การจำลองการกักเก็บในชั้นธรณีของคาร์บอนไดออกไซด์ในบริเวณอ่าวไทย

นางสาวมนฐิชา ระวังภัย

วิทยานิพนธ์นี้เป็นส่วนหนึ่งของการศึกษาตามหลักสูตรปริญญาวิศวกรรมศาสตรมหาบัณฑิต
สาขาวิชาวิศวกรรมทรัพยากรธรณี ภาควิชาวิศวกรรมเหมืองแร่และปิโตรเลียม
คณะวิศวกรรมศาสตร์ จุฬาลงกรณ์มหาวิทยาลัย
ปีการศึกษา 2558

Simulation On Geological Storage Of Carbon Dioxide In The Gulf Of Thailand.

Miss Monthicha Rawangphai

A Thesis Submitted in Partial Fulfillment of the Requirements
for the Degree of Master of Engineering Program in Georesources Engineering
Department of Mining and Petroleum Engineering
Faculty of Engineering
Chulalongkorn University
Academic Year 2015

Thesis Title	Simulation On Geological Storage Of Carbon Dioxide In The Gulf Of Thailand.
By	Miss Monthicha Rawangphai
Field of Study	Georesources Engineering
Thesis Advisor	Assistant Professor Kreangkrai Maneeintr, Ph.D.

Accepted by the Faculty of Engineering, Chulalongkorn University in Partial Fulfillment of the Requirements for the Master's Degree

.....Dean of the Faculty of Engineering
(Associate Professor Supot Teachavorasinskun, D.Eng.)

THESIS COMMITTEE

.....Chairman
(Assistant Professor Sunthorn Pumjan, Ph.D.)
.....Thesis Advisor
(Assistant Professor Kreangkrai Maneeintr, Ph.D.)
.....External Examiner
(Associate ProfessorPinyo Meechumna, Ph.D.)

มนฐิชา ระวังภัย : การจำลองการกักเก็บในชั้นธรณีของคาร์บอนไดออกไซด์ในบริเวณอ่าวไทย (Simulation On Geological Storage Of Carbon Dioxide In The Gulf Of Thailand.) อ.ที่ปรึกษาวิทยานิพนธ์หลัก: ผศ. ดร. เกรียงไกร มณีอินทร์, 95 หน้า.

ปัจจุบันสภาวะโลกร้อนเป็นหนึ่งในปัญหาสำคัญ เนื่องจากการเพิ่มขึ้นของปริมาณก๊าซคาร์บอนไดออกไซด์ในชั้นบรรยากาศ โดยก๊าซคาร์บอนไดออกไซด์เป็นองค์ประกอบที่สำคัญที่สุดของก๊าซเรือนกระจก ซึ่งมาจากอุตสาหกรรม เช่น การผลิตกระแสไฟฟ้า การดักจับและกักเก็บคาร์บอนไดออกไซด์ เป็นเทคโนโลยีที่ช่วยลดปริมาณก๊าซคาร์บอนไดออกไซด์ โดยเฉพาะการกักเก็บในชั้นธรณี ในประเทศไทยพื้นที่ที่มีศักยภาพสำหรับการกักเก็บในชั้นธรณีอยู่ในบริเวณอ่าวไทย อย่างไรก็ตามการวิจัยลักษณะที่ในประเทศไทยยังมีน้อย ดังนั้นในงานวิจัยนี้จึงเน้นการสร้างแบบจำลองของการกักเก็บก๊าซคาร์บอนไดออกไซด์ในชั้นธรณีบริเวณอ่าวไทย โดยมีการประมาณค่าของปริมาณกักเก็บและความดันที่เกิดการแตกหัก ความดันที่เพิ่มขึ้นและการกระจายตัวได้จากการสร้างแบบจำลองโดยอาศัยปัจจัยต่างๆด้วยเช่นกัน การอัดฉีดก๊าซคาร์บอนไดออกไซด์ใช้ในอัตรา 1,000-4,000 ตันต่อวัน ในระดับความลึกตั้งแต่ 2,160-2,510 เมตร และได้มีการตรวจวัดผลจากการศึกษาเป็นเวลา 50 ปี โดยจากผลแสดงให้เห็นว่าพื้นที่นี้มีศักยภาพในการกักเก็บก๊าซคาร์บอนไดออกไซด์ ซึ่งประกอบด้วยลักษณะเฉพาะของชั้น นอกจากนี้ยังรวมถึงความดันที่เพิ่มขึ้นและการกระจายตัวได้แสดงในระยะเวลา 50 ปี งานวิจัยนี้เป็นเหมือนความรู้พื้นฐานสำหรับการกักเก็บก๊าซคาร์บอนไดออกไซด์ในบริเวณพื้นที่นอกชายฝั่งในประเทศไทย

ภาควิชา วิศวกรรมเหมืองแร่และปิโตรเลียม ลายมือชื่อนิสิต .....

สาขาวิชา วิศวกรรมทรัพยากรธรณี ลายมือชื่อ อ.ที่ปรึกษาหลัก .....

ปีการศึกษา 2558

5670476521 : MAJOR GEORESOURCES ENGINEERING
KEYWORDS: CARBON CAPTURE AND STORAGE / OFFSHORE GEOLOGICAL STORAGE / PLUME MIGRATION / THE GULF OF THAILAND / CO2 MONITORING

MONTHICHA RAWANGPHAI: Simulation On Geological Storage Of Carbon Dioxide In The Gulf Of Thailand.. ADVISOR: ASST. PROF. KREANGKRAI MANEEINTR, Ph.D., 95 pp.

Climate change is one of the most concern problems currently because of the increase of the amount of greenhouse gases in the atmosphere. CO_2, the most important component of greenhouse gases, comes from industries like power generation. Carbon capture and storage (CCS) is the practical technology to mitigate CO_2 especially geological storage. In Thailand, the main potential of geological storage is in the Gulf of Thailand. However, the research on this in Thailand is scarce. Consequently, this work is focusing on the simulation of CO_2 geological storage in formations at the Gulf of Thailand. The storage capacity and the fracture pressure have been estimated. Also, the pressure buildup and plume migration have been simulated with various conditions. CO_2 injection is used from 1,000-4,000 tons per day with the depth from 2,160 – 2,510 meters and the results are studied for 1-50 years for monitoring period. The results show that CO_2 storage in this area has potential with the formation characteristics. Moreover, pressure buildup and plume migration are illustrated for the period of 50 years. This study can contribute as a fundamental knowledge for CO_2 storage in an offshore area in Thailand.

Department:	Mining and Petroleum Engineering	Student's Signature	.....
		Advisor's Signature	.....
Field of Study:	Georesources Engineering		
Academic Year:	2015		

ACKNOWLEDGEMENTS

First of all, I would like to express my sincere gratitude to Associate professor Dr. Kreangkrai Maneeintr, my thesis advisor for support and knowledge for my experiment.

I am grateful to the Department of Mineral Fuels (DMF), Ministry of Energy of Thailand. For support data used in this research.

I appreciate to The 90th Anniversary of Chulalongkorn University, Rachadapisak Sompote Fund and Graduate School Thesis Grant, Chulalongkorn University for financial support.

I would like to thankful for my Georesources Engineering friends for help and good friendship. Finally, I would like to thank my beautiful family for great support and always stay besides me no matter what happen.

CONTENTS

Page

LIST OF FIGURE

LIST OF TABLE

CHAPTER 1
INRODUCTION

1.1 Introduction

The changing of temperature in many parts of the world may cause climate change and global warming. Not only temperature increasing but also includes other situations such as weather changing, ice caps melting and arising of sea levels. All occurrences affect the human lives (global-greenhouse-warming, 2016).It is a result of greenhouse effect. The temperature of the earth's surface should be -18 ˚c without greenhouse effect (Staša et al., 2013).Therefore it is the advantage of greenhouse gases that make the earth's surface warmer. The greenhouse gases absorb infra-red radiation in the atmosphere thus making the earth warmer but currently greenhouse gases emission are enhanced in every years. So, the earth's temperatures increase immoderately and have an effect on human lives. The human activities are contributed to increase of greenhouse gases in the atmosphere.

1.2 Sources of carbon dioxide

The largest sources of greenhouse gases emission come from energy activities such as fossil fuel burning (Freund, 2013);(Staša et al., 2013). As shown in Figure 1.1.

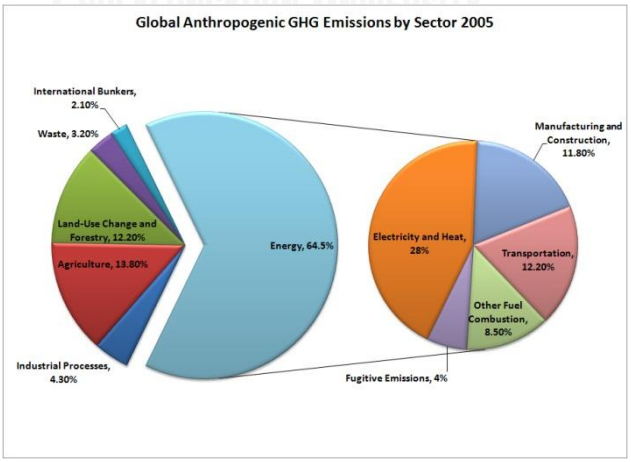

Figure 1.1 Global greenhouse gases emission in 2005
(Center for climate and energy solusions)

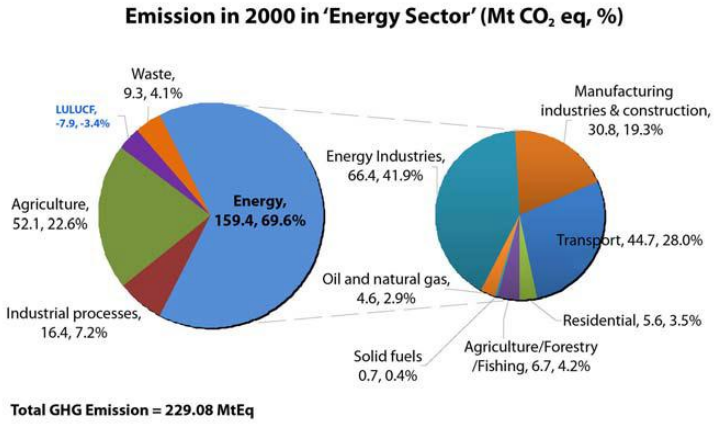

Figure 1.2 Greenhouse gases emission in Thailand in 2000
(Center for climate and energy solusions)

The trend of greenhouse gas emission in Thailand is similar as global emissions. Figure 1.2 shows the percent of sector for CO_2 emission and it shown that energy sector is the largest part which is separated into two sections. First section is fuel combustion, energy industries, manufacturing industries & construction, transportation and other sectors. Second section is fugitive emission. The greenhouse gases consist of carbon dioxide (CO_2), methane (CH_4), nitrous oxide (N_2O), hydro fluoride (HFC), per fluorocarbon (PFC) and sulfur hexafluoride (SF_6) as presented in Figure 1.3 (Office of Natural Resources and Environmental Policy and Planning, 2010). CO_2 is the most important component of greenhouse gases.

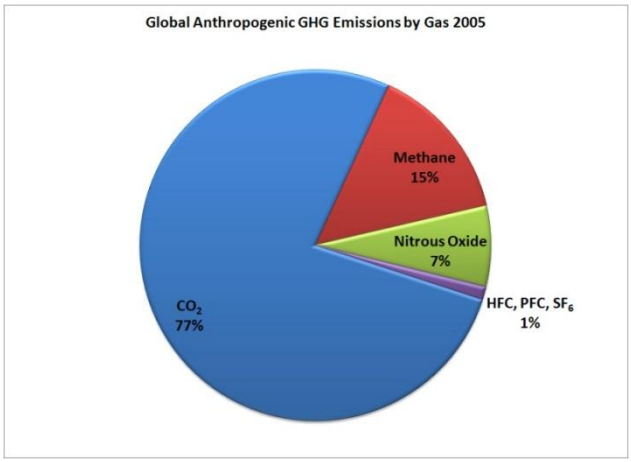

Figure 1.3 Global anthropogenic GHG emissions in 2005
(Center for climate and energy solusions)

1.3 Carbon Capture and Storage technology

With the adverse effect, CO_2 is needed to reduce or mitigate. Currently, the effective technology to do so is carbon capture and storage technology or CCS in order to reduce CO_2 emission to the atmosphere.

Carbon Capture and Storage technology has a potential to reduce 85-95% of CO_2 emission in the atmosphere (IPCC, 2005) .There are 3 processes in CCS, CO_2 capture, CO_2 transportation and CO_2 storage.

- CO_2 capture: This technology is for capture CO_2 from emission sources such as fossil power plant, natural gas processing etc. The process are capturing, dehydrating and compressing CO_2 from emission sources (Asian Development Bank, 2013).
- CO_2 transportation: The process is transported CO_2 from capture to storage via pipeline or ship to a storage site.
- CO_2 storage: The process is injected CO_2 in deep underground for permanent storage CO_2 (Asian Development Bank, 2013).

1.3.1 CO_2 storage

This research focuses on only CO_2 storage. There are 3 types of CO_2 storage such as ocean storage, mineral storage and geological storage.

1. Ocean storage

CO_2 can be transported by pipeline and ship to inject to the ocean or sea floor at depth below 3,000 m as presented in Figure 1.4. At that depth CO_2 is denser than water and form as a lake. It's only in small scale experiment. The good point of this storage is easy to inject because CO_2 can be injected directly into the ocean. However, if injected less than 3,000 m. depth, CO_2 will dissolve in sea water so it will increase in acidity and affect to marine ecosystem. Presently, ocean storage is still in research phase (IPCC, 2005).

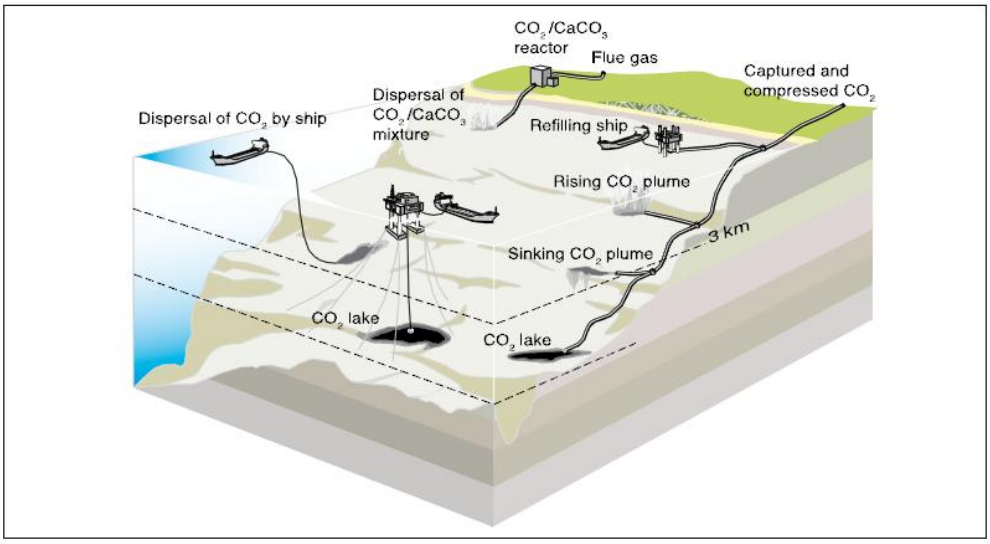

Figure 1.4 Ocean storage
(IPCC, 2005)

2. Mineral storage

Mineral storage is the method that CO_2 is reacted with metal oxide making calcium and the byproduct in solid form of a mineral carbonate. The advantage of solid form is stability but the natural reaction is very slow and uses more energy for pre-treatment of minerals. Other method is industrial uses but the CO_2 utilization is small scale and lifetime that CO_2 is retained too short. It is still in the development stage (IPCC, 2005).

The pros and cons from these 2 types of storage show that the potential for storage is not good enough. So the third type is interesting for this study. The third type is geological storage.

3. Geological storage

Geological storage is the storage of CO_2 in geological formation. The CO_2 is trapped in deep underground and its must be injected down to a depth of over 800 meters, where the ambient pressure and temperature will result in CO_2 being in liquid or supercritical state. Geological storage can be divided into 3 categories such as oil and gas field, saline formation and coal seams (IPCC, 2005) as shown in Figure 1.5.

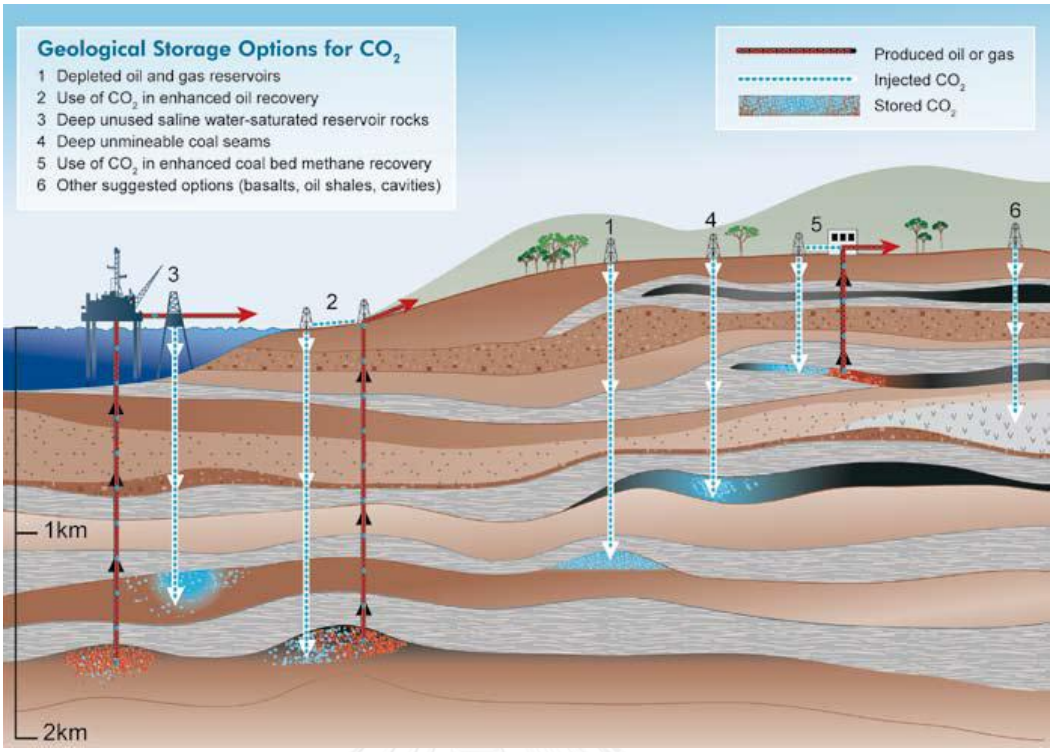

Figure 1.5 Geological storage
(IPCC, 2005)

1.3.2 Types of geological storage

1) Oil and gas field

A) Abandoned oil and gas fields: CO_2 is injected into the depleted oil and gas reservoirs. This research is focusing on this type especially in offshore field. This approach is attractive because these structures are known by geological structure and physical properties that studied before. The oil and gas are traps by structural and stratigraphic of formation. So that's why this area is safe for CO_2 storage. The simulation model that developed from oil and gas industry is used to predict the movement, displacement behavior and trapping. Finally, infrastructures are already in place (IPCC, 2005).

B) Enhanced oil recovery (EOR): CO_2 is injected for enhanced oil recovery (EOR) and economic benefit may be increased by increasing oil production.5-40% oil is recovered by conventional primary production (Holt, Jensen, & Lindeberg, 1995).

C) Enhanced gas recovery: the method injects CO_2 for enhanced gas recovery but it's only in pilot scale (IPCC, 2005).

2) Saline formations is the injection of CO_2 into sedimentary rock about 800-1,000 depth. This area is very large storage capacity (IPCC, 2005).

3) Coal seams

A) Unmineable coal seams: is CO_2 injected into unmineable coal seams.

B) Enhanced coal bed methane recovery (ECBM): is CO_2 injected into unmineable coal seams and replacing methane, thereby enhancing coal bed methane recovery (IPCC, 2005).

4.) Other geological media (basalt, oil or gas shale, salt caverns and abandoned mine): is CO_2 injected into geological media.

1.3.3 Existing CO_2 storage projects

Almost of existing CO_2 storage projects are geological storage such as the Sleipner project in the North sea, the Weyburn project in Canada and the In Salah project in Algeria (IPCC, 2005) as shown in Table 1.1.

Table 1.1 Existing CO_2 storage projects.
(IPCC, 2005)

Project name	Country	Injection start (year)	Approximate average daily injection rate (tCO_2 day^{-1})	Total (planned) storage (tCO_2)	Storage reservoir type
Weyburn	Canada	2000	3,000-5,000	20,000,000	EOR
In Salah	Algeria	2004	3,000-4,000	17,000,000	Gas field
Sleipner	Norway	1996	3,000	20,000,000	Saline formation
K12B	Netherlands	2004	100 (1,000 planned for 2006+)	8,000,000	Enhanced gas recovery
Frio	U.S.A	2004	177	1600	Saline formation
Fenn Big Valley	Canada	1998	50	200	ECBM
Qinshui Basin	China	2003	30	150	ECBM
Yubari	Japan	2004	10	200	ECBM
Recopol	Poland	2003	1	10	ECBM
Gorgon (planned)	Australia	~2009	10,000	unknown	Saline formation
Snøhvit (planned)	Norway	2006	2,000	unknown	Saline formation

Each types of storage has their own advantages and disadvantages. Nowadays geological storage is on demonstrate phase, ocean storage is in small scale experiment and mineral storage is in development stage. As shown in Table 1.2.

Table 1.2 Current maturity of CCS system component.
(modified from (IPCC, 2005)

CCS Component	CCS Technology		Research	Demonstration phase	Economically feasible under specific conditions	Mature
Geological storage	Enhanced oil recovery (EOR)					x
	Gas or oil fields				x	
	Saline formations				x	
	Enhanced Coal Bed Methane recovery (ECBM)			x		
Ocean storage	Direct injection (dissolution type)		x			
	Direct injection (lake type)		x			
Mineral storage	Mineral carbonate	Natural silicate minerals	x			
		Waste materials		x		
	Industrial uses					x

The storage in deep onshore, offshore geological formations use the same technology of oil and gas industry. The various technologies such as geophysical and geochemical are applied for survey the potential area (Ringrose et al., 2013). Site study for this work is in the gulf of Thailand because the target sources of CO_2 emission are in offshore oil and gas industries. CO_2 emissions from offshore oil and gas production in UK were 24.4 Mt. in 2001 (Vanner, 2005) and assume that in Thailand are 10-20 % of CO_2 emissions from offshore oil and gas production in UK. So this research is focusing on geological storage especially in depleted gas reservoir in order to reduce CO_2 emission. Other reasons include these structures are well known and infrastructures are in place already. In the future this method can apply to enhance oil recovery (EOR) to gain more profit in business.

1.4 Objectives of this project

The objective of this study is to evaluate the CO_2 storage in depleted gas or oil reservoir in the offshore fields by using a simulation model for observing the effects of various parameters on CO_2 storage such as in the reservoir.

The contributions of this research are to reduce CO_2 emissions from the industrial especially in offshore field and simulate CO_2 storage in depleted gas or oil reservoir at the Gulf of Thailand. This is a preliminary study on CO_2 storage. Accordingly, it can be apply to enhance oil/gas recovery for increase project value in the future.

The contents in this thesis are consisting of chapter 2, 3, 4 and 5. After the source of problem and basic knowledge are referred in Chapter 1, Chapter 2 presents about an important theory and literature review that used in this research such as properties of rock and petroleum fluids, porosity and permeability, temperature gradient, pressure gradient and plume migration. The simulation method and geology data are presented in Chapter 3. Chapter 4 presents the result and discussion described in term of pressure buildup, plume migration, shutin time and storage capacity. The last chapter is Chapter 5 presenting conclusion and recommendation of this research.

CHAPTER 2
THEORY AND LITERATURE REVIEW

This chapter presents the basic knowledge and theory of CO_2 geological storage as well as the literature review of previous study on CO_2 storage and existing projects.

2.1 Properties of rock and petroleum fluids

2.1.1 Properties of CO_2

The carbon dioxide emissions include anthropogenic activities such as fuel combustion, fermentation and the other source is natural source such as volcanic activities etc. CO_2 is not only disadvantage but it is necessary for plant in photosynthesis also.

The carbon dioxide is small quantities in the atmosphere. It is a chemical compound that consists of carbon and oxygen. In normal temperature and pressure, CO_2 is a gas. The general characteristics of CO_2 gas are colorless and disturbing odour. The CO_2 gas is denser than air. The properties of CO_2 consist of physical properties and chemical properties. The chemical properties of CO_2 have shown as a solubility of CO_2. When temperature, pressure and water salinity are increasing, the solubility of CO_2 in water will decreasing. The physical properties are about the state or phase of CO_2 that varies with temperature and pressure. Phase such as vapor, liquid and supercritical (IPCC, 2005).

2.1.2 Phase

Phase of CO_2 change according to temperature and pressure. CO_2 behaves as a gas in the air at standard temperature and pressure (STP). When temperature and pressure are increasing, CO_2 can be adapted properties between gas and liquid, it behave as a supercritical fluid above critical temperature (304.25 K) and critical pressure (72.9 atm) e.g. liquid-like density and gas-like viscosity (Wilcox, 2011)as shown in Figure 2.1.

The CO_2's behavior is an important aspect for storage (IPCC, 2005).The great depth for target reservoir that will be supported this condition is below 800 m. This is to be confidence that CO_2 will remain in dense state and to reduce its buoyancy in reservoir (Global CCS Institute, 2013)

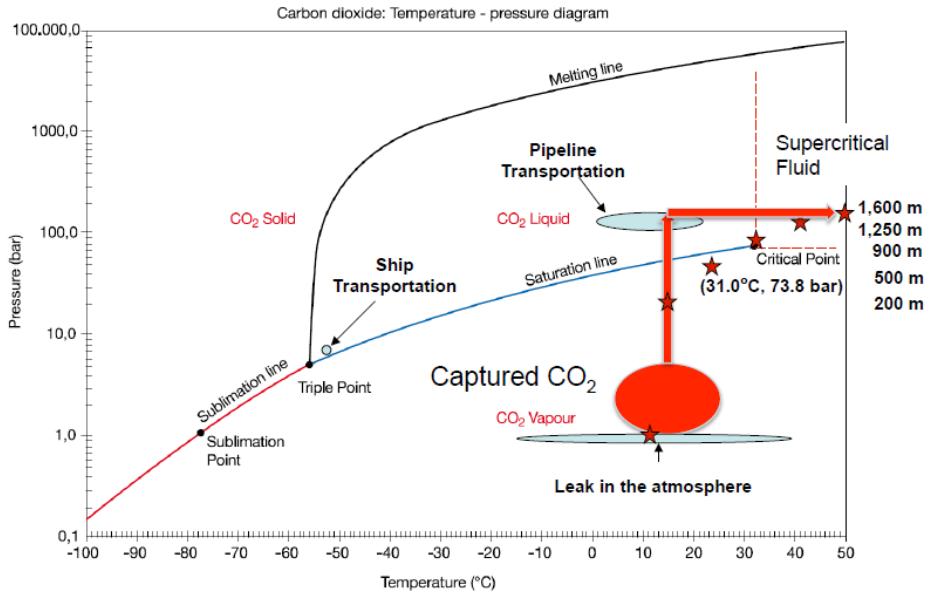

Figure 2.1 CO_2 temperature pressure diagram.

(Wilcox, 2011)

2.1.3 Density

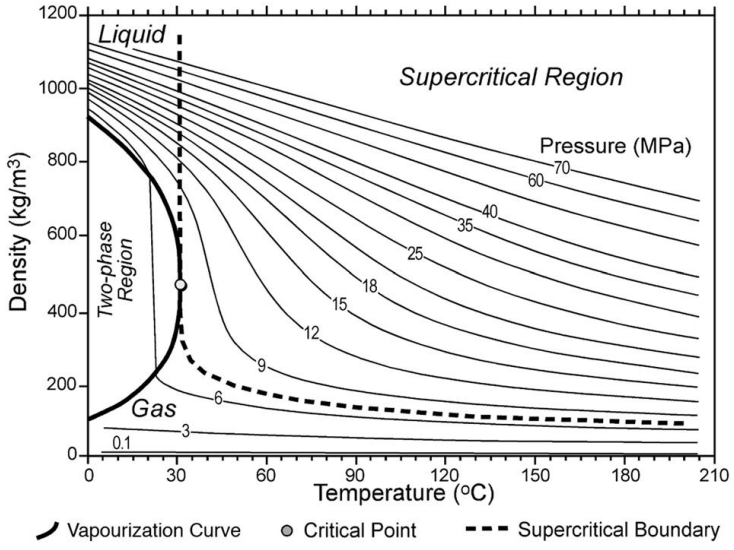

Figure 2.2 Variation of CO_2 density.
(Bachu, 2003)

Density is a ratio of mass (kg) and volume (m^3). It is used to indicate volume per tonne of CO_2 and to increase efficiency of geological storage and transportation (Wilcox, 2011). The variation of density depends on temperature and pressure (Bachu, 2003) as shown in Figure 2.2. It is used to calculate to amount of CO_2 storage in the formation for given conditions

2.1.4 Viscosity

Viscosity is used for indicates the resistance properties of the fluid flow. The influence of viscosity affects injection CO_2 to reservoir (Prakiat & Jeemsantia, 2011). Not only liquid viscosity can be resistance to the flow but the gas as well (ChemWiki). The viscosity can measure the ease of molecule mobility depending on attractive force (Blaber, 2005).Viscosity is inverse variation with temperature in liquid phase. The viscosity of liquid is decreasing when temperature is increasing. On the other hand, the viscosity in gas phase is increasing as temperature increases. This is a physical basic property of viscosity (Urroz, 2005)

2.1.5 Compressibility

Compressibility is fractional change in volume per unit change in pressure. The amounts of CO_2 injected depend on compressibility of pore space in reservoir (Pickup, 2013). Moreover, the compressibility is one of variable that use to calculate the storage coefficient especially in closed system if there are contain highly faults or compartment areas, effective storage resource is limited by compressibility of pore and maximum pressure buildup in formation (Gorecki et al., 2009).The benefit of compressibility is to know the pressure increase in reservoir (Prakiat & Jeemsantia, 2011)

2.1.6 Surface tension

The attractive force between molecules in liquid is the cohesion force. That will pull the molecules into liquid body then liquid try to change shape until that has minimize surface area. So, it will be less force of cohesion then liquid can flow. Surface tension is magnitude of force that control shape (Purdue university,

2004).Surface tension is tension that occurs on the surface of liquid (Wilcox, 2011). It is because attraction between molecules. It's like a thin film and opposes to breaking (Clark, 1969).

2.2 Porosity and permeability of formation

Porosity

The grains that make up the sandstone beds are not fit together. There is a pore space between grains. So it can be accumulate oil, gas or fluids. That is one characteristic of rock. Pore space or porosity in rock gives ability to absorb and hold fluids. Porosity is measured as a percent of total rock volume (Clark, 1969). It is a proportion of pore space in rock volume. The average porosity of sandstone is approximately 10 – 25 % as shown in Equation 2.1 (Wilcox, 2011)

$$\phi = \frac{V_V}{V_T} \tag{2.1}$$

Where V_v = Volume of void

V_T = Volume of total rock volume

Permeability

Permeability (k) is the ease that fluids can move through the interconnected pore space (Wilcox, 2011). The permeability of rock is more or less depending on the fluids that can pass great or less ease. Many rocks are porous but they still have less permeability than clay, shale and some other sandstones etc. Due to the interconnection between less void spaces, permeability it must be considered in term of forces that let fluids flow as presented in Equation 2.2 (Clark, 1969).

$$k = \frac{-Q\mu}{A(\frac{p_b - p_a}{x})} \tag{2.2}$$

Where μ = Viscosity(Pa·s)

x = Length (m)

Q = Volumetric flow rate (m^3/s)

A = Area (m^2)

p = Pressure (Pa)

There are many factors that affect porosity and permeability of sand stone regardless of size, shape of sand grains, compacted and cemented materials (Clark, 1969).

2.3 Darcy's law

Darcy's empirical flow law is the principles of fluid dynamic flow. Those fluids are flown through porous rock (Dake, 1977). Darcy's law varies directly with numerical quantity and pressure but varies reversely with viscosity of fluid as illustrate in Equation 2.3 (Clark, 1969).

$$Q = -\frac{k\rho g A(h_b - h_a)}{\mu L} \qquad (2.3)$$

Where Q = Volumetric flow rate (m^3/s)

k = Permeability (m^2)

ρ = Fluid density (Kg/m^3)

g = Gravitational acceleration (m/s^2)

A = Cross section area (m^2)

μ = Fluid viscosity (Pa-s)

h_a = Hydraulic head at point a (m)

h_b = Hydraulic head at point b (m)

L = Length (m)

2.4 Temperature gradient

Temperature is increasing when depth is increasing respectively (Wilcox, 2011).The estimate temperature gradient to around 25 ^{o}C to 30 ^{o}C per depth in kilometer as show in Equation 2.4 and 2.5

$$\frac{dt}{dz} \approx 25^{o}C \text{ to } 30^{o}C/km \qquad (2.4)$$

$$T(z) = T_s + \int_0^z \frac{dT}{dz} dz = T_s + \frac{d\overline{T}}{dz} z \qquad (2.5)$$

Where T_s = mean annual ground surface temperature (◦C) ~14.6°C

z = depth below ground surface (m)

2.5 Pressure gradient

Fluid pressure increase with depth that below water table as presented in Equation 2.6 (Wilcox, 2011).

$$P = P_{atm} + \int_0^d \rho_w g dz \approx P_{atm} + \overline{\rho_w} g d \qquad (2.6)$$

Where ρ_w = Density of groundwater (kg/m3) ~ 1,000 kg/m3,

g = Gravitational acceleration (9.81 m/s2),

z = Depth below the watertable (m), and

d = Depth of interest (m).

2.6 Pressure

2.6.1 Maximum pressure

Fracture pressure is a pore pressure affecting the formation in that it can break the rock to produce the fracture of caprock. Consequently, it can be implied to use as a maximum pressure that caprock can be tolerated. Basically 90% of fracture pressure

is applied as maximum pressure (Ruanman, 2015). During CO_2 injection, pressure must not exceed to 90% of fracture pressure to prevent the breaking caprock (Mathias et al., 2009). There are many equations of fracture pressure calculation one of them is the Hubbert and Willis Equation. The fundamental principal is "the minimum wellbore pressure required to extend an existing fracture is given as the pressure needed to overcome the minimum principle stress" as shown in Equation 2.7 (Bourgoyne et al., 1986)

$$P_{ff} = \sigma_{\min} + P_f \tag{2.7}$$

Where P_{ff} = Formation fracture pressure
P_f = Formation pressure
$\sigma_{\min}$ = Minimum matrix stress

The fracture pressure is expressed by (shokir)

$$F_{\min} = \frac{1}{3}\left(1 + \frac{2P}{D}\right) \tag{2.8}$$

Where F_{min} = Fracture gradient
P/D = Pore pressure gradient (psi/ft). Normal pore pressure gradient is 0.465 psi/ft (Nguyan, 2013)

2.6.2 Pressure buildup

Pressure buildup during CO_2 injection depends on the flow in both the multiphase and single phase regions. The estimation of pressure buildup consist of many properties such as permeability, thickness, viscosity of fluid, rock compressibility and CO_2 density. The pressure buildup which approach to maximum pressure buildup will determine to maximum CO_2 storage (Pickup, 2013). The pressure buildup equation is shown in Equation 2.8 (Wilcox, 2011).

$$\Delta P = \frac{Q \times \mu_W \times W}{4 \times \pi \times k \times b} + \frac{Q \times \mu_{CO_2}}{2 \times \pi \times k \times b} \times \left[\ln\left(\frac{r_f}{r_w}\right) + \left(\frac{f_{CO_2}}{K_{r_{CO_2}}} - 1\right)\left(1 - \frac{r_w}{r_f - r_w} \times \ln\left(\frac{r_f}{r_w}\right)\right)\right] \tag{2.8}$$

Where b = Reservoir thickness (m)

C_t = Total compressibility (Pa-1)

k = Permeability (m^2)

Q = Injection rate (m^3/s)

r_f = Radius to the front (m)

r_w = Well radius (m)

t = Time (s)

ϕ = Porosity

μ_W = Viscosity of water (Pa•s)

μ_{CO_2} = Viscosity of CO_2 (Pa•s)

2.7 Storage capacity

The area inside the formation is affected amount of CO_2 capacity. It depends on boundaries of area. There are closed, semi-closed and open systems as shown in Figure 2.3. In this research, it is assumed that the studied area is a closed system because in this area compartment boundaries are limited by faults in that basin.

Swarbrick et al., (2013) studies closed system and the reservoir is trapped by top seal, bottom seal and side seals. Top and bottom seals are fined-grained such as shale which is low permeability and side seals is occurred by lateral change or fault. There can be determined the maximum storage capacity for each area.

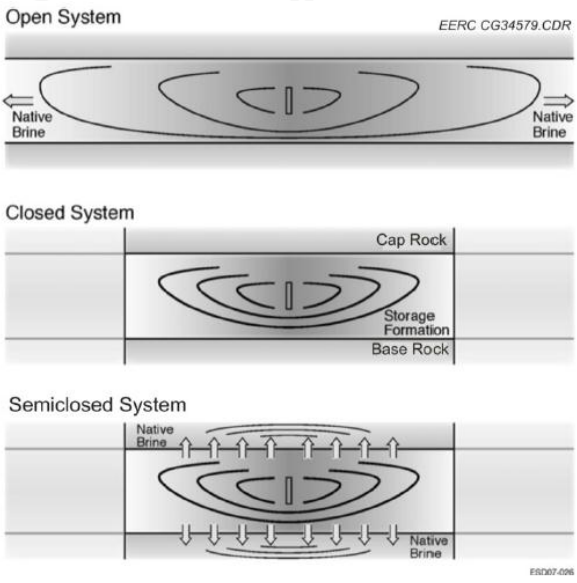

Figure 2.3 Diagram of storage system.
(Gorecki et al., 2009)

Storage capacity is amount of CO_2 that will be contained in the reservoir. CO_2 storage in depleted oil or gas reservoir can be calculated directly. The basic data for calculation consist of reservoir and rock properties. The volume of CO_2 that is stored in reservoir should to equal volume of oil or gases which are produced (Pickup, 2013). Equation 2.9 is applied to calculate for amount of CO_2 stored in the formation.

$$V_{CO_2} = R_f \times A \times H \times \phi \times (1-S_{wc}) \qquad (2.9)$$

Where V_{CO_2} = Volume of CO_2

R_f = The recovery factor

A = Area

H = Thickness

ϕ = Porosity

S_{wc} = The connate water saturation

2.8 Plume migration

After injection of CO_2 into geological formation, CO_2 will be kept in the injected zone for a while. Although, CO_2 is still in supercritical state, it is a result from buoyancy-driven (Silin et al., 2009). The widespread of plume migration can be produced in a thin layer of targeted reservoir. In the formation with low injection pressure gradient, there is a risk of leakage but if the concern in overlooked, then this area is possible for CO_2 storage. Moreover, low permeability will accentuate pressure buildup in area and then CO_2 outflow will be limited (Chasset et al., 2011).

2.9 Literature review

Ringrose et al.,(2013) studied the CO_2 at Central Algeria. This project is a pioneer of onshore CO_2 capture and storage. CO_2 is injected into carboniferous sandstone unit at the Krechba field. Injections start from 2004 and store 3.8 Mt. of CO_2 .The storage potential in subsurface has been monitored by using geophysical and geochemical methods. The modeling that goal of CO_2 storage modeling are for understand dynamic process in storage unit that controls injectivity and storage capacity and simulation of migration pathway (Ringrose et al., 2013).

Staša et al.,(2013) studied the CO_2 storage in geological layers as a method to reduce CO_2. The area should be monitor for the performance of CO_2 storage. CO_2 is compressed into a dense liquid. The injection pressure must be higher than outside reservoir pressure. The amounts of injection wells depend on quantity of CO_2, injection rate, permeability, reservoir thickness, maximum pressure and type of wells. If injection pressure is more than maximum pressure, storage and seal rock will be destroyed. The numerical simulations are used to assess the impact that would happen to reservoir and seal rock (Staša et al., 2013).

Plasynski et al.,(2008) studied at CO_2 injection Weybern oil field in Saskatchewan, Canada. CO_2 is transported from Dakota gasification plant in North Dakota by pipeline. Injection start from October 2005. This project expects the recovery of oil for 30 years. The objective is to determine the long-term storage risk and monitoring migrate risk (Plasynski et al., 2008).

Torp & Gale (2004) study the demonstrating storage at Sleipner gas field in North Sea and injected CO_2 into sand layer " Utsira formation" in deep saline aquifer. The project is the first commercial project application of CO_2 in deep saline aquifer in the world. Injection starts from October 1996 and the amount of CO_2 approximately 5 Mt. The monitoring use by 3D seismic survey to see geological storage reservoir and reservoir simulation to observe the movement of CO_2 (Torp & Gale, 2004).

Bouc et al.,(2009) studied the determining safety criteria for CO_2 geological storage under CRISCO$_2$ project. The aims of the project is to evaluate the risk by using model and to define various requirement that should have less impact on human health and safety, environment and other underground resources. This project began in December 2006 until December 2009. In the conclusion the CRISCO2 project developed tools to identified risk, represent risk events and assess the uncertainty parameters. These tools can apply to any sites. Example case is in an aquifer in the Paris basin for testing the effective of safety criteria (Bouc et al., 2009).

Chadwick & Eiken (2013) study CO_2 storage in Sleipner natural gas in offshore field. That is the world longest running industrial scale of CO_2 storage. This offshore field produces natural gas at 3,400-3,600 m deep. The 9% of CO_2 in this field must be reduced to less than 2.5%. For CO_2 injected to Utsira Sand, this is large formation in subsurface. The Utsira Sand is saline aquifer. Injection point is at 1,012

m under sea level. At the beginning, 1 Mt of CO_2 injected in 1996. Until 2011, there are 13 Mt of CO_2 stored in this area. 3D map show the Utsira Sand structure consist of valleys and small domes. CO_2 injected into beneath small dome. Diameter of dome is 1-2 km which elongated structure. The fault are cut the Utsira Sand but it does not effect to reservoir and caprock. From wireline log, 70% is sand and thin mudstones in this area. Thickness of mudstone is only 50-100 m that is barrier in reservoir sand. From core sample, the result from laboratory porosity is in the range 27-42%. The regional porosity form wireline log is 35-40%. Permeability is 1-8 Darcy. The initial temperature is 29˚C at top of reservoir and temperature at injection depth is 35 ˚C. The CO_2 is injected in dense phase form with pressure 6.2-6.6 MPa. During injection, if pressure is buildup, injection rate will decrease, density will increases and pressure increase. Then effect to temperature change (Chadwick & Eiken, 2013).

Swarbrick et al.,(2013) studies the pressure control in carbon capture and storage. Pressure is an important property to measure storage capacity in area and define injection pressure. In addition phase and characteristic of CO_2 in the layer controlled by pressure. This can identify the suitable sites. The ways that subsurface pressures are impacted on CO_2 storage consist of

1)subsurface pressure to control the CO_2 phase: CO_2 is in condensed state at 800 m. So this is maximum volume that can be stored.

2)the pore fluid pressure during CO_2 injection does not over than shear failure limit.

3)Fluid pressure used for identified system in area such as closed or open system and

4) Degree of overpressure is calculated by fluid pressure etc.

There are 3 types of pressure important in this study; pore fluid pressure (pressure is increasing while injecting CO_2), fracture pressure (increasing with depth) and lithostatic pressure. There are 2 type of storage site, 1) closed system is compartment or highly fault that the maximum storage defined by top seal hydraulic failure. Initial high pressure volume of injection is less. In depleted gas field, pressure will decrease and then it can store large volume of CO_2 and 2) open system is open aquifer to surface (Swarbrick et al., 2013).

Whittaker & Perkins (2013) study the technology of CO_2 EOR. EOR is enhanced oil recovery technology that connects with CO_2 storage. The method is to inject CO_2 in oil reservoir then densed CO_2 will dissolve to oil that increases the

amount of oil. There are 130 commercial projects for EOR around the world. Almost all of projects in United States that located in Permain basin. Source of CO_2 is from coal-fired power plants. CO_2 is compressed form gas to densed phase or as a supercritical state to transport and inject. The property of supercritical state is density like liquid and mobility like gas. At 800 m depth or more, CO_2 will in the form of supercritical phase and CO_2 will be retaining in reservoir with lower buoyancy force. Moreover, porosity and permeability are affected to inject CO_2. The purpose of storage is CO_2 still remain in target reservoir (Whittaker & Perkins, 2013).

Underschultz et al.,(2011) studies CO_2 storage in depleted gas field. That is the CO2CRC Otway project in Australia. This is demonstrating storage. The injection is beginning in 2008 and paused it at 2009. There are 65,445 tonnes of CO_2 stored in reservoir. The injection rate is 870 tonnes per week. The K12B field is in the North Sea that located at onshore of Otway basin. This is depleted gas field and the data in area are well known. Not only CO_2 storage but also enhanced gas recovery is investigated in this project (Underschultz et al., 2011).

CHAPTER 3
SIMULATION

This chapter presents the simulation model created by CMG software. The fundamental and geological data of this studied area are obtained from the Department of Mineral Fuels (DMF), Ministry of Energy and presented in this chapter. The model is shown in 3D model. Also, the conditions of simulation are presented here.

3.1 CMG program

CMG program is developed by Computer Modeling Group. It is a simulation software to build the 3D models.There are three types of simulator consisting of GEM, IMEX and STAR. IMEX is black oil simulator with three phases. That is used for modeling primary depletes and secondary recovery process in oil and gas reservoir. STAR is advance process for recovery process that concern with thermal; inject steam, solvent, air and chemical. GEM is compositional reservoir simulator. GEM is generalized equation of state model reservoir simulator. The modeling shows the effect of fluid composition to reservoir. The models of GEM are asphaltenes, coal bed methane and the geochemistry of sequestration of gases comprise CO_2 and acid gases (CMG, 2011).

This research uses GEM of CMG simulation for study the ability of this area and storage capacity that injected CO_2 in depleted gas field. Peng-Robinson is the equation of state used to predict phase equilibrium of composition and density of gas phase. It will support to various parts for computing properties of gas. At the beginning, Cartesian grid to create grid is set. It represents a geological formation (Basbug, 2005). In this case, the permit of CMG program is for academic purpose. So the maximum member of grids is only 10,000 grids in I, J and K direction. It can be vary thickness and depth. Afterward component properties including component of reservoir and gas, rock fluid type and initial conditions are specified. In this step, the important things are injection rate and fracture pressure. That will affect the storage capacity of CO_2. Finally, validation of dataset and run normal immediately are performed. The result of program shows in a 3D model.

3.2 Fundamental and geological data

For this research, the fundamental and geological data are obtained from the Department of Mineral Fuels (DMF), Ministry of Energy of Thailand. The study area is north Malay basin in the Gulf of Thailand as shown in Figure 3.1. The reason to select the area because the information is limited to available while information of this area are received from DMF. Furthermore, there are a lot of oil/gas industry in North Malay Basin therefore the facilities in this area can use in CO_2 storage technology in the future.

The fundamental data for depleted gas reservoirs are acquired from DMF consist of temperature, porosity, depth and etc. as shown in Table 3.1. However, the data are not enough for simulation thus it needs to assume and calculate some data such as area, storage capacity and fracture pressure (maximum pressure) in order to get the simulation model and results.

Table 3.1 List of fundamental data.

Parameters	Values
Depth (m)	2,160 – 2,510
Thickness (m)	8-24
Pressure at layer (MPa)	9-12
Pressure current of well (MPa)	9-13
Maximum pressure (MPa)	28-34
Density of CO_2 (Kg/m^3)	202-233
Porosity (%)	16-27
Permeability (md)	69 - 450
Temperature (˚C)	87-97
Temperature of well (˚C)	74-92

Geology of Gulf of Thailand

The Gulf of Thailand is on the southern edge of the Eurasian plate. The area are 270,000 km^2. Almost of basins in the Gulf of Thailand are in Tertiary. The location is

approximately latitude 6°-14° N and longitude 94°-103°E in the southeast of Thailand (Kongkanoi, 2008). The area is cut by two major fault system consist of Three pagoda fault and Ranong fault (Chochawalit, 1985). The structural basins in the Gulf of Thailand are made up by movement of the Indian plate and the following collision with Eurasian plate in the Eocene (Morley & Racey, 2010) The basins in Thailand are presented in Figure 3.1. In black box is Malay Basin.

The basins are formed as a grabens and half grabens in N-S orientation. The area is divided into two main region by Ko Kra Ridge. The western areas are small basin compose of Hua Hin basin, Kra and Wetern basins, East Kra Basin, Chomphon Basin,Songkhla and Nakorn Basins. The eastern areas are two major basins consist of Pattani and Malay basin. The sediment are contained 8000 m. and 4000 m for western area (Polachan et al., 1991)

Geology of North Malay basin

The North Malay Basin is in the northern part of Malay Basin as shown on Figure 3.2 and 3.3. In Figure 3.2 is shown location of Malay basin and Figure 3.3 presented map of North Malay Basin.This is elongate basin that occurred by rift activity in late Eocene to Oligocene (Khositchaisri, 2005). That developed by extrusion tectonic. It occurred throughout Southeast Asia after t the collision of Indian and Eurasian plate in early Cenozoic (Chotpitayasunon, 2005). The structural trend or main faults are NW-SE and N-S orientation. The fault form graben and horst pattern which sets pending syn-rift and post rift period (Kananithikorn, 2005).Malay basin is hydrocarbon basin. That found in Oligocene and Miocene sandstone. For the reason, Oligocene and Miocene sediment are source rock (Khositchaisri, 2005)

The geological histories in Cenozoic of the North Malay Basin are similar to Pattani basin as shown a Figure 3.4 that is cross section of Pattani Basin and Malay Basin. The stratigraphy of two basins is same in the Miocence-Recent. In this area, there are expanded oil and gas exploration and development. The part of Thailand thin the North Malay Basin are two mains production and exploration blocks : Arthit and Bongkot (Morley & Racey, 2010)

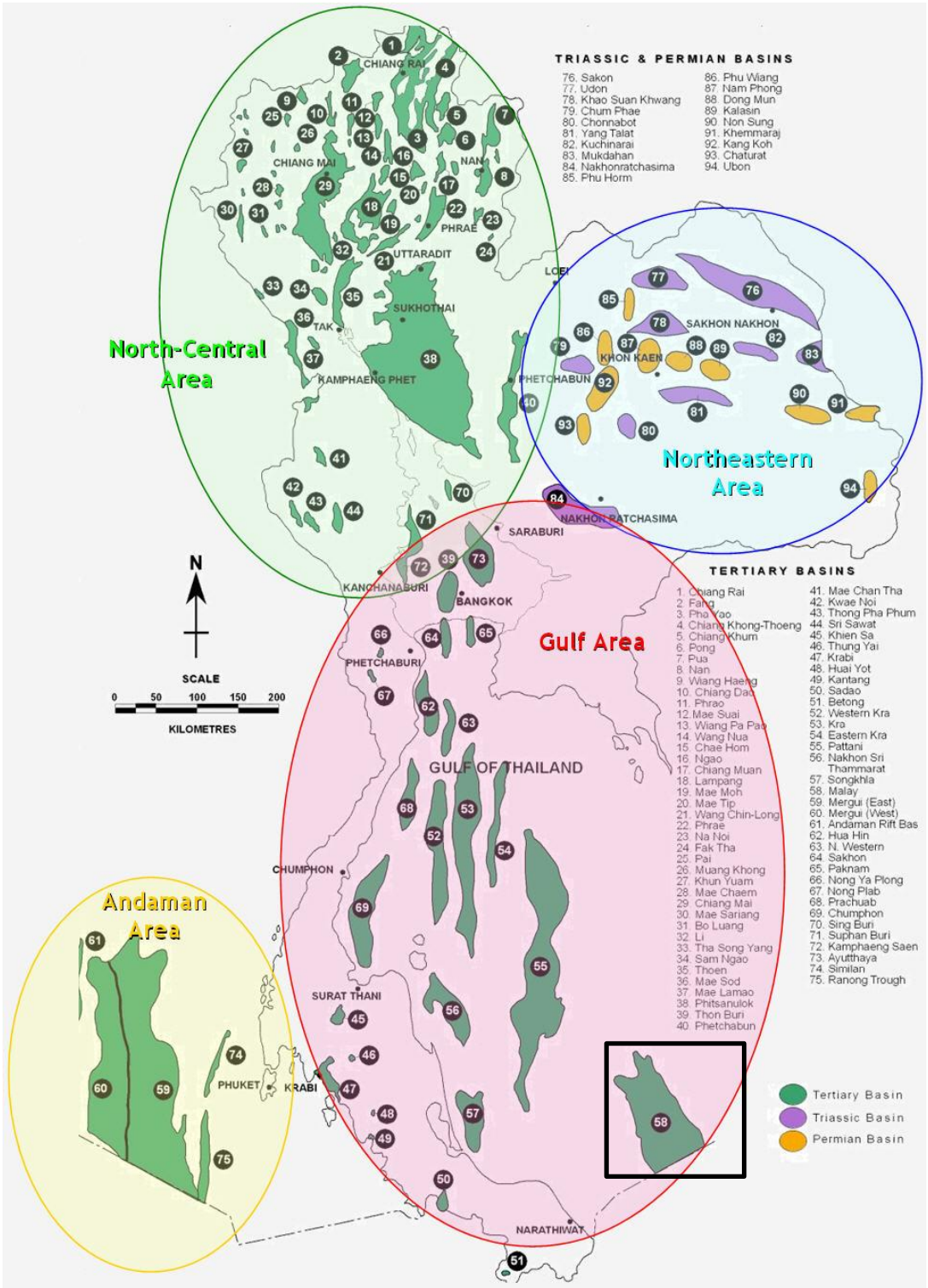

Figure 3.1 Basins in Thailand.
(Ministry of energy)

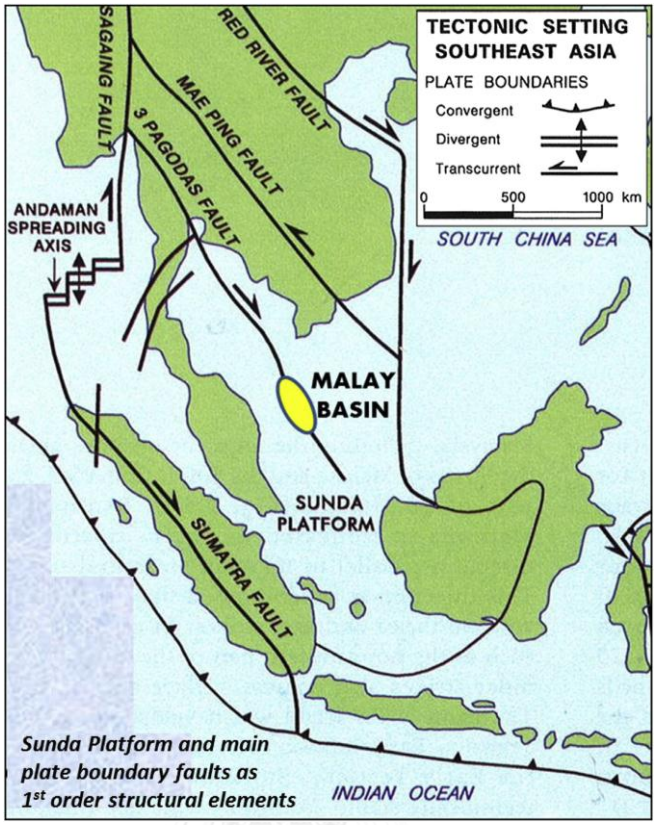

Figure 3.2 Map of location Malay basin.
(Mansor, Rahman, Menier, & Pubellier, 2014)

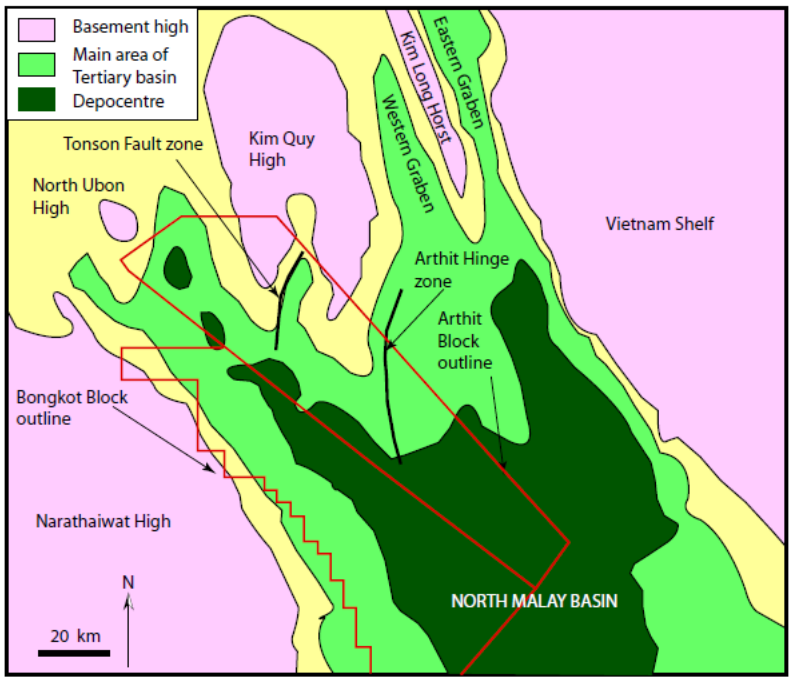

Figure 3.3 Regional map of North Malay Basin.
(Morley & Racey, 2010)

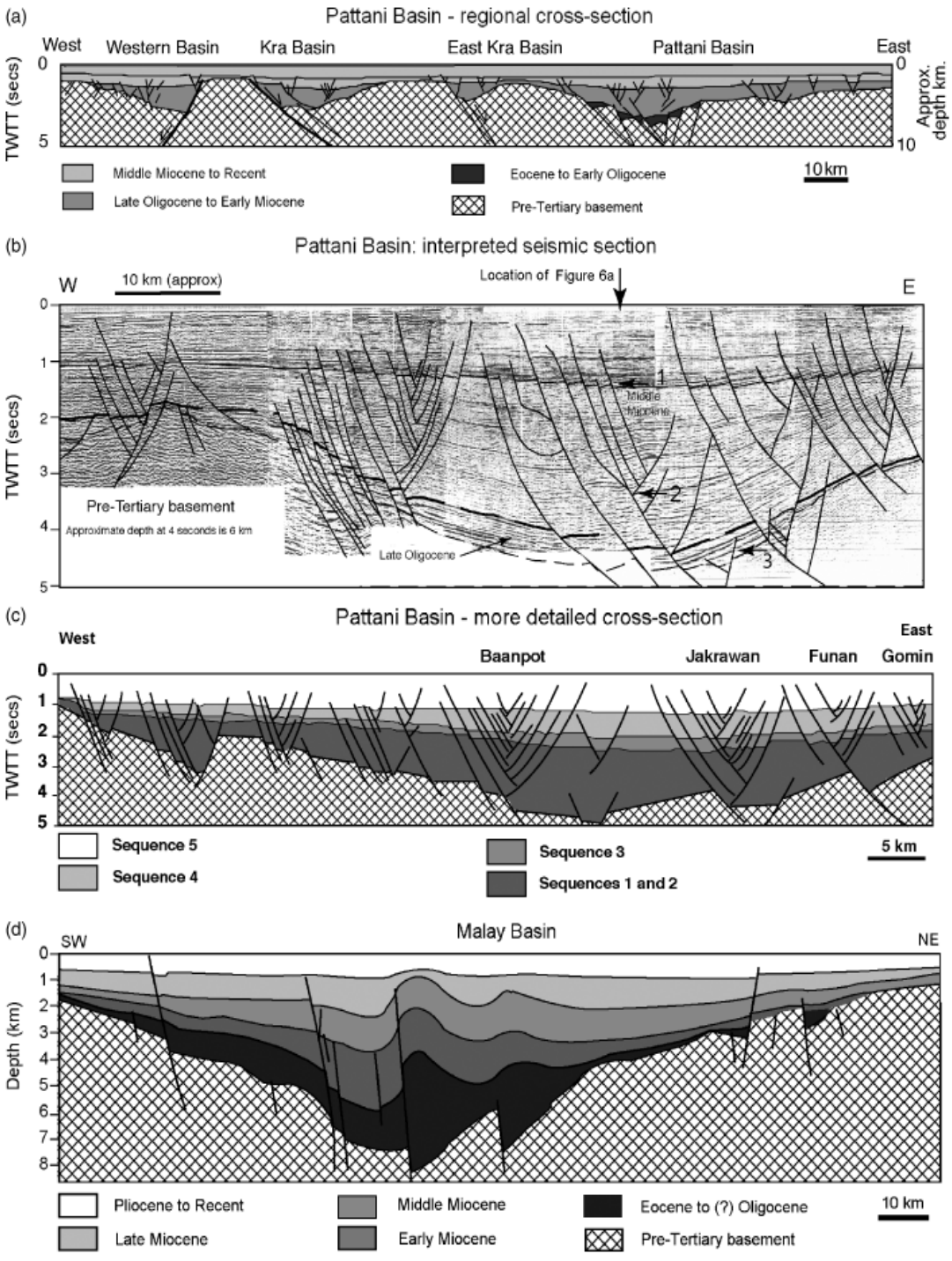

Figure 3.4 Cross section of Pattani basin and Malay basin.
(Morley & Westaway, 2006)

(Khositchaisri, 2005), (Chotpitayasunon, 2005)The strata of this basin can be divided into 4 formations that begin with oldest unit as shown in Figure 3.5. The formations are related with tectonic history.

The first formation is formation 0, there are gray to black shale and sandstone that deposited in syn-rift phase.

Formation 1 and Formation 2, that deposited in sag phase or post rift. Formation 1 is red bed unit consist of claystone, siltstone and sandstone.The gross thickness of sand is 20 meters.In this formation is fluvial-lacustrine deposits. Formation 2 can divided into 5 units as 2A, 2B, 2C, 2D and 2E. The depositional is delta plain to delta front from lower to upper sequence. It is the most thickness formation.

Formation 3, the depositional occur in regional subsidence phase. The result of offshore marine. There are shale interbedded with fine sandstone.

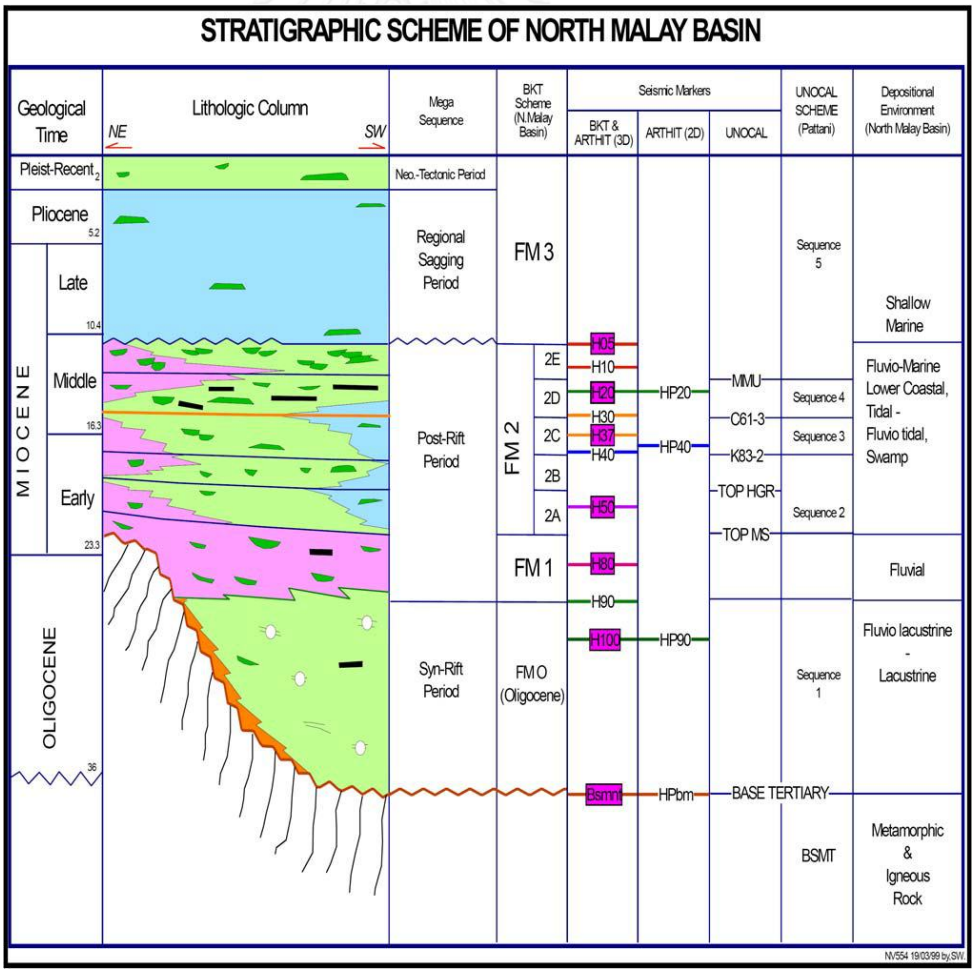

Figure 3.5 Stratigraphic column of North Malay Basin.
(Kongkanoi, 2008)

3.3 Simulation model

The simulation model of this work is created in 3D model. The model shows that CO_2 is injected and retained at in the targeted formation. Moreover, the storage capacity, plume migration and pressure buildup are shown in the results from the model.

3.3.1 Methodology

After starting up the GEM-CMG program. First of all, reservoir properties that consist of gird creation and properties of area are set. Grid creation is the procedure to define area for CO_2 injected. Cartesian grid for area is show in Figures 3.6 – 3.11. Grid block are defined 25 x 25 in I and J direction for every well but in K direction it depends on thickness in each layer. Block width, I direction is 250 m as same as in J direction. Due to the fact that the geology data is not enough and limited number of grid. So the appearance of the result is box 3D. The next step is to set the component that are reservoir temperature and component of fluid injected. The third step is to set the rock-fluid properties. The forth step is to specify the initial conditions. The last step is to set the wells and recurrent which is an important part which part is related to injection demand. Another important parameter is an injection rate. There are 4 injection rates: 1,000, 2,000, 3,000 and 4,000 t/d. The simulation program will shutin by maximum pressure that defined in wells and recurrent. After that validation with GEM and running normal immediately are performed. That is run simulation process. If the data is not correct it will warn error. Therefore, it must recheck the input data. But if the simulation can be run without error, the result will show in 3D model. Flow chart of methodology is presented in Figure 3.12. And the operation conditions are presented in Table 3.2.

Table 3.2 Operation condition.

.

Operation condition	
Grid block	25x25xk
Block width I direction	25x10
Block width J direction	25x10
Injection rate (t/d)	1,000-4,000

3.3.2 Well data

In this research, there are 3 wells consisting of Well 1, Well 2 and Well 3 in the North Malay Basin. CO_2 in supercritical state are injected into geological formation (depleted gas field) for all these 3 wells with the depth approximately 2,160 – 2,510 m. in supercritical state. The fundamental data in each well are show in Tables 3.3, 3.4 and 3.5, respectively. In this case, porosity and permeability are varied randomly in every layers ranging of 16 – 27 % for porosity and 69 – 450 md for permeability. The maximum pressure is calculated for each layer and used as criteria to terminate the simlation. It is calculated by Equation 2.7.

Table 3.3 Fundamental data of Well 1.

Parameter	1st Layer of sand	2nd Layer of sand
Depth (m)	2485.14-2508.4	2232.1-2255.8
Thickness (m)	23.26	23.7
Pressure at layer (MPa)	11.24	10.09
Maximum pressure (MPa)	32.52	29.21
Density of CO_2 (Kg/m^3)	232.47	209.29
Temperature (˚C)	96.58	89.5
Temperature of well (˚C)	74.5	
Porosity (%)	16 – 27	
Permeability (md)	69 – 450	
Pressure current of well (MPa)	9.63	

Table 3.4 Fundamental data of Well 2.

Parameter	1st Layer of sand	2nd Layer of sand	3rd Layer of sand
Depth (m)	2310.48 - 2326.9	2294.17 - 2307.35	2265.21-2276.24
Thickness (m)	16.42	13.18	11.03
Pressure at layer (MPa)	10.45	10.38	10.25
Maximum pressure (MPa)	30.24	30.02	29.65
Density of CO_2 (Kg/m^3)	217.53	215.9	212.89
Temperature (˚C)	91.7	91.24	90.43
Temperature of well (˚C)	67.78		
Porosity (%)	16 – 27 %		
Permeability (md)	69 – 450		
Pressure current of well (MPa)	10.76		

Table 3.5 Fundamental data of Well 3.

Parameter	1st Layer of sand	2nd Layer of sand	3rd Layer of sand	4th Layer of sand
Depth (m)	2331.42 - 2346.05	2245.77 - 2258.87	2181.76 - 2191.21	2162.27 - 2171.2
Thickness (m)	14.63	13.1	9.45	8.93
Pressure at layer (MPa)	10.55	10.16	9.87	9.78
Maximum pressure (MPa)	33.9	29.4	28.56	28.31
Density of CO_2 (Kg/m^3)	219.67	210.89	204.49	202.79
Temperature (˚C)	92.28	89.88	88.09	87.54
Temperature of well (˚C)	91.75			
Porosity (%)	16 – 27			
Permeability (md)	69 – 450			
Pressure current of well (MPa)	12.18			

For each layer there is its own permeability and porosity. Figures 3.6 – 3.11 presented grid block of 3 wells. There are different colors in each layer it depending on the value of porosity and permeability. Figures 3.6, 3.8 and 3.10 show a variation of permeability for Well 1, Well 2 and Well 3, respectively. Figures 3.7, 3.9 and 3.11 present the difference of porosity value in each well. Because the value of porosity and permeability are not totally difference and it is identified with color. Some of these values are in the same color; so some layers have the same color but in detail there are difference values.

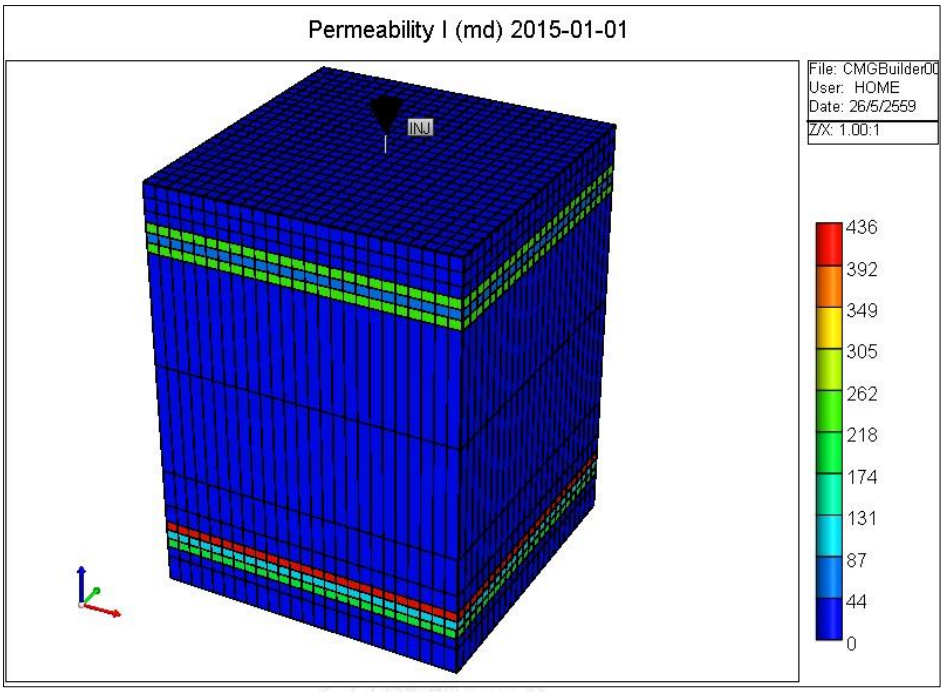

Figure 3.6 Grid block of Well 1 shows permeability.

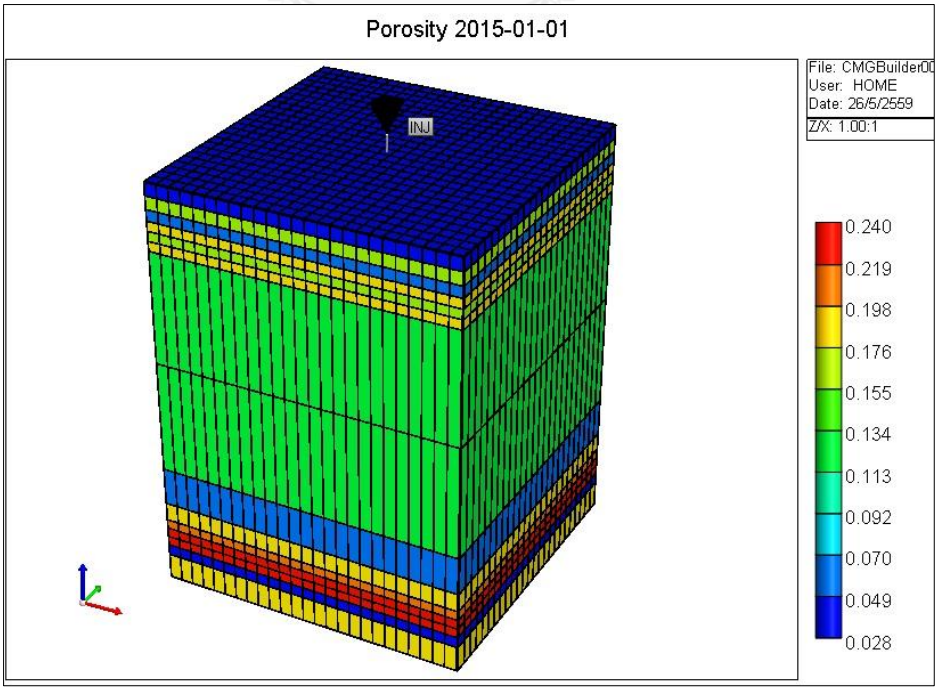

Figure 3.7 Grid block of Well 1 shows porosity.

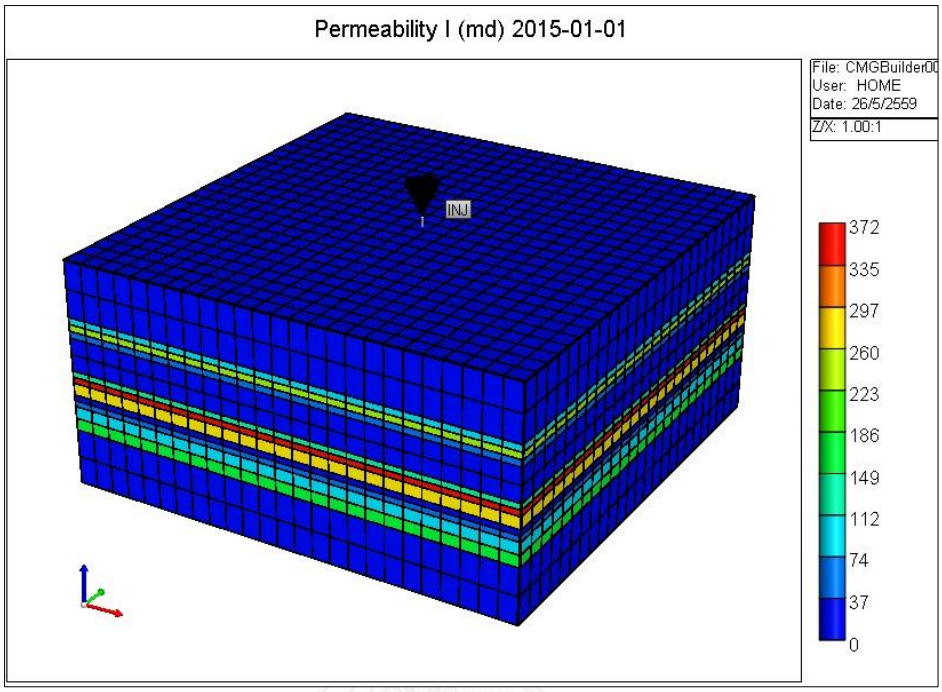

Figure 3.8 Grid block of Well 2 shows permeability.

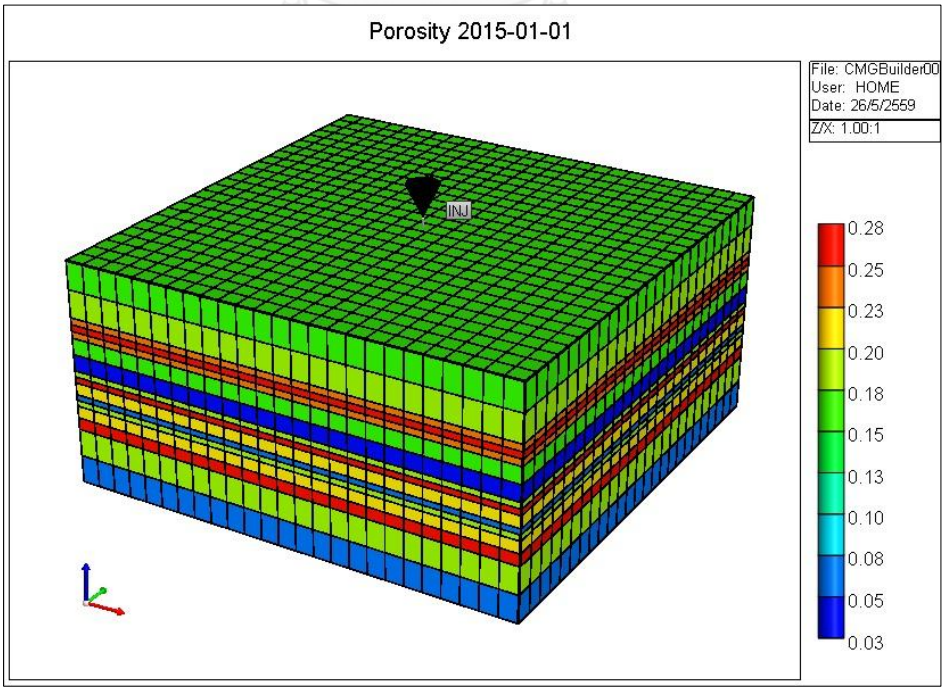

Figure 3.9 Grid block of Well 2 shows porosity.

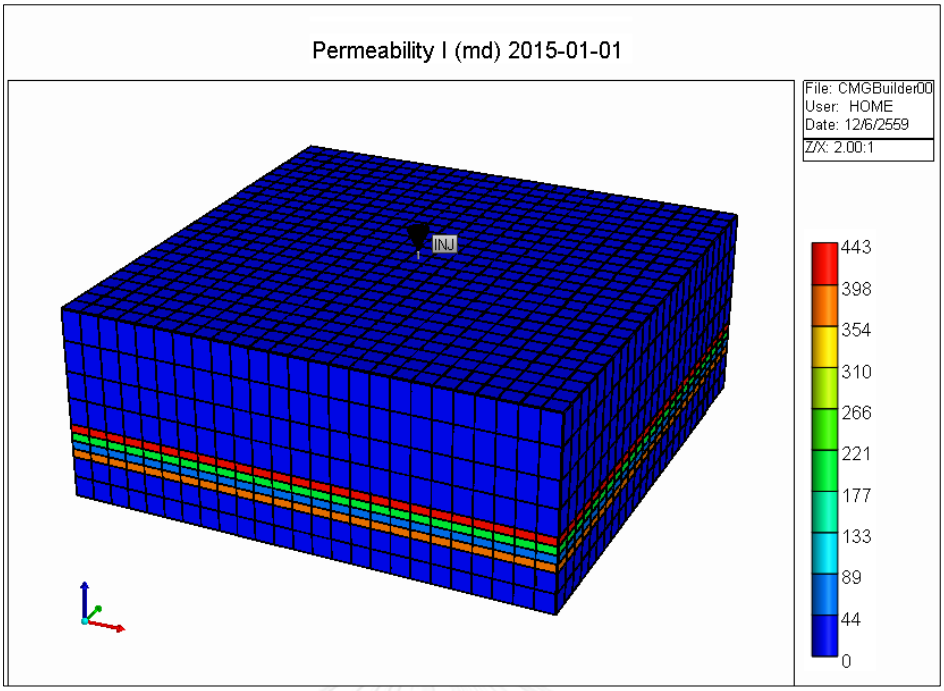

Figure 3.10 Grid block of Well 3 shows permeability.

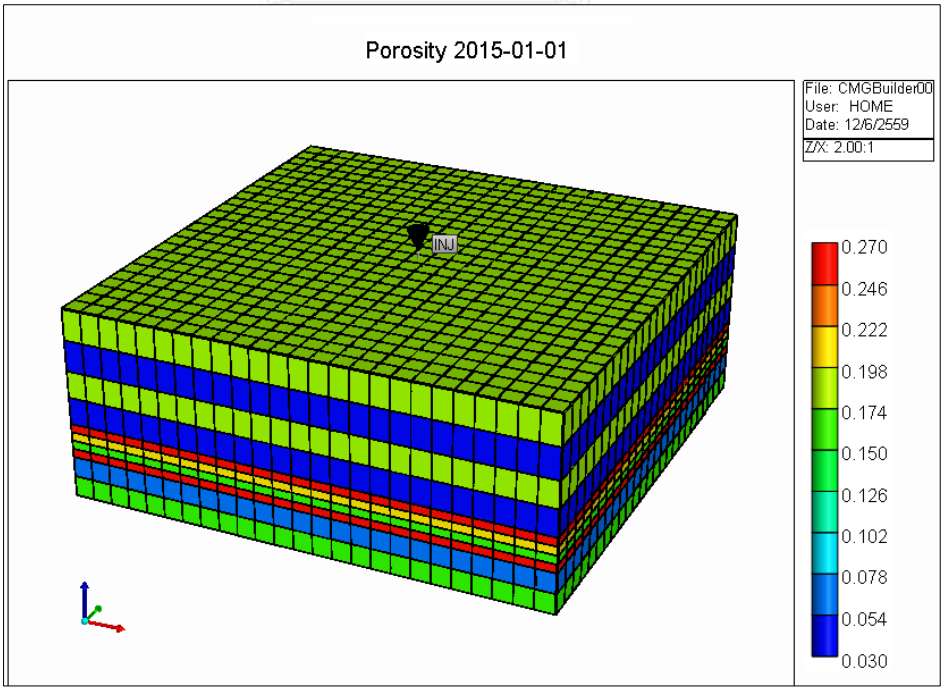

Figure 3.11 Grid block of Well 3 shows porosity.

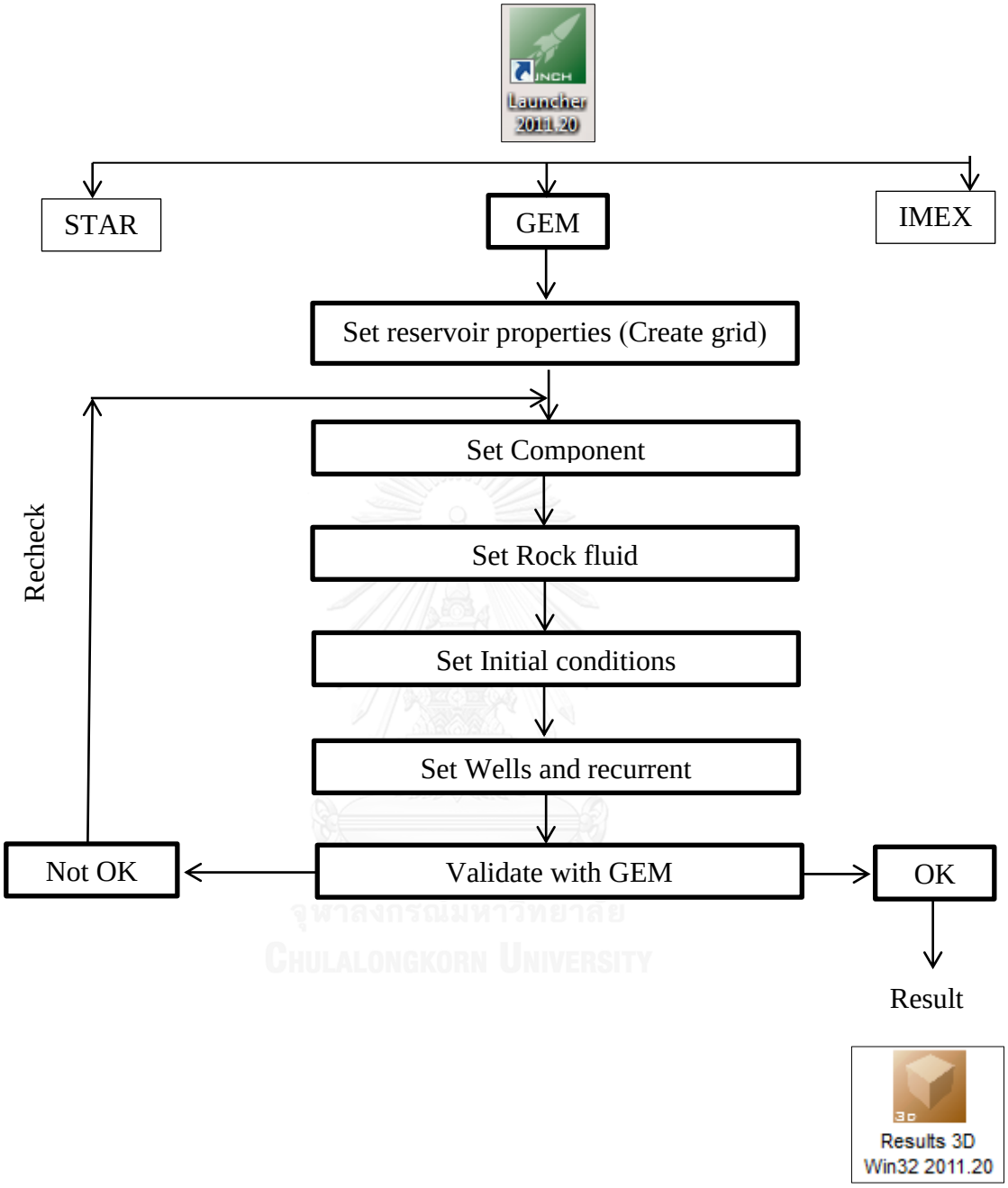

Figure 3.12 Flow chart of CMG program.

CHAPTER 4
RESULTS AND DISCUSSION

For this study, there are 3 wells for CO_2 injection into geological formation (depleted oil or gas field). The target depth is ranging from 2,160 – 2,510 m. In each well, CO_2 is injected into the sand layers with the injection rate of 1,000, 2,000, 3,000, and 4,000 t/d obtained from literate review and previous work. Period of time for study is retain 50 years with time step for monitoring is 1 month. The results from simulation are presented and discussed in this chapter for pressure buildup, plume migration and storage capacity which is controlled by shutin time.

4.1 Pressure buildup and shutin time

The injection rates of CO_2 are induced pressure to increase. However, maximum pressure should not exceed 90% of fracture pressure during injection CO_2 (Mathias et al., 2009) to prevent caprock breaking.

4.1.1 Well 1

For Well 1, there are 2 sand layers for injected CO_2. The 1st layer is bottom sand layer and 2nd layer is top sand layer. The fundamental data is shown in Table 3.3 and is brought to present here again. The simulation results of CO_2 injection in Well 1 are presented in Table 4.1 and Figures 4.1-4.4.

Table 3.3 Fundamental data of Well 1.

Parameter	1st Layer of sand	2nd Layer of sand
Depth (m)	2485.14-2508.4	2232.1-2255.8
Thickness (m)	23.26	23.7
Pressure at layer (MPa)	11.24	10.09
Maximum pressure (MPa)	32.52	29.21
Density of CO_2 (Kg/m^3)	232.47	209.29
Temperature (˚C)	96.58	89.5
Temperature of well (˚C)	74.5	
Porosity (%)	16 – 27	
Permeability (md)	69 – 450	
Pressure current of well (MPa)	9.63	

Table 4.1 Pressure buildup each injection rate in Well 1.

		Year	1000 t/d	2000 t/d	3000 t/d	4000 t/d	Max.Pressure
Well 1	2nd layer [MPa]	0	10.09	10.09	10.09	10.09	29.2
		1	17.18	21.57	24.60	27.71	29.2
		5	24.77	26.11	25.31	23.01	29.2
		10	28.49	25.43	24.95	22.81	29.2
		20	28.08	25.39	24.92	22.78	29.2
		50	28.03	25.35	24.88	22.76	29.2
	1st layer [MPa]	0	11.24	11.24	11.24	11.24	32.52
		1	18.34	25.39	24.36	26.98	32.52
		5	25.13	31.08	29.77	27.78	32.52
		10	32.11	30.41	29.55	27.71	32.52
		20	31.50	30.40	29.54	27.70	32.52
		50	31.48	30.38	29.53	27.68	32.52

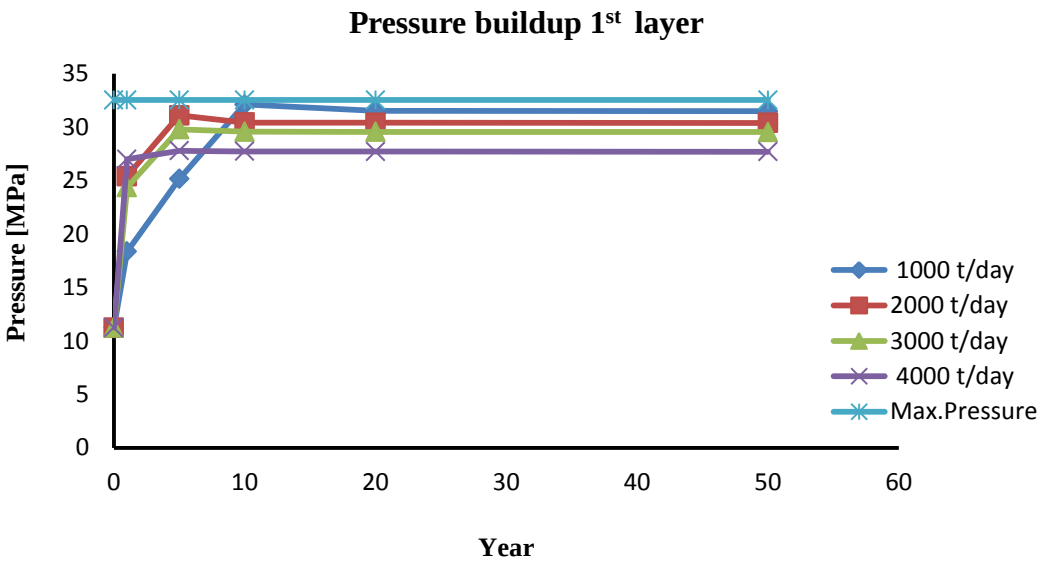

Figure 4.1 Graph of pressure buildup of 1st layer in Well 1.

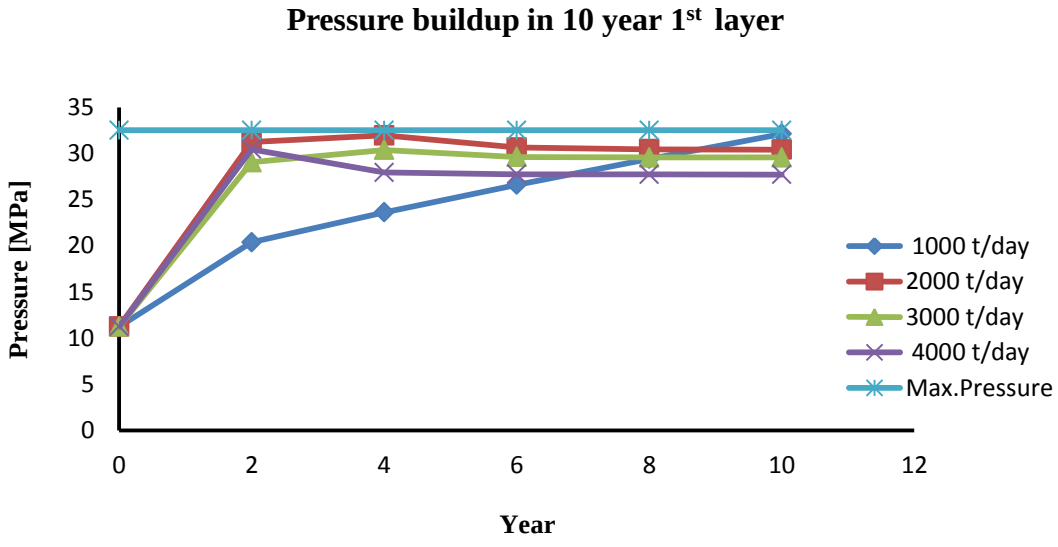

Figure 4.2 Graph of pressure buildup of 1st layer in Well 1 in 10 years.

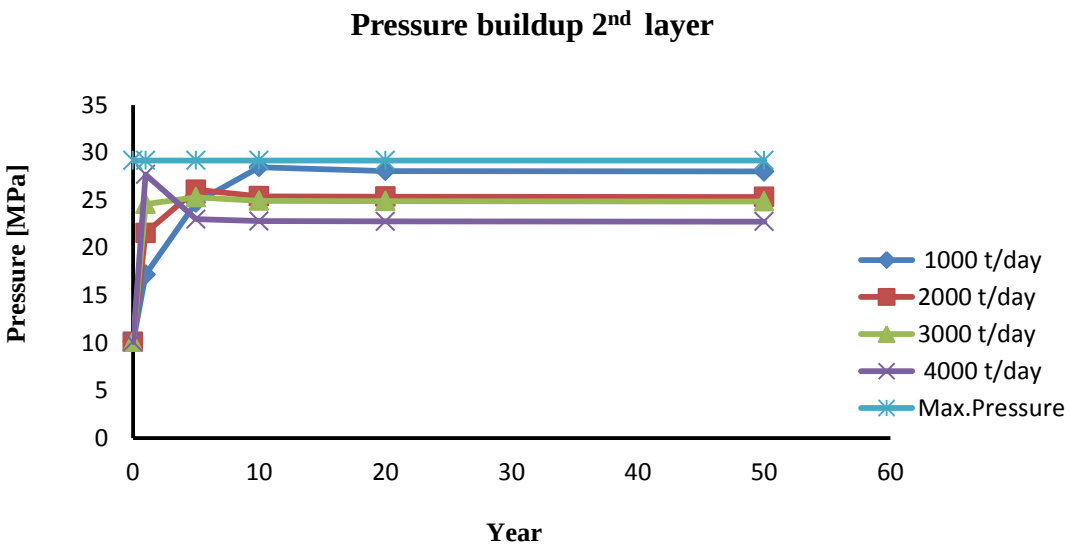

Figure 4.3 Graph of pressure buildup in 2nd layer in Well 1.

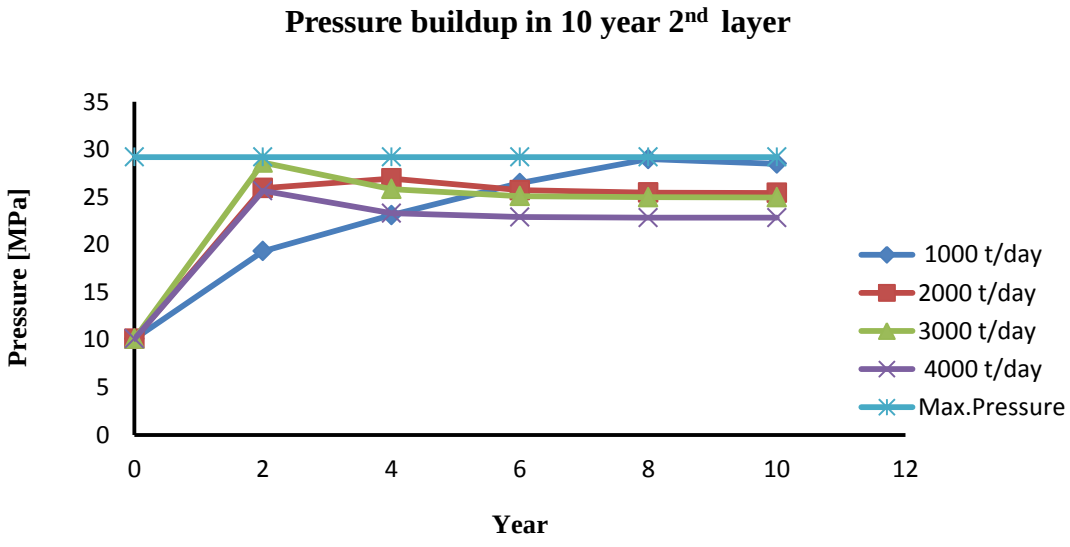

Figure 4.4 Graph of pressure buildup of 2nd layer in Well 1 in 10 years.

Figures 4.1- 4.4 show pressure buildup in Well 1 that consists of 2 layers of sand. Figures 4.1 and 4.3 show pressure buildup in 50 years in 1st and 2nd layer. Figures 4.2 and 4.4 show pressure buildup in 10 years in 1st and 2nd layer. The pressure in every injection rate is increasing but the pressure does not exceed the

fracture pressure. The result of 2 layers shown in Figure 4.1 is getting along well with Figure 4.3. CO_2 injection is beginning at to bottom of 1st layer until it full then start to inject to bottom of 2nd layer. The pressure at injection rate 1,000 t/d is increasing gradually. Meanwhile 2,000, 3,000 and 4,000 t/d are increasing sharply at the beginning. A pressure buildup in 1,000 t/d is increased highest and follows by 2,000, 3,000 and 4,000 t/d, respectively. The results show large amount of CO_2 injected will effect to pressure buildup. On the other hand, the lower amount of CO_2 injection is increasing gradually. Therefore, shutin time is effected by pressure buildup. When pressure increasing sharply, shutin time will be short because it prevents the pressure over maximum pressure as presented in Table 4.2. In 1st layer, injection rate at 1,000 t/d is shutin at 10.5 year with pressure of 32.095 MPa. Injection rate at 2,000 t/d is shutin at 4.5 years with pressure of 31.46 MPa. Injection rate at 3,000 t/d is shutin at 3 years with pressure of 31.12 MPa and injection rate at 4,000 t/d is shutin at 2 years with pressure of 30.44 MPa. Trend of pressure and shutin time in 2nd layer is get along with 1st layer. Shutin time for injection rate 1,000-4,000 t/d are 8, 3, 2 and 1.25 years with pressure at 28.97, 27.54, 28.61 and 27.21 MPa respectively.

The maximum pressure for 1st layer is 32.52 MPa and 29.2 MPa for 2nd layer. That is criteria to set shutin for stop injection. The pressures in each injection rate are increasing until shutin time as presented in Table 4.2.

Table 4.2 Shutin time in Well 1.

			1,000t/d	2,000t/d	3,000t/d	4,000t/d	Max. Pressure
Well 1	2nd layer	shutin time	28.97 MPa [8years]	27.54 MPa [3years]	28.61 MPa [2years]	27.21 MPa [1.25years]	29.20 MPa
	1st layer	shutin time	32.09 MPa [10.5years]	31.46 MPa [4.5years]	31.12 MPa [3years]	30.44 MPa [2years]	32.52 MPa

4.1.2 Well 2

For Well 2, there are 3 sand layers in this well consist of 1st layer is bottom sand, 2nd layer is middle sand and 3rd layer is top sand. The fundamental data has shown in Table 3.4 and is brought to present here again.

Table 3.4 Fundamental data of Well 2.

Parameter	1st Layer of sand	2nd Layer of sand	3rd Layer of sand
Depth (m)	2310.48 - 2326.9	2294.17 - 2307.35	2265.21-2276.24
Thickness (m)	16.42	13.18	11.03
Pressure at layer (MPa)	10.45	10.38	10.25
Maximum pressure (MPa)	30.24	30.02	29.65
Density of CO_2 (Kg/m^3)	217.53	215.9	212.89
Temperature (˚C)	91.7	91.24	90.43
Temperature of well (˚C)	67.78		
Porosity (%)	16 – 27 %		
Permeability (md)	69 – 450		
Pressure current of well (MPa)	10.76		

The simulation results of CO_2 injection in Well 2 are presented in Table 4.3 and Figures 4.5-4.10.

Table 4.3 Pressure buildup each injection rate in Well 2

		Year	1,000 t/d	2,000 t/d	3,000 t/d	4,000 t/d	Max. Pressure
Well 2	3rd layer [MPa]	0	10.25	10.25	10.25	10.25	29.64
		1	21.49	28.15	28.73	28.44	29.64
		5	29.35	29.04	28.74	28.44	29.64
		10	29.35	29.04	28.73	28.43	29.64
		20	29.33	29.02	28.71	28.41	29.64
		50	29.27	28.96	28.65	28.35	29.64
	2nd layer [MPa]	0	10.38	10.38	10.38	10.38	30.02
		1	25.969	29.77	29.3	29.3	30.02
		5	29.82	29.74	29.27	29.27	30.02
		10	29.82	29.73	29.26	29.26	30.02
		20	29.81	29.72	29.24	29.25	30.02
		50	29.7	29.62	29.14	29.14	30.02
	1st layer [MPa]	0	10.45	10.45	10.45	10.45	30.23
		1	22.52	26.12	26.1	22.51	30.23
		5	29.64	26.13	26.11	22.52	30.23
		10	29.64	26.13	26.11	22.52	30.23
		20	29.64	26.13	26.11	22.52	30.23
		50	29.64	26.13	26.11	22.52	30.23

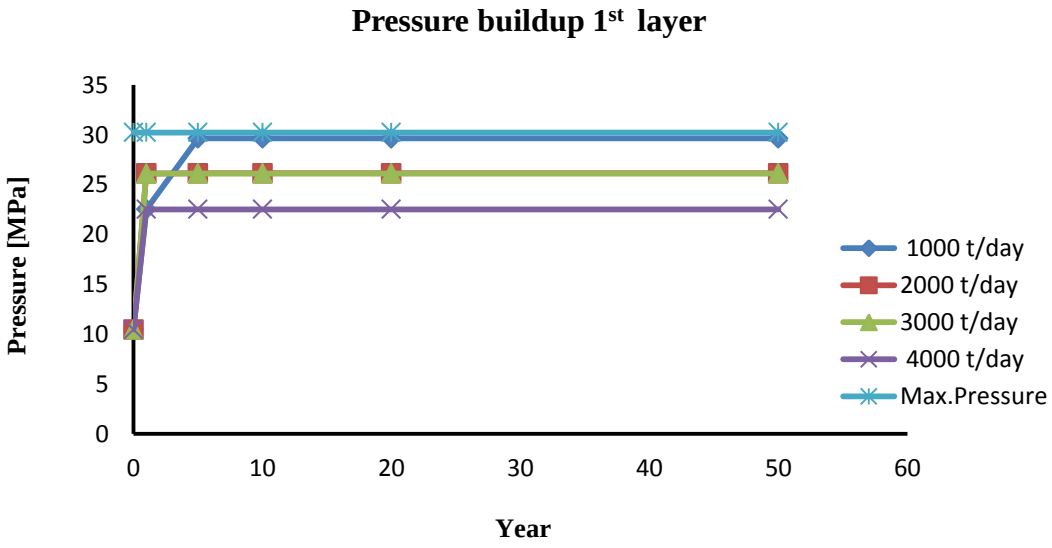

Figure 4.5 Graph of pressure buildup of 1st layer in Well 2.

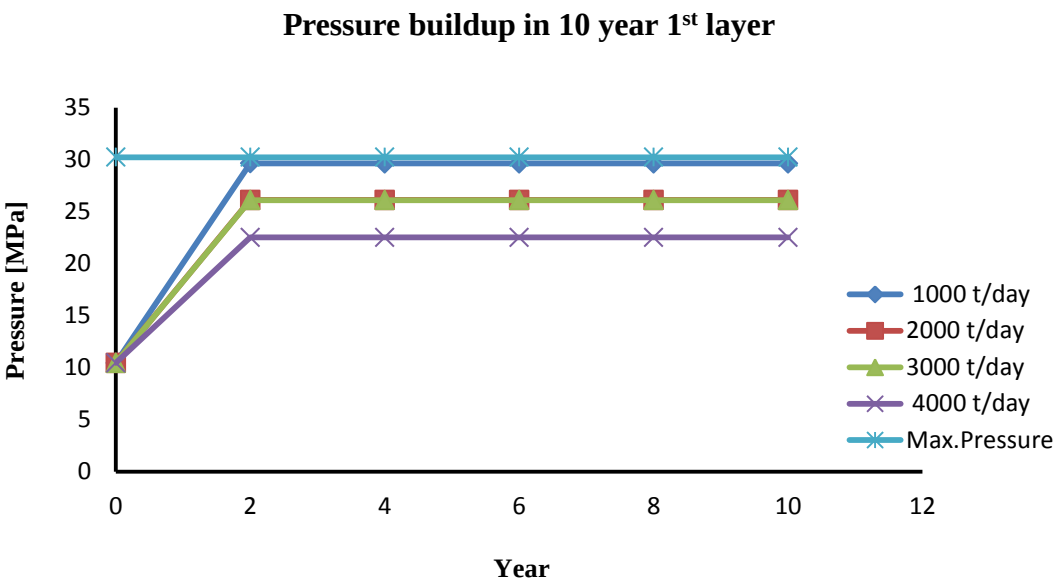

Figure 4.6 Graph of pressure buildup of 1st layer in Well 2 in 10 years.

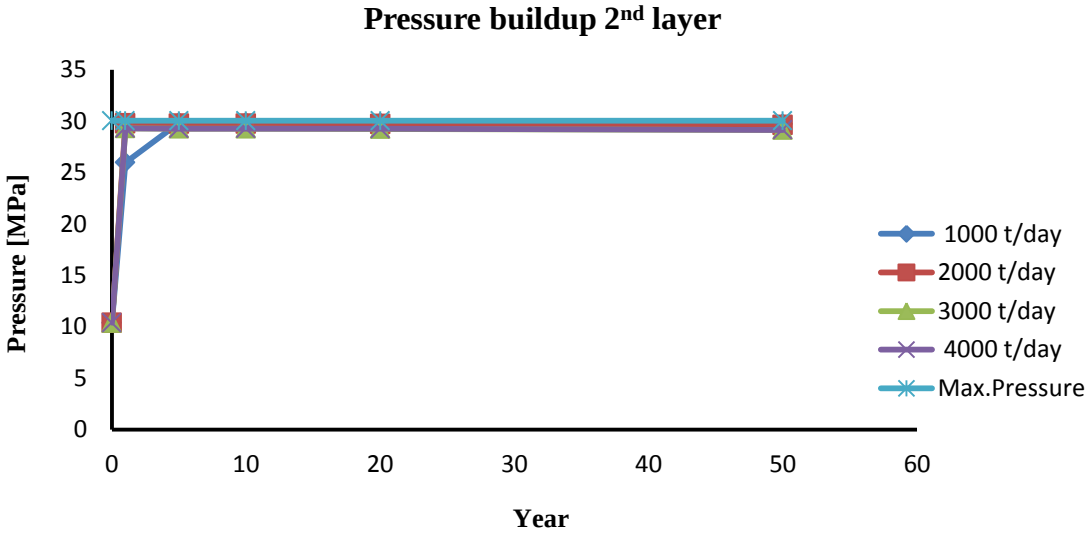

Figure 4.7 Graph of pressure buildup of 2nd layer in Well 2.

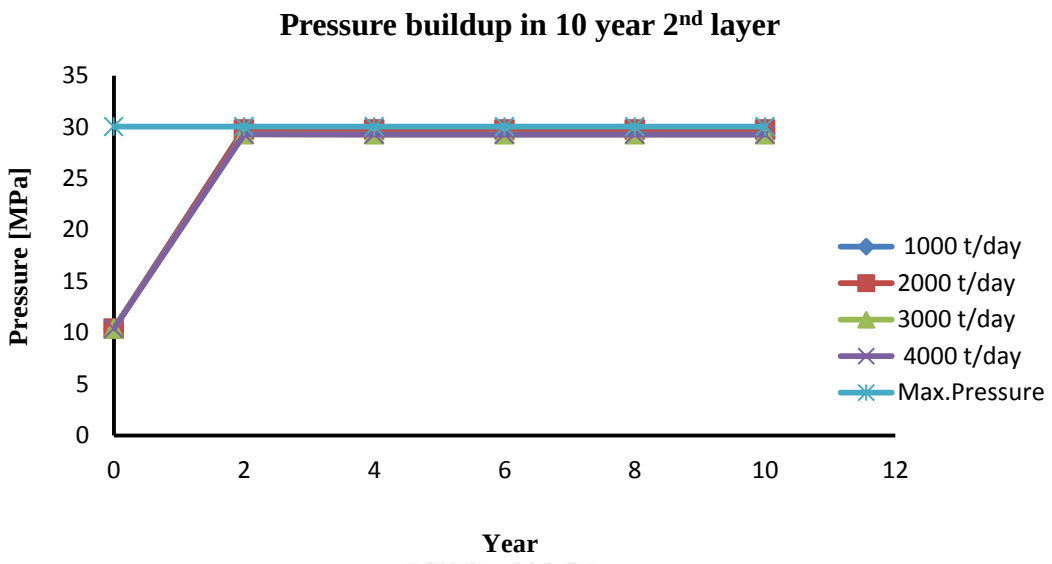

Figure 4.8 Graph of pressure buildup of 2nd layer in Well 2 in 10 years.

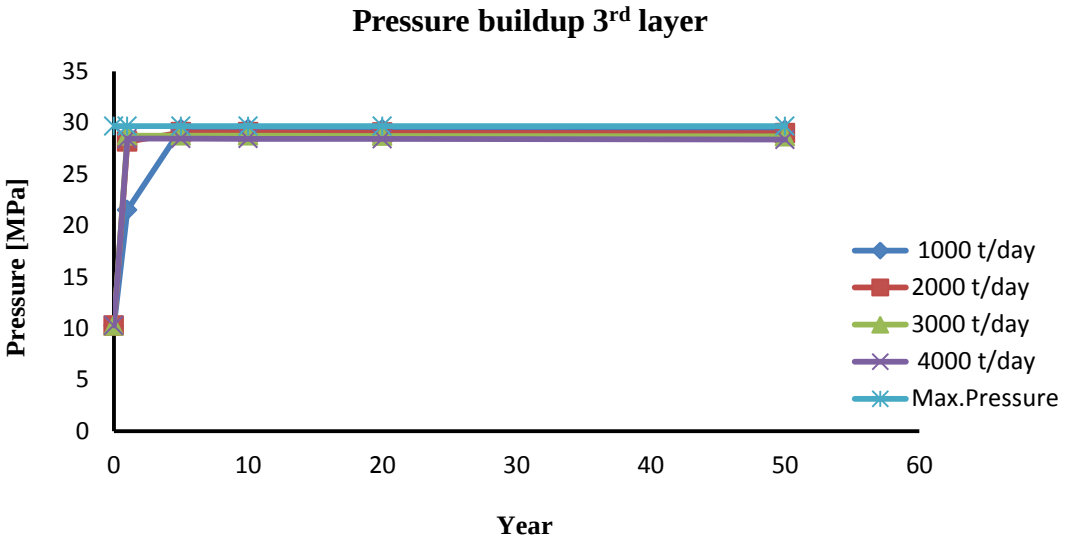

Figure 4.9 Graph of pressure buildup of 3rd layer in Well 2

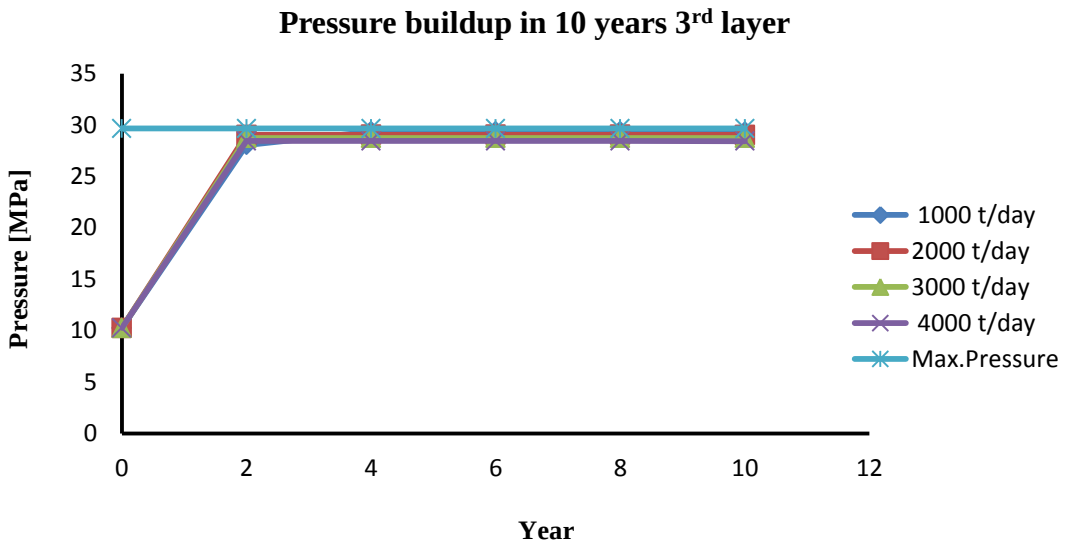

Figure 4.10 Graph of pressure buildup of 3rd layer in Well 2 in 10 years.

Table 4.3 show pressure buildup in each injection rate in Well 2. The maximum pressure in 1st layer is 30.23 MPa, 2nd layer is 30.02 MPa and 3rd layer is 29.64 MPa. That is used to set shutin time as shown in Table 4.4. Figures 4.5, 4.7 and 4.9 show pressure buildup by for 50 years. Figures 4.6, 4.8 and 4.10 show pressure buildup in 10 years. Generally, 1,000 t/d are increasing gradually while 2,000, 3,000 and 4,000 t/d are increasing aggressively. At the beginning, CO_2 injected into bottom of 1st layer. After shutin time start to inject into 2nd layer and 3rd layer at the last. The 1st layer thickness is 16.42 m in the bottom of well. Pressure buildup in injection rate 1,000 t/d is higher than other until shutin time is on 2.25 years with pressure is 29.63 MPa. The Injection rate 2,000 t/d is shutin at 1 year with pressure is 26.12 MPa. The injection rate 3,000 t/d and 4,000 t/d are shutin at 0.75 and 0.5 years with pressure 26.09 and 22.39 MPa respectively. After shutin, pressure will be decreasing gradually by the time.

The 2nd layer is 13.18 m thickness. It is middle sand layer. The injection rate 1,000 t/d is shutin at 1.4 years with 29.86 MPa of pressure. Injection rate 2,000 t/d is shutin at 0.7 years with 29.8 MPa. Injection rate 3,000 t/d is shutin at 0.5 years with 29.35 MPa of pressure and injection rate 4,000 t/d is shutin at 0.4 years with 29.35 MPa. A trend of pressure buildup graph in 2nd layer is as same as 1st layer. The last layer is top layer or 3rd layer. Thickness of layer is 11.03 m. Shutin time 2.27 years

with 29.43 MPa pressure at 1,000 t/d injection rate. Shutin time 1.12 years with 29.24 MPa pressure at 2,000 t/d injection rate. Shutin time 0.75 years with 29.05 MPa pressure at 3,000 t/d injection rate and shutin time 0.55 years with 28.88 MPa pressure at 4,000 t/d injection rate

From the results, it shows that pressure buildup at shutin time are not comparatively difference but shutin time is so different. Because the amount of injection is effected from pressure buildup in well as shown in Figures 4.5-4.10. The large amount of CO_2 injected influences to produce pressure buildup increasing sharply with shorter shutin time

Table 4.4 Shutin time in Well 2.

			1,000t/d	2,000t/d	3,000t/d	4,000t/d	Max. Pressure
Well 2	3rd layer	shutin time	29.43 MPa [2.27years]	29.24 MPa [1.12years]	29.05MPa [0.75years]	28.88 MPa [0.55years]	29.64 MPa
	2nd layer	shutin time	29.86MPa [1.4years]	29.8MPa [0.7years]	29.35MPa [0.5years]	29.35MPa [0.4years]	30.02 MPa
	1st layer	shutin time	29.63 MPa [2.25years]	26.12 MPa [1 years]	26.09MPa [0.75years]	22.39 MPa [0.5years]	30.23 MPa

4.1.3 Well 3

For Well 3, there are 4 sand layers in this well consisting of 1st layer, as a bottom sand, 2nd layer, 3rd layer and the last 4th layer as a top layer. The fundamental data has shown in Table 3.5 and is brought to present here again. The simulation results of CO_2 injection in Well 3 are presented in Table 4.5 and Figure 4.11 to Figure 4.18.

Table 3.5 Fundamental data of Well 3.

Parameter	1st Layer of sand	2nd Layer of sand	3rd Layer of sand	4th Layer of sand
Depth (m)	2331.42 - 2346.05	2245.77 - 2258.87	2181.76 - 2191.21	2162.27 - 2171.2
Thickness (m)	14.63	13.1	9.45	8.93
Pressure at layer (MPa)	10.55	10.16	9.87	9.78
Maximum pressure (MPa)	33.9	29.4	28.56	28.31
Density of CO_2 (Kg/m^3)	219.67	210.89	204.49	202.79
Temperature (˚C)	92.28	89.88	88.09	87.54
Temperature of well (˚C)	91.75			
Porosity (%)	16 – 27			
Permeability (md)	69 – 450			
Pressure current of well (MPa)	12.18			

Table 4.5 Pressure buildup each injection rate in Well 3.

		Year	1,000 t/d	2,000 t/d	3,000 t/d	4,000 t/d	Max. Pressure
Well 3	4^{th} layer [MPa]	0	9.78	9.78	9.78	9.78	28.30
		1	24.70	27.96	27.38	26.70	28.30
		5	28.17	27.92	27.35	26.66	28.30
		10	28.10	27.85	27.3	26.61	28.30
		20	28.00	27.74	27.23	26.53	28.30
		50	27.90	27.65	27.13	26.44	28.30
	3^{rd} layer [MPa]	0	9.87	9.87	9.87	9.87	28.56
		1	24.26	28.33	27.84	27.36	28.56
		5	28.39	28.27	27.78	27.31	28.56
		10	28.34	28.23	27.74	27.26	28.56
		20	28.31	28.2	27.71	27.24	28.56
		50	28.29	28.17	27.69	27.21	28.56
	2^{nd} layer [MPa]	0	10.16	10.16	10.16	10.16	29.39
		1	17.59	21.37	24.27	27.04	29.39
		5	28.84	29.05	27.98	26.66	29.39
		10	28.81	29.05	27.97	26.65	29.39
		20	28.8	29.04	27.96	26.64	29.39
		50	28.78	29.02	27.94	26.62	29.39
	1^{st} layer [MPa]	0	10.54	10.54	10.54	10.54	33.91
		1	19.68	24.16	28.25	32.11	33.91
		5	33.29	33.27	33.26	31.73	33.91
		10	33.27	33.22	33.21	31.68	33.91
		20	33.18	33.13	33.11	31.59	33.91
		50	33.06	33.00	32.98	31.45	33.91

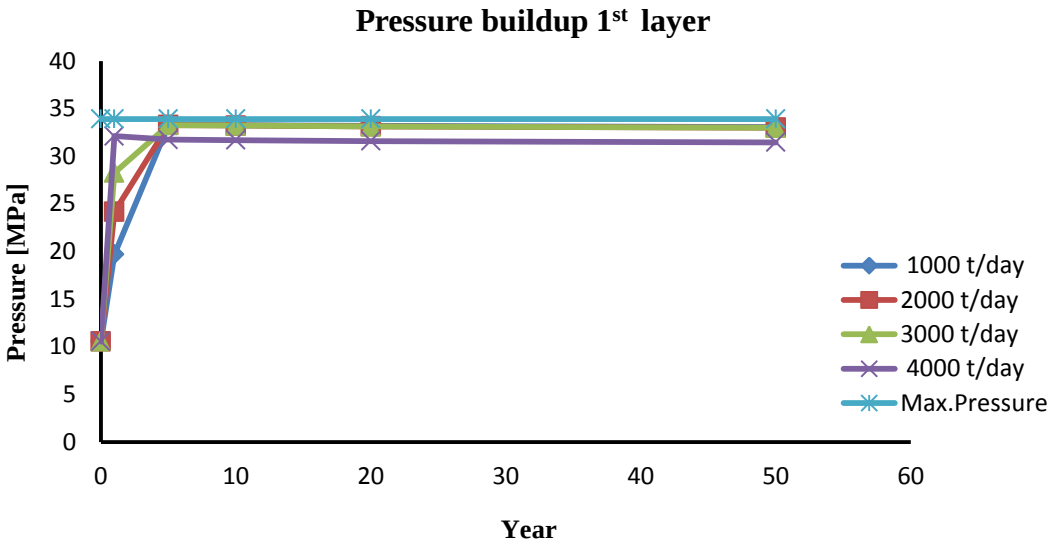

Figure 4.11 Graph of pressure buildup of 1st layer in Well 3.

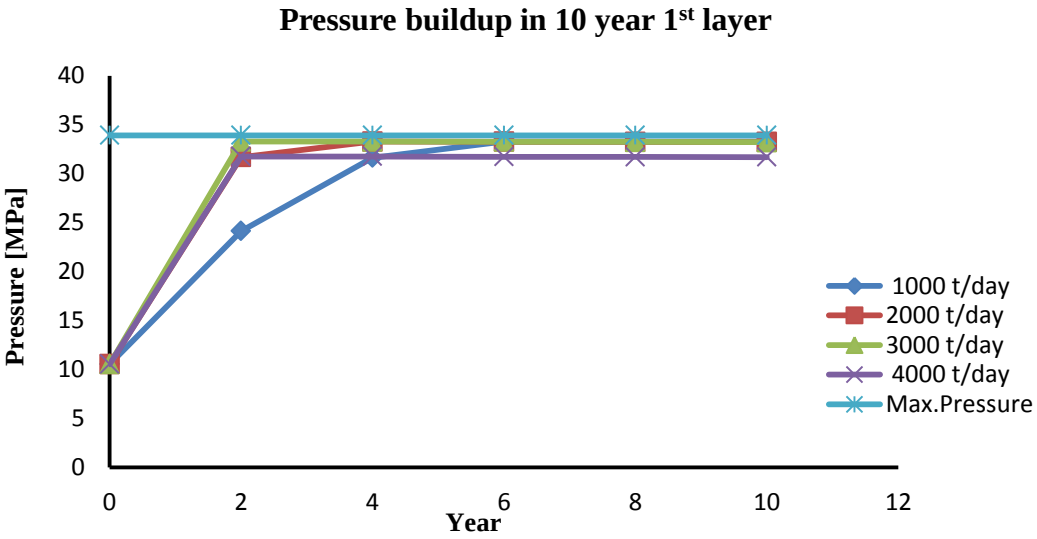

Figure 4.12 Graph of pressure buildup of 1st layer in Well 3 in 10 years.

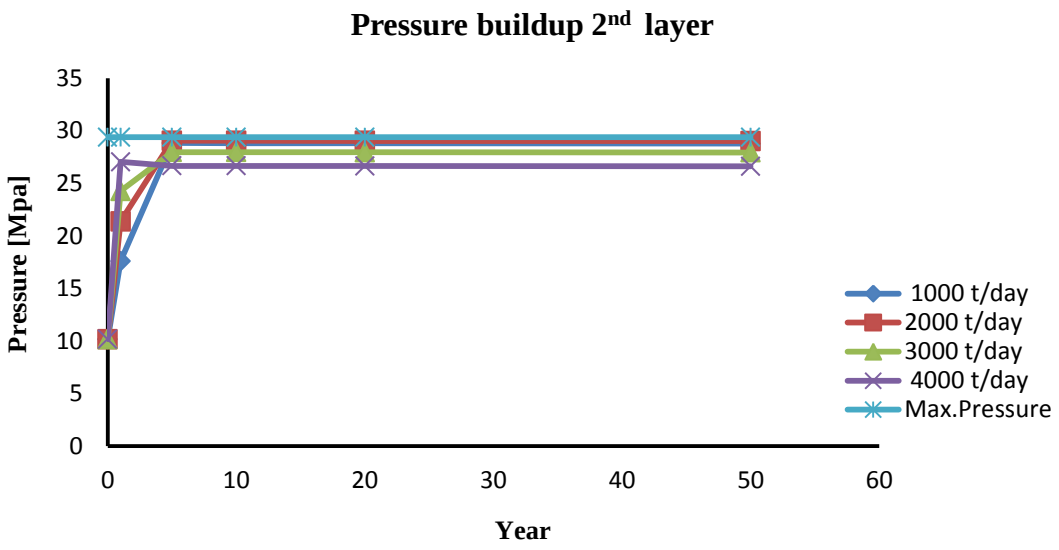

Figure 4.13 Graph of pressure buildup of 2nd layer in Well 3.

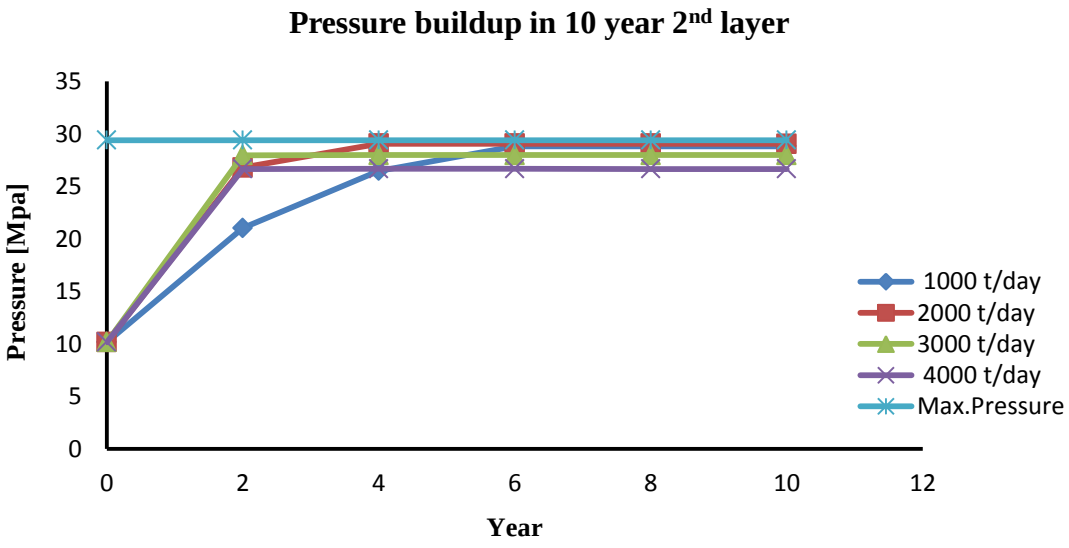

Figure 4.14 Graph of pressure buildup of 2nd layer in Well 3 in 10 years.

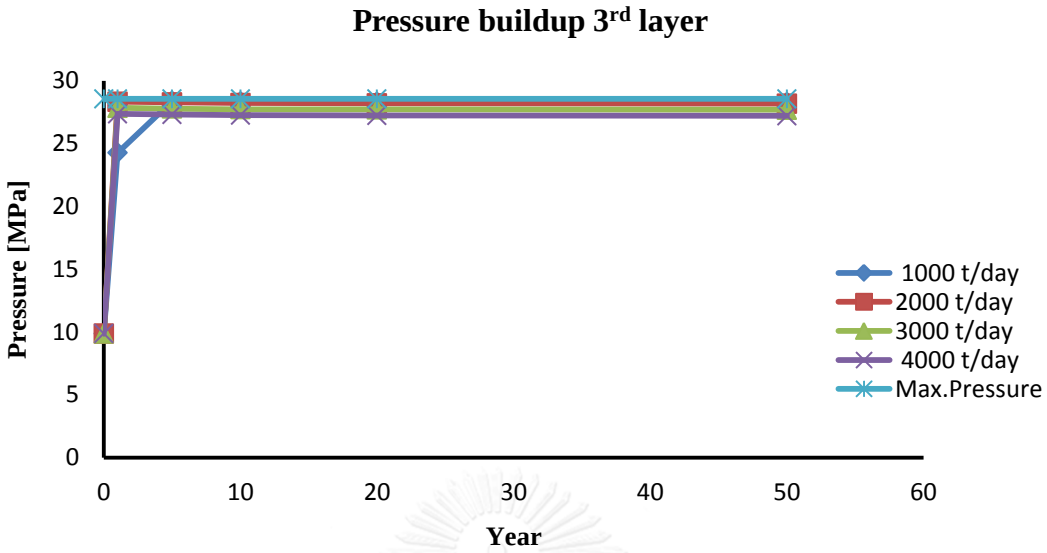

Figure 4.15 Graph of pressure buildup of 3rd layer in Well 3

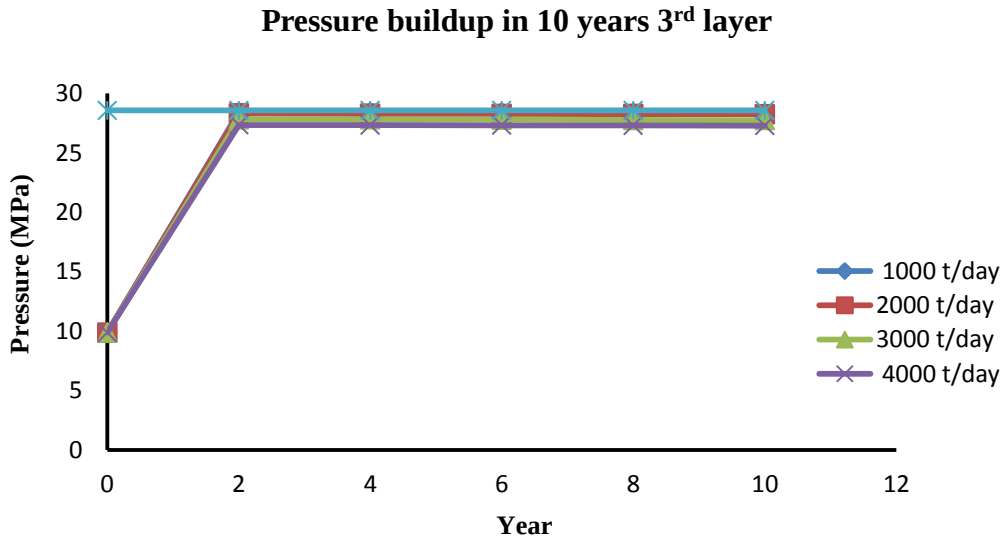

Figure 4.16 Graph of pressure buildup of 3rd layer in Well 3 in 10 years.

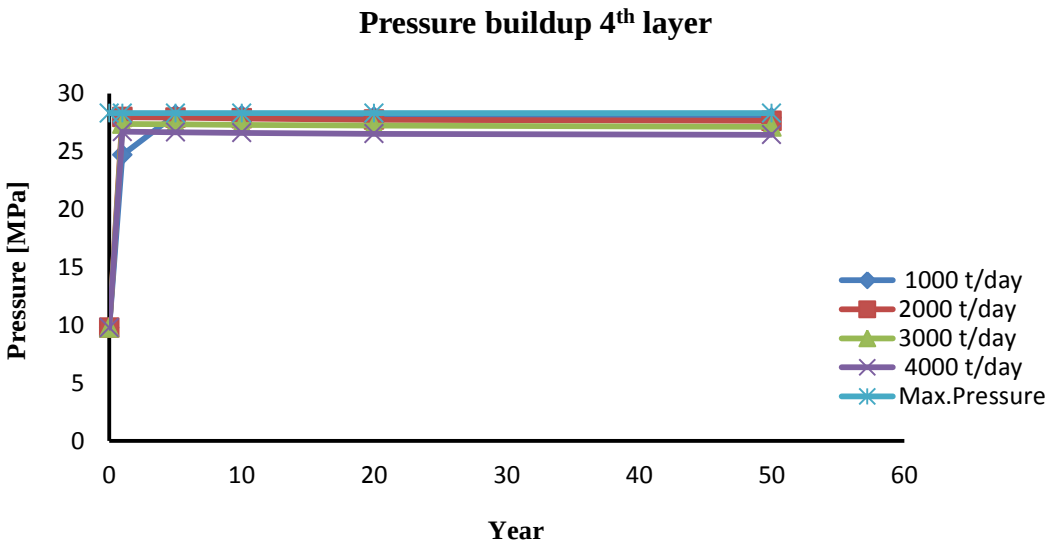

Figure 4.17 Graph of pressure buildup of 4th layer in Well 3.

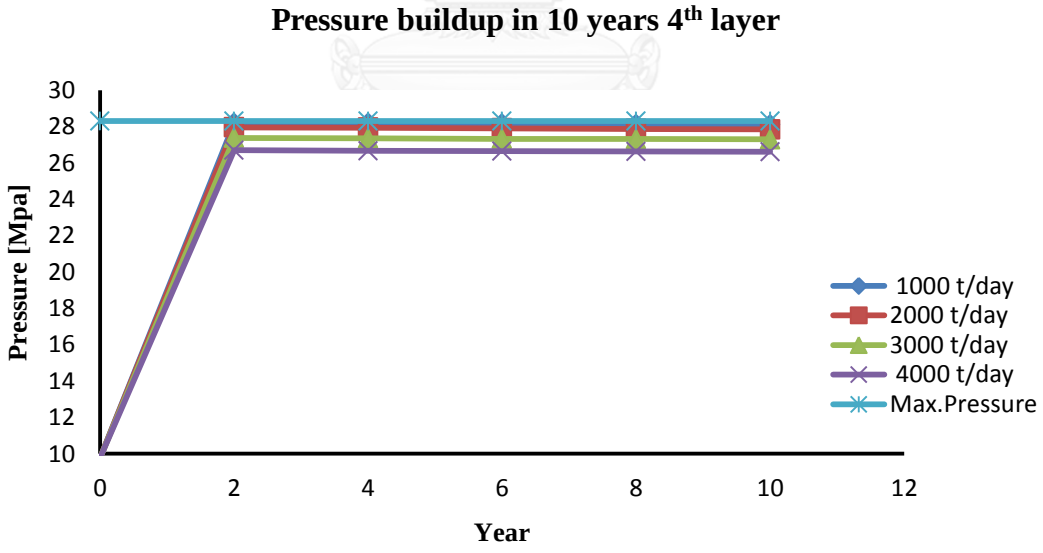

Figure 4.18 Graph of pressure buildup of 4th layer in Well 3 in 10 years.

The pressure buildups of Well 3 are shown in Table 4.5. The maximum pressure for set shutin are 33.91 MPa for 1st layer, 29.39 MPa for 2nd layer, 28.56 MPa for 3rd layer and 28.3 MPa for 4th layer. Figure 4.11 shows pressure buildup in the bottom sand. Trend of graph is the same as Well 1 and Well 2. Figures 4.12-4.18 show the graph of pressure buildup in 2nd layer, 3rd layer and 4th layer, respectively. Table 4.6 presents shutin time related with pressure buildup. Starting injection at bottom of 1st layer until shutin and then injection at 2nd layer, 3rd layer and the last one, 4th layer.

From the results it is shown that in 1st layer has 14.63 m thickness with the injection rate of 1,000 t/d shutin time at 4.75 years with pressure of 33.29 MPa, injection rate 2,000 t/d shutin at 2.5 years with pressure of 33.27 years, injection rate 3,000 t/d is shutin at 1.75 years with pressure of 33.27 MPa and injection rate 4,000 t/d is shutin at 1.25 years with pressure of 31.71 MPa. Trends of pressure buildup in other layers are different.

The sequence of maximum pressure buildup in 2nd layer ranging from high to low is 2,000, 1,000, 3,000 and 4,000 t/d. Injection rate 2,000 t/d has to shutin 2.75 years with pressure at 29.07 MPa. Injection rate 1,000 t/d is shutin at 5.25 years with pressure 28.81 MPa, Injection rate 3,000 t/d has to shutin at 0.5 years with pressure 27.96 MPa and injection rate 4,000 t/d has to shutin at 1.25 years with pressure is 26.69 MPa. Thickness of 2nd layer is 13.1 m.

The 3rd layer has thickness of 9.45 m. Injection rate 1,000 t/d shutins at 1.5 years with pressure of 28.41 MPa. Injection rate 2,000 t/d shutins at 0.77 years with pressure at 28.35 MPa. Injection rate 3,000 t/d shutins at 0.49 years with pressure of 27.69 MPa and injection rate 4,000 t/d shutins at 0.36 years with pressure of 27.64 MPa. The last layer is 4th layer. Thickness is 8.93 m. Injection rate 1,000 t/d shutins at 1.4 years with 28.19 MPa, Injection rate 2,000 t/d shutins at 0.71 years with 27.95 MPa. Injection rate 3,000 t/d shutins at 0.44 years with 27.44 MPa and injection rate 4,000 t/d shutins at 0.33 years with 26.89 MPa.

The 3rd layer and 4th layer are thin sand layers. Therefore, it effects on pressure increasing sharply at early shutin time.

Table 4.6 Shutin time in Well 3.

			1,000 t/d	2,000 t/d	3,000 t/d	4,000 t/d	Max .Pressure
Well 3	4th layer	shutin time	28.19 MPa [1.4years]	27.95 MPa [0.71years]	27.44 MPa [0.44years]	26.89 MPa [0.33years]	28.30 MPa
	3rd layer	shutin time	28.41 MPa [1.5years]	28.35 MPa [0.77years]	27.96 MPa [0.49years]	27.64 MPa [0.36years]	28.56 MPa
	2nd layer	shutin time	28.81 MPa [5.25years]	29.07 MPa [2.75years]	27.96 MPa [1.75years]	26.69 MPa [1.25years]	29.39 MPa
	1st layer	shutin time	33.29 MPa [4.75years]	33.27 MPa [2.5years]	33.27 MPa [1.75years]	31.73 MPa [1.25years]	33.91 MPa

The pressure is increasing rapidly in closed system than open system. The overall system when pressure increases, will decrease (Mackay, 2013). Almost trends line in every wells for injection rates at 1,000 t/d are gradually increasing. At the same time 2,000, 3,000 and 4,000 t/d injection rate are increasing sharply. In first 10 years, there is a variation in pressure buildup. Pressure reaches to the maximum pressure. After shutin time the pressure decreasing gradually by time. Mackay.E.J,(2013) has studied CO_2 injection leading to changes in pressure and saturation. During injection, pore pressure has changed. The pressure changes immediately since CO_2 is injected.

4.2 Storage capacity

The storage capacity from simulation is calculated with cumulative injection (Gorecki et al., 2009).The result of storage capacity is shown in the section.

4.2.1 Well 1

The result of Well 1 is shown in Table.4.7 and Figures 4.19-4.20. For each injection rate, capacity of CO_2 increases in every year until shutin. Table 4.7 presents storage capacity in each layer for each injection rate. In 1st layer, the storage capacities of injection rate from 1,000-4,000 t/d are consist of 3.74, 2.33, 3.01 and 2.56 Mt and in 2nd layer storage capacities of injection rate from 1,000-4,000 t/d are 2.83, 2.1, 1.9 and 1.46 Mt, respectively. Storage capacity is related to pressure buildup and shutin time. From Figures 4.19-4.20, both layers in period of 1 year, there are a lot of capacity variation because this time is before shutin time. The capacity still increases until shutin time. After that storage capacity is constant. From Figure 4.19 show that the storage capacity of injection rate 2,000, 3,000 and 4,000 t/d are constant in 5 years because there are shutin at 4.5 years, 3 years and 2 years. But injection rate 1,000 t/d is still inject and shutin at 10.5 years. That why capacity at injection rate 1,000 t/d still is increasing as well as 2nd layer that present in Figure 4.20. Injection rate 1,000 t/d is shutin at 8 years therefore storage capacity is still increasing while injection rate 2,000, 3000 and 4,000 t/d is shutin at 3 years, 2 years and 1.25 years, respectively. So the storage capacity are constant in period 5 years.

Total storage capacity in Well 1 for 1,000 t/d injection rate is 6.57 Mt, 4.43 Mt at 2,000 t/d injection rate, 3,000 t/d injection rate is 4.91 Mt and 4,000 t/d injection rate is 4.02 Mt. In 4 injection rate, 1,000 t/d is contained highest storage capacity. By the time others 3 injection rates, storage capacity are not totally difference. Therefore injection rate 4,000 t/d is suitable for use. Because it is shutin in immediately with high storage capacity.

Table 4.7 Storage capacity in Well 1.

		Storage capacity (Mt)			
		1,000 t/d	2,000 t/d	3,000 t/d	4,000 t/d
Well 1	2nd layer	2.83	2.1	1.9	1.46
	1st layer	3.74	2.33	3.01	2.56
	Total	6.57	4.43	4.91	4.02

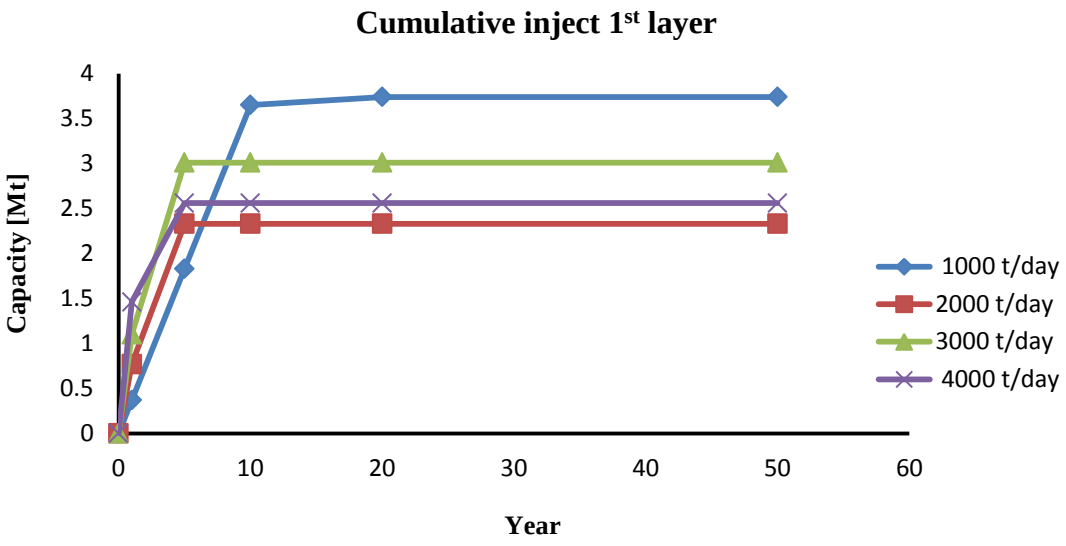

Figure 4.19 Storage capacity in 1st layer in Well 1.

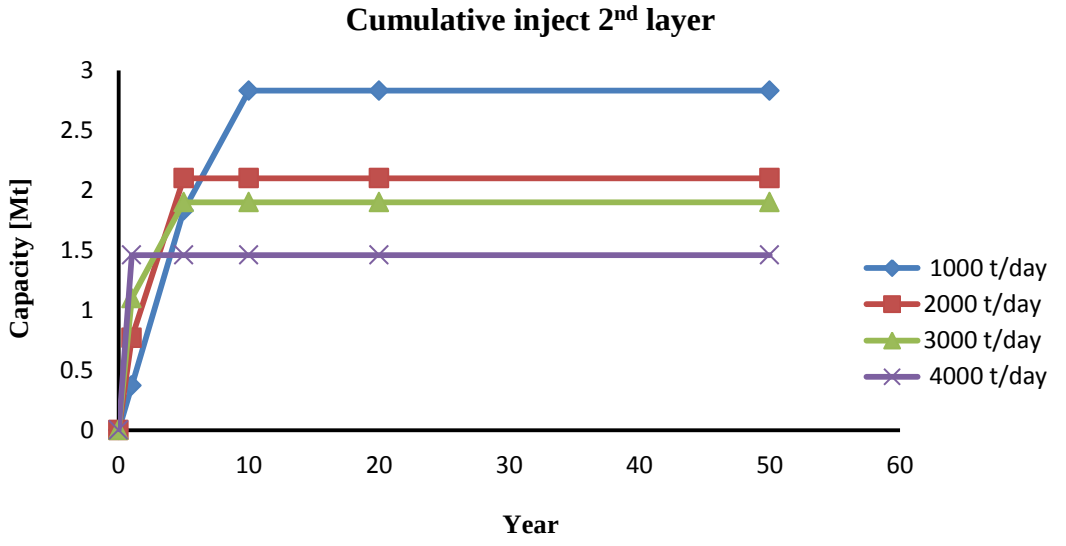

Figure 4.20 Storage capacity in 2nd layer in Well 1.

4.2.2 Well 2

From Figures 4.21-4.23 presented storage capacity in 3 layer that consist of 1st layer, 2nd layer and 3rd layer. The storage capacity is shown in Table.4.8. The storage capacity in 1st layer is 0.73, 0.55, 0.54 and 0.36 Mt for injection rate of 1,000-4,000 t/d. The storage capacity in 2nd layer 0.5, 0.5, 0.48 and 0.48 Mt for injection rate of 1,000-4,000 t/d. The top layer is 3rd layer can be obtained CO_2 0.82, 0.8, 0.78 and 0.76 Mt for injection rate of 1,000-4,000 t/d. Figure 4.21 shows storage capacity that increases in every year in the 1st layer. Storage capacities for injection rate of 2,000, 3,000 and 4,000 t/d are constant in year 1 because of their shutin period which are 1, 0.75 and 0.5 years, respectively. 1,000 t/d injection rate shutins at 2.25 years so it is still increasing until period 5 years. The 2nd layer and 3rd layer get along well with 1st layer. That 2nd layer, 1,000 t/d injection rate is shutin at 1.44 years so in Figure 4.22 storage capacity is continuous increase. 2,000 – 4,000 t/d injection rate is shutin at 0.7, 0.5 and 0.4 years, respectively. The 3rd layer, injection rate 1,000 t/d is still highest storage capacity as show in Figure 4.23 because shutin time is 2.27 years. While 2,000 – 4,000 t/d injection rate are shutin at 1.12, 0.75 and 0.55 years, respectively. Thus their capacities are constant since period 1 year.

Total storage capacity in Well 2 for 2.05 Mt at 1,000 t/d injection rate. 1.85 Mt at 2,000 t/d injection rate. 1.8 Mt at 3,000 t/d injection rate and 1.6 Mt at 4,000 t/d injection rate. As opposed to shutin time, injection rate 3,000 t/d is valuable.

Table 4.8 Storage capacity in Well 2.

		Storage capacity (Mt)			
		1,000 t/d	2,000 t/d	3,000 t/d	4,000 t/d
Well 2	3rd layer	0.82	0.8	0.78	0.76
	2nd layer	0.5	0.5	0.48	0.48
	1st layer	0.73	0.55	0.54	0.36
	Total	2.05	1.85	1.8	1.6

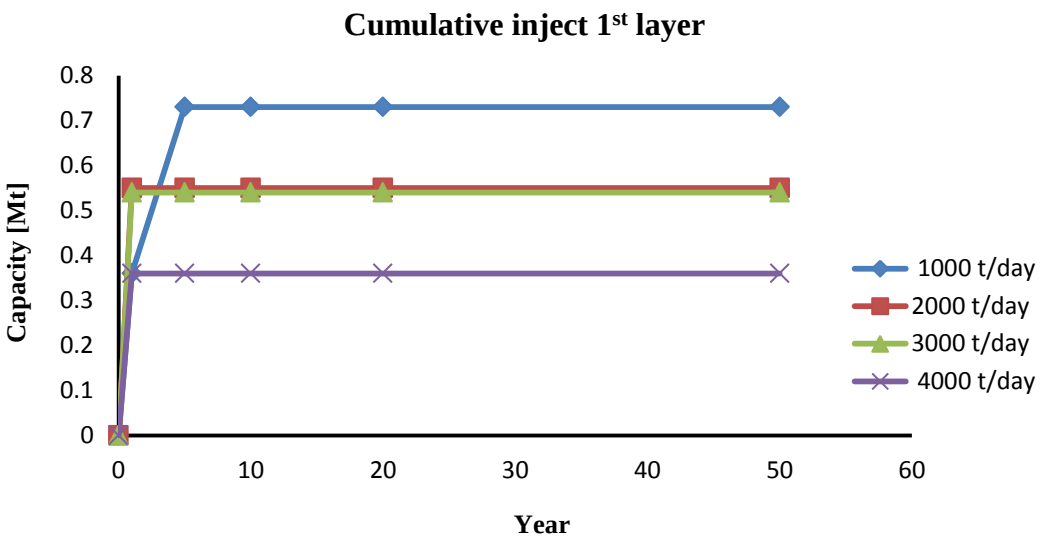

Figure 4.21 Storage capacity in 1st layer in Well 2.

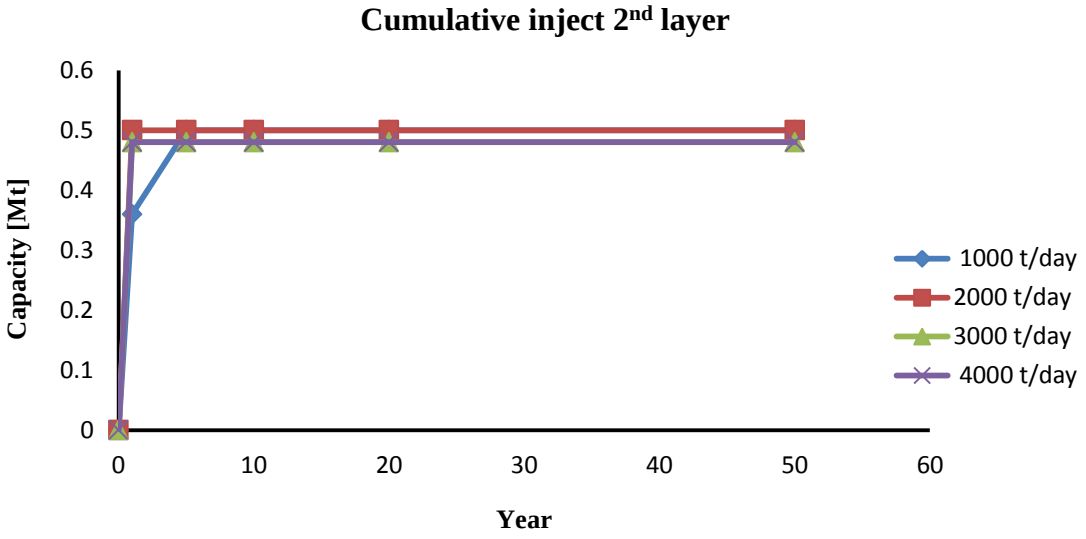

Figure 4.22 Storage capacity in 2nd layer in Well 2.

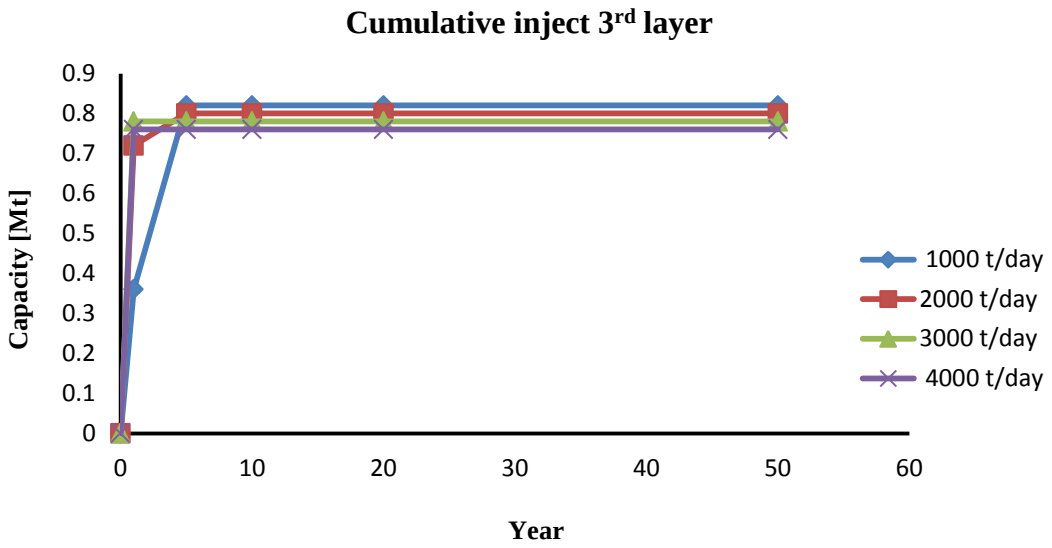

Figure 4.23 Storage capacity in 3rd layer in Well 2

4.2.3 Well 3

Figures 4.24-4.27 present storage capacity increasing by the time. The storage capacity in 4 layers in Well 3 is presented in Table.4.9. The storage capacity of 1st layer is consisting of 1.6, 1.64, 1.64 and 1.46 Mt in injection rate 1,000-4,000 t/d, respectively. The 2nd layer is consisting of 1.83, 1.82, 1.64 and 1.46 Mt in injection rate 1,000-4,000 t/d, respectively. The 3rd layer is 0.54, 0.54, 0.51 and 0.48 Mt in injection rate 1,000-4,000 t/d, respectively and the 4th layer is 0.5, 0.5, 0.45 and 0.43 Mt in injection rate 1,000-4,000 t/d, respectively. Storage capacity is increased by the time until shutin time. Figure 4.24 shown storage capacity in the 1st layer. 4,000 t/d injection rate is constant in period of year 1 because shutin time is 1.25 years. The storage capacity at 1,000-3,000 t/d injection rates are increasing until years 5. Shutin time are 4.75, 2.5and 1.75 years for 1,000-3,000 t/d injection rate, respectively. Figure 4.25 presents storage capacity in 2nd layer. 4,000 t/d injection rate shutins at 1.25 years and storage capacity is increased until year 1 period. 1,000-3,000 t/d injection rate are increasing until 5 years. Shutin time are 5.25, 2.75 and 1.75 years, respectively. While storage capacity in the 3rd layer and 4th layer at 2,000-3,000 t/d injection rate are constant since year 1 period. 1,000 t/d injection rate in both layers are increases until year 5 period. The 3rd layer and 4th layer are thin sand; so, it cannot obtain CO_2 inject significantly.

Total storage capacity in well for 1,000 t/d injection rate is 4.47 Mt. 2,000 t/d injection rate is 4.8 Mt. 3,000 t/d injection rate is 4.24 Mt and 4,000 t/d injection rate is 3.83 Mt. For this well 3,000 t/d injection rate is the most valuable to inject. Because of early time for shutin and storage capacity that can be obtained.

Table 4.9 Storage capacity in Well 3.

		Storage capacity (Mt)			
		1,000 t/d	2,000 t/d	3,000 t/d	4,000 t/d
Well 3	4th layer	0.5	0.5	0.45	0.43
	3rd layer	0.54	0.54	0.51	0.48
	2nd layer	1.83	1.82	1.64	1.46
	1st layer	1.6	1.64	1.64	1.46
	Total	4.47	4.5	4.24	3.83

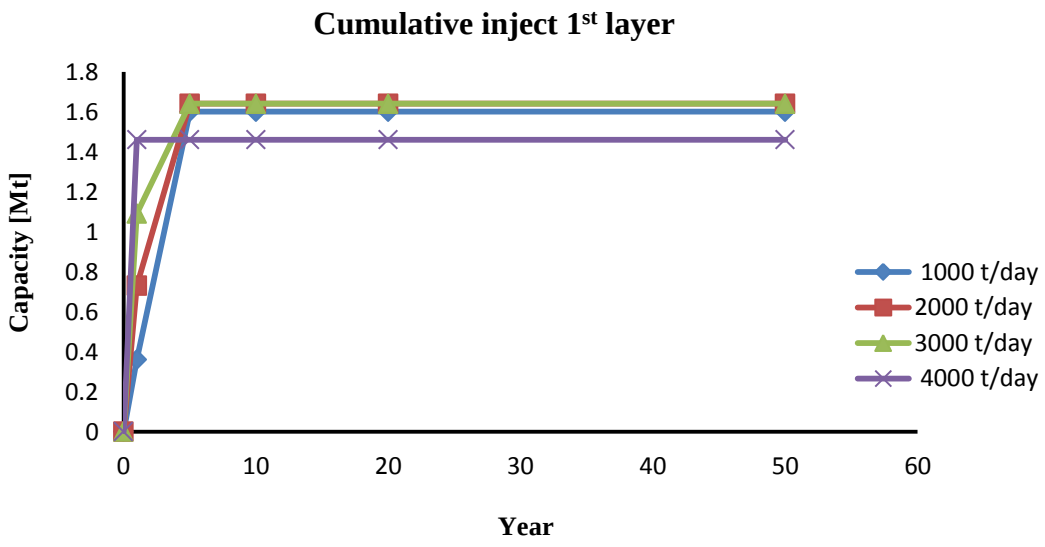

Figure 4.24 Storage capacity in 1st layer in Well 3.

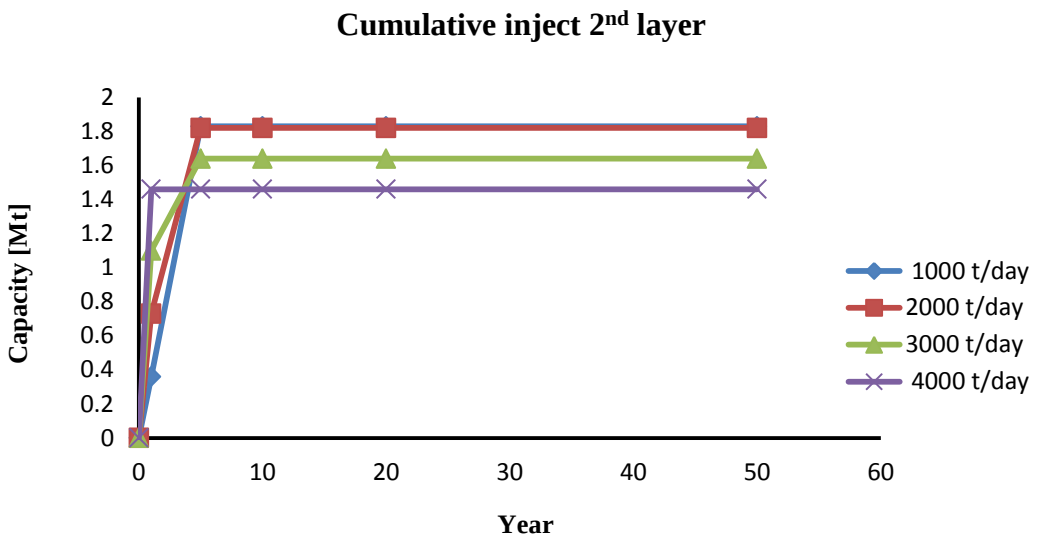

Figure 4.25 Storage capacity in 2nd layer in Well 3.

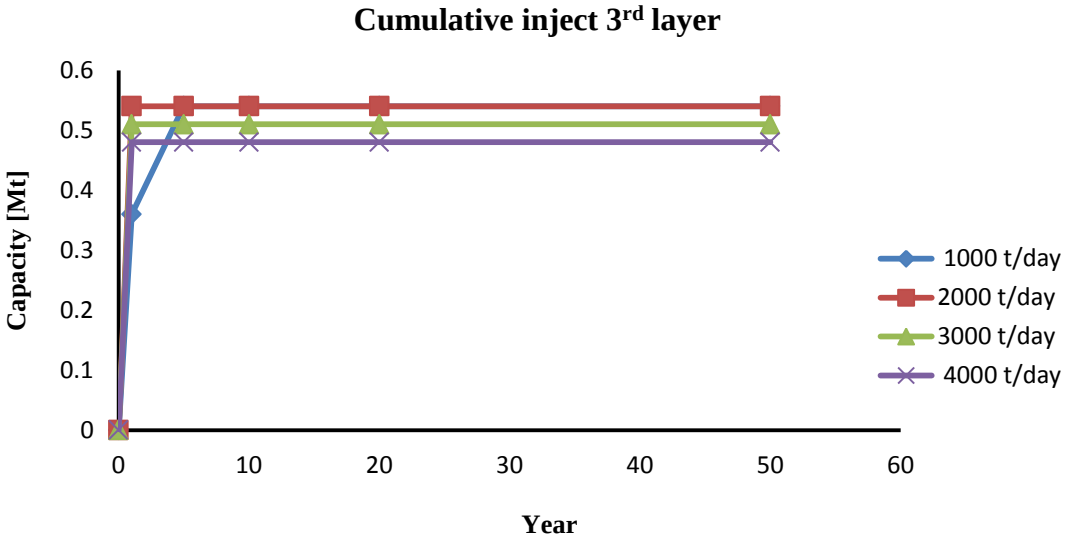

Figure 4.26 Storage capacity in 3rd layer in Well 3.

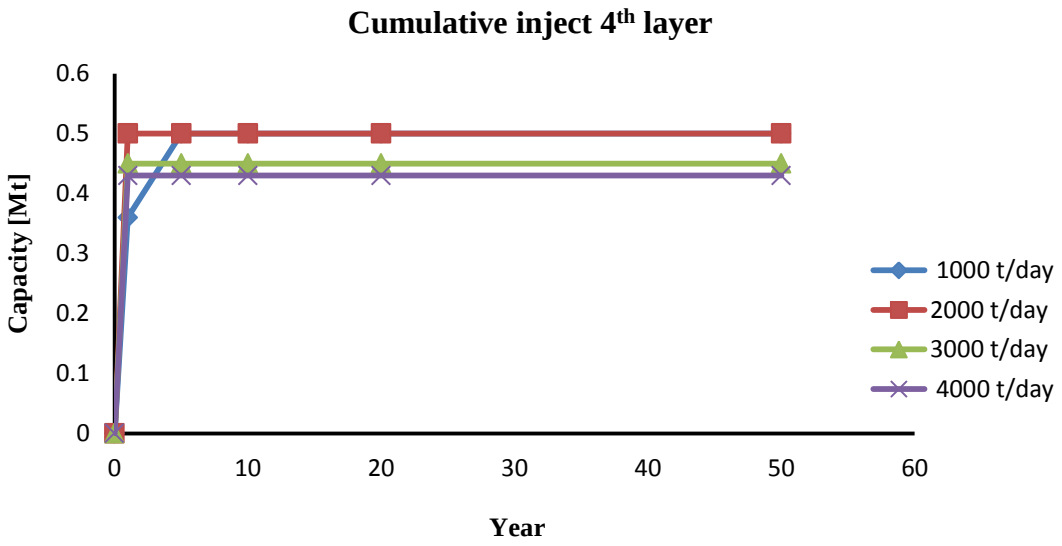

Figure 4.27 Storage capacity in 4th layer in Well 3.

4.3 Plume migration

During CO_2 injection, the fluid saturation in formation has changed. Even injection of CO_2 has stopped, plume migration of CO_2 is continuing. The plume migration continues for year, 10 years, centuries or millennia because of buoyancy (Mackay, 2013) CO_2 migrate faster in high permeability. The radius or area of plume migration is increasing as a pressure increasing while injection CO_2.

4.3.1 Well 1

The results of plume migration are presented in Table 4.10 for area and Table 4.11 for radius of migration. Also, plume migration has shown in Figures 4.28-4.31. Figures 4.28 and 4.30 present the area of plume migration. Figures 4.29 and 4.31 show the radius of plume migration. The trend of radius of CO_2 migration gets along well with area of plume migration with the period of time. The plume migration of CO_2 is expanding to large area until shutin time. After that plume are slightly decreasing because pressure decrease and solubility trapping. In the first 5 year, there are a lot of variations. In the period of 10-50 years, plume migration for all injection rates are constant and starts to decrease gradually. For Well 1, plume migration for injection rate of 1,000 t/d are expanded largest.

Table 4.10 Area of plume migration in Well 1.

		Year	1,000 t/d	2,000 t/d	3,000 t/d	4,000 t/d
Well 1	2nd layer [km^2]	0	0	0	0	0
		1	0.011	0.017	0.019	0.021
		5	0.034	0.039	0.037	0.031
		10	0.048	0.039	0.037	0.031
		20	0.048	0.038	0.036	0.031
		50	0.046	0.036	0.034	0.028
	1st layer [km^2]	0	0	0	0	0
		1	0.009	0.014	0.017	0.019
		5	0.027	0.037	0.036	0.033
		10	0.038	0.037	0.035	0.032
		20	0.037	0.035	0.033	0.030
		50	0.031	0.027	0.024	0.019

Table 4.11 Radius of plume migration in Well 1.

		Year	1,000 t/d	2,000 t/d	3,000 t/d	4,000 t/d
Well 1	2nd layer [km]	0	0	0	0	0
		1	0.060	0.073	0.077	0.082
		5	0.104	0.111	0.109	0.100
		10	0.123	0.111	0.108	0.100
		20	0.123	0.110	0.107	0.099
		50	0.121	0.107	0.104	0.094
	1st layer [km]	0	0	0	0	0
		1	0.055	0.067	0.073	0.078
		5	0.093	0.109	0.107	0.103
		10	0.110	0.108	0.105	0.101
		20	0.109	0.105	0.102	0.097
		50	0.099	0.092	0.087	0.078

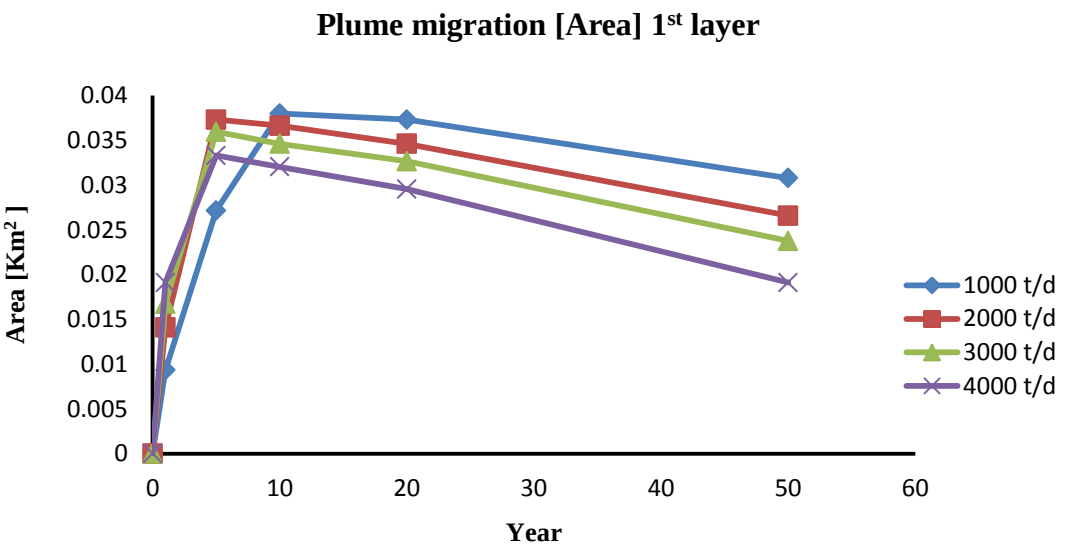

Figure 4.28 Area of plume migration in 1st layer in Well 1.

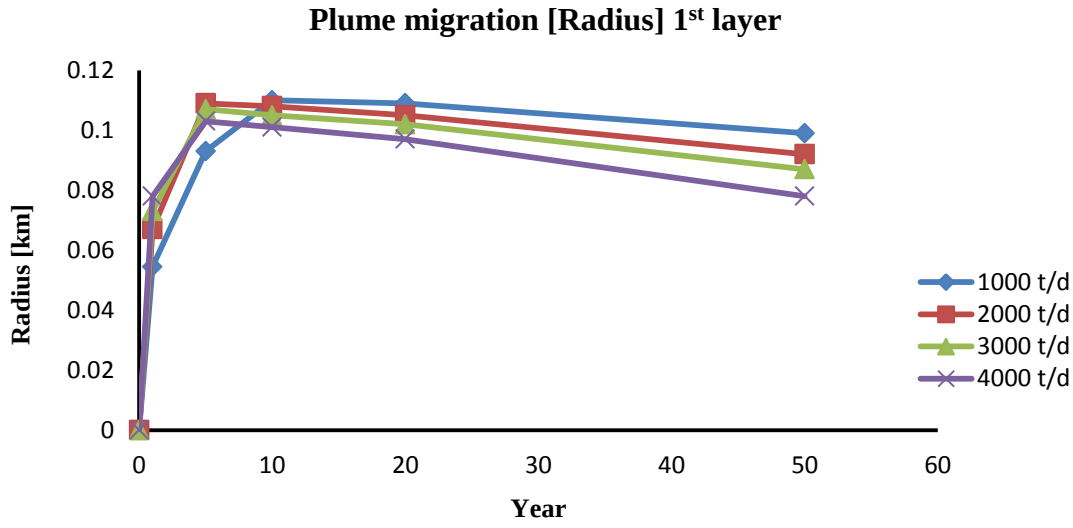

Figure 4.29 Radius of plume migration in 1st layer in Well 1.

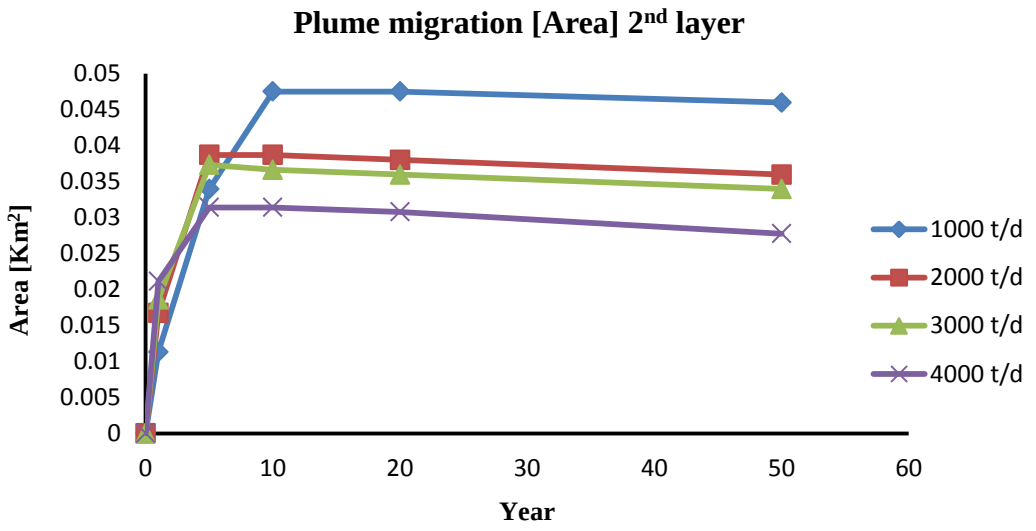

Figure 4.30 Area of plume migration in 2nd layer in Well 1.

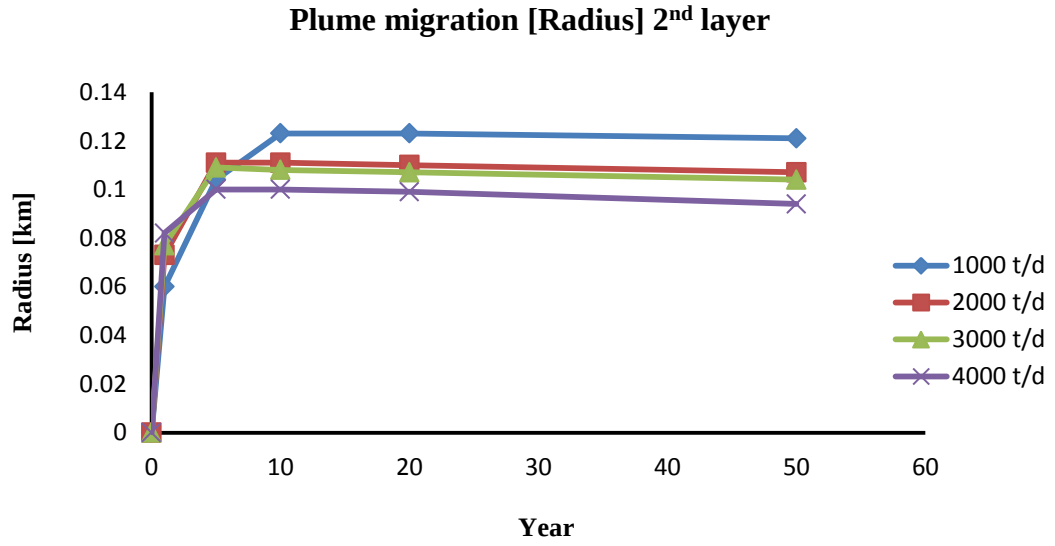

Figure 4.31 Radius of plume migration in 2nd layer in Well 1.

4.3.2 Well 2

The results present in Table 4.12 in the terms of plume migration and Table 4.13 in radius of plume migration. Figures 4.32, 4.34 and 4.36 present are area of plume migration in 1st layer, 2nd layer and 3rd layer, respectively. And Figures 4.33, 4.35 and 4.37 have shown as a radius of plume migration. The expansion of CO_2 is increases until shutin time. Then plume migration is slightly decreasing after 5 year. In this well, plume migration in 1,000 t/d injection rate is larger area than others. In 1st layer, 1,000 t/d injection rate is largest area followed by 2,000, 3,000 and 4,000 t/d, respectively. In 2nd layer, 1,000 t/d injection rate still has largest area follow by 2,000, 4,000 and 3,000 t/d injection rate that according with pressure buildup. As same as 3rd layer, the largest plume is in injection rate 1,000 t/d. The next one is injection rate 2,000 t/d, 3,000 t/d and 4,000 t/d, respectively. For overall, plume migration is increased until shutin time and the it will decreased gradually.

Table 4.12 Area of plume migration in Well 2.

		Year	1,000 t/d	2,000 t/d	3,000 t/d	4,000 t/d
Well 2	3rd layer [km^2]	0	0	0	0	0
		1	0.011	0.015	0.015	0.015
		5	0.020	0.020	0.020	0.020
		10	0.020	0.020	0.020	0.019
		20	0.020	0.020	0.019	0.019
		50	0.019	0.019	0.019	0.018
	2nd layer [km^2]	0	0	0	0	0
		1	0.012	0.014	0.015	0.015
		5	0.018	0.018	0.017	0.017
		10	0.017	0.017	0.017	0.017
		20	0.017	0.017	0.016	0.017
		50	0.015	0.015	0.015	0.014
	1st layer [km^2]	0	0	0	0	0
		1	0.009	0.011	0.012	0.011
		5	0.023	0.019	0.019	0.015
		10	0.023	0.019	0.019	0.015
		20	0.023	0.019	0.018	0.014
		50	0.022	0.017	0.017	0.012

Table 4.13 Radius of plume migration in Well 2.

		Year	1,000 t/d	2,000 t/d	3,000 t/d	4,000 t/d
Well 2	3rd layer [km]	0	0	0	0	0
		1	0.058	0.068	0.070	0.070
		5	0.081	0.080	0.079	0.079
		10	0.080	0.080	0.079	0.078
		20	0.080	0.079	0.079	0.078
		50	0.078	0.078	0.077	0.076
	2nd layer [km^2]	0	0	0	0	0
		1	0.062	0.068	0.069	0.069
		5	0.075	0.075	0.074	0.074
		10	0.075	0.074	0.073	0.073
		20	0.074	0.073	0.072	0.072
		50	0.070	0.069	0.068	0.067
	1st layer [km^2]	0	0	0	0	0
		1	0.055	0.060	0.061	0.060
		5	0.086	0.078	0.078	0.068
		10	0.086	0.078	0.078	0.068
		20	0.085	0.077	0.077	0.066
		50	0.083	0.074	0.074	0.063

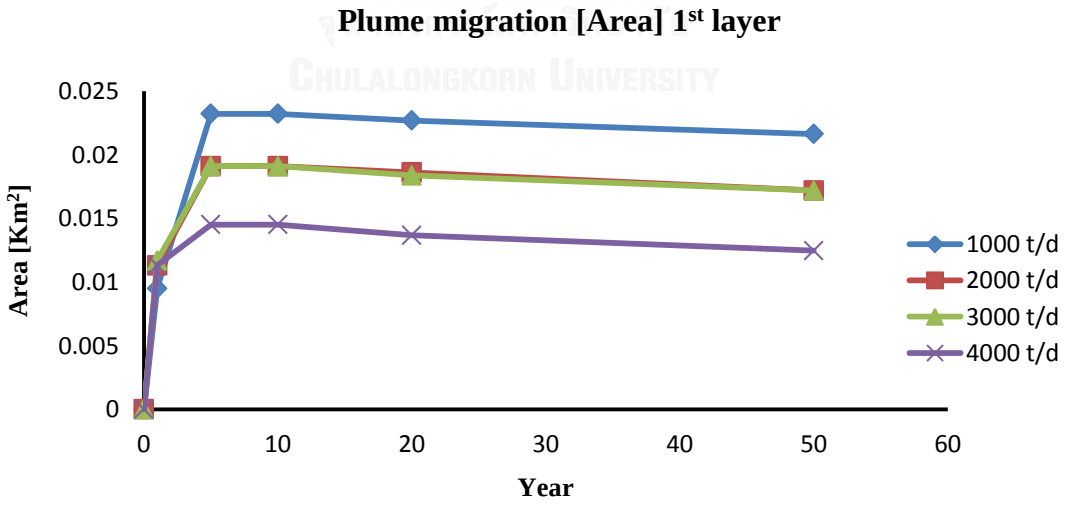

Figure 4.32 Area of plume migration in 1st layer in Well 2.

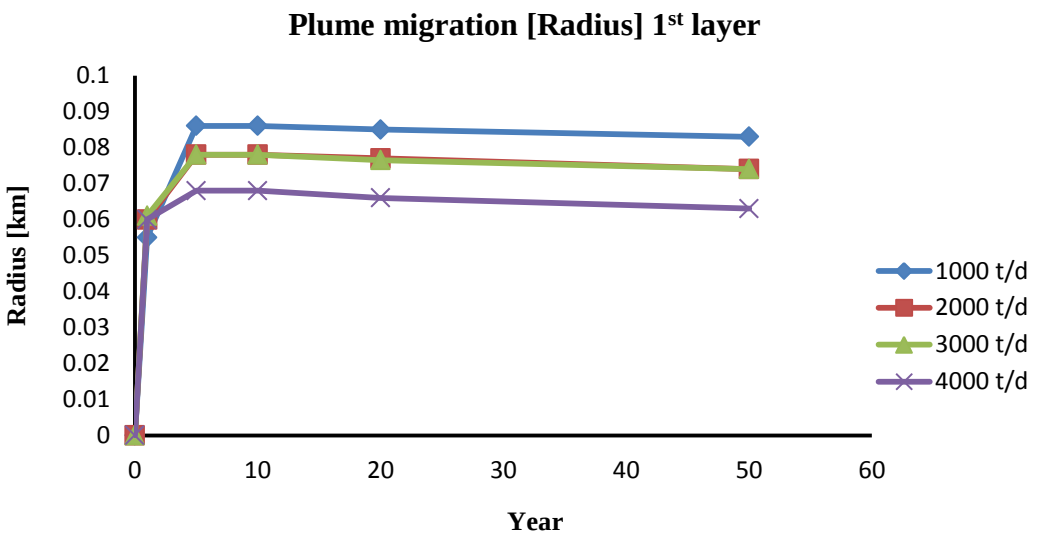

Figure 4.33 Radius of plume migration in 1st layer in Well 2.

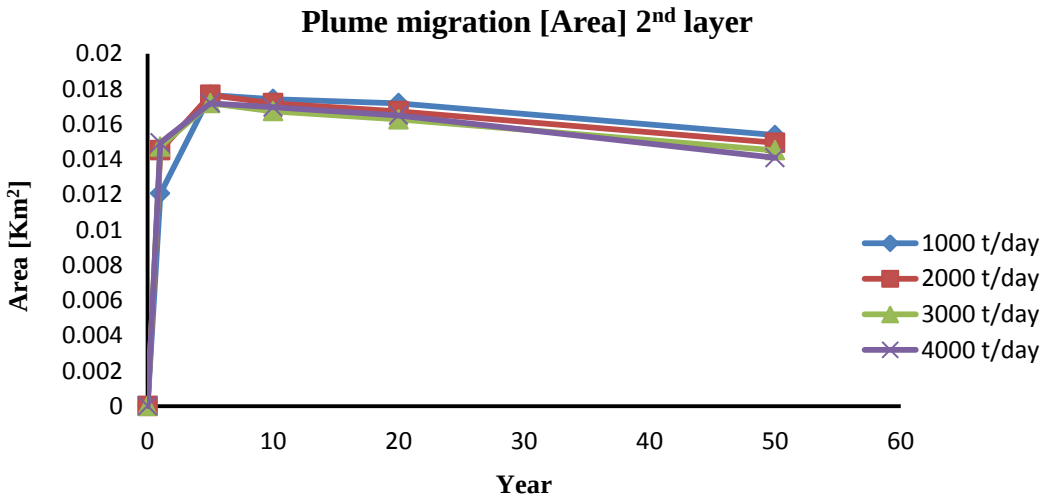

Figure 4.34 Area of plume migration in 2nd layer in Well 2.

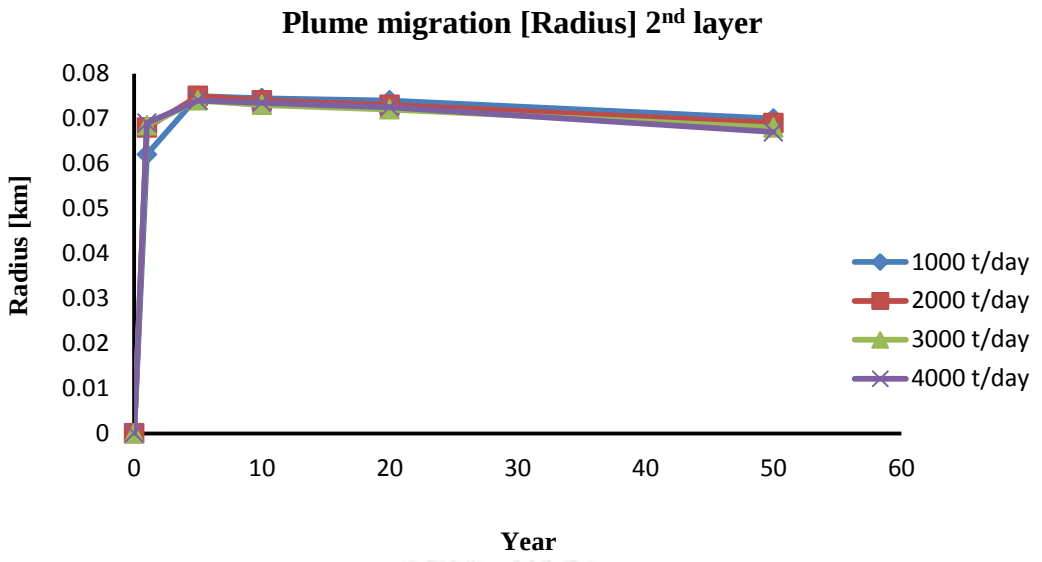

Figure 4.35 Radius of plume migration in 2nd layer in Well 2.

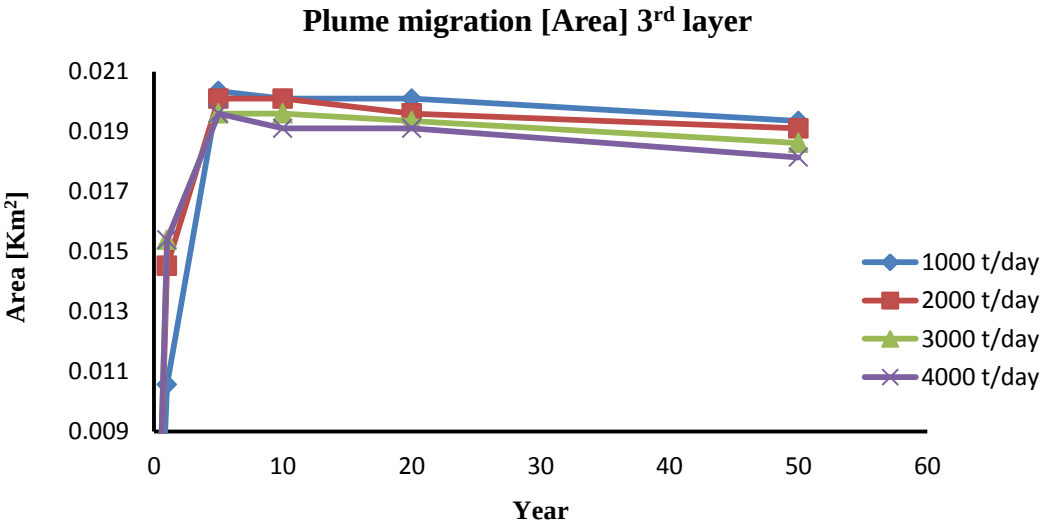

Figure 4.36 Area of plume migration in 3rd layer in Well 2.

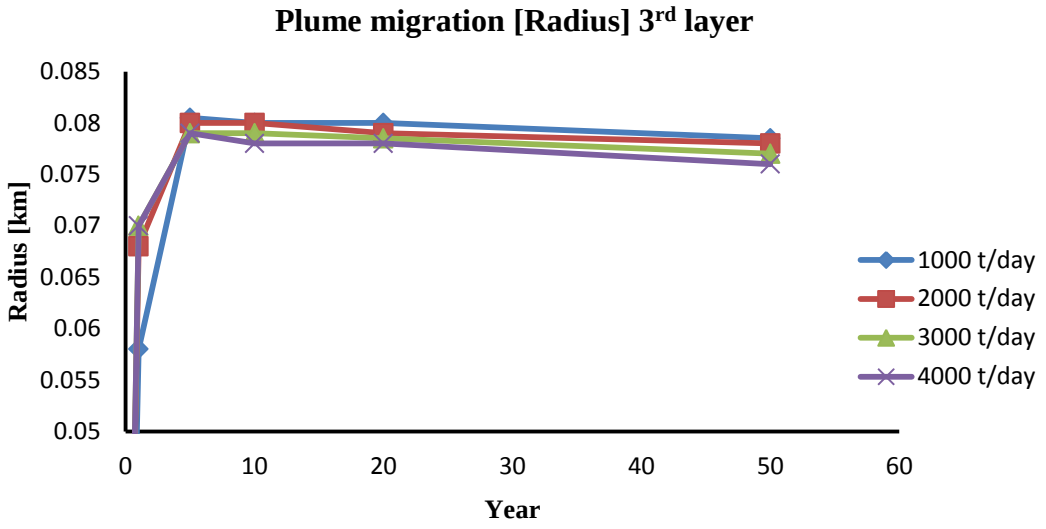

Figure 4.37 Radius of plume migration in 3rd layer in Well 2.

4.3.3 Well 3

The result of plume migration in Well 3 is the same as Well 1 and Well 2 presented in Table 4.14 for area of plume migration and Table 4.15 for radius of plume migration. Figures 4.38, 4.40, 4.42 and 4.44 are the results of plume migration in area. Figure 4.39, 4.41, 4.43 and 4.45 are radius of plume migration. The result present in 4 sand layers of Well 3. There are consisting of 4th layer, 3rd layer, 2nd layer and 1st layer. In all layers, plume of CO_2 are expanding in large area. The maximum area is in 5 year. Afterwards, the areas of plume are decreasing. CO_2 migrated in 1,000 t/d injection rate is larger area than other except plume in layer 1st. In 1st layer, the expansions of CO_2 in injection rate 3,000 t/d are largest. The sequence of radius and area of plume migration from large to small is 3,000, 2,000, 1,000 and 4,000 t/d injection rate that is affected from pressure buildup. Because pressure at shutin time of this layer at 1,000, 2,000 and 3,000 t/d injection rate are similar. In 2nd layer, 1,000 t/d injection rate is created plume large area followed by 2,000, 3,000 and 4,000 t/d after shutin time. In 3rd layer and 4th layer trends are same that the largest area is created by 1,000, 2,000 and 3,000 t/d injection rate is similar and the last is 4,000 t/d. The reason is related to pressure buildup and shutin time. Moreover, the 3rd layer and 4th layer has a thin layer; so, it can be satored CO_2 not too much that effected to plume migration. From that result plum migration in 3rd layer and 4th layer are small as which

is difference from the 1st layer and 2nd layer as the result of buoyancy force. In addition CO_2 moves up to the top layer and accompanies by thin layer of sand.

Table 4.14 Area of plume migration in Well 3.

		Year	1,000 t/d	2,000 t/d	3,000 t/d	4,000 t/d
Well 3	4th layer [km^2]	0	0	0	0	0
		1	0.016	0.021	0.019	0.019
		5	0.022	0.021	0.019	0.019
		10	0.021	0.021	0.019	0.019
		20	0.021	0.020	0.018	0.018
		50	0.018	0.017	0.015	0.015
	3rd layer [km^2]	0	0	0	0	0
		1	0.017	0.022	0.021	0.020
		5	0.021	0.022	0.021	0.019
		10	0.021	0.021	0.019	0.018
		20	0.018	0.018	0.016	0.015
		50	0.005	0.006	00.006	0.006
	2nd layer [km^2]	0	0	0	0	0
		1	0.023	0.031	0.036	0.039
		5	0.054	0.056	0.053	0.049
		10	0.057	0.056	0.053	0.049
		20	0.056	0.056	0.053	0.049
		50	0.056	0.055	0.051	0.048
	1st layer [km^2]	0	0	0	0	0
		1	0.019	0.026	0.030	0.032
		5	0.039	0.040	0.041	0.039
		10	0.038	0.039	0.039	0.037
		20	0.035	0.037	0.038	0.034
		50	0.025	0.025	0.025	0.017

Table 4.15 Radius of plume migration in Well 3.

		Year	1,000 t/d	2,000 t/d	3,000 t/d	4,000 t/d
Well 3	4^{th} layer [km]	0	0	0	0	0
		1	0.071	0.083	0.079	0.079
		5	0.083	0.083	0.079	0.078
		10	0.082	0.082	0.078	0.077
		20	0.081	0.081	0.075	0.075
		50	0.076	0.075	0.070	0.069
	3^{rd} layer [km]	0	0	0	0	0
		1	0.074	0.083	0.082	0.080
		5	0.083	0.083	0.081	0.079
		10	0.081	0.081	0.078	0.076
		20	0.076	0.075	0.072	0.069
		50	0.039	0.043	0.043	0.042
	2^{nd} layer [km]	0	0	0	0	0
		1	0.086	0.1	0.107	0.112
		5	0.132	0.134	0.130	0.126
		10	0.135	0.134	0.130	0.125
		20	0.134	0.133	0.130	0.125
		50	0.133	0.132	0.128	0.124
	1^{st} layer [km]	0	0	0	0	0
		1	0.077	0.091	0.098	0.102
		5	0.112	0.113	0.114	0.111
		10	0.111	0.111	0.112	0.109
		20	0.106	0.108	0.111	0.104
		50	0.090	0.090	0.089	0.074

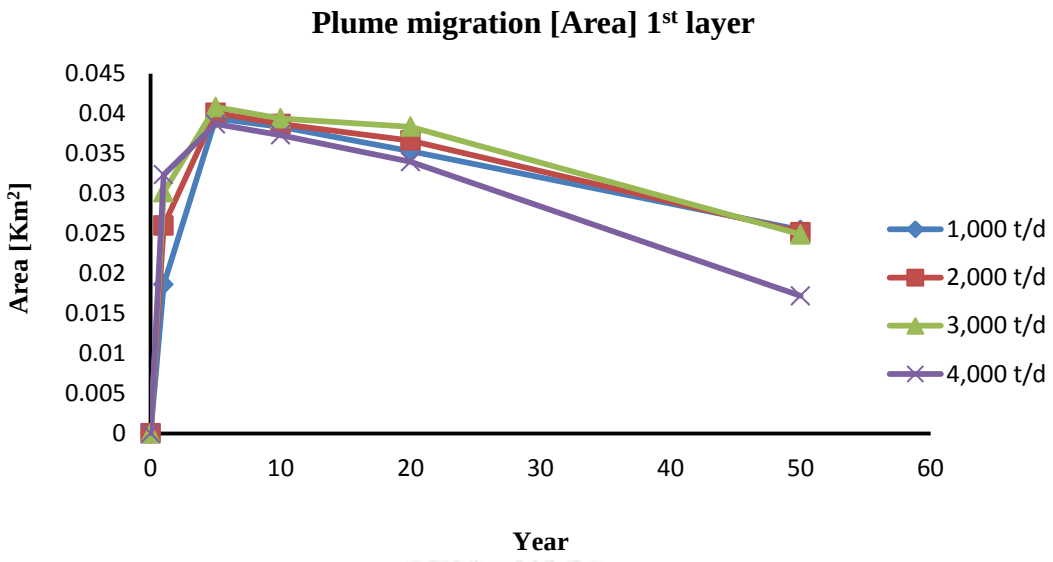

Figure 4.38 Area of plume migration in 1st layer in Well 3.

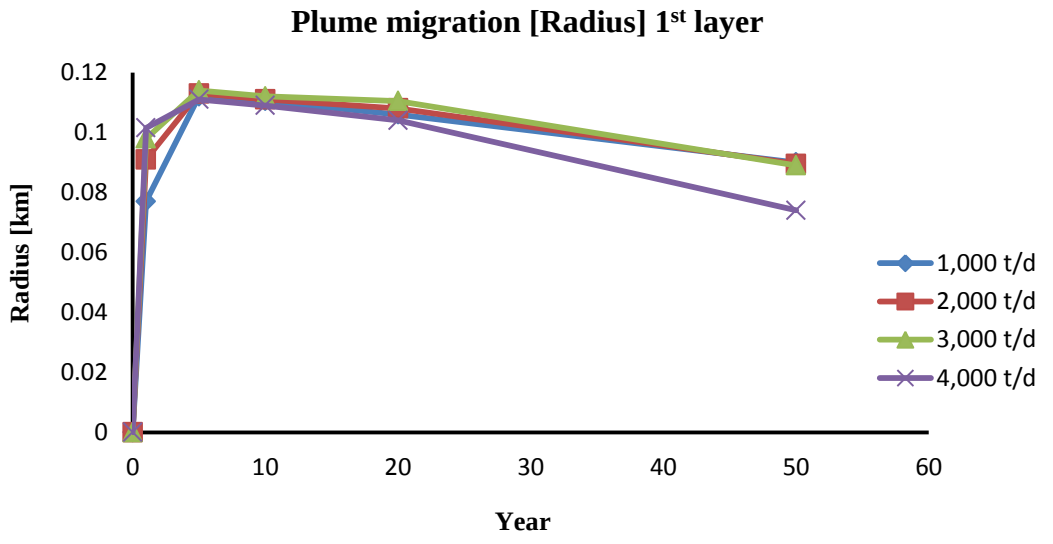

Figure 4.39 Radius of plume migration in 1st layer in Well 3.

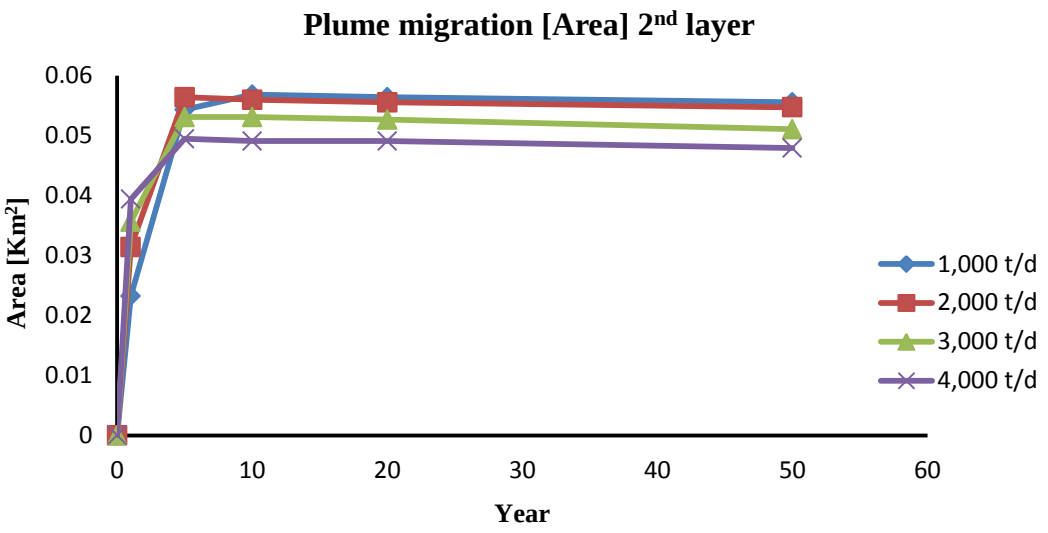

Figure 4.40 Area of plume migration in 2nd layer in Well 3.

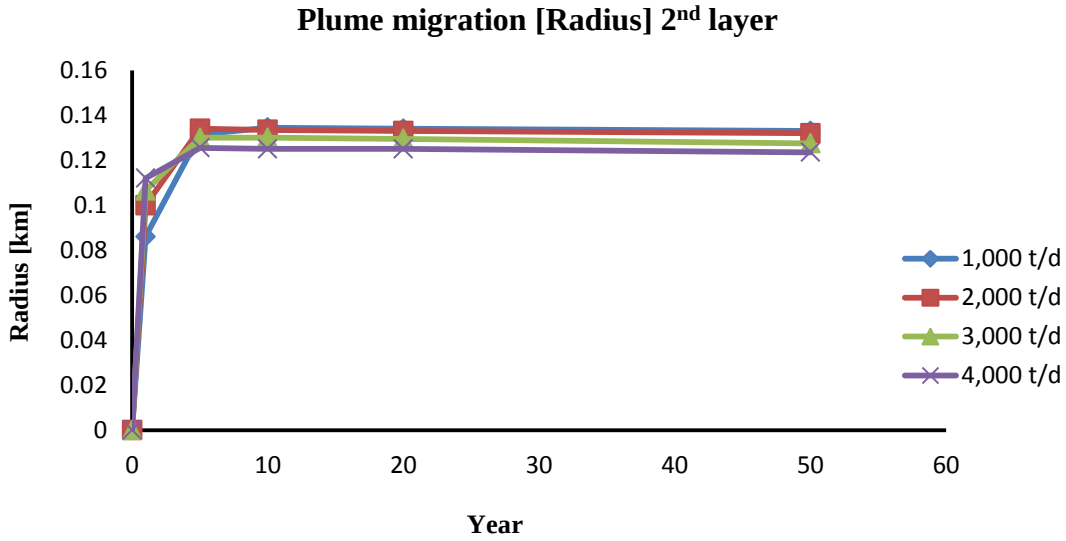

Figure 4.41 Radius of plume migration in 2nd layer in Well 3.

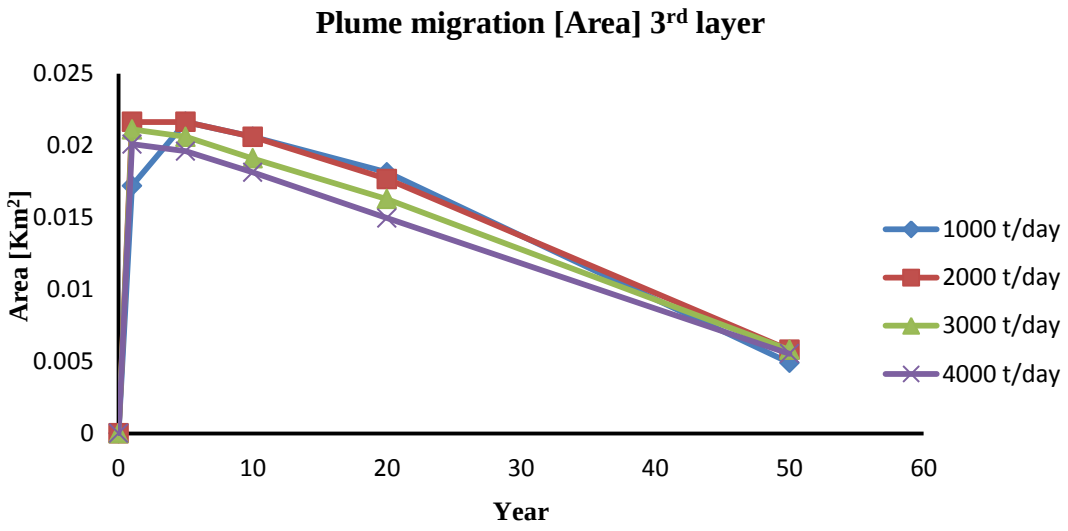

Figure 4.42 Area of plume migration in 3rd layer in Well 3.

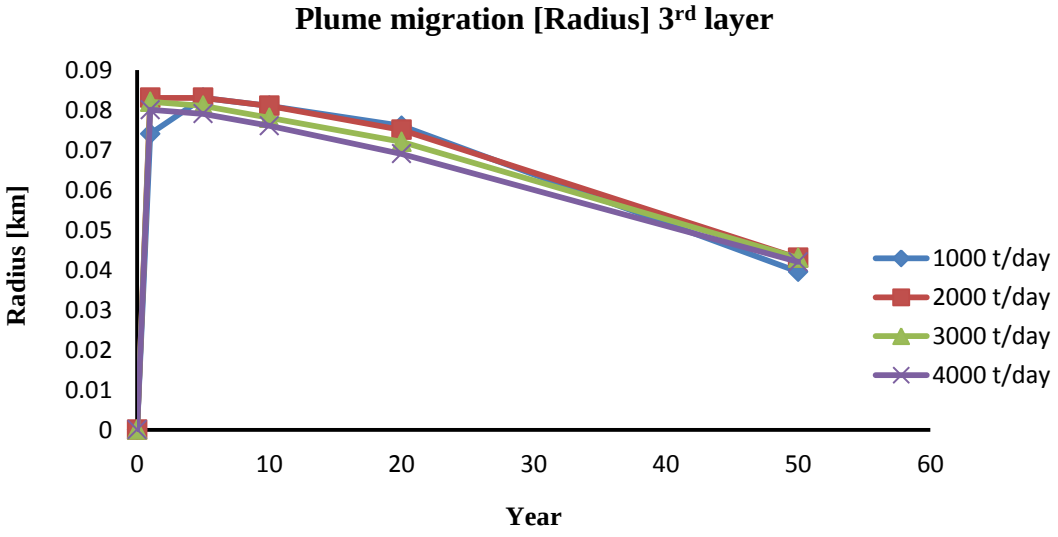

Figure 4.43 Radius of plume migration in 3rd layer in Well 3.

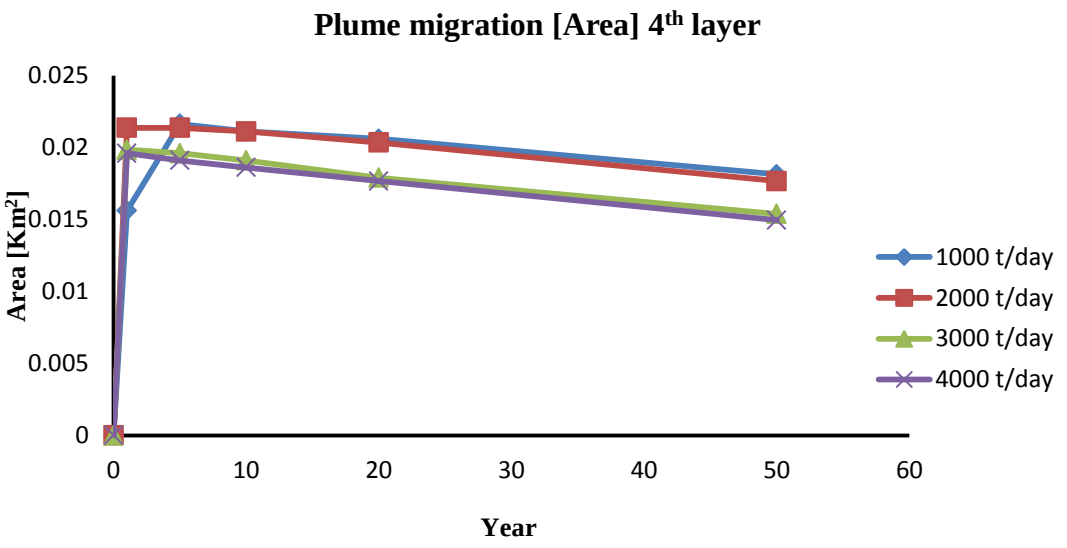

Figure 4.44 Area of plume migration in 4th layer in Well 3.

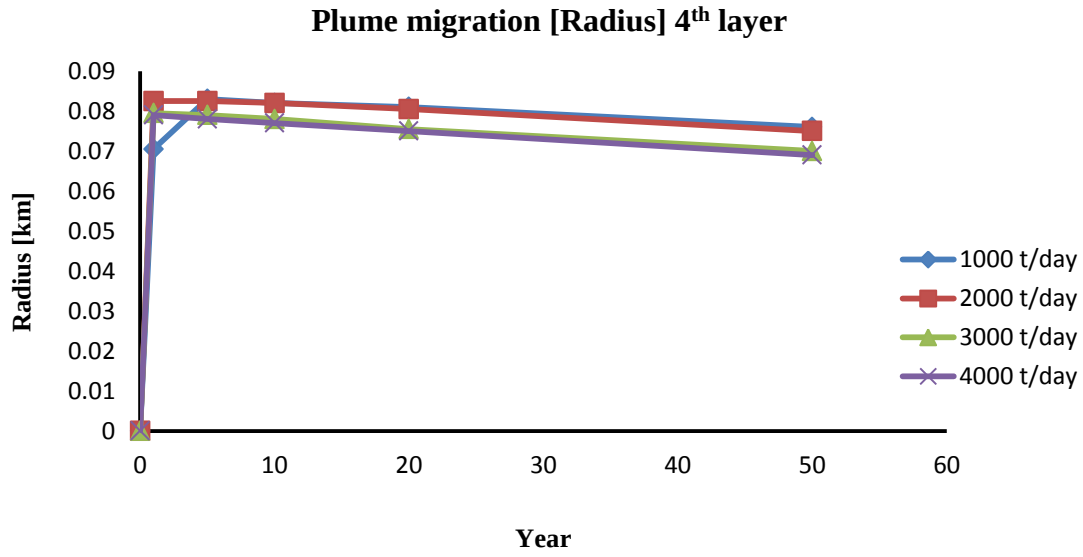

Figure 4.45 Radius of plume migration in 4th layer in Well 3.

The results of plume migration in horizontal from injection well as shown in Figures 4.45-4.60. Firstly, CO_2 injected into the bottom of each layer. Then CO_2 moves up to top sand layer. The CO_2 should stay to beneath shale layer. But in this research, the simulation show the CO_2 can leak into bottom shale layer. CO_2 that leaks to shale layer are in small amount. In this case, it will occur because of permeability and porosity of rock formations. Figure 4.45-4.60 show the CO_2 moves up to the top layer in 4,000 t/d injection rate in Well 1. The detail and other result of injection rate are show in appendix. Figure 4.45-4.50 present plume migration of 4,000 t/d injection rate in all layer at Well 1. Figure 4.51-4.55 present plume migration of 4,000 t/d injection rate in 1^{st} layer at Well 1 and Figure 4.56-4.60 present plume migration of 4,000 t/d injection rate in 2^{nd} layer at Well 1. The result from simulation show plume migration increasing by period of time until shutin time. After shutin trend of plume migration is decreasing gradually.

From Table 4.16 presents the results of 3 Wells that show the efficiency of area. The maximum storage capacity from all Wells that can be obtained 13.059 Mt and 9.45 Mt is minimum storage capacity in area. The maximum pressure buildup is 33.29 MPa and the minimum pressure buildup is 26.69 MPa depending on shutin time. Therefore, the maximum of shutin time is 10.5 years and minimum of shutin time is 0.5 years. CO_2 can be expanded largest radius is 0.135 km and smallest radius is 0.068 km. And in area, maximum area is 0.057 km^2 and minimum area is 0.015 km^2. Thus, this area has a potential for CO_2 storage.

Table 4.16 The result of 3 wells.

	Layer	Maximum pressure (MPa)	Pressure buildup (MPa)	Shutin time (Years)	Radius (km)	Area (km^2)	Storage capacity (Mt)
Well 1	2^{nd} layer	29.20	27.21-28.97	1.25-8	0.100-0.123	0.031-0.048	1.90-2.83
	1^{st} layer	32.52	30.44-32.09	2-10.5	0.103-0.110	0.033-0.038	2.33-3.74
	Total						4.02-6.57
Well 2	3^{rd} layer	29.64	28.88 -29.43	0.55-2.27	0.079-0.081	0.019-0.020	0.76-0.82
	2^{nd} layer	30.02	29.35-29.86	0.4-1.4	0.074-0.075	0.017-0.018	0.48-0.5
	1^{st} layer	30.23	22.39-29.63	0.5-2.5	0.068-0.086	0.015-0.023	0.36-0.73
	Total						1.6-2.05
Well 3	4^{th} layer	28.30	26.89-28.19	0.33-1.4	0.073-0.089	0.019-0.022	0.43-0.5
	3^{rd} layer	28.56	27.64-28.41	0.36-1.5	0.080-0.083	0.020-0.022	0.48-0.54
	2^{nd} layer	29.39	26.69-29.07	1.25-5.25	0.126-0.135	0.049-0.057	1.46-1.83
	1^{st} layer	33.91	31.73-33.29	1.25-4.75	0.111-0.114	0.039-0.041	1.46-1.64
	Total						3.83-4.47

a.

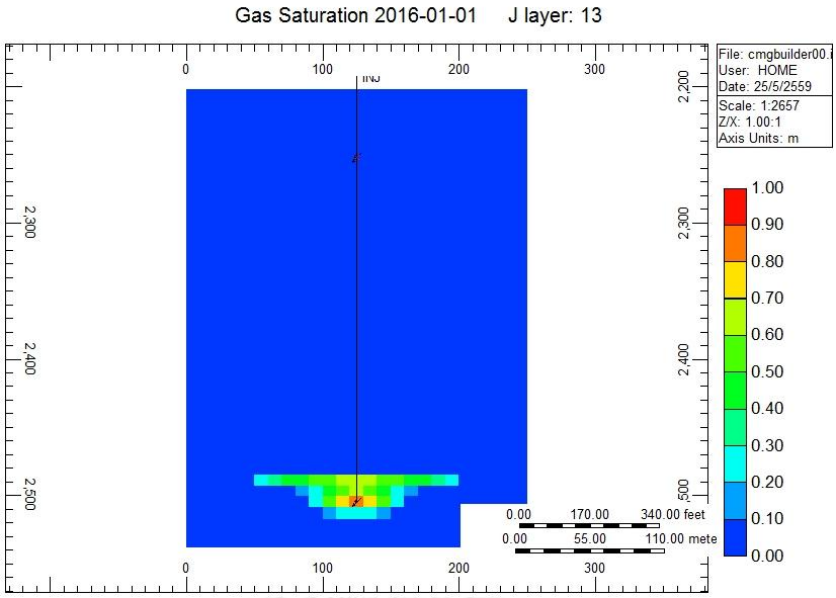

b.

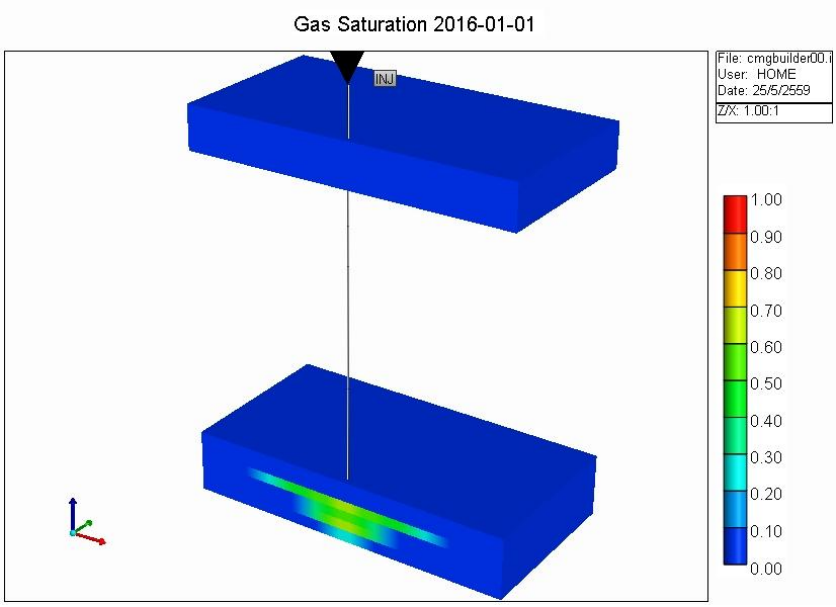

Figure 4.46 a. migration area from side in all layer at Well 1 (1 year)
b. migration area from 3D in all layer at Well 1 (1 year)

a.

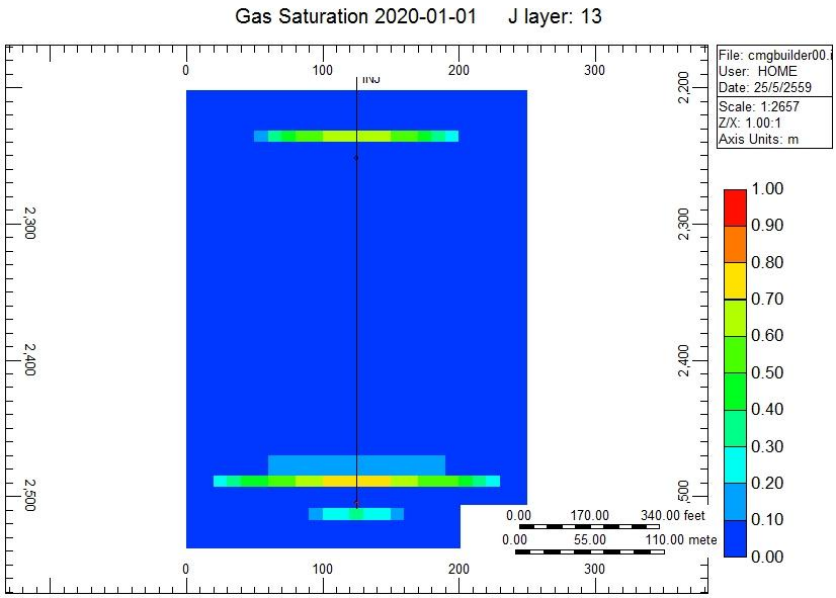

b.

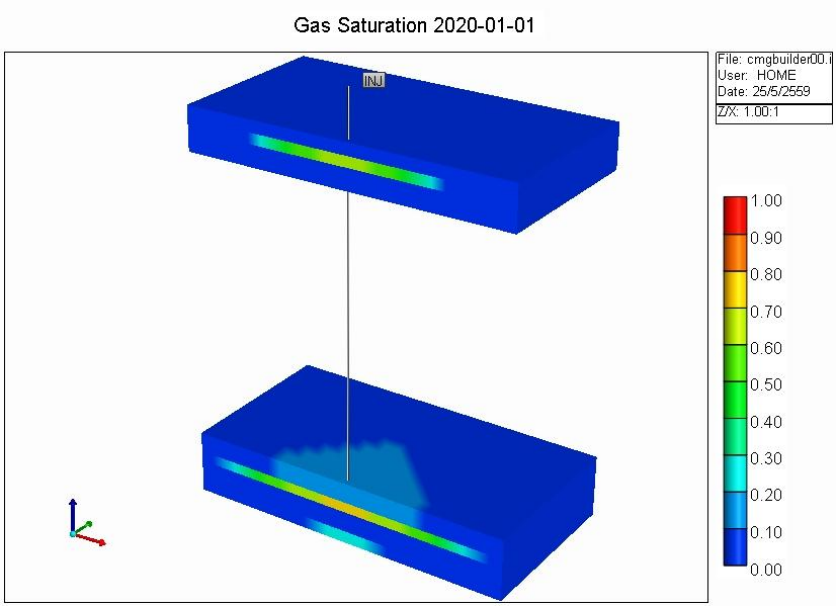

Figure 4.47 a. migration area from side in all layer at Well 1 (5 years)
b. migration area from 3D in all layer at Well 1 (5 years)

a.

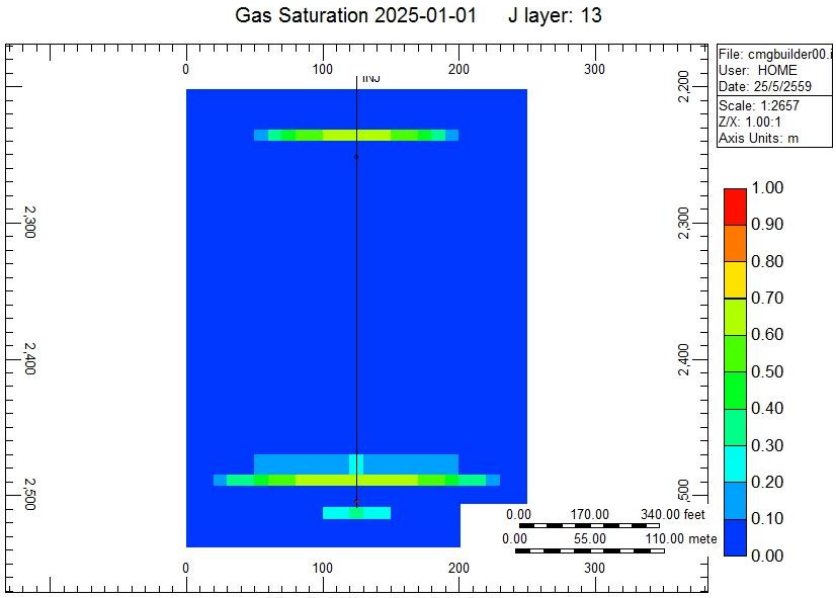

b.

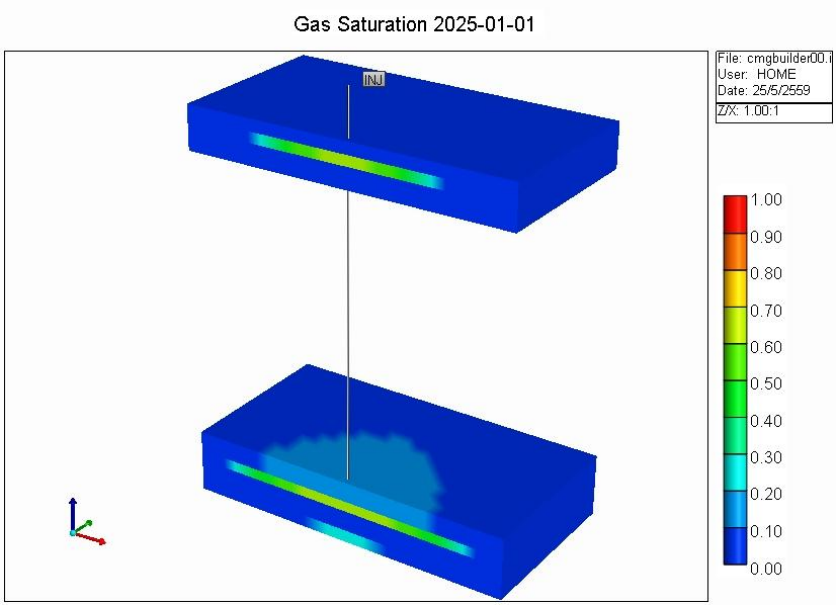

Figure 4.48 a. migration area from side in all layer at Well 1 (10 years)
b. migration area from 3D in all layer at Well 1 (10 years)

a.

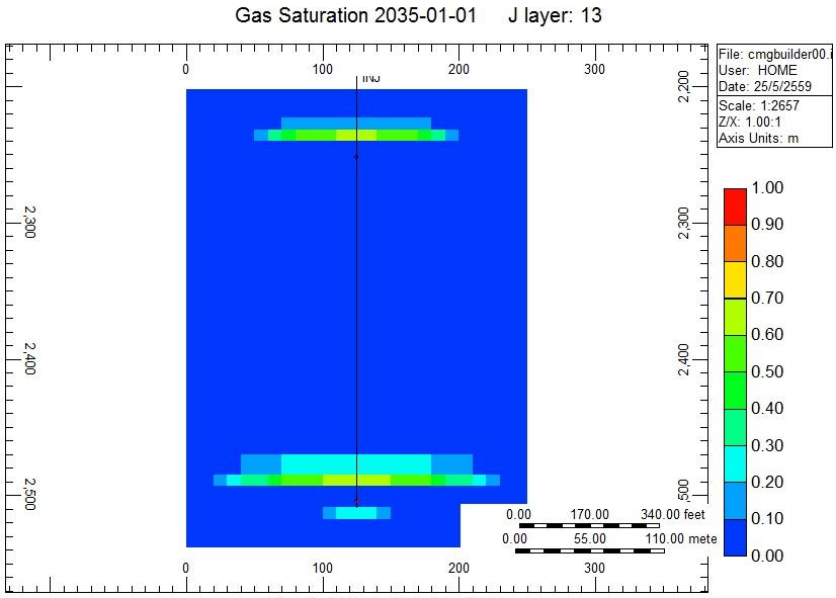

b.

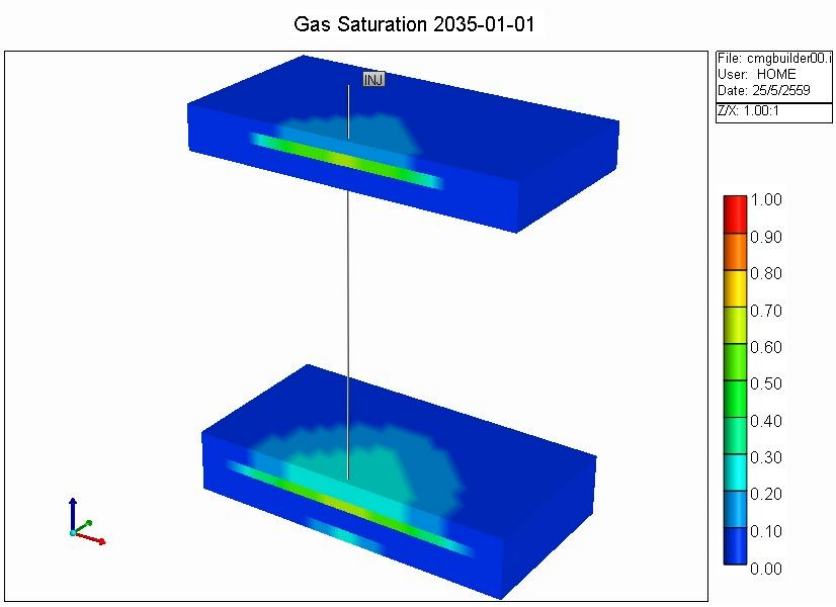

Figure 4.49 a. migration area from side in all layer at Well 1 (20 years)
b. migration area from 3D in all layer at Well 1 (20 years)

a.

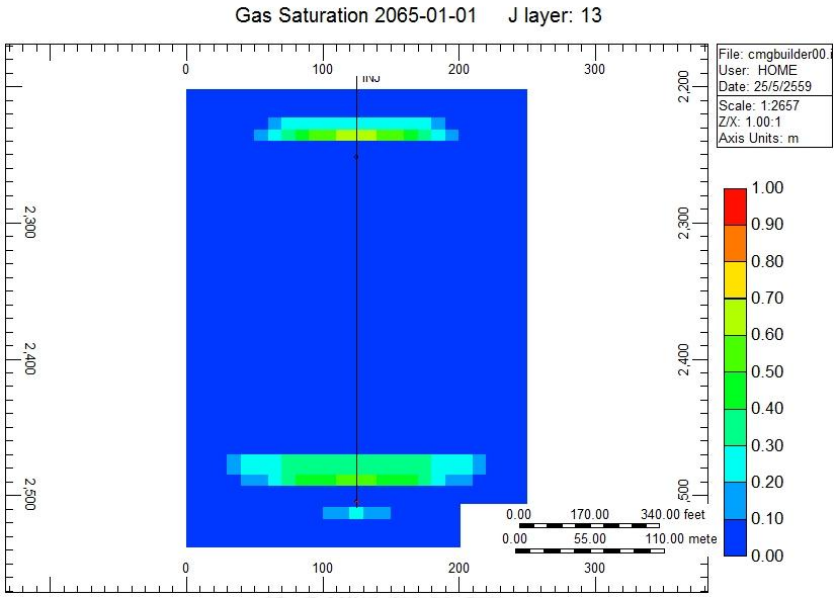

b.

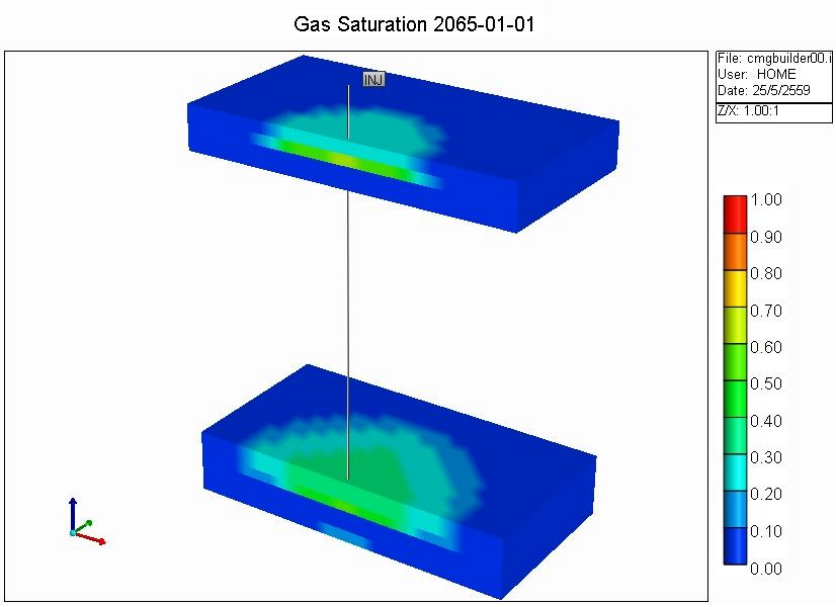

Figure 4.50 a. migration area from side in all layer at Well 1 (50 years)
b. migration area from 3D in all layer at Well 1 (50 years)

a.

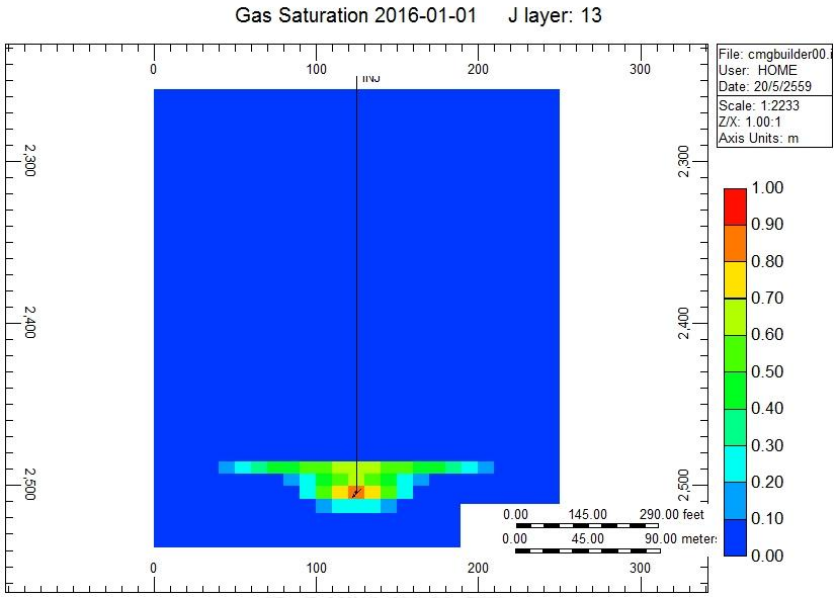

b.

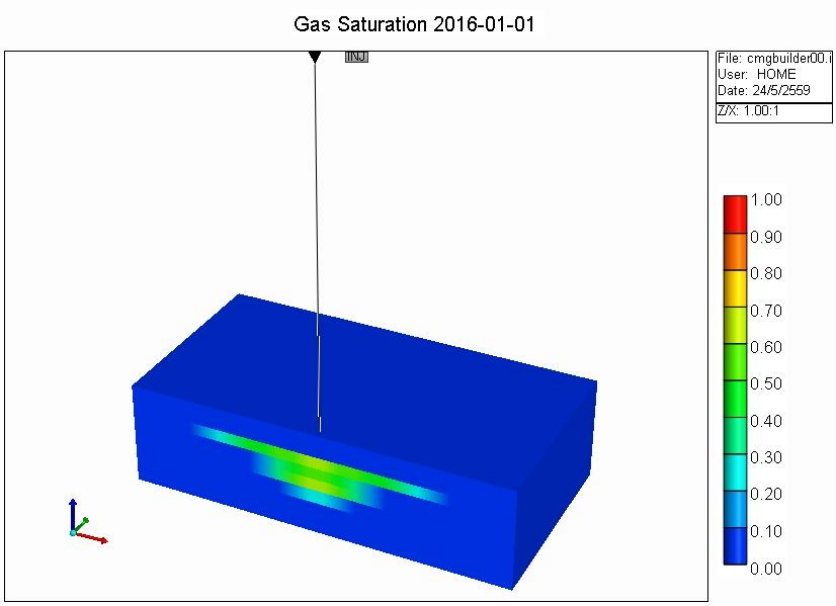

Figure 4.51 a. migration area from side in 1st layer at Well 1 (1 year)
b. migration area from 3D in 1st layer at Well 1 (1 year)

a.

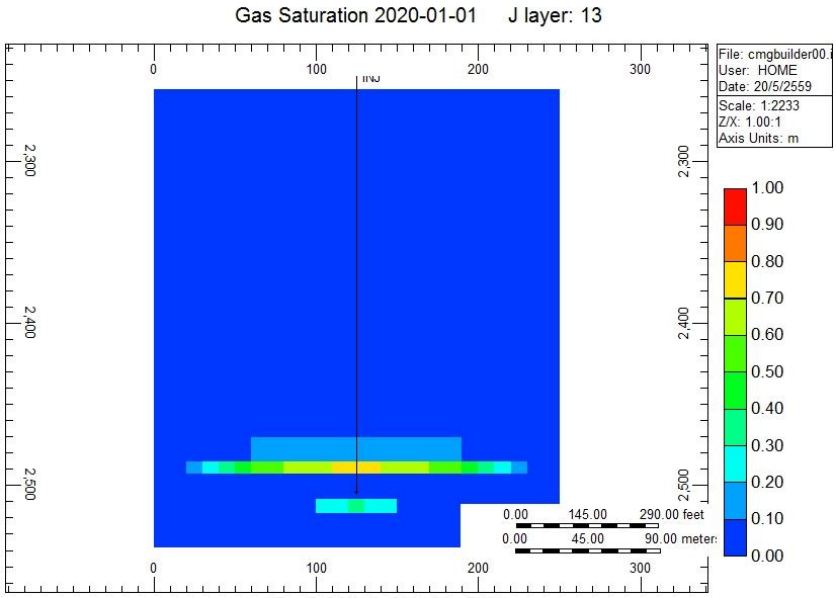

b.

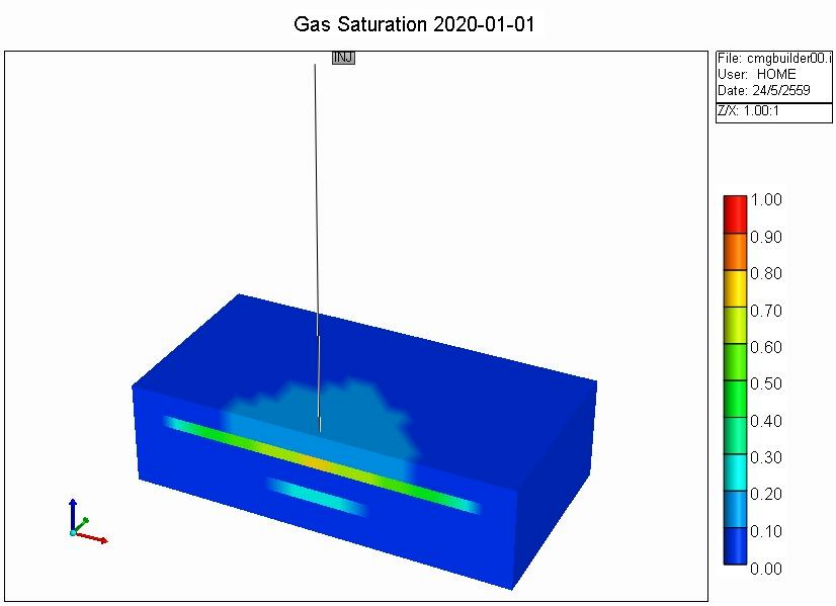

Figure 4.52 a. migration area from side in 1st layer at Well 1 (5 years)
b. migration area from 3D in 1st layer at Well 1 (5 years)

a.

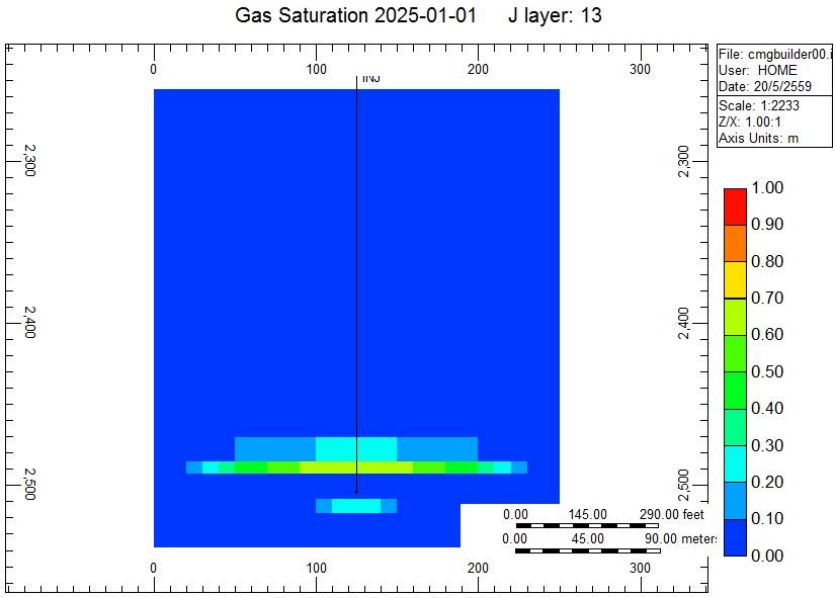

b.

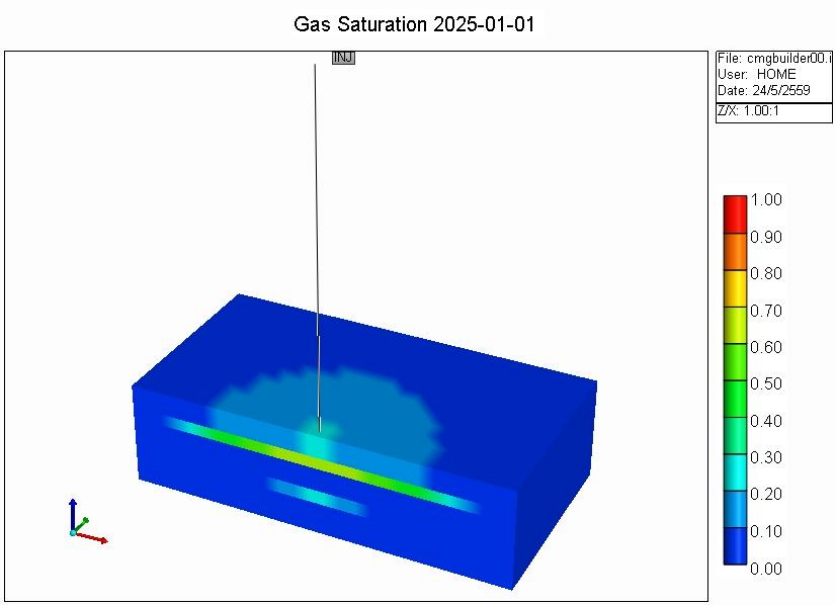

Figure 4.53 a. migration area from side in 1st layer at Well 1 (10 years)
b. migration area from 3D in 1st layer at Well 1 (10 years)

a.

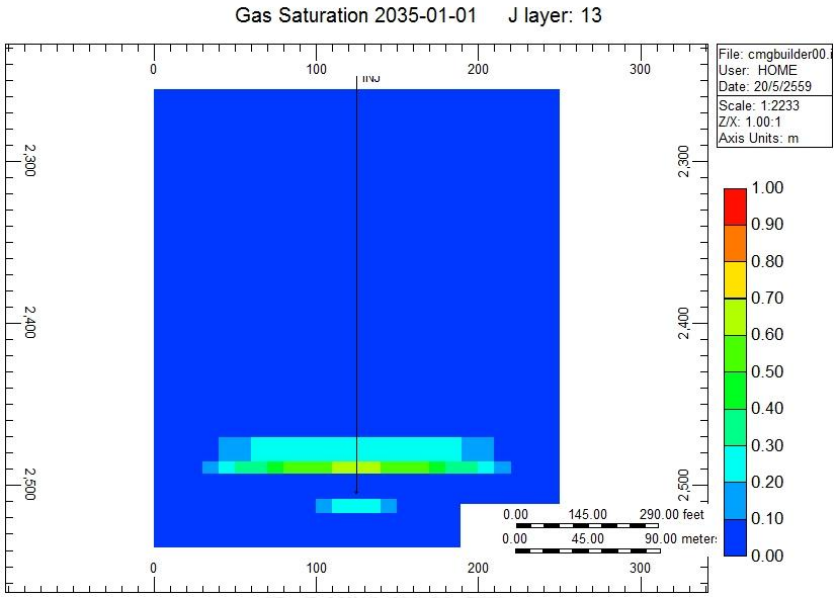

b.

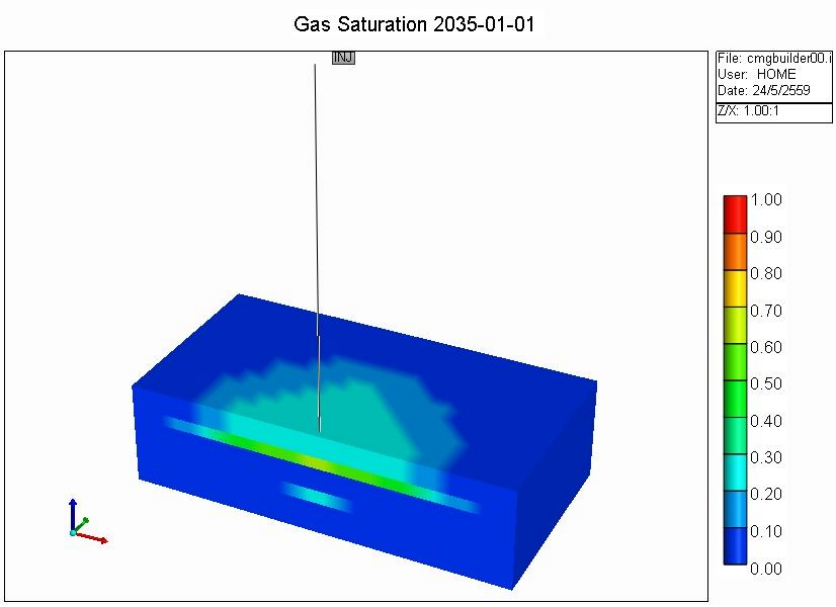

Figure 4.54 a. migration area from side in 1st layer at Well 1 (20 years)
b. migration area from 3D in 1st layer at Well 1 (20 years)

a.

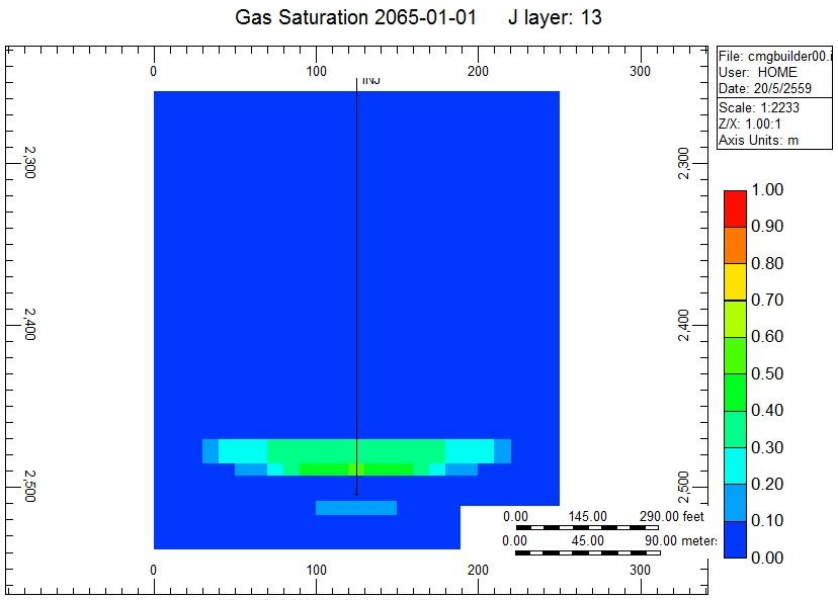

b.

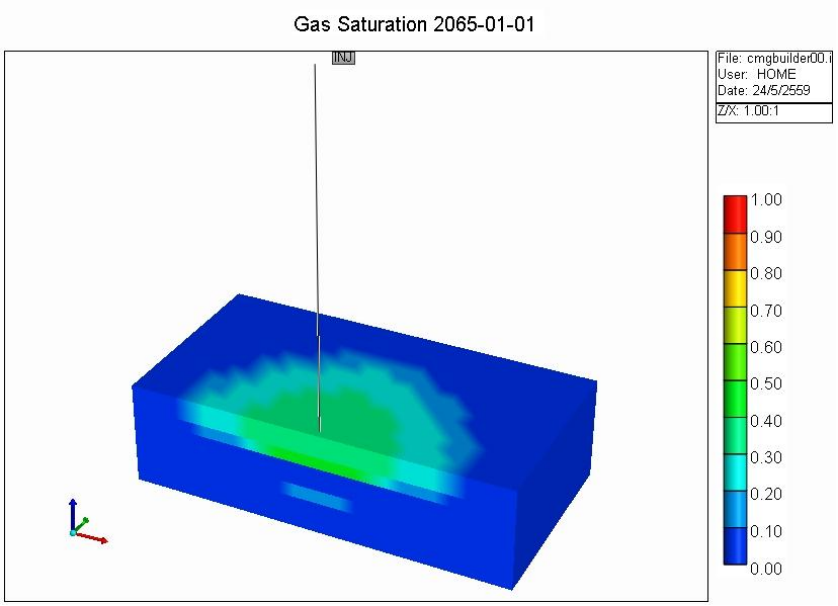

Figure 4.55 a. migration area from side in 1st layer at Well 1 (50 years)
b. migration area from 3D in 1st layer at Well 1 (50 years)

a.

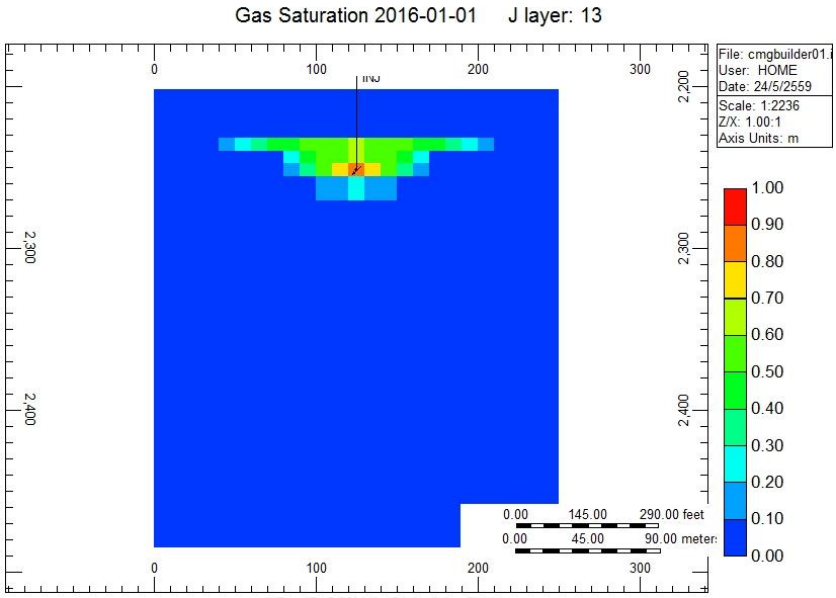

b.

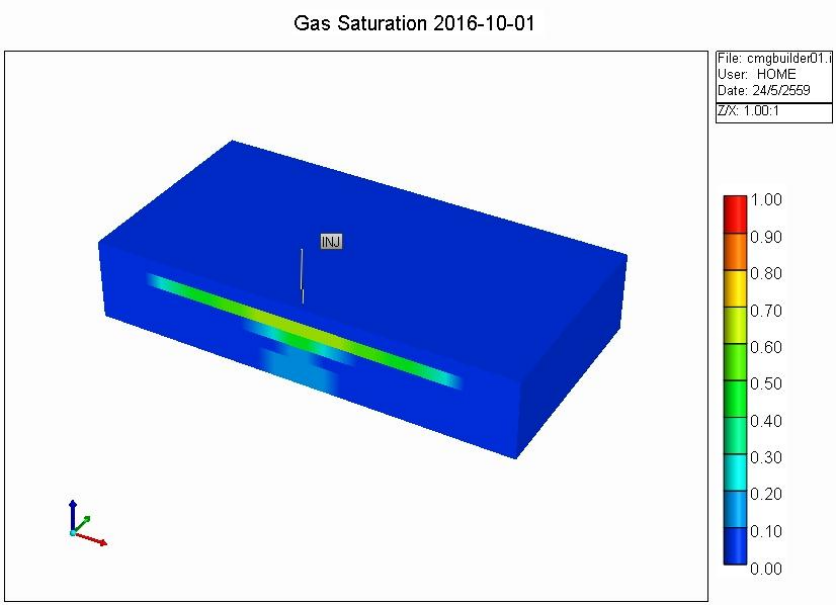

Figure 4.56a. migration area from side in 2nd layer at Well 1 (1 year)
b. migration area from 3D in 2nd layer at Well 1 (1 year)

a.

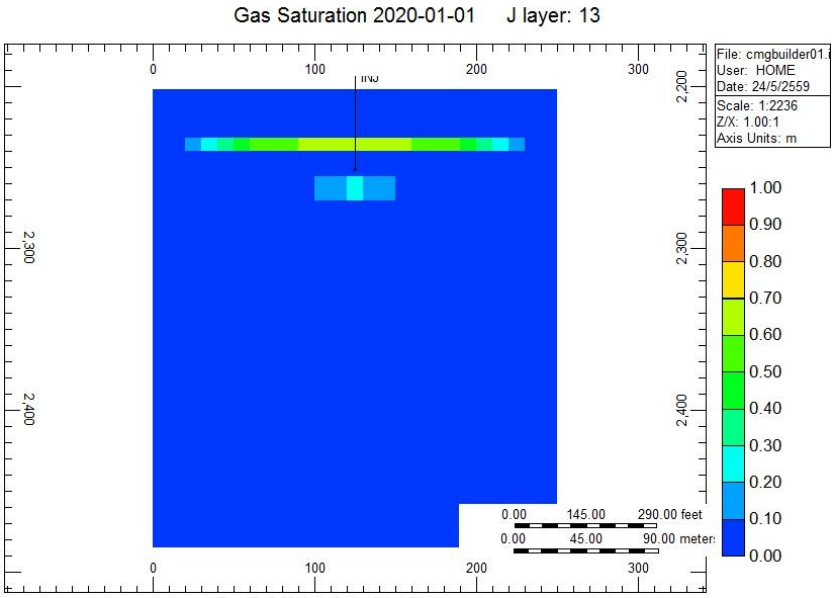

b.

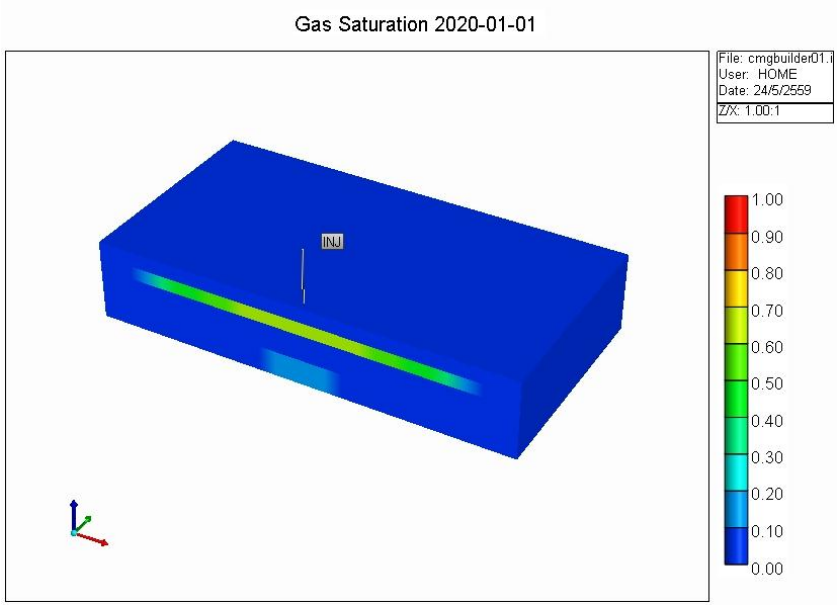

Figure 4.57 a. migration area from side in 2nd layer at Well 1 (5 years)
b. migration area from 3D in 2nd layer at Well 1 (5 years)

a.

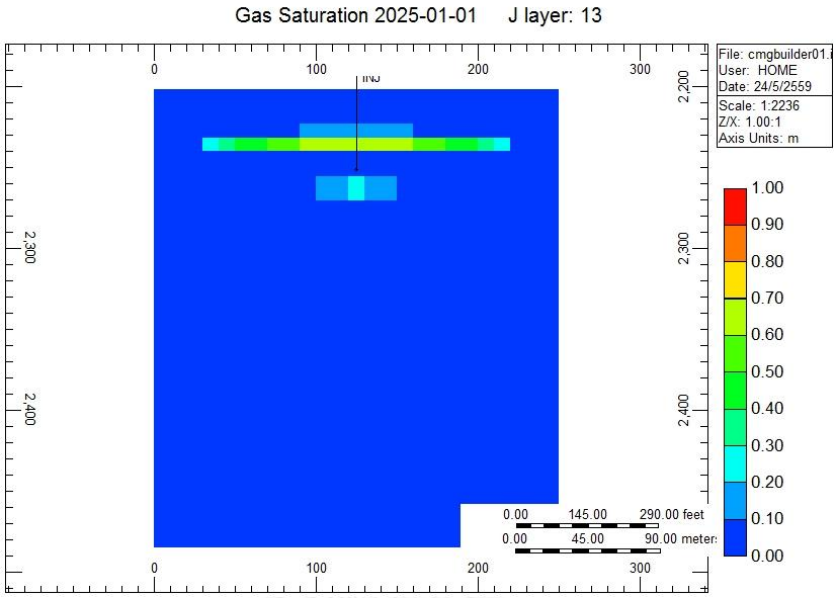

b.

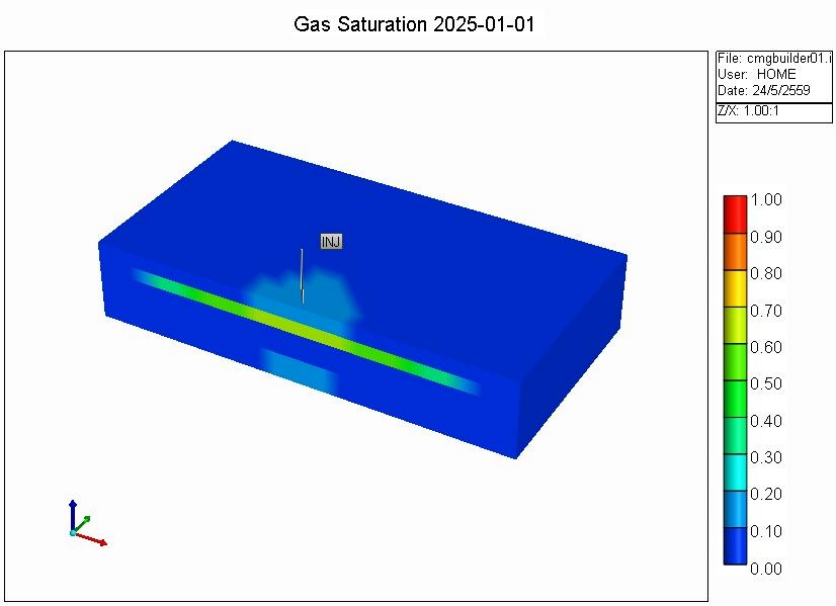

Figure 4.58 a. migration area from side in 2nd layer at Well 1 (10 years)
b. migration area from 3D in 2nd layer at Well 1 (10 years)

a.

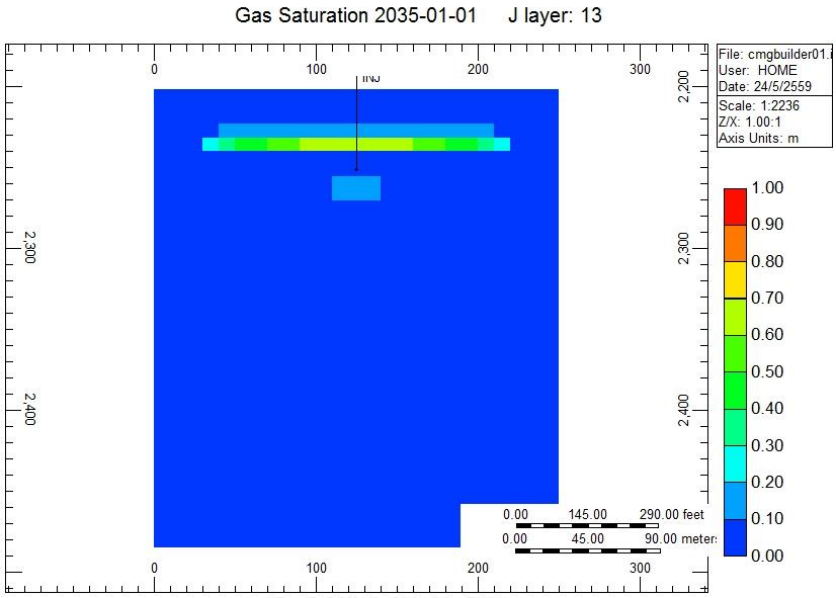

b.

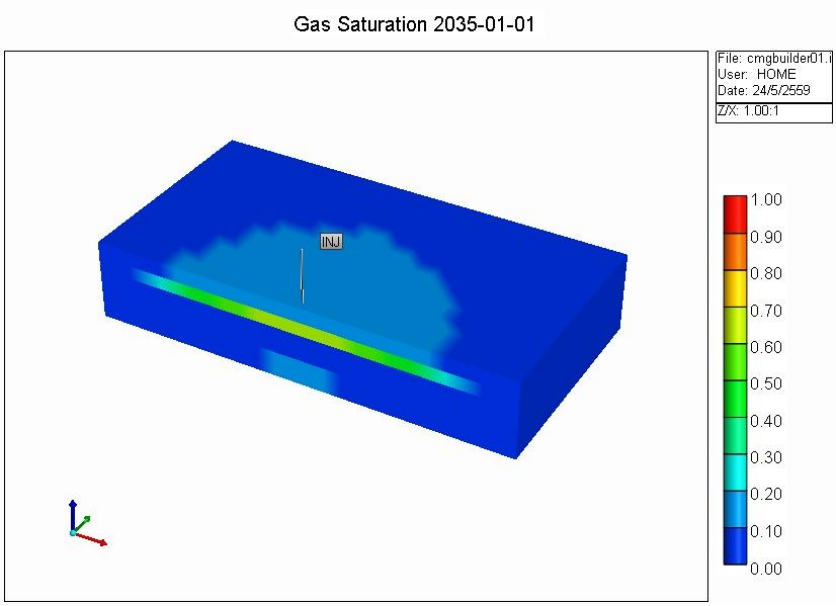

Figure 4.59 a. migration area from side in 2nd layer at Well 1 (20 years)
b. migration area from 3D in 2nd layer at Well 1 (20 years)

a.

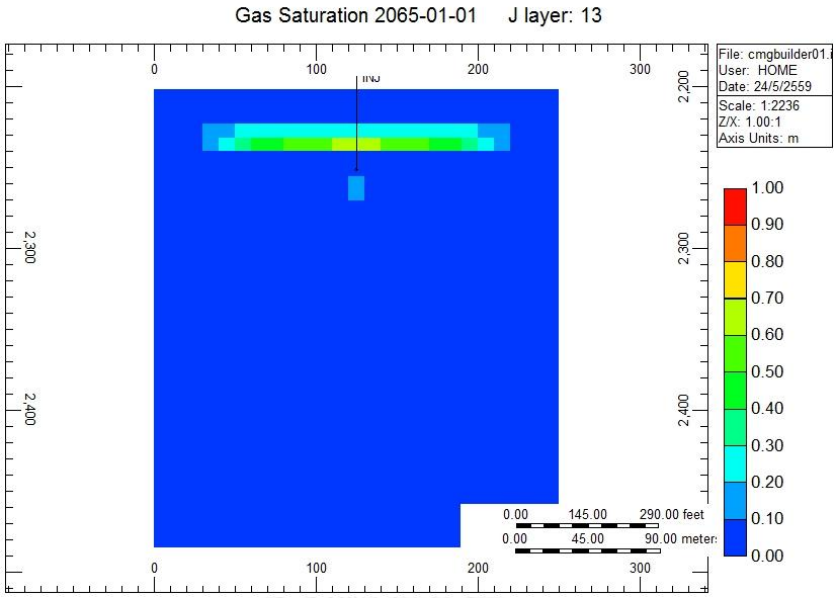

b.

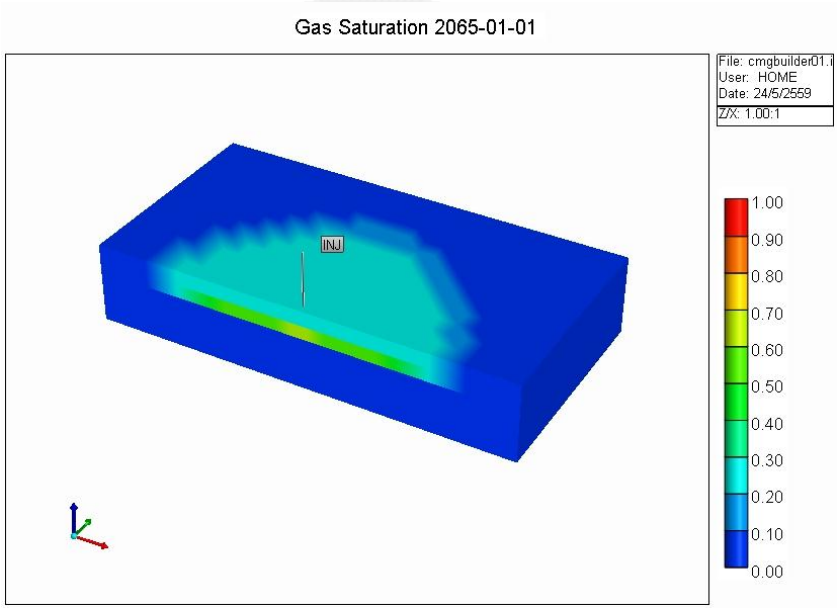

Figure 4.60 a. migration area from side in 2nd layer at Well 1 (50 years)
b. migration area from 3D in 2nd layer at Well 1 (50 years)

CHAPTER 5
CONCLUSIONS AND RECOMMENDATION

In this chapter conclusion and recommendation from simulation are presented. The study area is in North Malay basin in the Gulf of Thailand. There are 3 wells for inject CO_2. Well 1 is consisting of 2 layer of sand. Well 2 is consisting of 3 sand layers and Well 3 is consisting of 4 sand layers. The parameters that studied are pressure buildup, shutin time, storage capacity and plume migration. With the various conditions such as injection rate of CO_2 are 1,000 – 4,000 t/d, depth of target formation is approximately 2,160 – 2,510 m. The periods of time for study are 0-50 years.

5.1 Conclusions

In various parameters that are mention above, important parameters are pressure buildup and injection rate of CO_2. Because other parameters (shutin time, storage capacity and plume migration) are varied with pressure buildup and injection rate.

- The fracture pressure is an importance determinant. The 90% of fracture pressure, maximum pressure is used to set shutin time.That used to prevent caprock breaking.
- Pressure buildup is increasing until shutin time. After that pressure is decreasing gradually by period of time. Pressure of injection rate at 1,000 t/d is increasing slightly. The injection rate 2,000, 3,000 and 4,000 t/d are increasing sharply with increasing time after shutin pressure is decreasing gradually. Storage capacity is increasing with increasing time same as pressure buildup. The maximum of storage capacity is in shutin time period. In almost every cases, injection rate 1,000 t/d has storage capacity higher than other.
- Like pressure buildup, storage capacity is increasing with increasing time. The maximum storage capacity is in shutin time period and constant. In almost every cases, injection rate at 1,000 t/d has storage capacity higher than others because of the longest shutin period.

- The consideration of plume migration of CO_2 in terms of area and radius of migration is investigated, the expansion in large area is occurred within shutin time period. Plume migration of CO_2 is increasing until shutin time and decreasing gradually by the time. The CO_2 injected is move up from the bottom sand (injection point) to top sand.
- Time step to monitor or observe the effect on pressure buildup, storage capacity and plume migration is also studied for 50 years. First 5 years are important to observe the pressure buildup.
- Selected formation of this study is thin layer sand affecting to storage capacity in each well. The 3D results from simulation have shown that the CO_2 can leak to shale layer. Therefore, in this area thin layer have possibility for CO_2 to leak to the top.
- From the 3D result, it shows that CO_2 can leak into caprock. Because sand layer in this area is thin and in some caprock layer is thin as well. According to (ADB (People's Republic of China), 2011) studied geological storage criteria. The properties of target site are should to more than 1,500 depth, permeability is 10–50 md, porosity are 15-20 % and 8-10 %, reservoir thickness is 10-20 m.

5.2 Recommendations

- The lack of some important information, to run simulation is the main problem for the study. Fundamental data is needed to put in program. Finally, the result will be more reliable. This is the benefit for project in the future.
- Reliable data is used to decide the site that suitable to inject CO_2. Furthermore, if the map of area is used to create grid that the result will more sensible.
- Time step can be varied to find the best range for monitoring. From the study, time step is one of the issues to monitor for future study.

REFERENCES

ADB (People's Republic of China). (2011). Roadmap for the Demonstration of Carbon Capture and Storage (CCS) in China.

Asian Development Bank. (2013). *Prospects for CARBON CAPTURE and STORAGE in SOUTHEAST ASIA*. Philippines.

Bachu, S. (2003). Screening and ranking of sedimentary basins for sequestration of CO2 in geological media in response to climate change. *Environmental Geology, 44*(3), 277-289. doi: 10.1007/s00254-003-0762-9

Basbug, B. (2005). *modeling of carbon dioxide sequestration in deep saline aquifer.* (Master).

Blaber, D. M. (2005). Retrieved 3/4, 2016, from http://www.mikeblaber.org/oldwine/chm1045/notes/Forces/Liquids/Forces03.htm

Bouc, O., Gale, J., Herzog, H., Braitsch, J., Bouc, O., Audigane, P., . . . Seyedi, D. (2009). Greenhouse Gas Control Technologies 9Determining safety criteria for CO2 geological storage. *Energy Procedia, 1*(1), 2439-2446. doi: http://dx.doi.org/10.1016/j.egypro.2009.02.005

Bourgoyne et al. (1986). *applied drilling engineering*.

Center for climate and energy solusions. Retrieved 4/2, 2016, from http://www.c2es.org/facts-figures/international-emissions

Chadwick, R. A., & Eiken, O. (2013). Offshore CO_2 storage: Sleinper natural gas field beneath the North Sea. In G. Jon & S. Mathais (Eds.), *Geological storage of carbon dioxide (CO2):Geoscience, technologies, environmental aspects and legal frameworks* (pp. 227-248): Woodhead publishing.

ChemWiki, U. D. Retrieved 3/4, 2016

Chochawalit, A. (1985). *Basin analysis of tertiary strata In the Pattani basin The gulf of Thailand.* (Doctor), The university of british Columbia.

Chotpitayasunon, T. (2005). *Depositional environment of formation 2,central part of Arthit area in the North Malay Basin,South of Thailand.* (Bachelor), Chulalongkorn university.

Clark, J. N. (1969). *Elements of petroleum reservoirs*.

CMG. (2011). User's Guide GEM Advanced Compositional and GHG Reservoir Simulator Version 2011.

Dake, L. P. (1977). *Fundamentals of reservoir enginerring* ELSEVIER SCIENCE B.V.

Freund, P. (2013). Anthropogenic climate change and the role of CO_2 capture and storage (CCS). In G. Jon & S. Mathais (Eds.), *Geological storage of carbon dioxide (CO_2):Geoscience, technologies, environmental aspects and legal frameworks* (pp. 1-23): Woodhead publishing

global-greenhouse-warming. (2016). Retrieved 03/15, 2016, from http://www.global-greenhouse-warming.com/

Global CCS Institute. (2013). The Global Status of CCS: 2013. Retrieved 3/4, 2016, from https://www.globalccsinstitute.com/publications/global-status-ccs-2013

Gorecki, C. D., Sorensen, J. A., Bremer, J. M., Knudsen, D., Smith, S. A., Steadman, E. N., & Harju, J. A. (2009). *Development of Storage Coefficients for Determining the Effective CO2 Storage Resource in Deep Saline Formations*.

Holt, T., Jensen, J. I., & Lindeberg, E. (1995). Underground storage of CO2 in aquifers and oil reservoirs. *Energy Conversion and Management, 36*(6–9), 535-538. doi: http://dx.doi.org/10.1016/0196-8904(95)00061-H

IPCC. (2005). *IPCC Special Report on Carbon Dioxide Capture and Storage,* (O. D. Bert Metz, Heleen de Coninck,Manuela Loos,Leo Meyer Ed.).

Kananithikorn, T. (2005). *Reservoir Geometry Study: An integration of 3D seismic and well log data of the North Malay Basin, Gulf of Thailand.* (Bachelor), Chulalongkorn university.

Khositchaisri, P. (2005). *The structural geolmetry analysis; relative of structure and reservoir geometry of block a in the North Malay Basin,Gulf of Thailand.* (bacherlor), Chulalongkorn university.

Kongkanoi, C. (2008). *ubsurface correlation of formation 1, platform B arthit project gulf of Thailand using the climate stratigraphic approach.* (Graduate School), Chiang Mai University.

Mackay, E. J. (2013). Modelling the injectivity,migration and trapping of CO_2 in carbon capture and storage (CCS). In G. Jon & S. Mathais (Eds.), *Geological storage of carbon dioxide (CO2):Geoscience, technologies, environmental aspects and legal frameworks* (pp. 45-65): Woodhead publishing.

Mansor, M. Y., Rahman, A. H. A., Menier, D., & Pubellier, M. (2014). Structural evolution of Malay Basin, its link to Sunda Block tectonics. *Marine and Petroleum Geology, 58, Part B*, 736-748. doi: http://dx.doi.org/10.1016/j.marpetgeo.2014.05.003

Mathias et al. (2009). Screening and selection of sites for CO2 sequestration based on pressure buildup. *International Journal of Greenhouse Gas Control, 3*(5), 577-585. doi: http://dx.doi.org/10.1016/j.ijggc.2009.05.002

Ministry of energy. The gulf of Thailand. Retrieved 3/5, 2015, from http://www2.dmf.go.th

Morley, & Westaway. (2006). Subsidence in the super-deep Pattani and Malay basins of Southeast Asia: a coupledmodel incorporating lower-crustal flowin response to post-rift sediment loading. *Basin Research, 18*, 51-84. doi: 10.1111/j.1365-2117.2006.00285.x

Morley , K. C., & Racey, A. (2010). Tertiary stratigraphy. In R. F. Ridd , A. J. Barber & M. J. Crow (Eds.), *The geology of Thailand*.

Nguyan, T. (2013). Well Design - PE 413:Chapter 1: Fracture Pressure. Retrieved 9/18, 2015, from infohost.nmt.edu/~petro/faculty/Nguyen/PE413/Presentation/C1/2_FracturePressure.ppt Well Design - PE 413 Chapter 1: Fracture Pressure

Office of Natural Resources and Environmental Policy and Planning. (2010). Thailand's Second National Communication under the United Nations Framework Convention on Climate Change In M. o. N. R. a. Environment. & Bangkok (Eds.).

Pickup, G. E. (2013). CO_2 storage capacity calculation using static and dynamic modelling. In G. Jon & S. Mathais (Eds.), *Geological storage of carbon dioxide (CO_2):Geoscience, technologies, environmental aspects and legal frameworks* (pp. 26-43): Woodhead publishing

Plasynski et al. (2008). Weyburn carbon dioxide sequestration project.

Polachan et al. (1991). Development of Cenozoic basins in Thailand. *Marine and Petroleum Geology,, 8*.

Prakiat, D., & Jeemsantia, A. (2011). *pportunity for Carbon Dioxide Storage in Thailand:Mae Moh Power Station Case Study.* (Bachelor), Chulalongkorn University.

Purdue university. (2004). Surface tension. Retrieved 4/21, 2016, from http://chemed.chem.purdue.edu/genchem/topicreview/bp/ch14/property.php

Ringrose et al. (2013). GHGT-11 Proceedings of the 11th International Conference on Greenhouse Gas Control Technologies, 18-22 November 2012, Kyoto, JapanThe In Salah CO2 Storage Project: Lessons Learned and Knowledge Transfer. *Energy Procedia, 37*, 6226-6236. doi: http://dx.doi.org/10.1016/j.egypro.2013.06.551

Ruanman, N. (2015). *numerical simulation on carbon dioxide storage in san sai area, fang basin.* (Master), Chulalongkorn University.

shokir, E. Fracture Gradients. Retrieved 9/23, 2015, from http://faculty.ksu.edu.sa/shokir/PGE472/Lectures/fracture%20gradient%20-%20Part%20I.pdf

Silin et al. (2009). A one-dimensional model of vertical gas plume migration through a heterogeneous porous medium. *International Journal of Greenhouse Gas Control, 3*(3), 300-310. doi: http://dx.doi.org/10.1016/j.ijggc.2008.09.003

Staša, P., Matsui, K., Kramadibrata, S., Chovancová, K., Kebo, V., Chovanec, J., & Kodym, O. (2013). International Conference on Earth Science and Technology Proceedings September 2012Research of CO2 Storage Possibilities to the Underground. *Procedia Earth and Planetary Science, 6*, 14-23. doi: http://dx.doi.org/10.1016/j.proeps.2013.01.002

Torp, A. T., & Gale, J. (2004). Demonstrating storage of CO2 in geological reservoirs: The Sleipner and SACS projects. *Energy, 29*(9–10), 1361-1369. doi: http://dx.doi.org/10.1016/j.energy.2004.03.104

Underschultz, J., Boreham, C., Dance, T., Stalker, L., Freifeld, B., Kirste, D., & Ennis-King, J. (2011). CO2 storage in a depleted gas field: An overview of the CO2CRC Otway Project and initial results. *International Journal of Greenhouse Gas Control, 5*(4), 922-932. doi: http://dx.doi.org/10.1016/j.ijggc.2011.02.009

Urroz, E. G. (2005). Ch 2 – Properties of Fluids - II.

Vanner, R. (2005). Energy Use in Offshore Oil and Gas Production:Trends and Drivers for Efficiency from 1975 to 2025.

Whittaker, S., & Perkins, E. (2013). Technologies aspects of carbon enhanced oil recovery and associated storage.

Wilcox, J., Rochana P., . (2011). Workshop on Carbon Capture and Storage.

APPENDIX A

This section shows parameters that use in CMG program.

Well 1
Setting data 1st layer

Parameter	1st layer
Grid type	Cartesian
Number of blocks (i x j x k)	25 x 25 x 9
Block widths in I direction	25 x 10
Block widths in J direction	25 x 10

Setting data 2nd layer

Parameter	2nd layer
Grid type	Cartesian
Number of blocks (i x j x k)	25 x 25 x 10
Block widths in I direction	25 x 10
Block widths in J direction	25 x 10

Setting data all layer

Parameter	2nd layer
Grid type	Cartesian
Number of blocks (i x j x k)	25 x 25 x 15
Block widths in I direction	25 x 10
Block widths in J direction	25 x 10

Reservoir properties

1st layer (Bottom layer)

Layer	Grid top(m)	Grid thickness(m)	Perm I	Porosity
1	2255.80	91.73	0.46	0.124
2	2347.53	91.73	0.29	0.12
3	2439.27	30.86	0.12	0.068
4	2470.14	15	0.8	0.18
5	2485.14	7.75	436.02	0.20
6	2492.89	7.75	104.47	0.24
7	2500.64	7.75	180.30	0.22
8	2508.40	9	0.053	0.029
9	2517.40	21	0.8	0.18

2nd layer (Top layer)

Layer	Grid top(m)	Grid thickness(m)	Perm I	Porosity
1	2202.10	10.50	0.02	0.028
2	2212.60	10.50	0.45	0.17
3	2223.10	9	0.12	0.06
4	2232.10	7.90	241.48	0.19
5	2240	7.90	80.72	0.17
6	2247.90	7.90	229.61	0.19
7	2255.80	15	0.46	0.12
8	2270.80	30.86	0.29	0.12
9	2301.60	91.73	0.12	0.068
10	2393.40	91.73	0.8	0.18

All layers

Layer	Grid top(m)	Grid thickness(m)	Perm I	Porosity
1	2202.10	10.5	0.018	0.02
2	2212.60	10.5	0.45	0.17
3	2223.10	9	0.12	0.06
4	2232.10	7.9	241.48	0.19
5	2240	7.9	80.72	0.17
6	2247.90	7.9	229.61	0.19
7	2255.80	91.73	0.46	0.12
8	2347.53	91.73	0.29	0.12
9	2439.27	30.86	0.12	0.068
10	2470.14	15	0.8	0.18
11	2485.14	7.75	436.02	0.20
12	2492.89	7.75	104.47	0.24
13	2500.64	7.75	180.30	0.22
14	2508.40	9	0.053	0.029
15	2517.40	21	0.8	0.18

Well 2

Setting data 1st layer

Parameter	1st layer
Grid type	Cartesian
Number of blocks (i x j x k)	25 x 25 x 8
Block widths in I direction	25 x 10
Block widths in J direction	25 x 10

Setting data 2nd layer

Parameter	2nd layer
Grid type	Cartesian
Number of blocks (i x j x k)	25 x 25 x 8
Block widths in I direction	25 x 10
Block widths in J direction	25 x 10

Setting data 3rd layer

Parameter	2nd layer
Grid type	Cartesian
Number of blocks (i x j x k)	25 x 25 x 8
Block widths in I direction	25 x 10
Block widths in J direction	25 x 10

Setting data all layer

Parameter	2nd layer
Grid type	Cartesian
Number of blocks (i x j x k)	25 x 25 x 16
Block widths in I direction	25 x 10
Block widths in J direction	25 x 10

Reservoir properties

1st layer (Bottom layer)

Layer	Grid top(m)	Grid thickness(m)	Perm I	Porosity
1	2307.35	3.13	0.13	0.07
2	2310.48	3.28	69.18	0.20
3	2313.76	3.28	104.47	0.24
4	2317.04	3.28	80.72	0.17
5	2320.33	3.28	236.05	0.28
6	2323.61	3.28	104.47	0.24
7	2326.90	15	0.80	0.18
8	2341.90	15	0.13	0.07

2nd layer (Middle layer)

Layer	Grid top(m)	Grid thickness(m)	Perm I	Porosity
1	2276.24	8.96	0.45	0.17
2	2285.21	4.96	0.05	0.03
3	2290.17	4	0.18	0.08
4	2294.17	3.29	136.14	0.18
5	2297.46	3.29	371.77	0.27
6	2300.76	3.29	136.14	0.18
7	2304.06	3.29	442.58	0.27
8	2307.35	3.13	0.12	0.07

3rd layer (Top layer)

Layer	Grid top(m)	Grid thickness(m)	Perm I	Porosity
1	2235.21	15.00	0.45	0.17
2	2250.21	7.50	0.80	0.18
3	2257.71	7.50	0.05	0.03
4	2265.21	3.68	104.47	0.24
5	2268.89	3.68	236.05	0.28
6	2272.56	3.68	64.57	0.23
7	2276.24	8.97	0.45	0.17
8	2285.2	8.97	0.05	0.03

All layers

Layer	Grid top(m)	Grid thickness(m)	Perm I	Porosity
1	2235.21	15	0.453	0.17
2	2250.21	15	0.8	0.18
3	2265.21	3.676	104.472	0.24
4	2268.89	3.676	236.048	0.28
5	2272.56	3.676	64.565	0.23
6	2276.24	8.965	0.453	0.17
7	2285.2	8.965	0.053	0.0298
8	2294.17	3.295	136.144	0.18
9	2297.46	3.295	371.773	0.26638
10	2300.76	6.59	289.37	0.225
11	2307.35	3.13	0.126	0.0684
12	2310.48	3.284	69.183	0.2
13	2313.76	6.568	92.599	0.21
14	2320.33	6.568	170.26	0.26
15	2326.9	15	0.8	0.18
16	2341.9	15	0.126	0.0684

Well 3

Setting data 1st layer

Parameter	1st layer
Grid type	Cartesian
Number of blocks (i x j x k)	25 x 25 x 13
Block widths in I direction	25 x 10
Block widths in J direction	25 x 10

Setting data 2nd layer

Parameter	2nd layer
Grid type	Cartesian
Number of blocks (i x j x k)	25 x 25 x 12
Block widths in I direction	25 x 10
Block widths in J direction	25 x 10

Setting data 3rd layer

Parameter	2nd layer
Grid type	Cartesian
Number of blocks (i x j x k)	25 x 25 x 10
Block widths in I direction	25 x 10
Block widths in J direction	25 x 10

Setting data 4th layer

Parameter	2nd layer
Grid type	Cartesian
Number of blocks (i x j x k)	25 x 25 x 10
Block widths in I direction	25 x 10
Block widths in J direction	25 x 10

Setting data all layer

Parameter	2nd layer
Grid type	Cartesian
Number of blocks (i x j x k)	25 x 25 x 16
Block widths in I direction	25 x 10
Block widths in J direction	25 x 10

Reservoir properties

1st layer (Bottom layer)

Layer	Grid top(m)	Grid thickness(m)	Perm I	Porosity
1	2258.87	24.18	0.13	0.07
2	2283.05	24.18	0.80	0.18
3	2307.23	12.09	0.45	0.17
4	2319.32	12.09	0.45	0.17
5	2331.42	2.44	442.59	0.27
6	2333.86	2.44	64.57	0.23
8	2336.30	2.44	436.02	0.20
9	2338.73	2.44	69.18	0.20
10	2341.17	2.44	277.67	0.23
11	2343.61	2.44	78.52	0.21
12	2346.05	15	0.13	0.07
13	2361.05	15	0.05	0.03

2nd layer (Middle layer)

Layer	Grid top(m)	Grid thickness(m)	Perm I	Porosity
1	2191.21	18.18	0.018	0.02
2	2209.40	18.18	0.12	0.06
3	2227.58	9.09	0.018	0.02
4	2236.67	9.09	0.018	0.02
5	2245.77	3.27	111.68	0.21
6	2249.05	3.27	136.14	0.18
7	2252.32	3.27	171.93	0.22
8	2255.60	3.27	273.52	0.26
9	2258.87	12.09	0.12	0.06
10	2270.96	12.09	0.80	0.18
11	2283.05	24.18	0.45	0.17
12	2307.24	24.18	0.45	0.17

3rd layer (Middle layer)

Layer	Grid top(m)	Grid thickness(m)	Perm I	Porosity
1	2171.21	5.28	0.13	0.07
2	2176.48	5.28	0.45	0.17
3	2181.76	2.36	273.53	0.26
4	2184.12	2.36	104.47	0.24
5	2186.49	2.36	180.30	0.22
6	2188.85	2.36	171.93	0.22
7	2191.21	9.09	0.45	0.17
8	2200.31	9.09	0.02	0.03
9	2209.40	18.19	0.13	0.07
10	2227.58	18.19	0.02	0.03

4th layer (Top layer)

Layer	Grid top(m)	Grid thickness(m)	Perm I	Porosity
1	2132.27	8	0.8	0.18
2	2140.27	8	0.05	0.03
3	2148.27	7	0.8	0.18
4	2155.27	7	0.05	0.03
5	2162.27	2.23	442.59	0.27
6	2164.50	2.23	180.30	0.22
7	2166.73	2.23	79.91	0.17
8	2168.97	2.23	371.77	0.27
9	2171.20	5.28	0.13	0.07
10	2176.48	5.28	0.45	0.17

All layers

Layer	Grid top(m)	Grid thickness(m)	Perm I	Porosity
1	2132.27	30	0.8	0.18
2	2162.27	4.46	442.59	0.27
3	2166.74	4.46	180.30	0.22
4	2171.20	5.28	0.05	0.029
5	2176.48	5.28	0.13	0.07
6	2181.76	4.72	79.91	0.17
7	2186.49	4.72	371.77	0.26
8	2191.21	27.28	0.45	0.17
9	2218.49	27.28	0.02	0.03
10	2245.77	6.55	273.53	0.26
11	2252.32	6.55	104.47	0.24
12	2258.87	36.27	0.13	0.07
13	2295.15	36.27	0.02	0.03
14	2331.42	7.315	180.30	0.22
15	2338.74	7.315	171.93	0.22
16	2346.05	30	0.12	0.07

APPENDIX B

This section shows the simulation result in Well 1, Well 2 and Well 3. That presented in 3D model and cross section. With time period 1, 5, 10, 20 and 50 years. Injection rate at 1,000-4,000 t/d

Well 1

All layer at 1,000 t/d injection rate.

a.

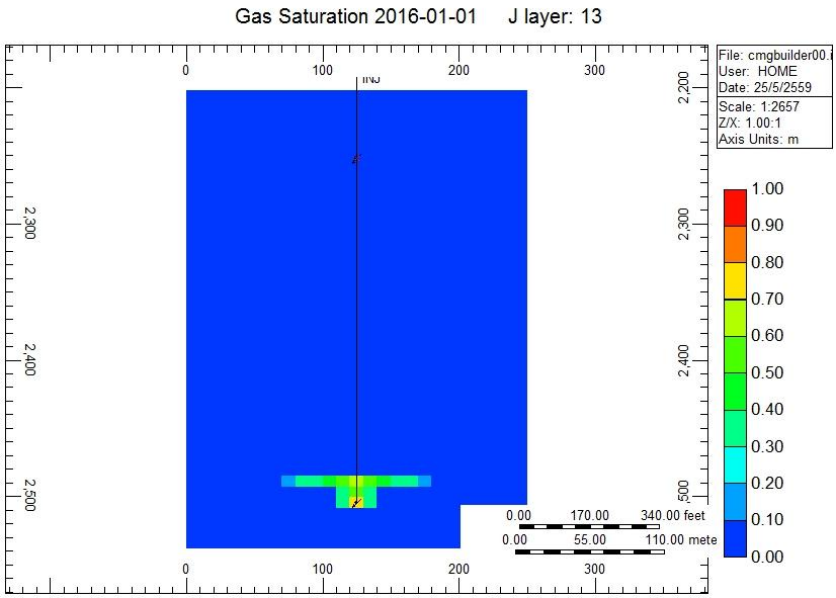

b.

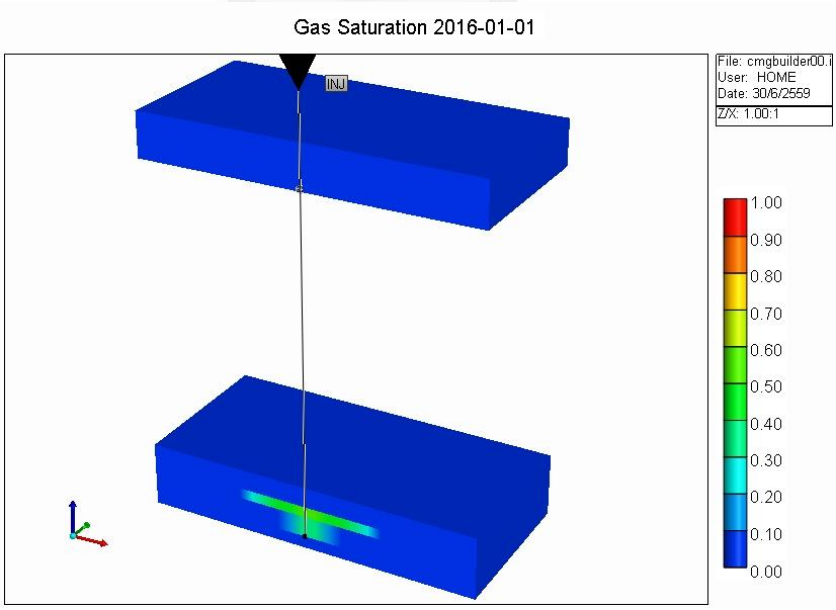

a. side view (1 year) and b. 3D view (1 year) in all layer at Well 1

a.

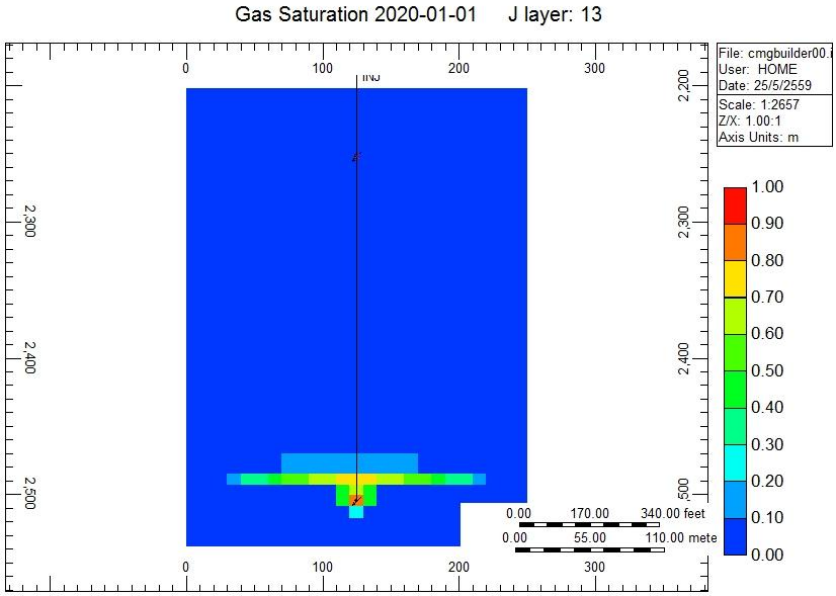

b.

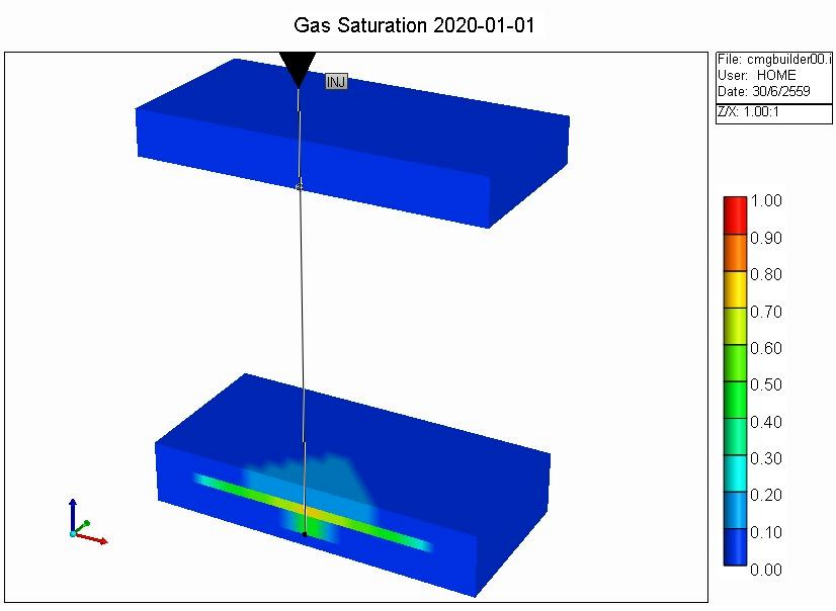

a. side view (5 years) and b. 3D view (5 years) in all layer at Well 1

a.

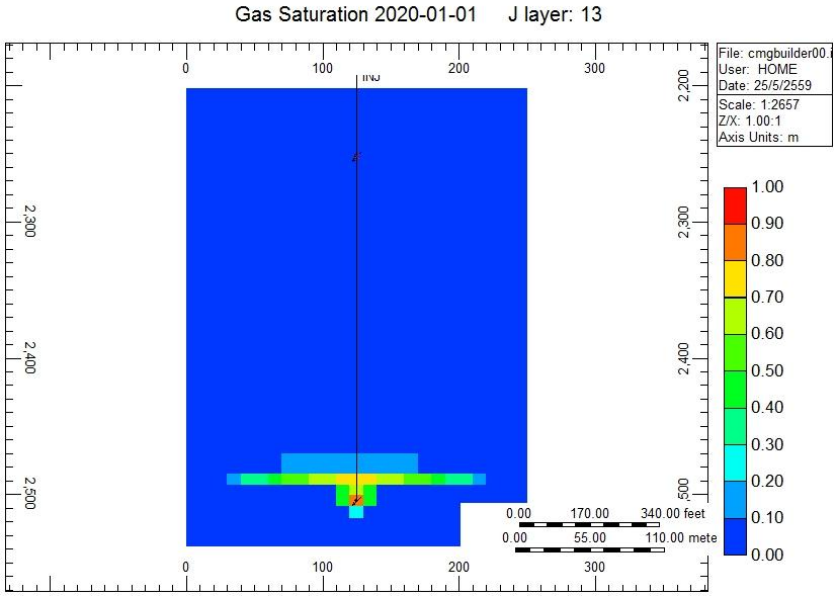

b.

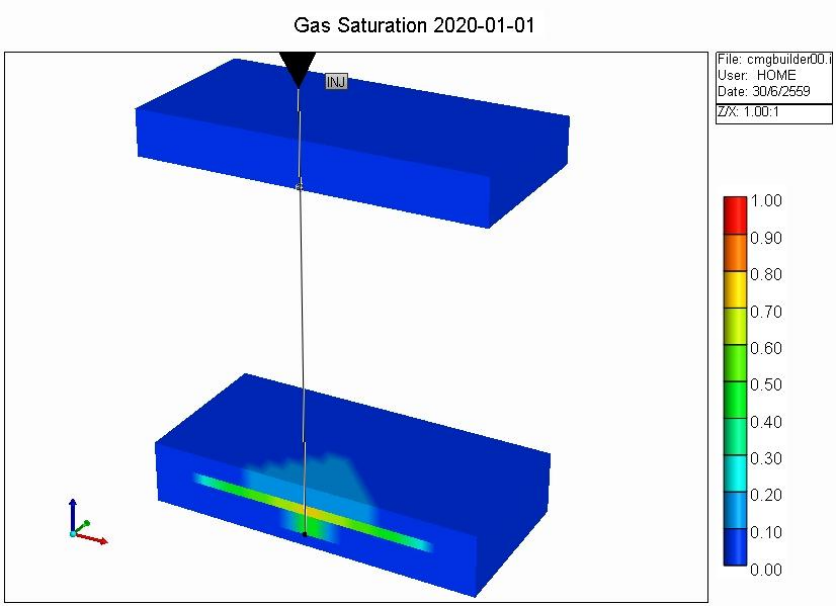

a. side view (10 years) and b. 3D view (10 years) in all layer at Well 1

a.

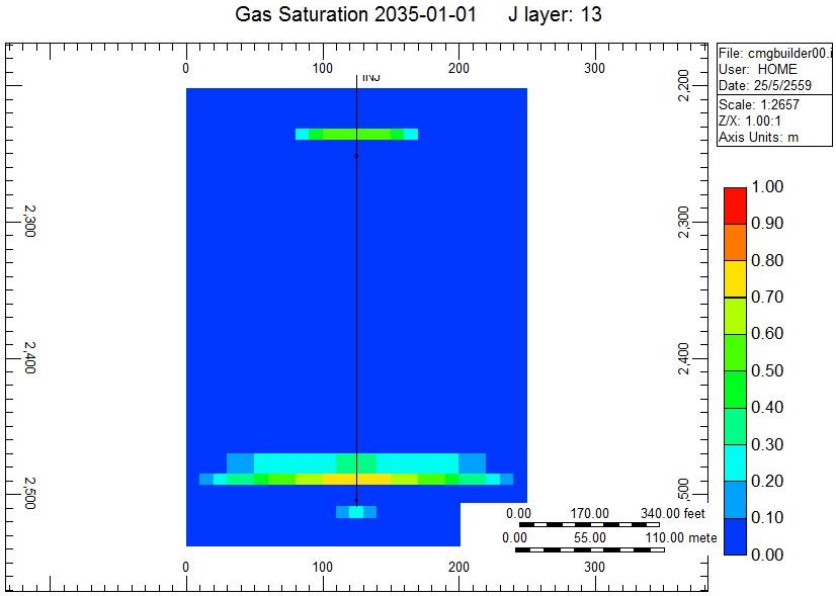

b.

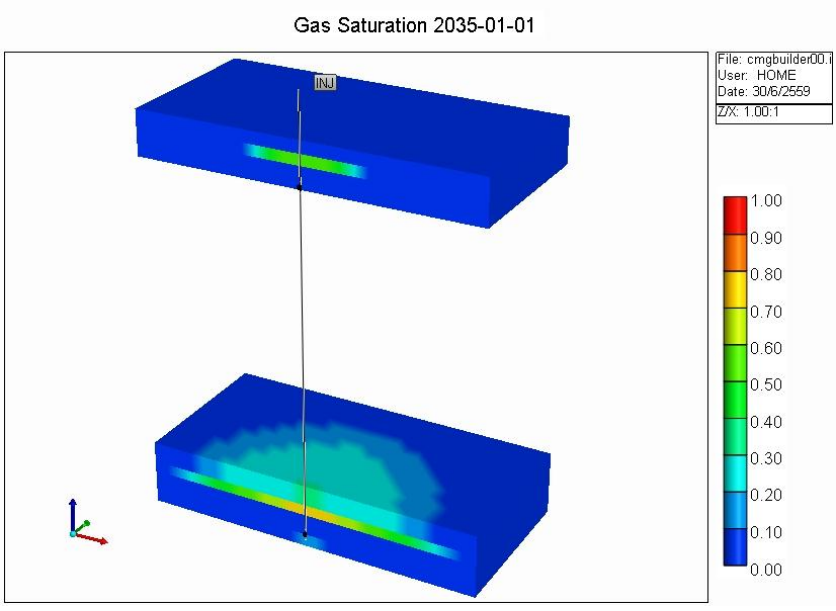

a. side view (20 years) and b. 3D view (20 years) in all layer at Well 1

a.

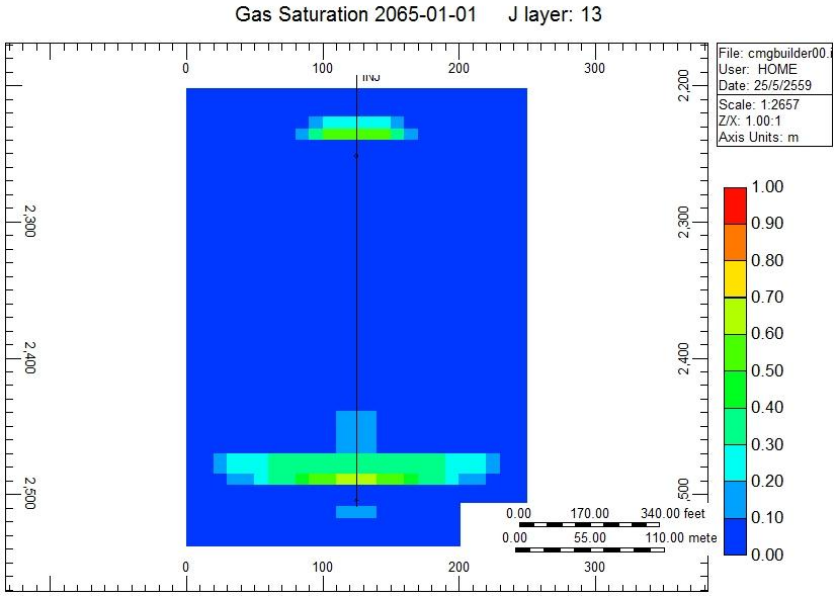

b.

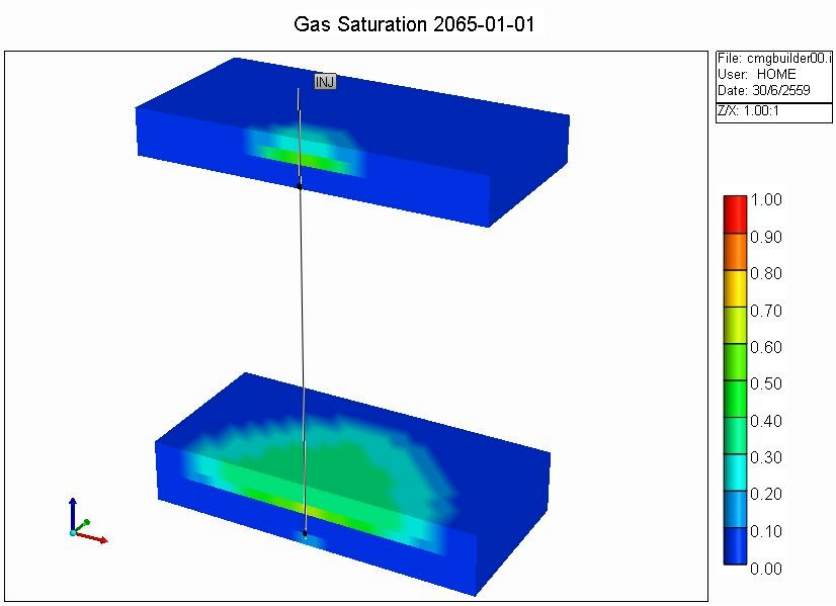

a. side view (50 years) and b. 3D view (50 years) in all layer at Well 1

All layer at 2,000 t/d injection rate.

a.

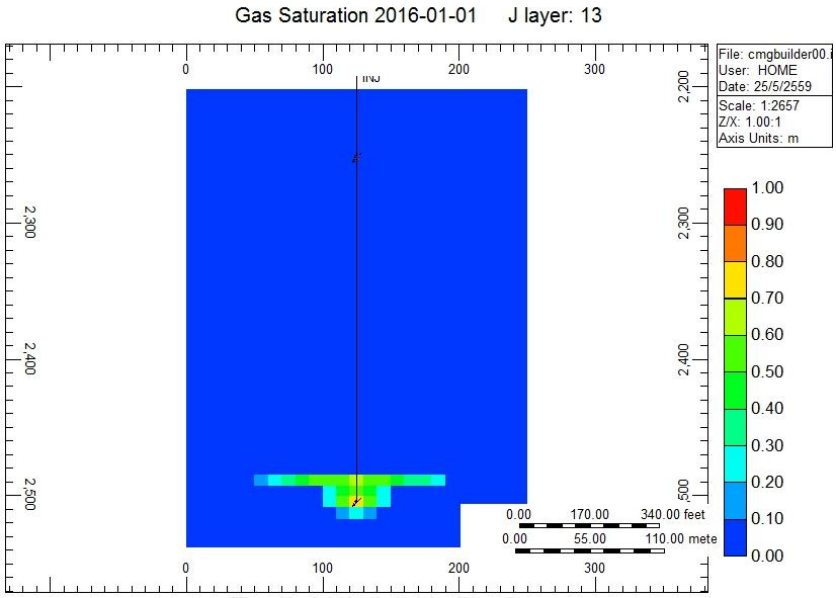

b.

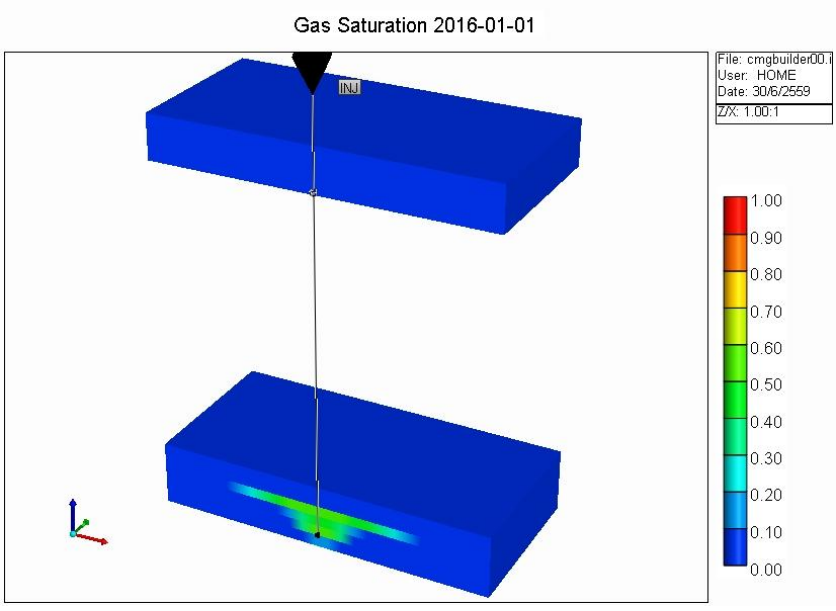

a. side view (1 year) and b. 3D view (1 year) in all layer at Well 1

a.

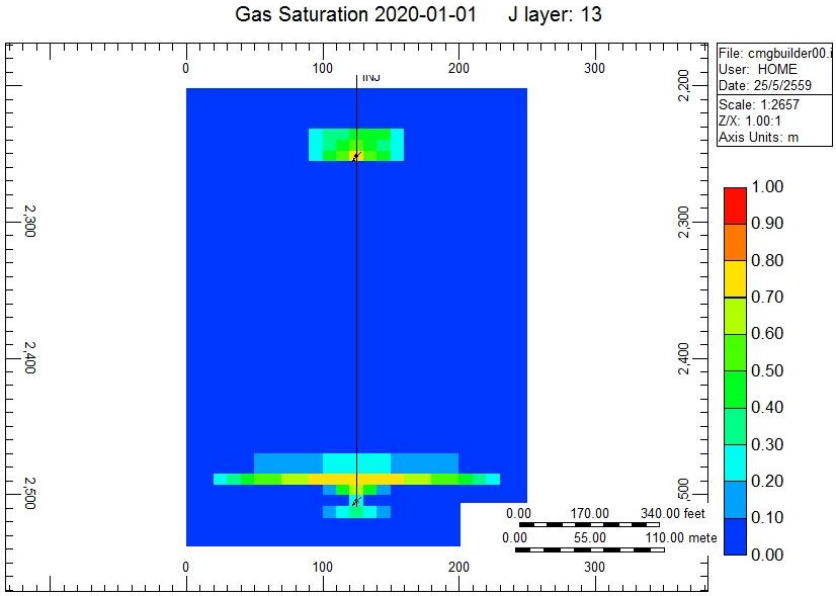

b.

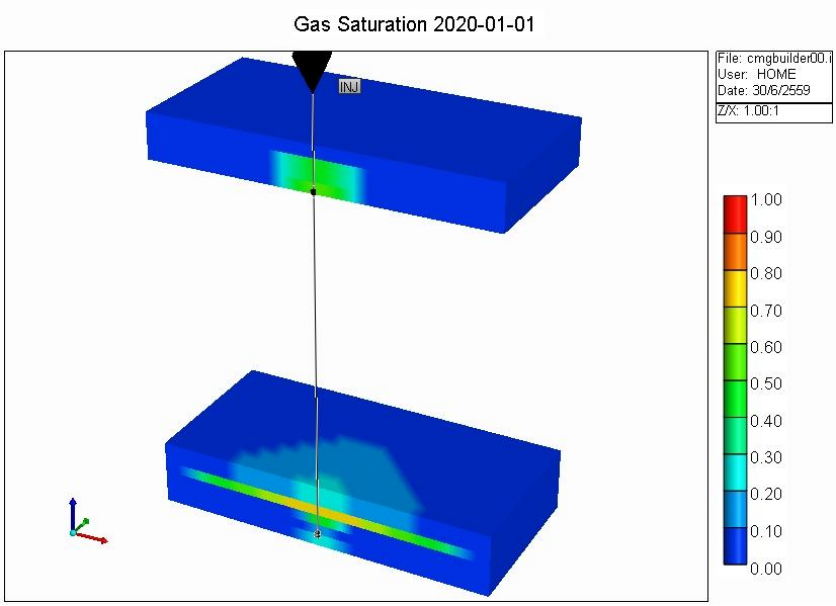

a. side view (5 years) and b. 3D view (5 years) in all layer at Well 1

a.

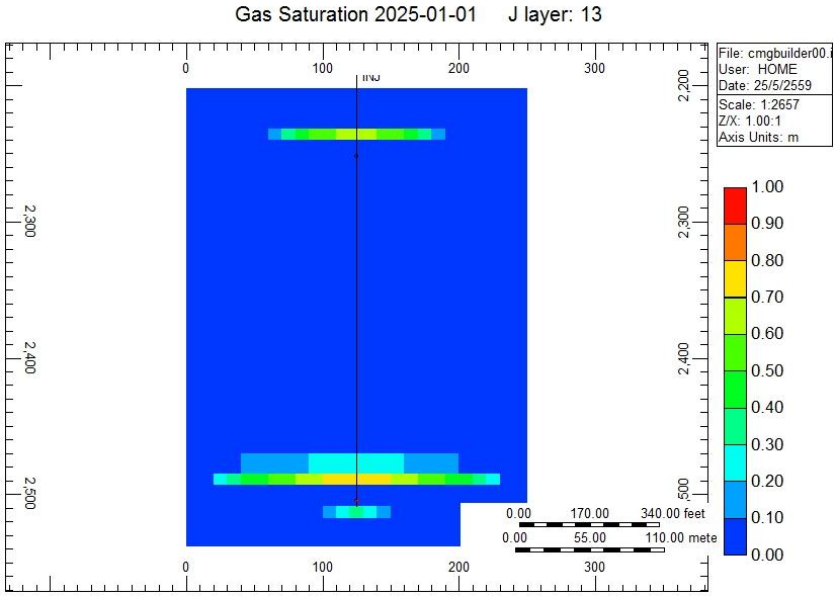

b.

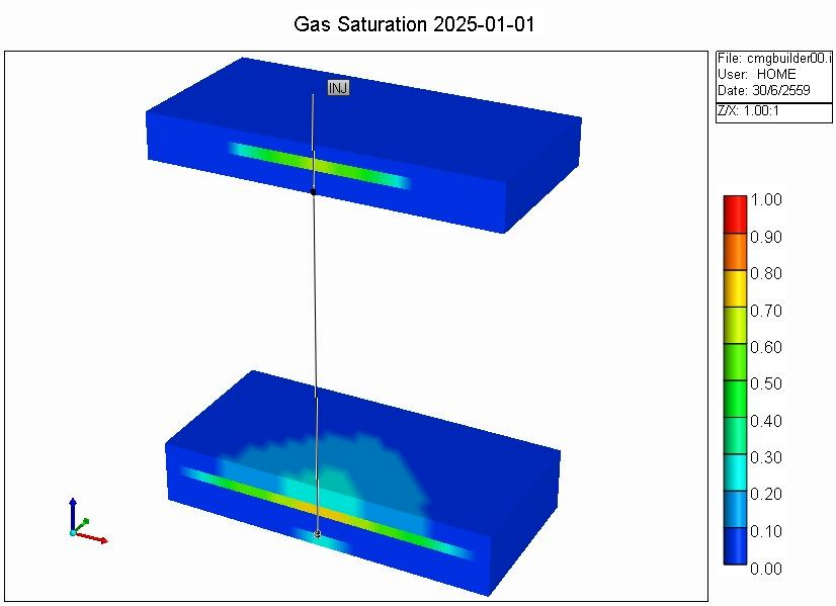

a. side view (10 years) and b. 3D view (10 years) in all layer at Well 1

a.

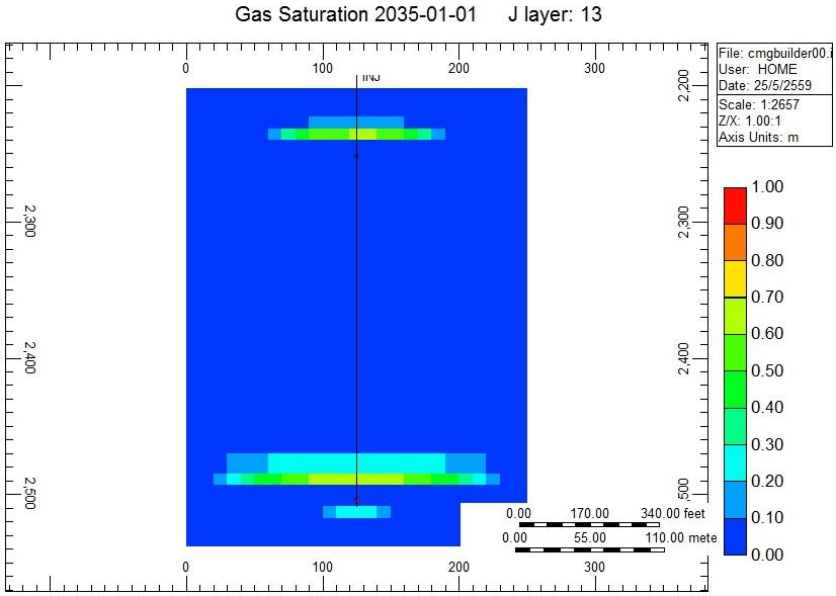

b.

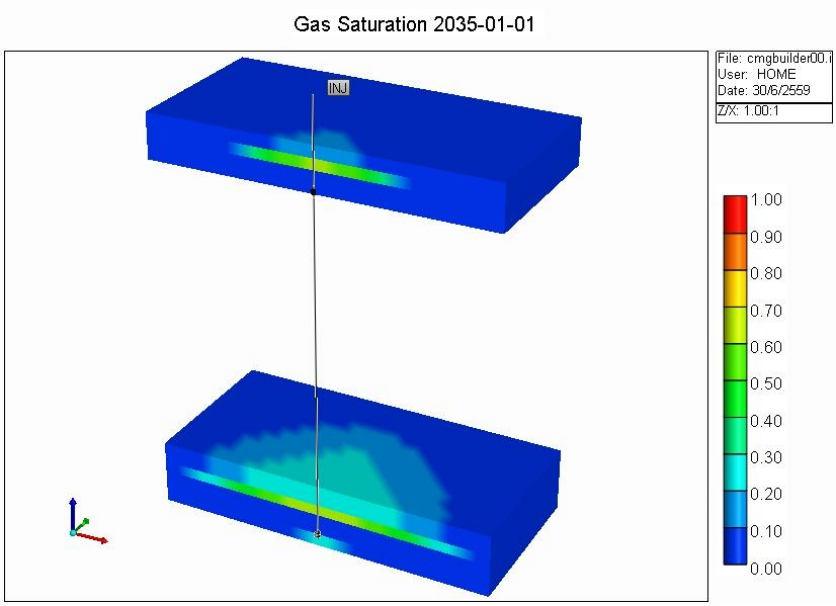

a. side view (20 years) and b. 3D view (20 years) in all layer at Well 1

a.

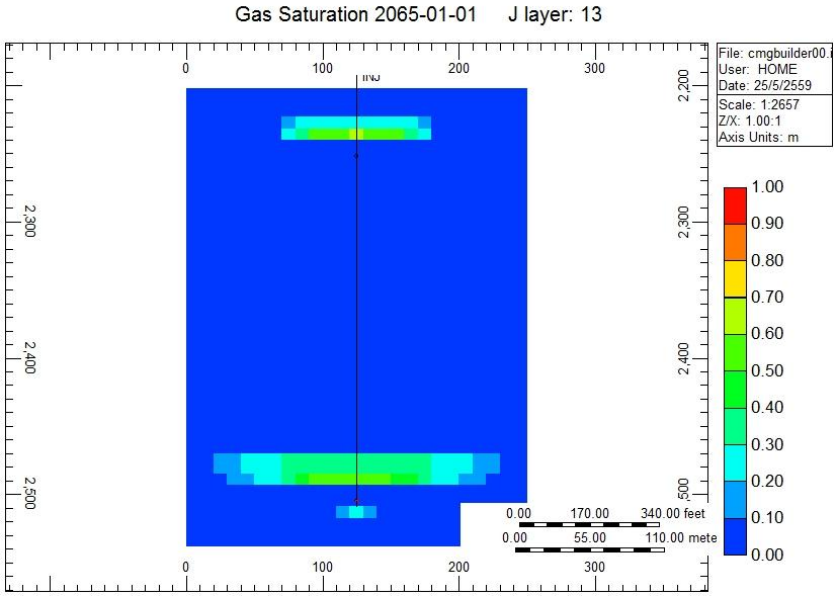

b.

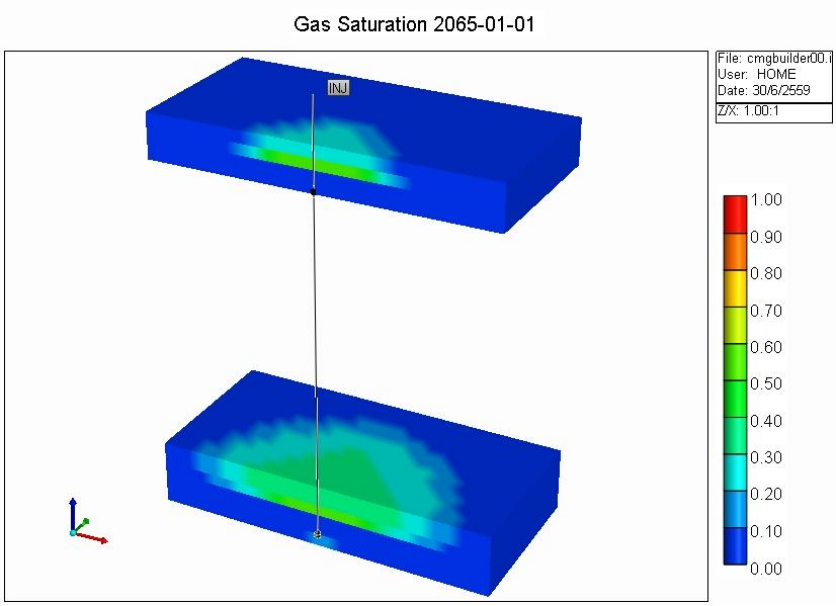

a. side view (50 years) and b. 3D view (50 years) in all layer at Well 1

All layer at 3,000 t/d injection rate.

a.

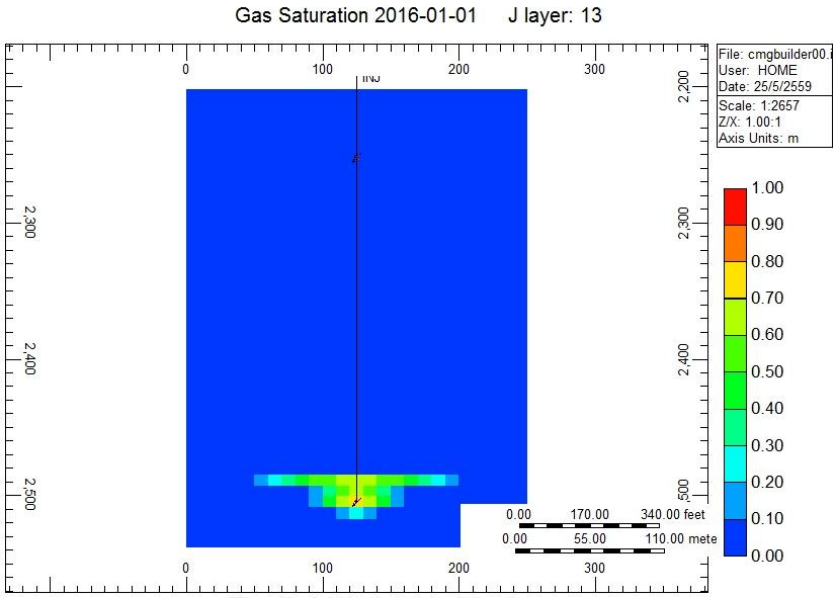

b.

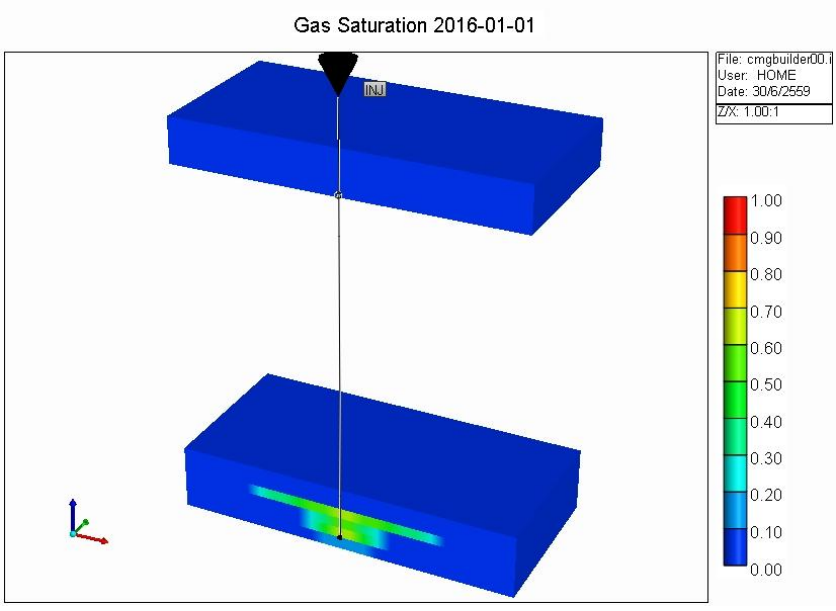

a. side view (1 year) and b. 3D view (1 year) in all layer at Well 1

a.

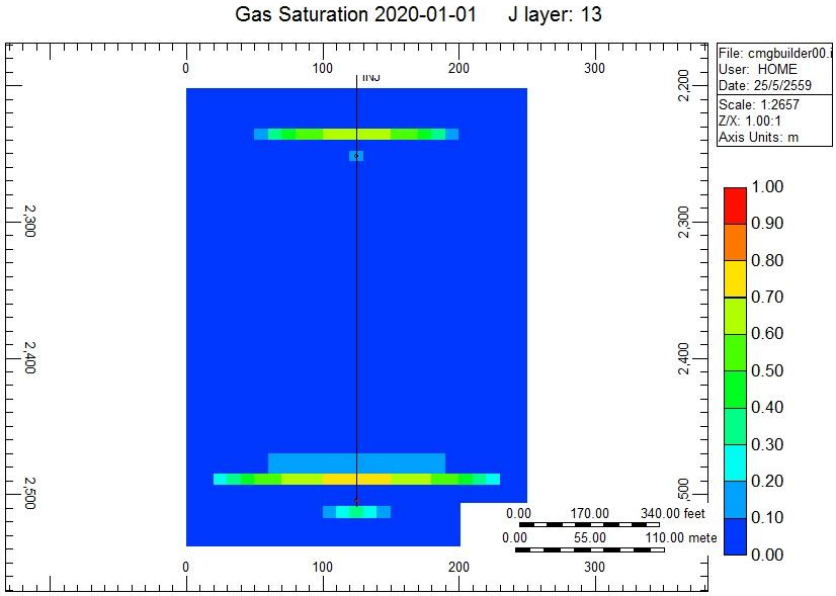

b.

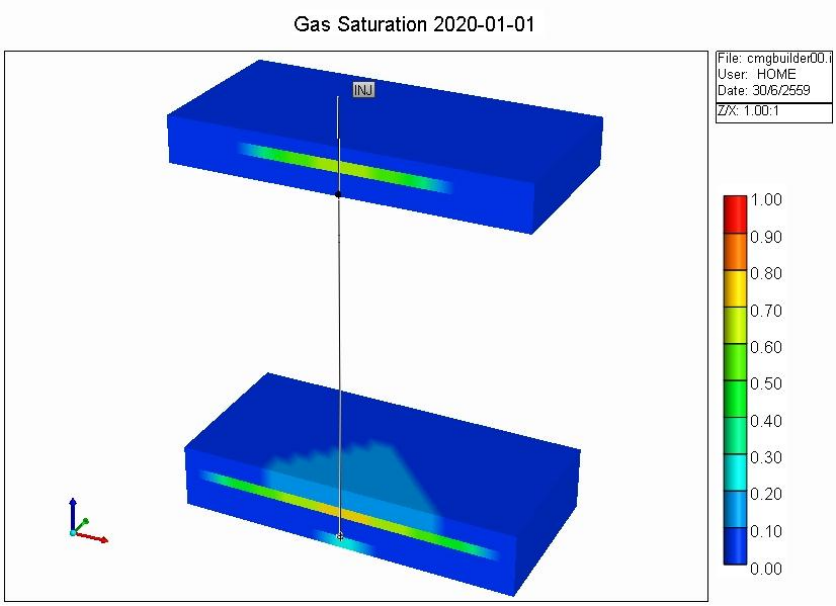

a. side view (5 years) and b. 3D view (5 years) in all layer at Well 1

a.

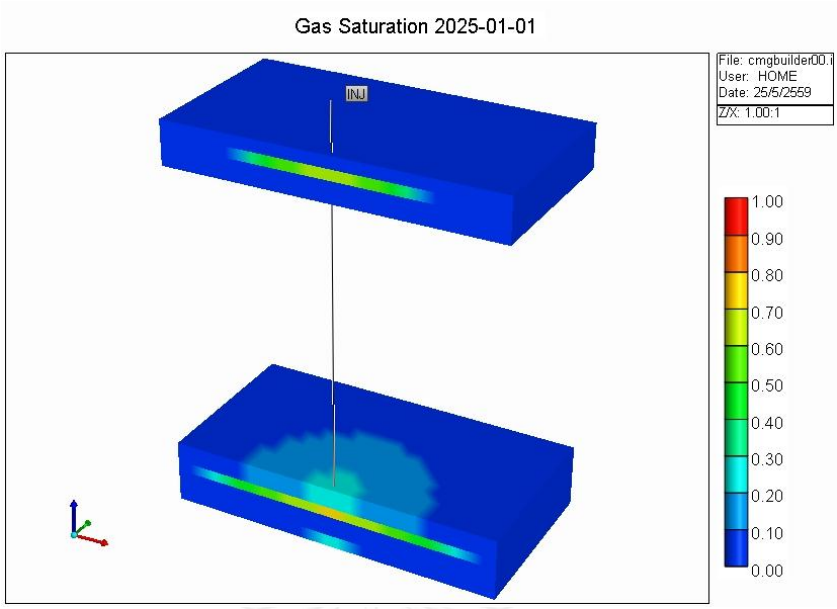

b.

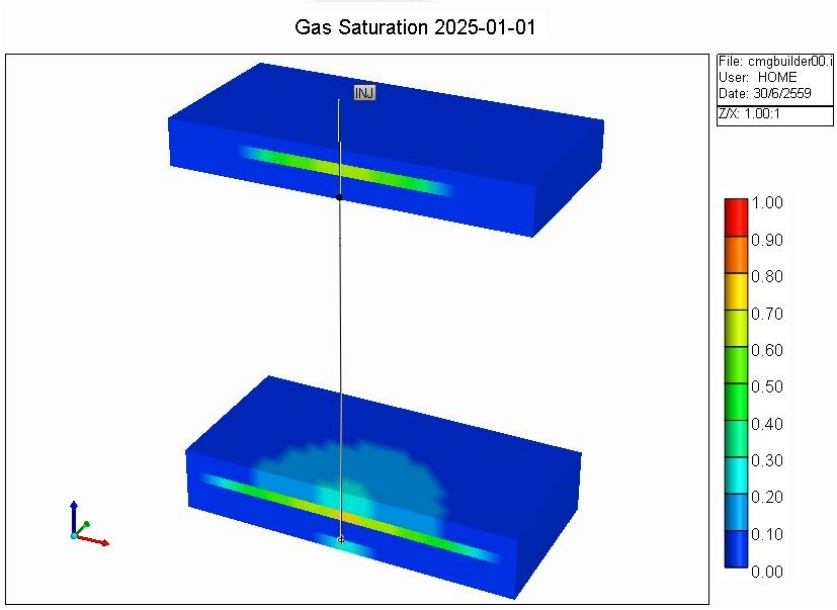

a. side view (10 years) and b. 3D view (10 years) in all layer at Well 1

a.

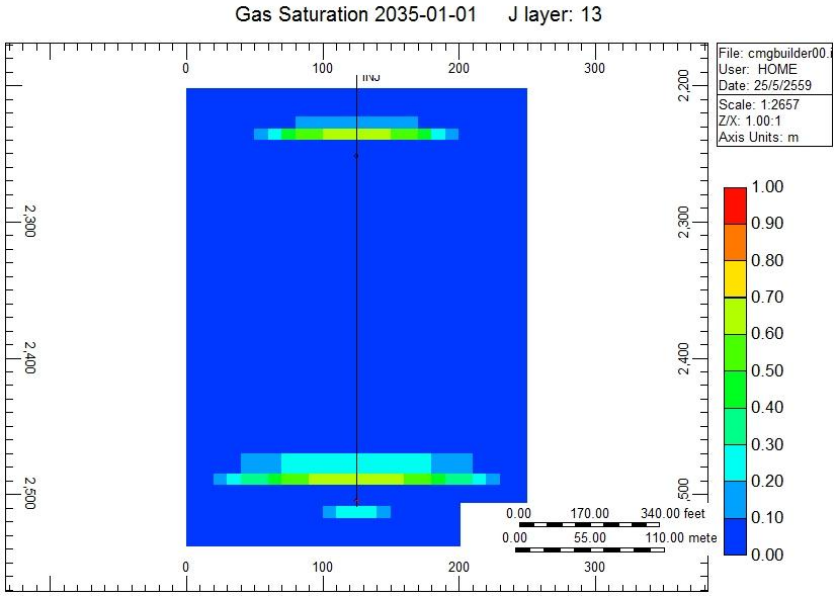

b.

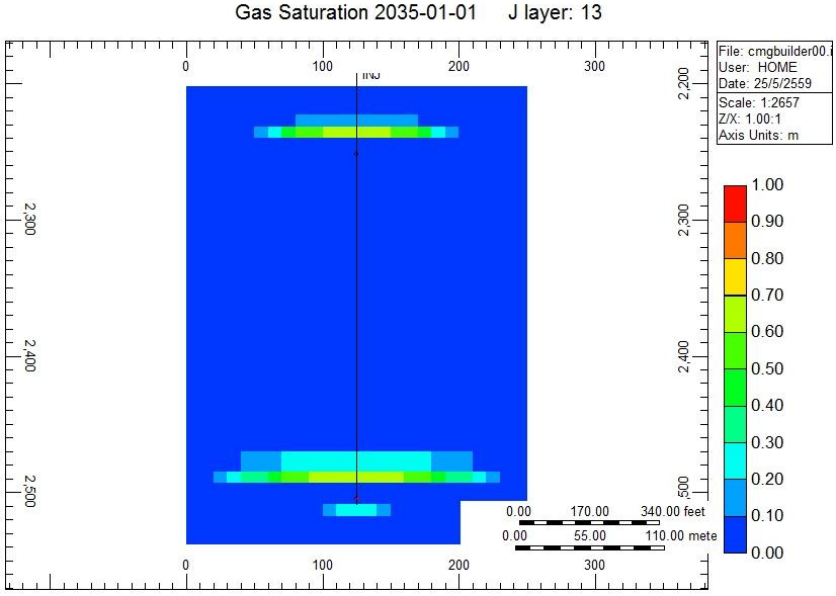

a. side view (20 years) and b. 3D view (20 years) in all layer at Well 1

a.

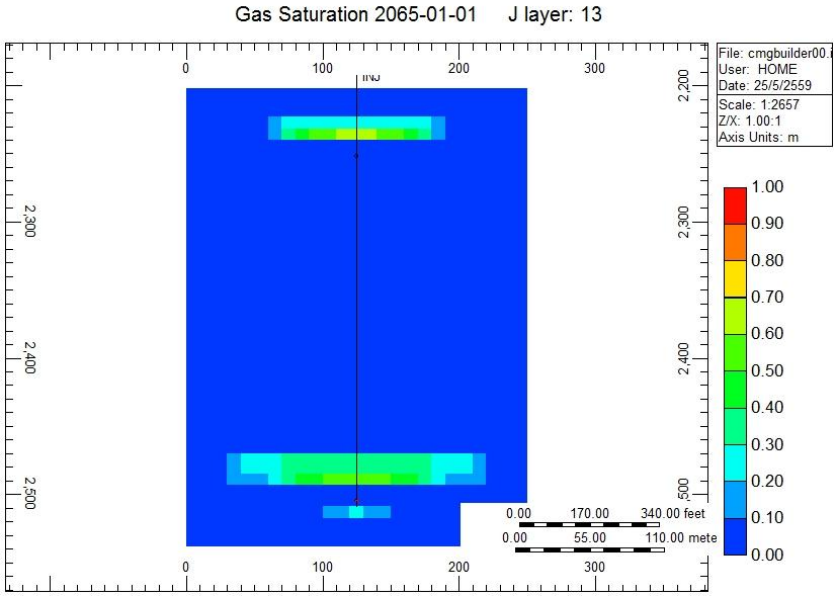

b.

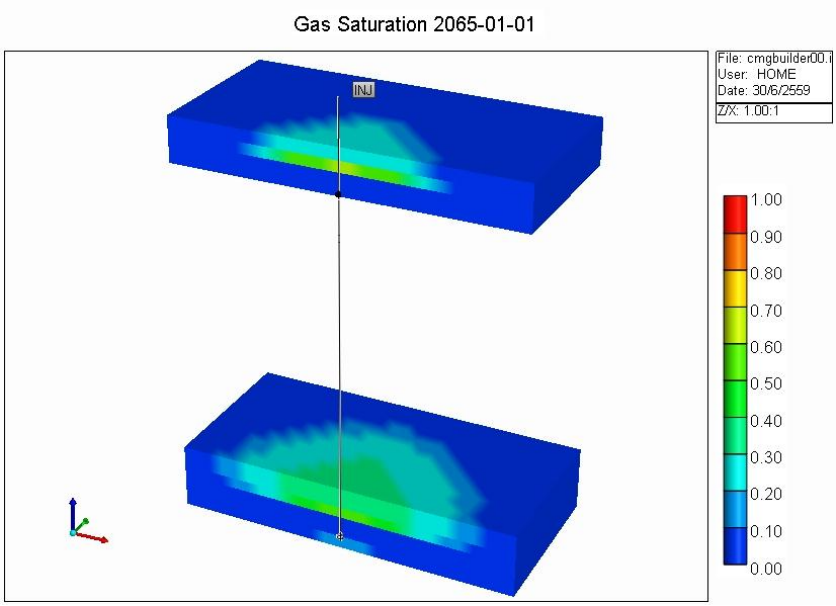

a. side view (50 years) and b. 3D view (50 years) in all layer at Well 1

All layer at 4,000 t/d injection rate.

a.

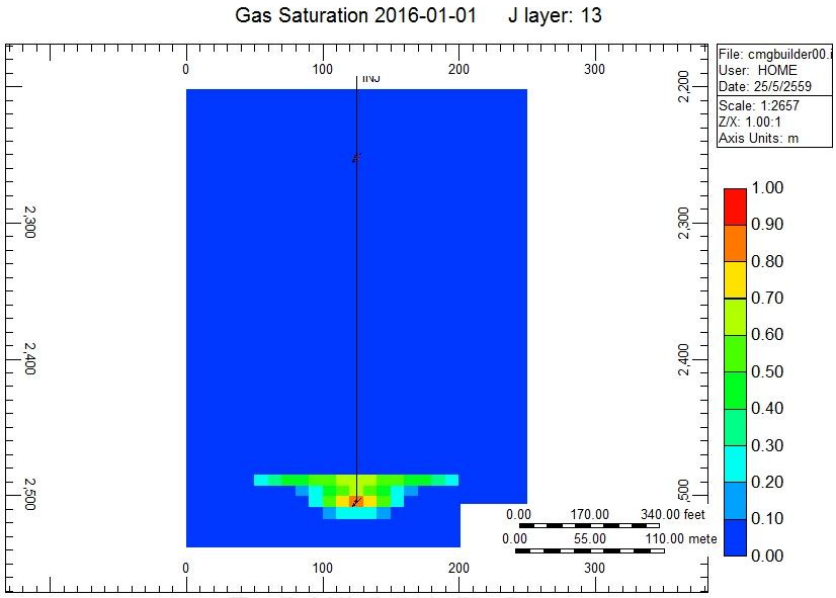

b.

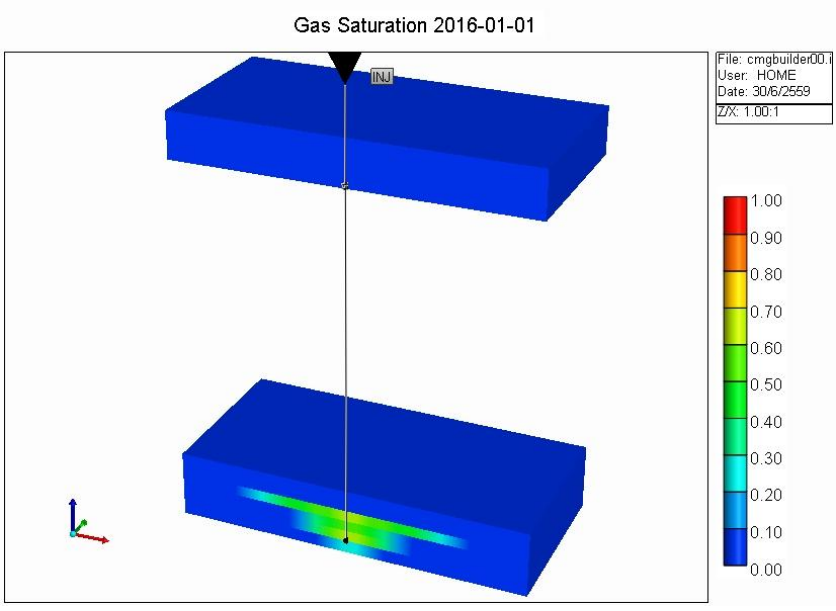

a. side view (1 year) and b. 3D view (1 year) in all layer at Well 1

a.

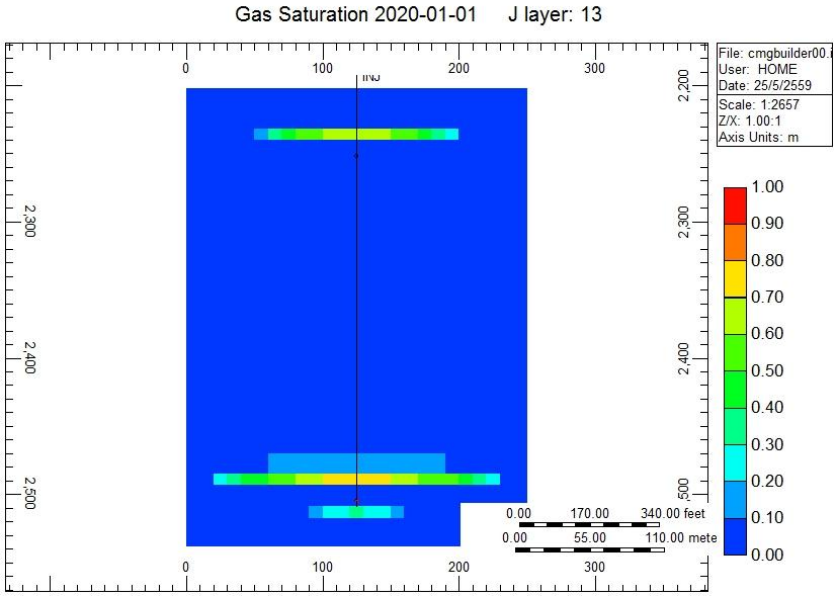

b.

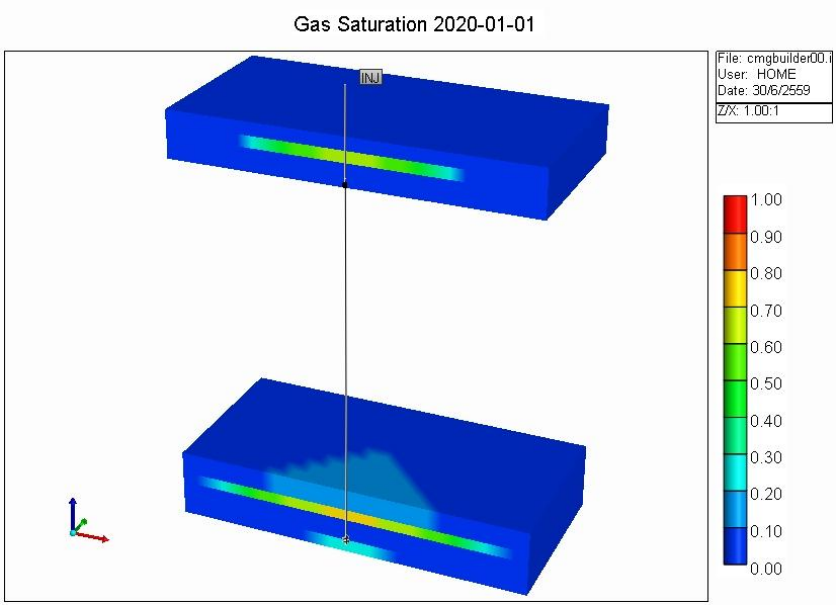

a. side view (5 years) and b. 3D view (5 years) in all layer at Well 1

a.

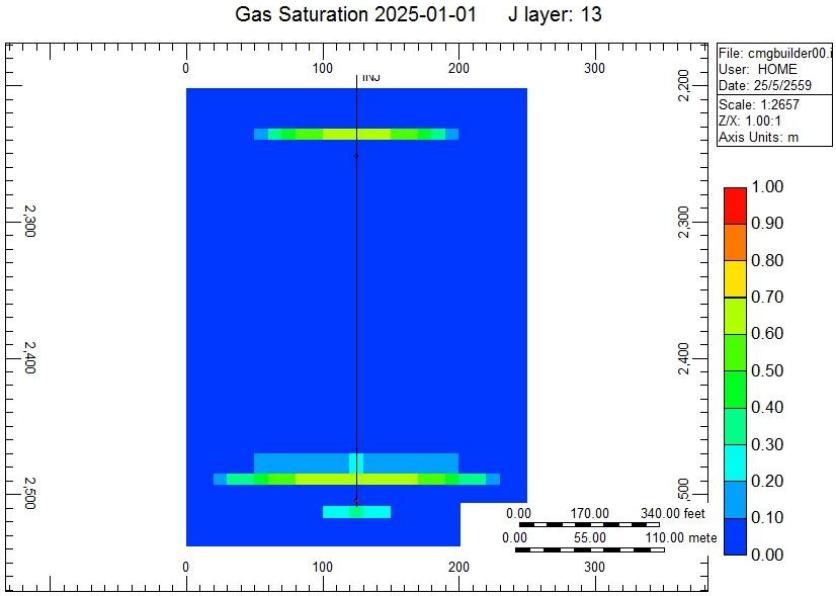

b.

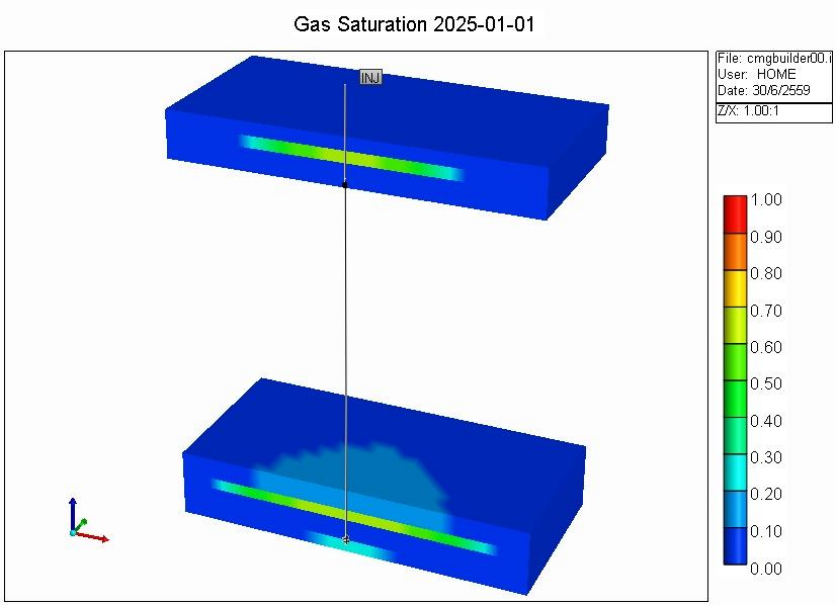

a. side view (10 years) and b. 3D view (10 years) in all layer at Well 1

a.

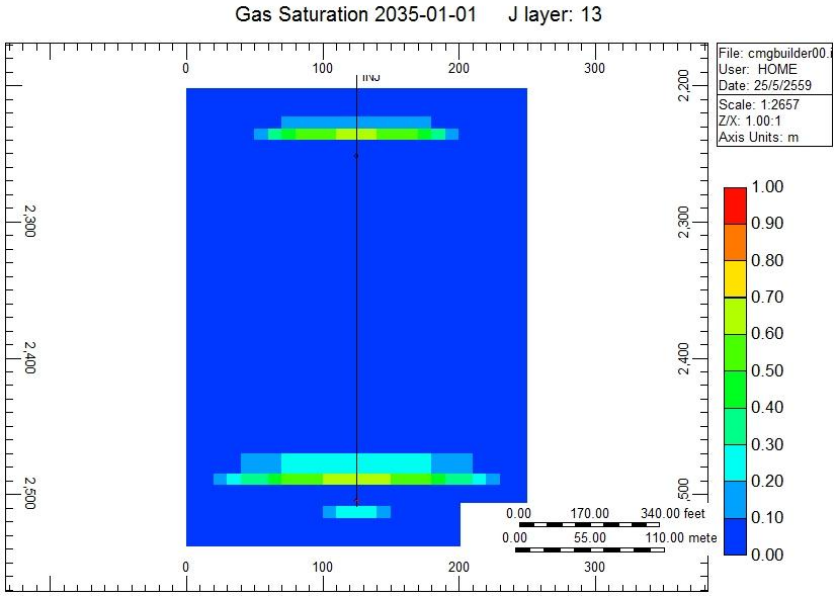

b.

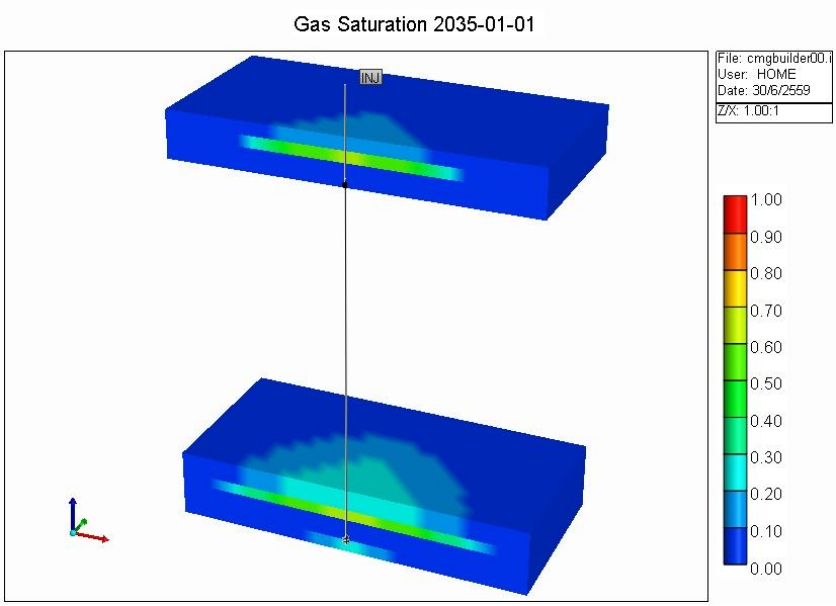

a. side view (20 years) and b. 3D view (20 years) in all layer at Well 1

a.

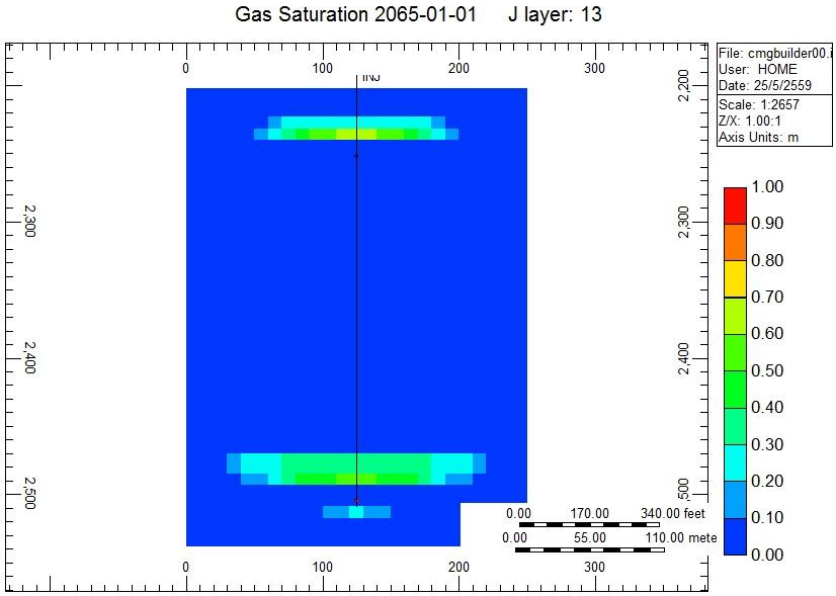

b.

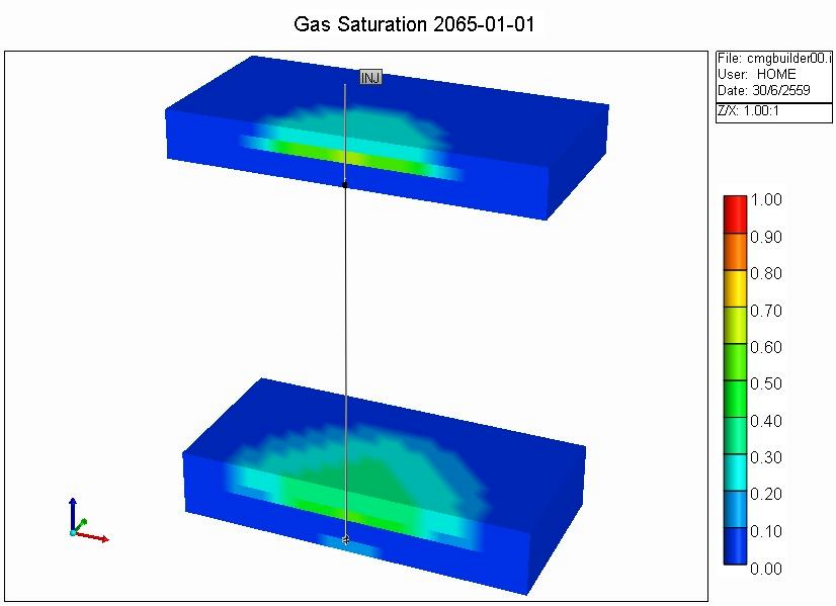

a. side view (50 years) and b. 3D view (50 years) in all layer at Well 1

Well 2

All layer at 1,000 t/d injection rate.

a.

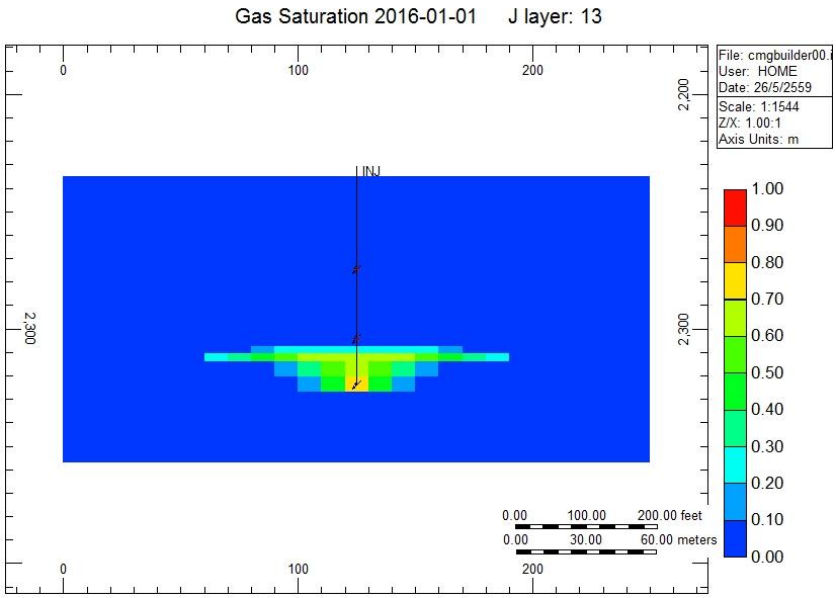

b.

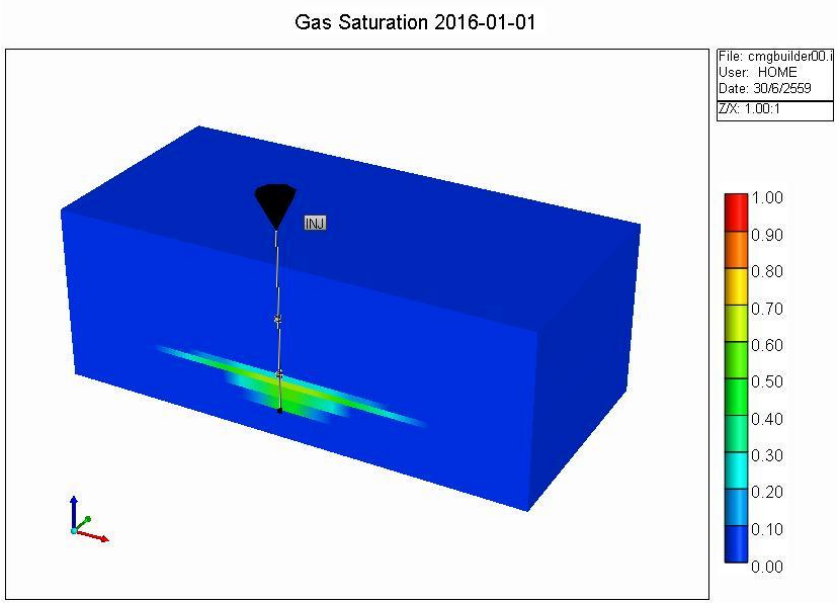

a. side view (1 year) and b. 3D view (1 year) in all layer at Well 2

a.

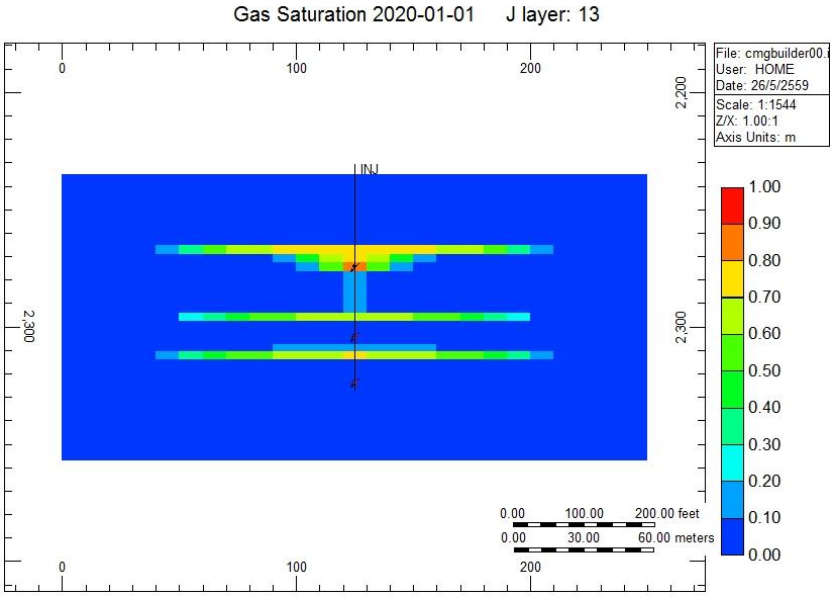

b.

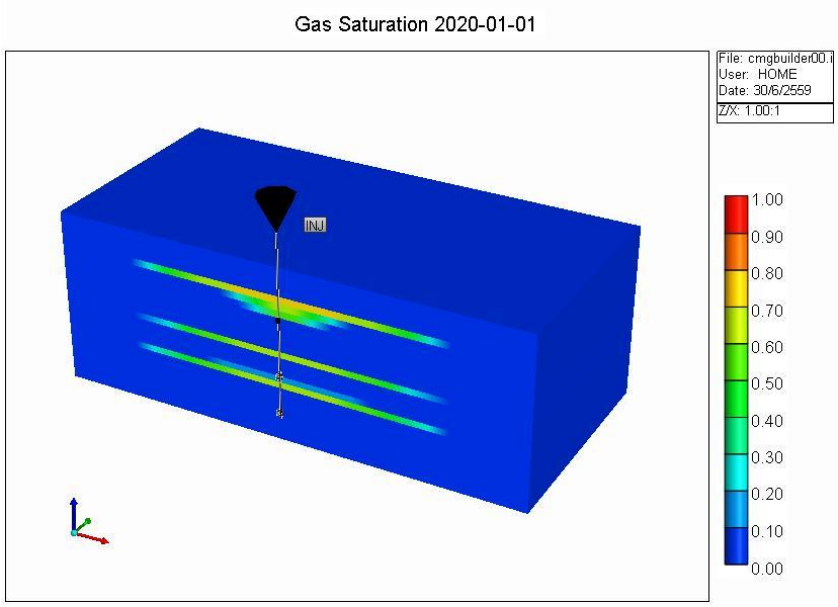

a. side view (5 years) and b. 3D view (5 years) in all layer at Well 2

a.

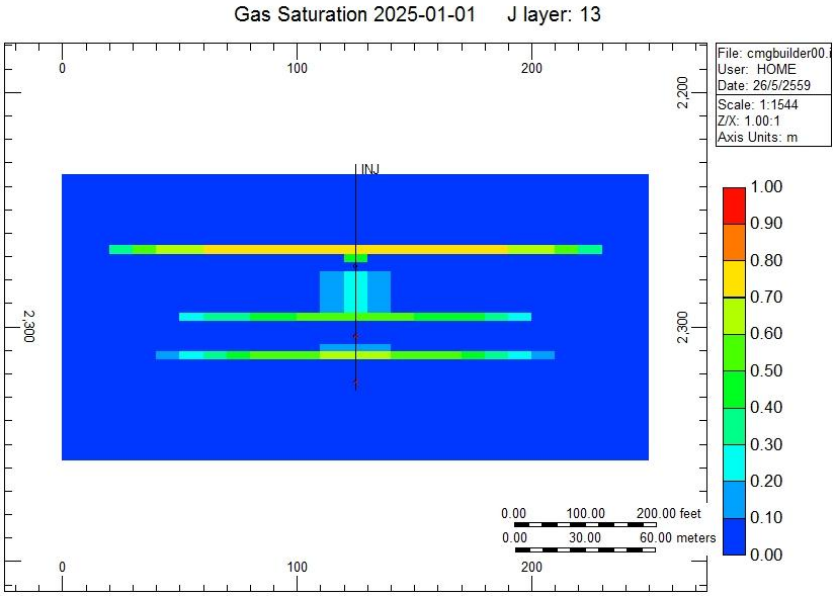

b.

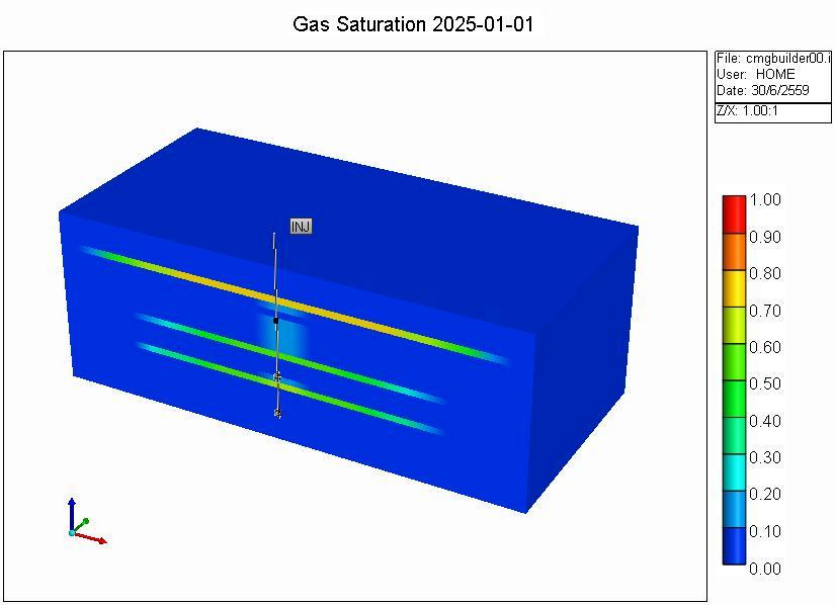

a. side view (10 years) and b. 3D view (10 years) in all layer at Well 2

a.

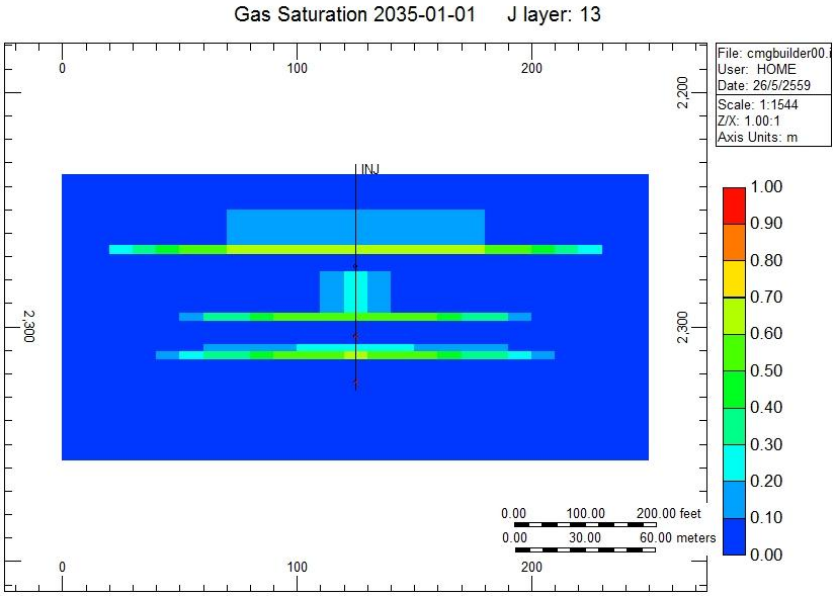

b.

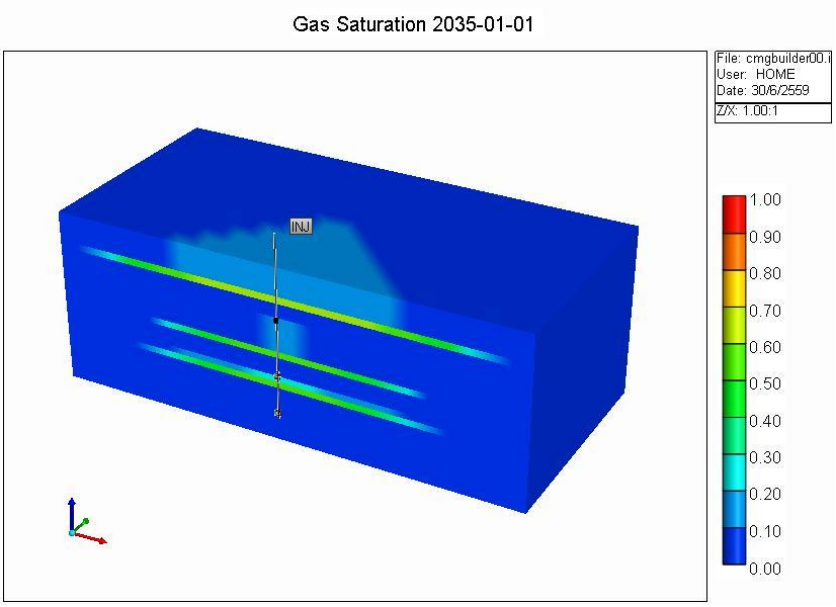

a. side view (20 years) and b. 3D view (20 years) in all layer at Well 2

a.

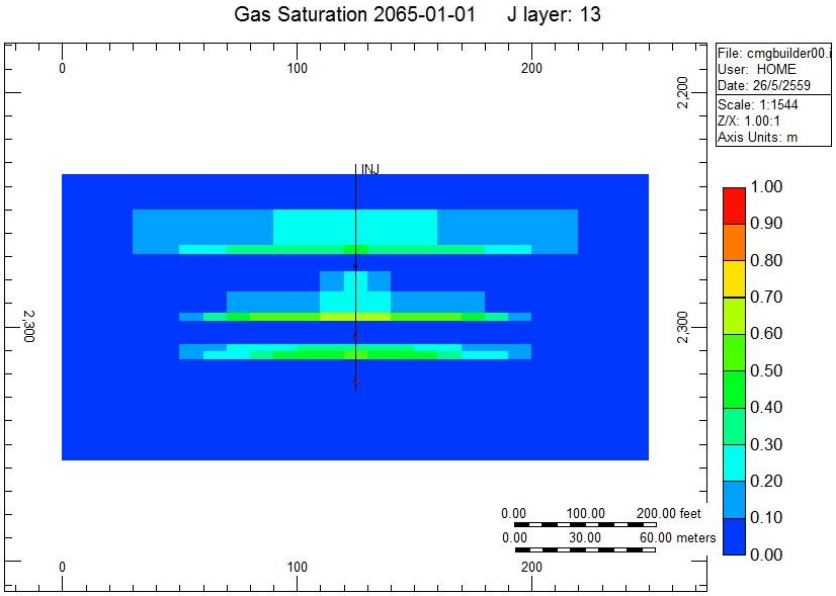

b.

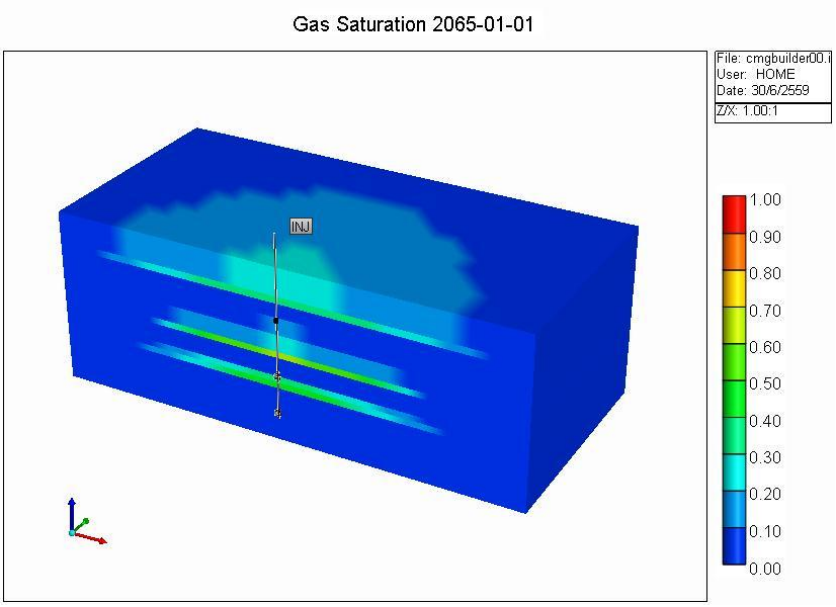

a. side view (50 years) and b. 3D view (50 years) in all layer at Well 2

All layer at 2,000 t/d injection rate.

a.

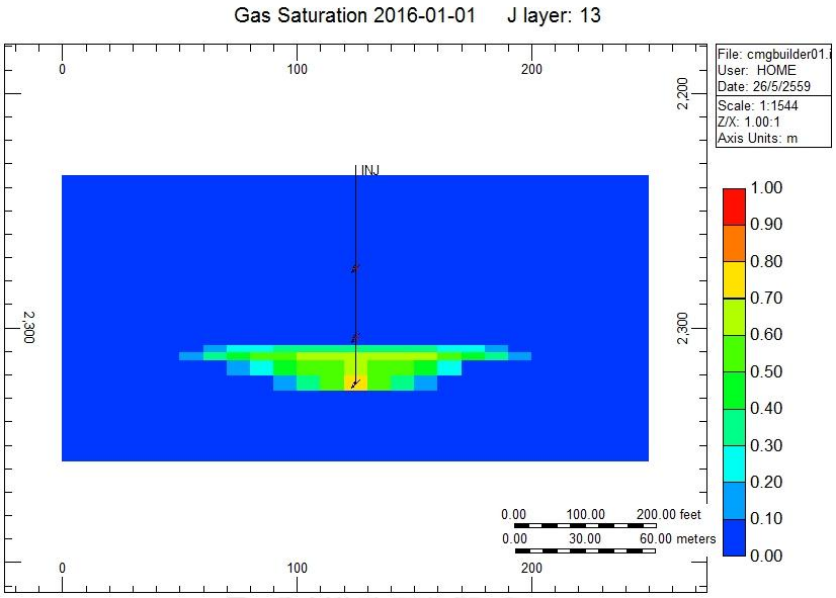

b.

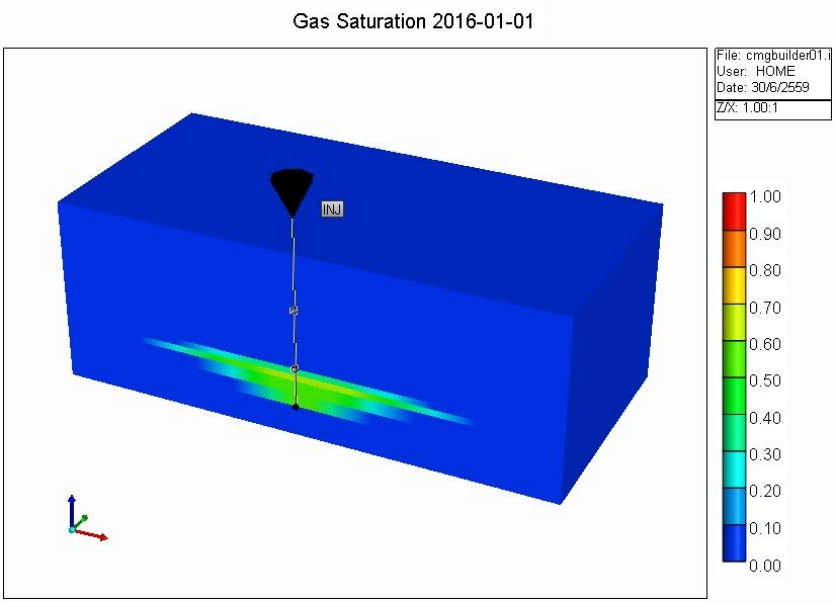

a. side view (1 year) and b. 3D view (1 year) in all layer at Well 2

a.

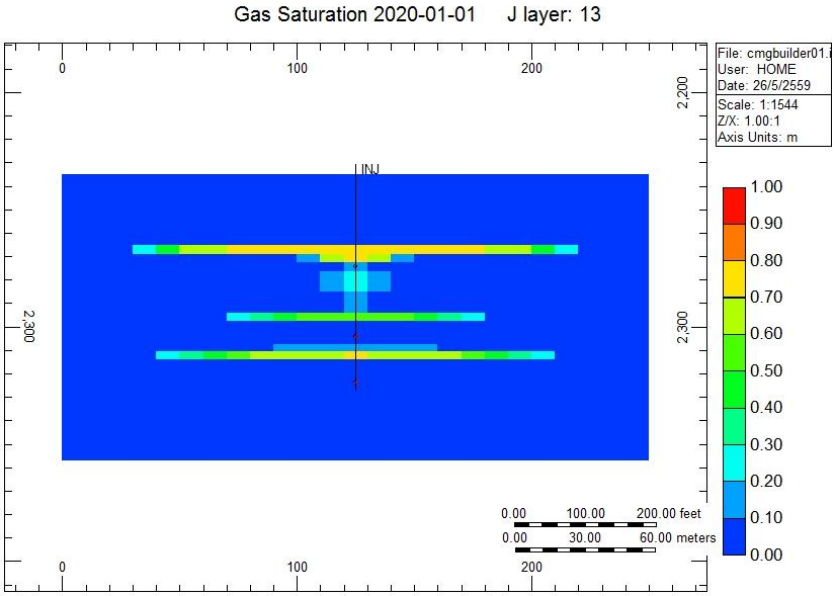

b.

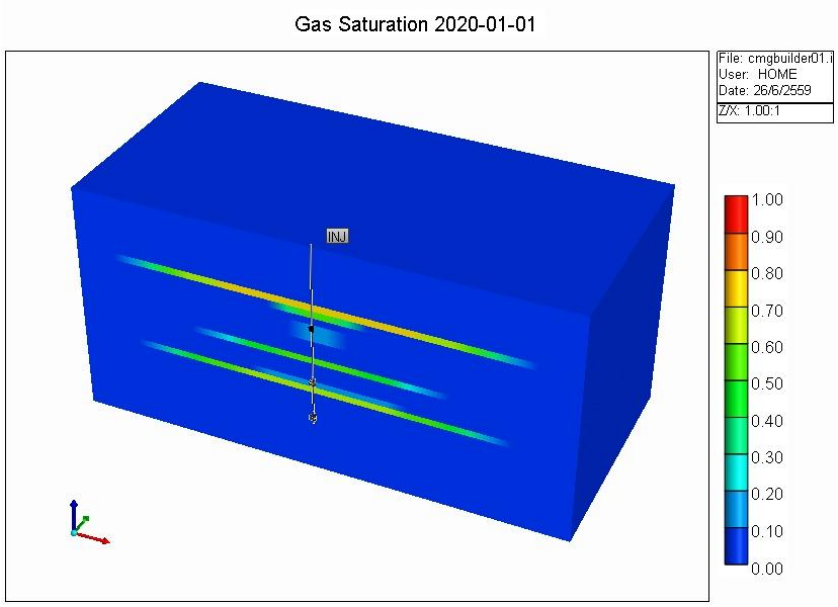

a. side view (5 years) and b. 3D view (5 years) in all layer at Well 2

a.

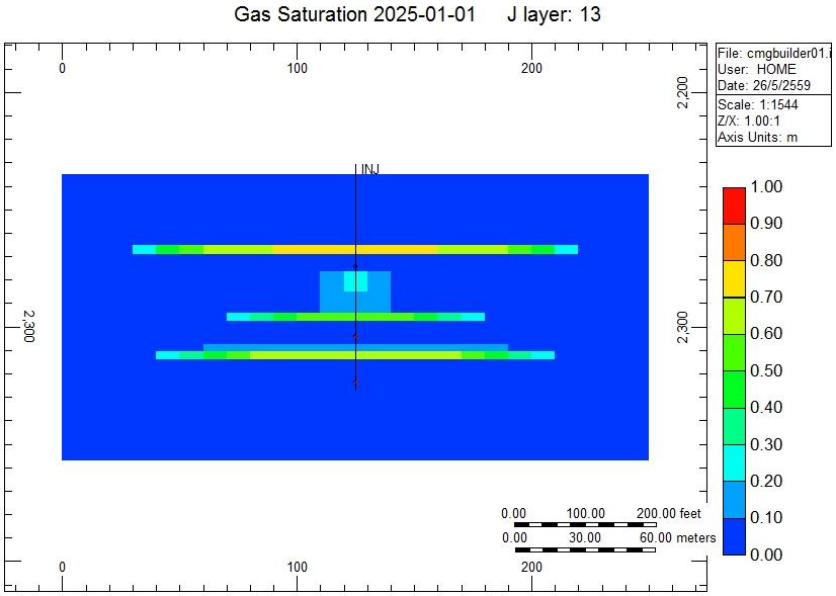

b.

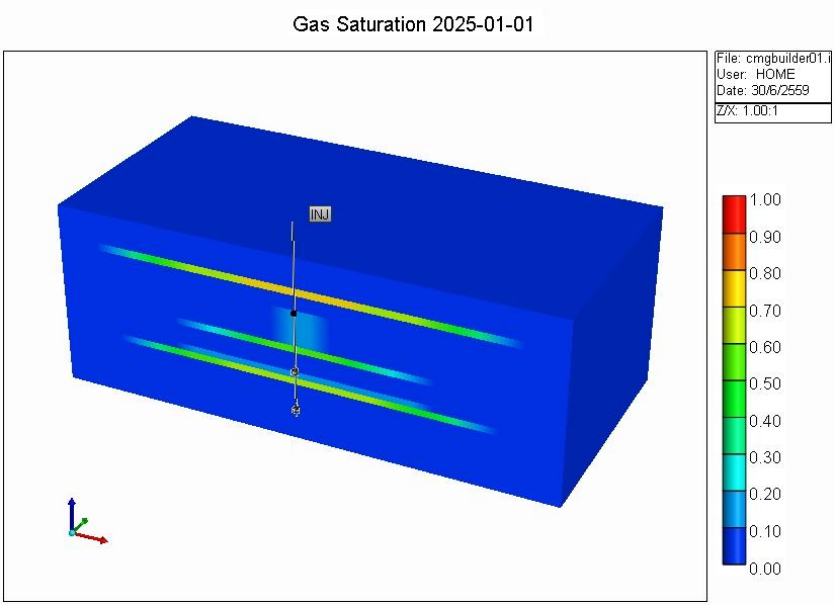

a. side view (10 years) and b. 3D view (10 years) in all layer at Well 2

a.

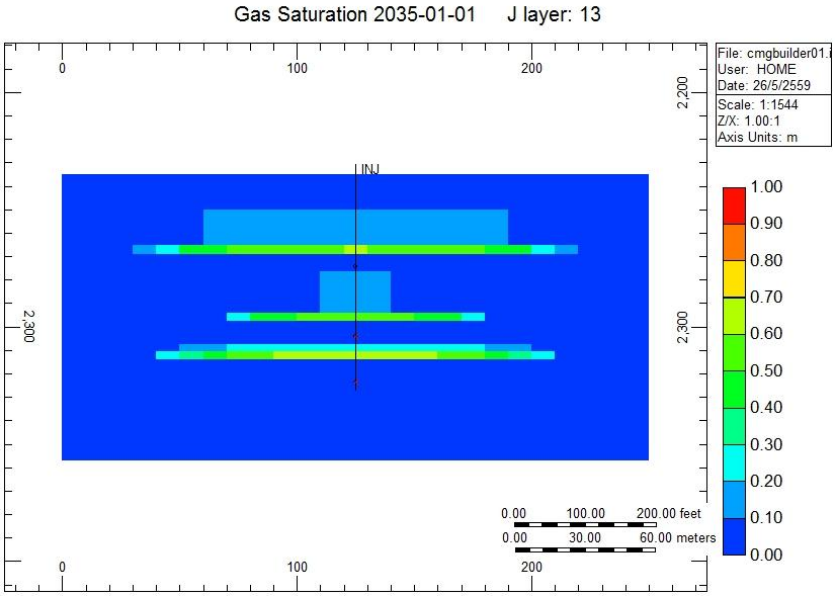

b.

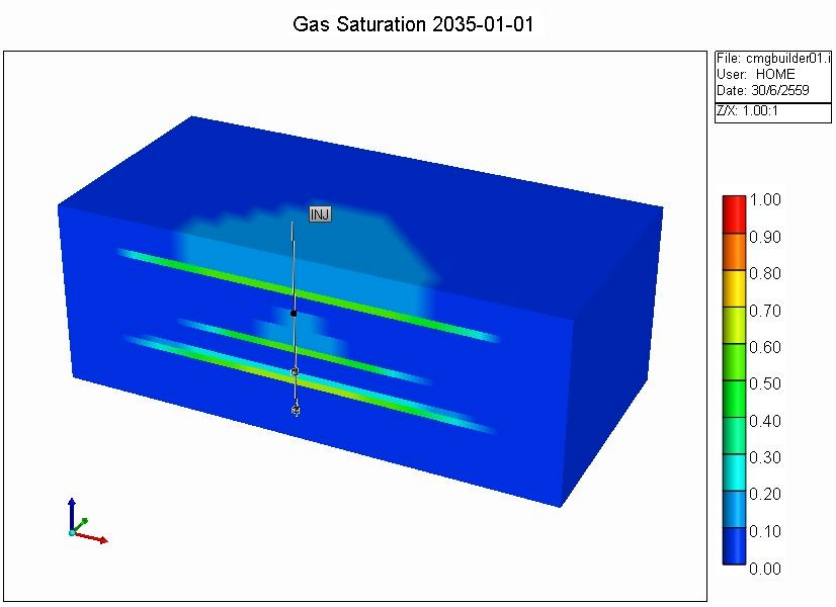

a. side view (20 years) and b. 3D view (20 years) in all layer at Well 2

a.

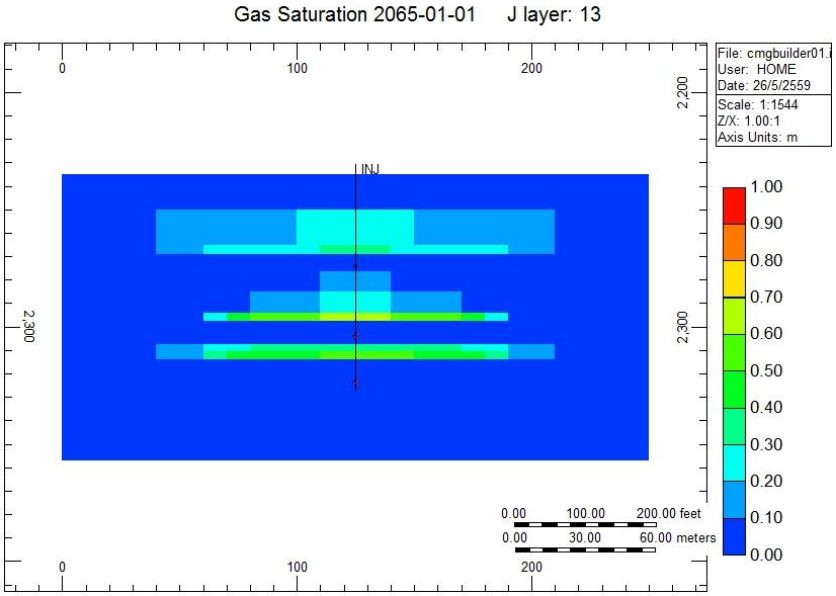

b.

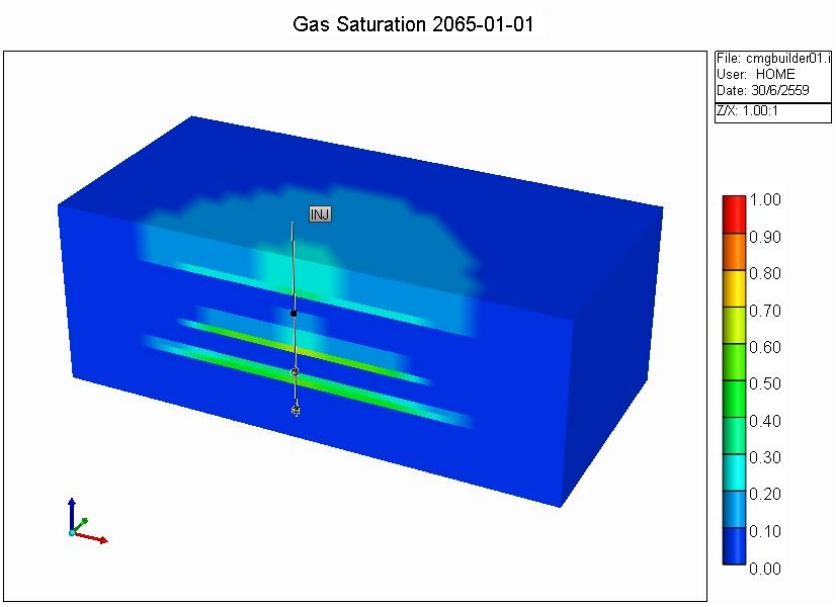

a. side view (50 years) and b. 3D view (50 years) in all layer at Well 2

All layer at 3,000 t/d injection rate.

a.

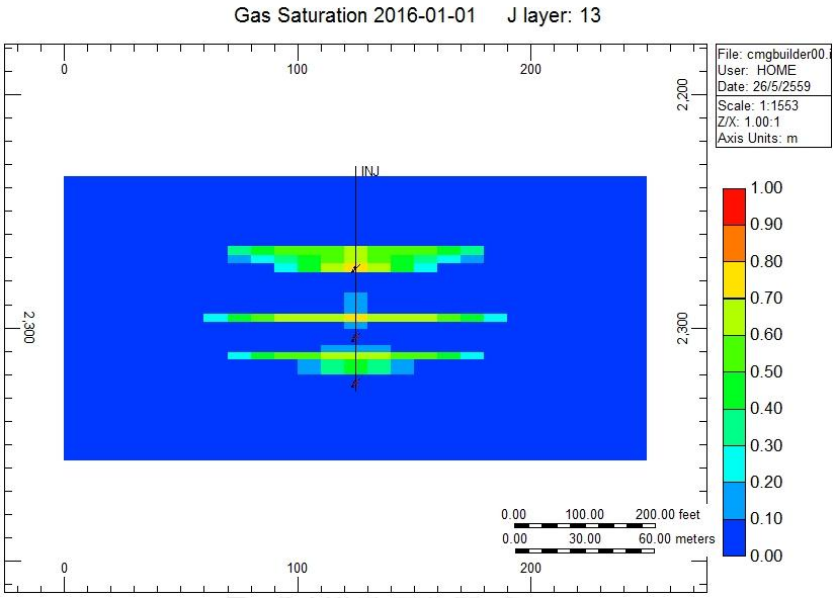

b.

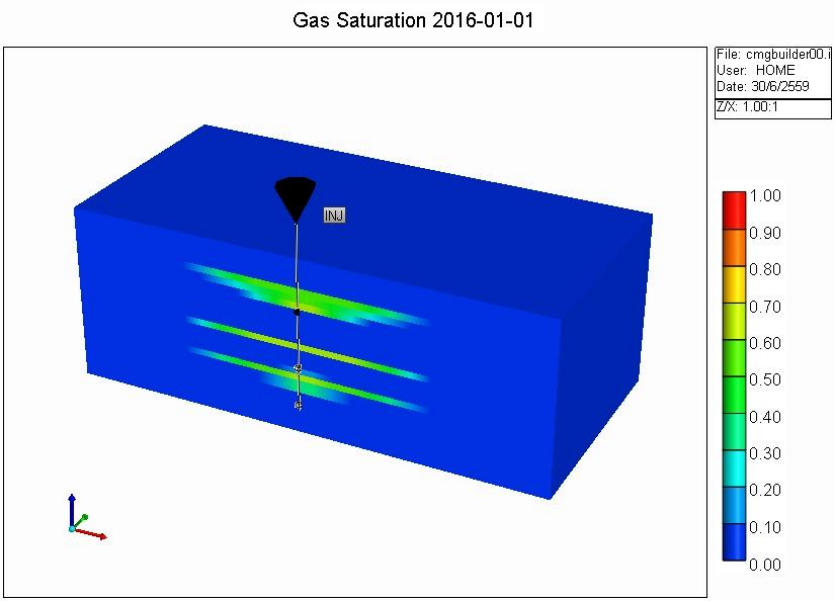

a. side view (1 year) and b. 3D view (1 year) in all layer at Well 2

a.

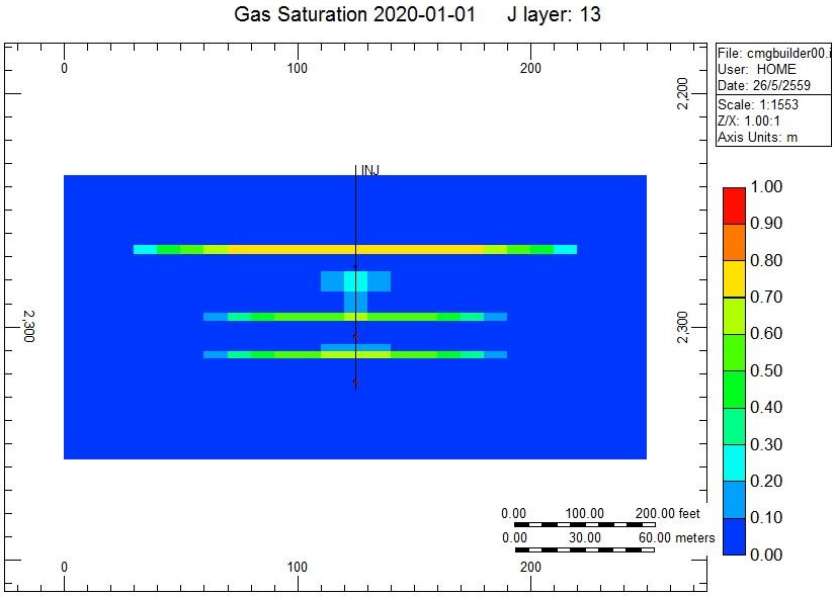

b.

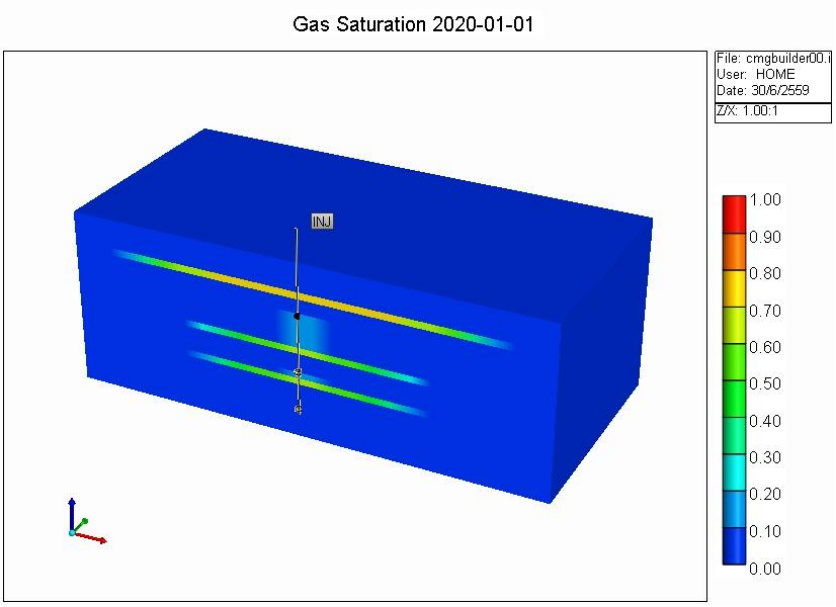

a. side view (5 years) and b. 3D view (5 years) in all layer at Well 2

a.

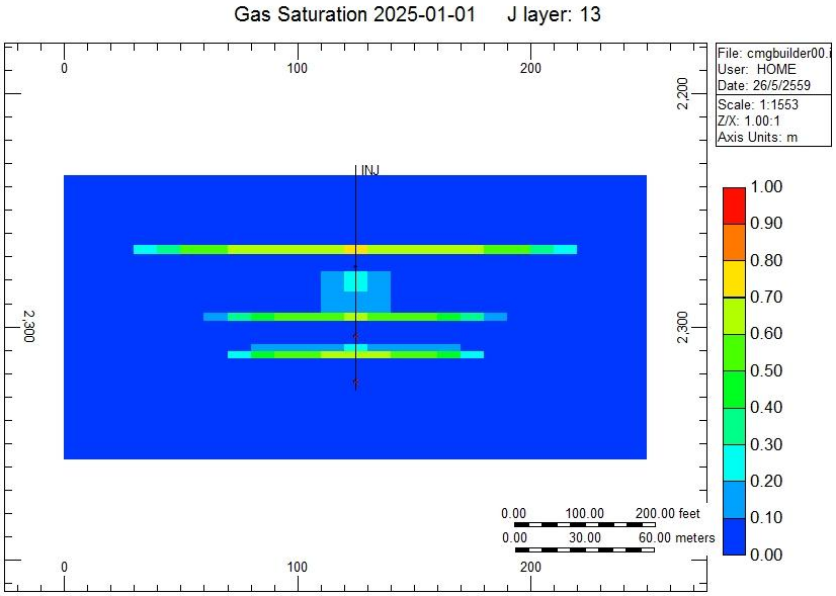

b.

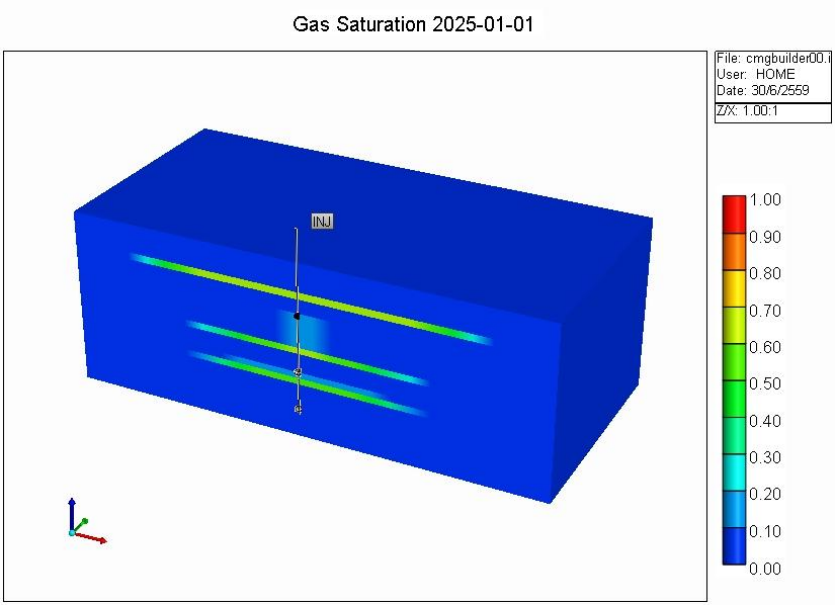

a. side view (10 years) and b. 3D view (10 years) in all layer at Well 2

a.

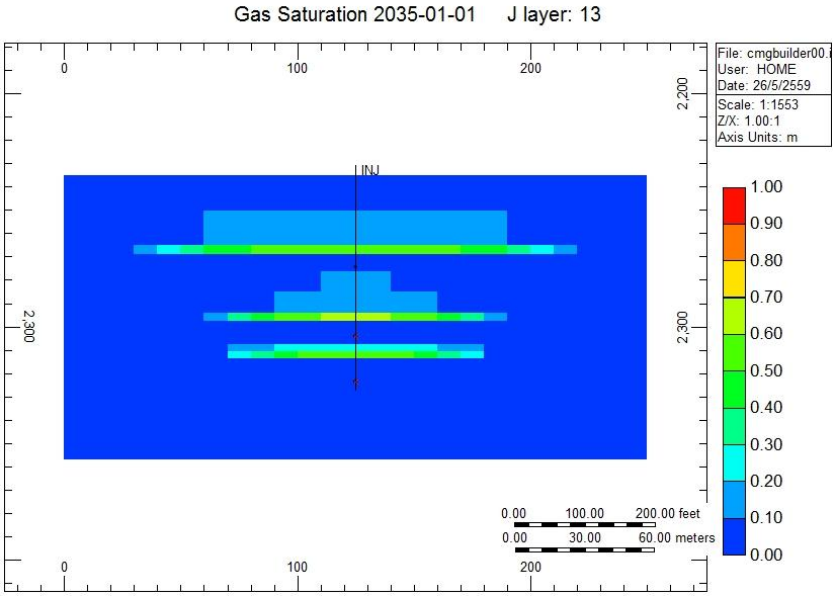

b.

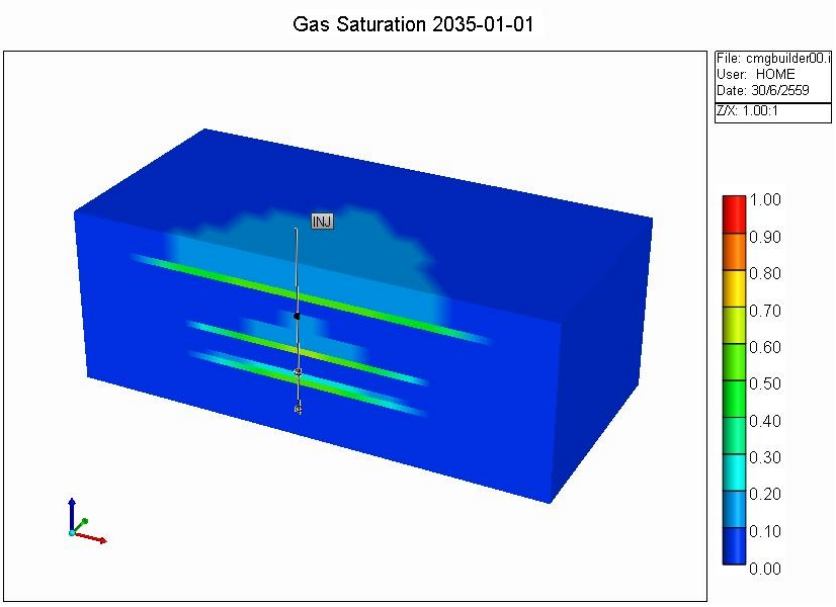

a. side view (20 years) and b. 3D view (20 years) in all layer at Well 2

a.

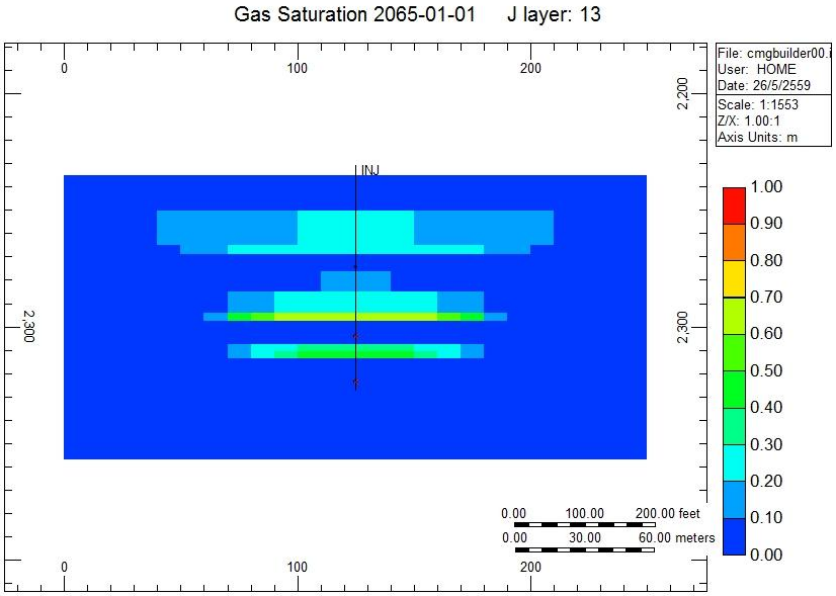

b.

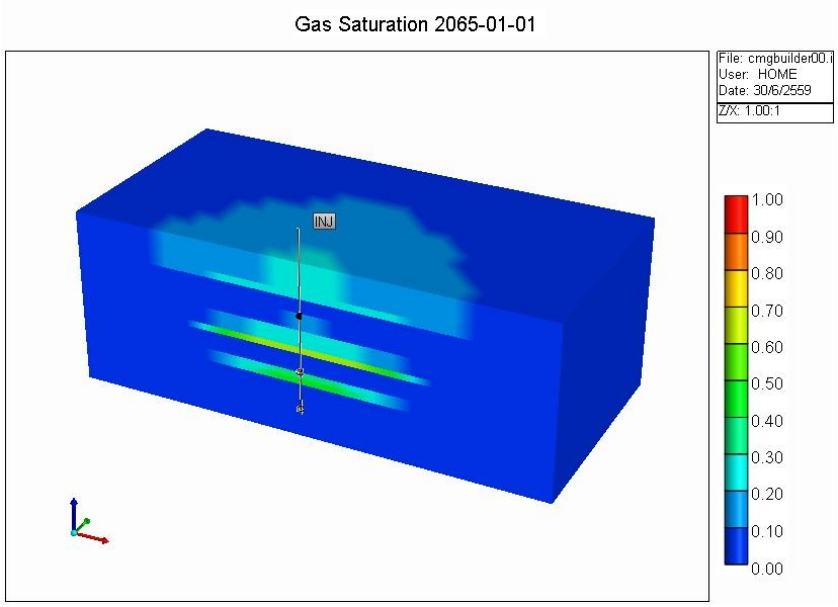

a. side view (50 years) and b. 3D view (50 years) in all layer at Well 2

All layer at 4,000 t/d injection rate.

a.

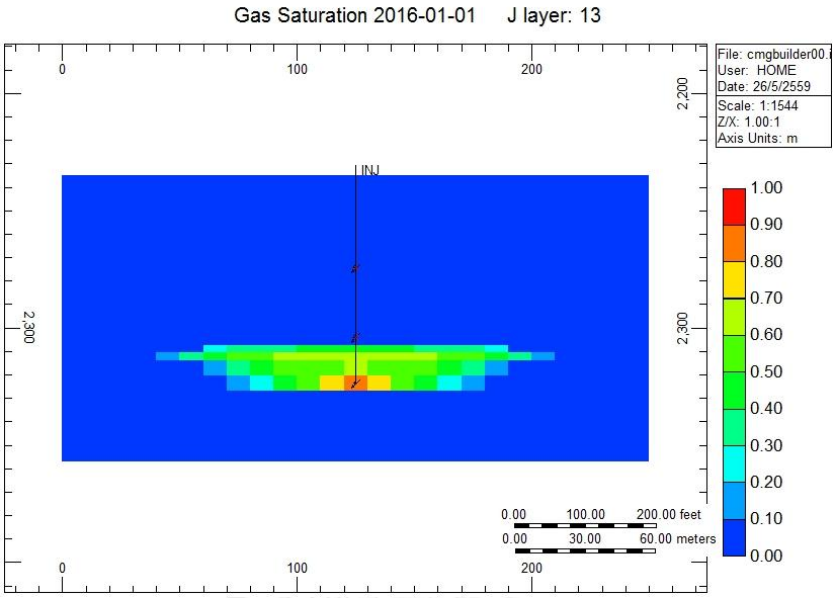

b.

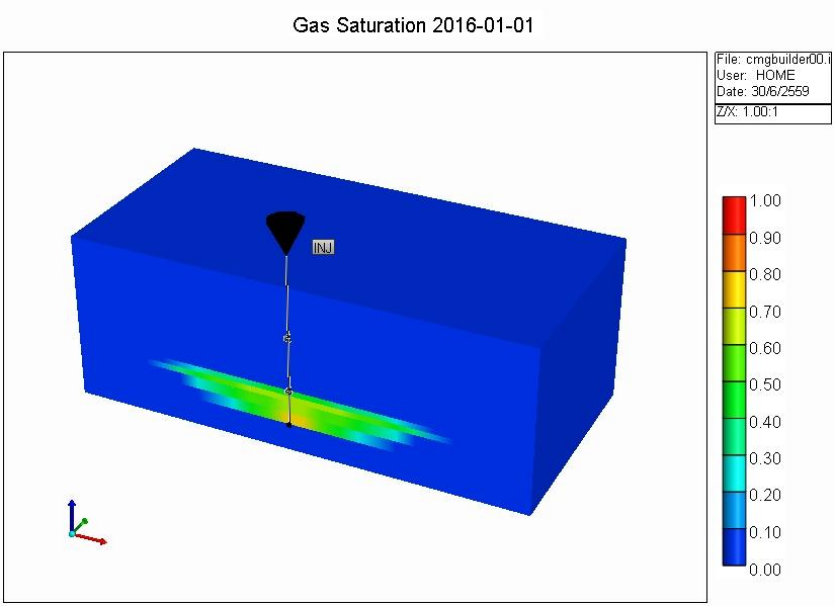

a. side view (1 year) and b. 3D view (1 year) in all layer at Well 2

a.

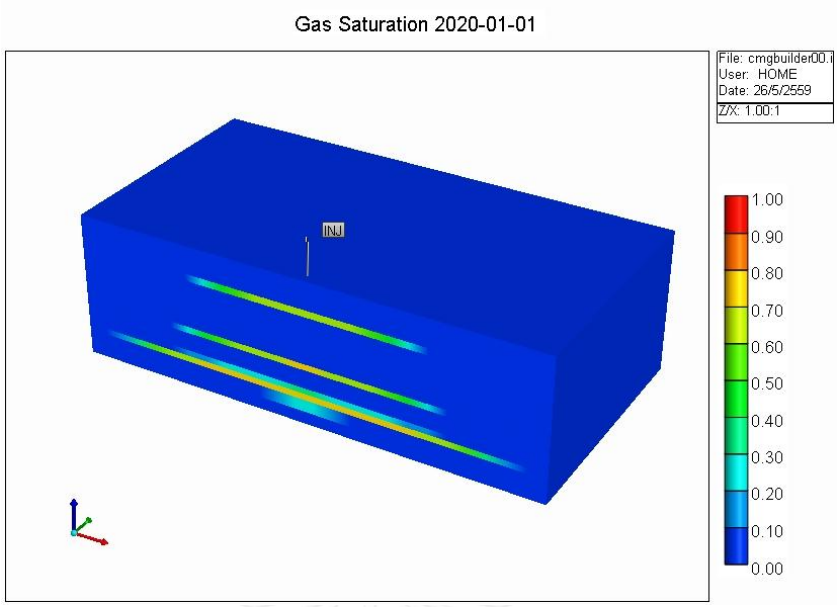

b.

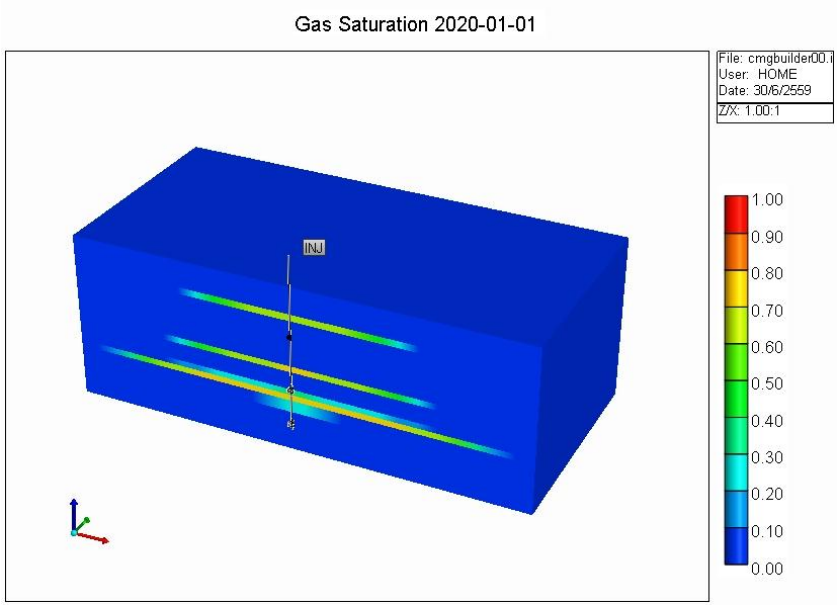

a. side view (5 years) and b. 3D view (5 years) in all layer at Well 2

a.

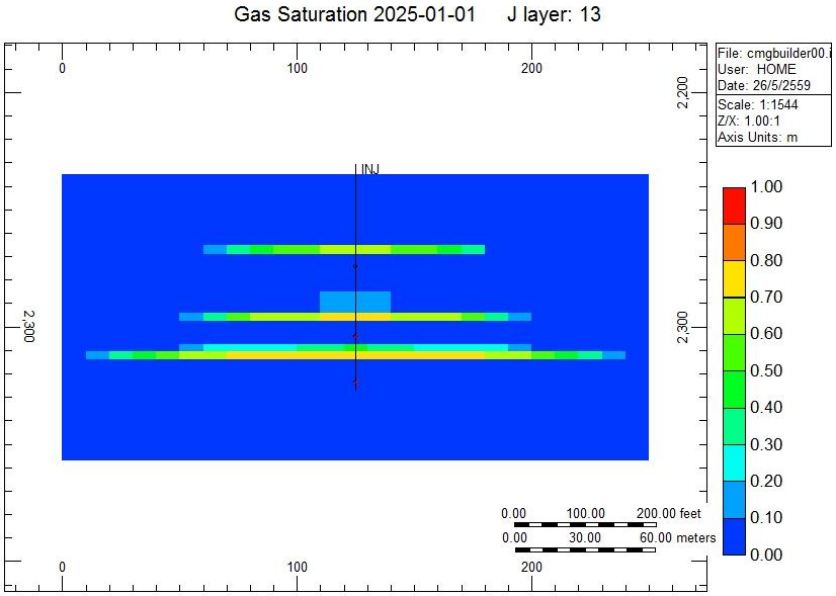

b.

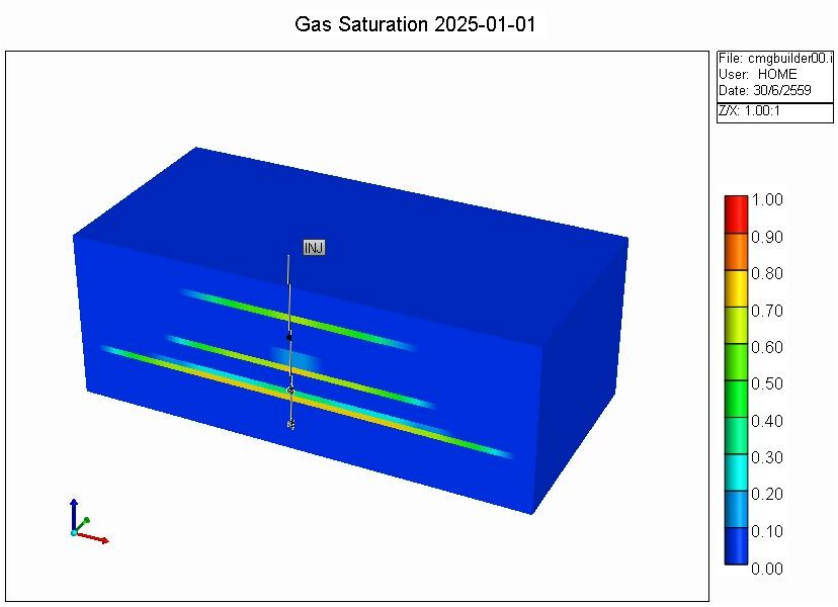

a. side view (10 years) and b. 3D view (10 years) in all layer at Well 2

a.

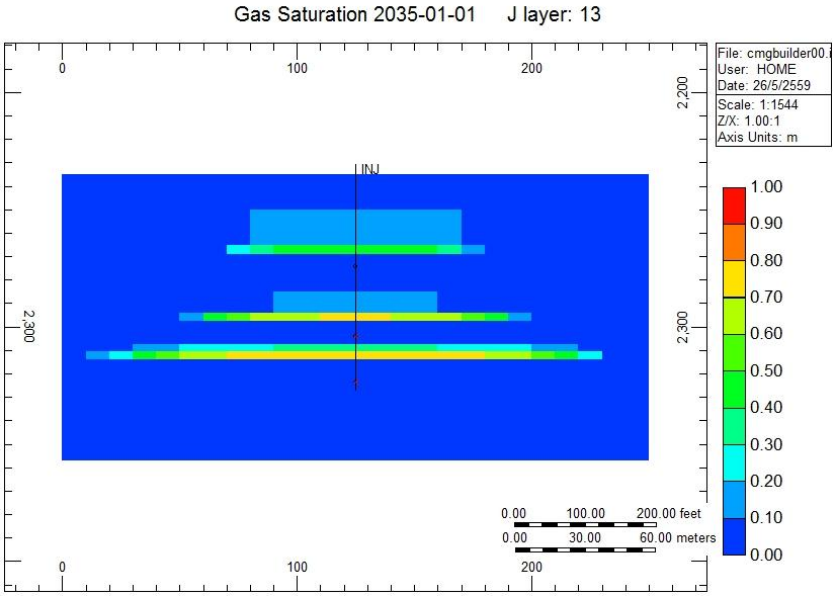

b.

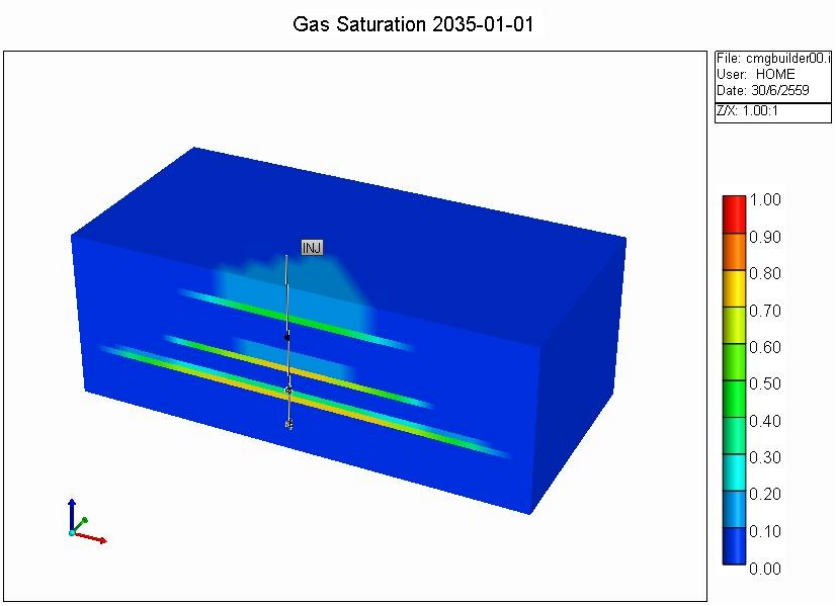

a. side view (20 years) and b. 3D view (20 years) in all layer at Well 2

a.

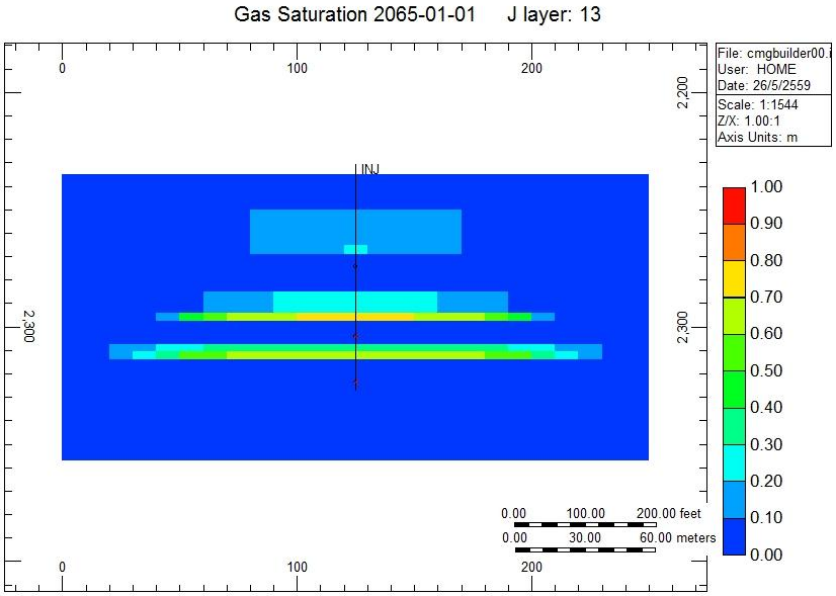

b.

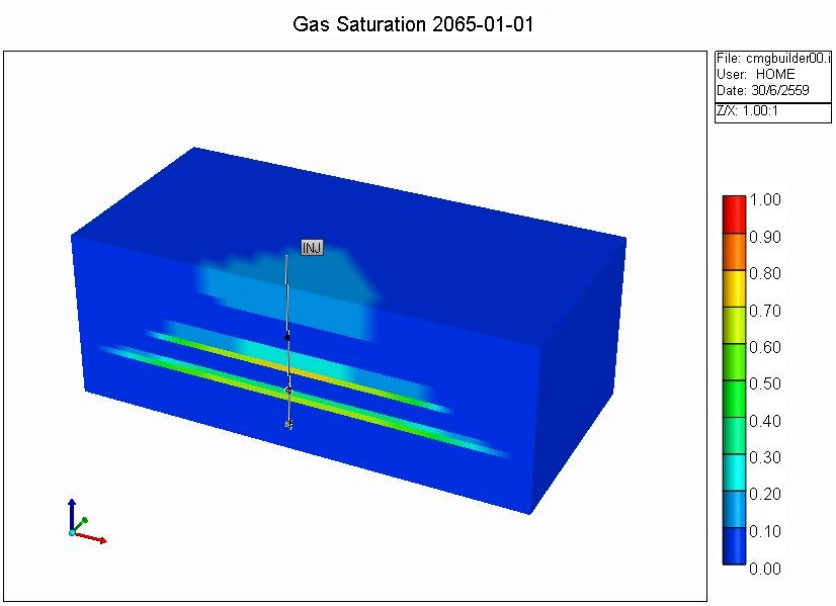

a. side view (50 years) and b. 3D view (50 years) in all layer at Well 2

Well 3

All layer at 1,000 t/d injection rate.

a.

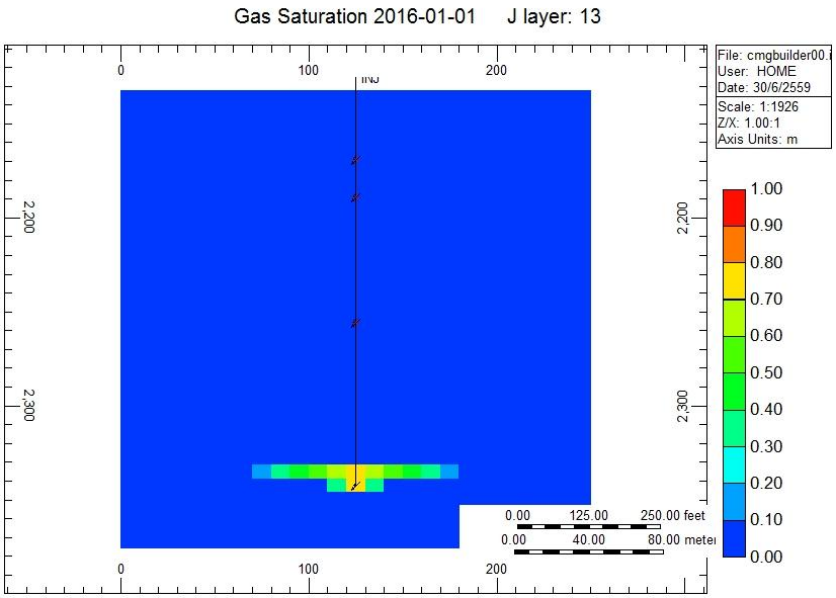

b.

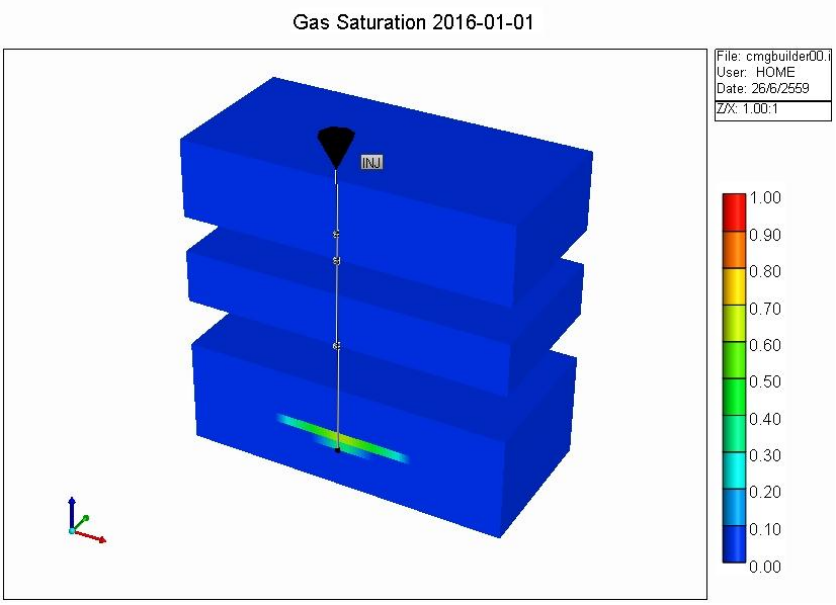

a. side view (1 year) and b. 3D view (1 year) in all layer at Well 3

a.

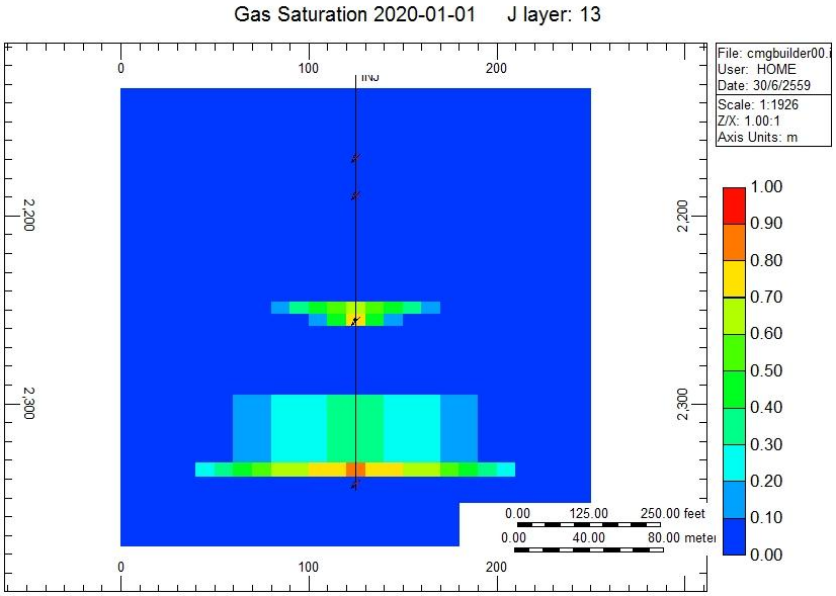

b.

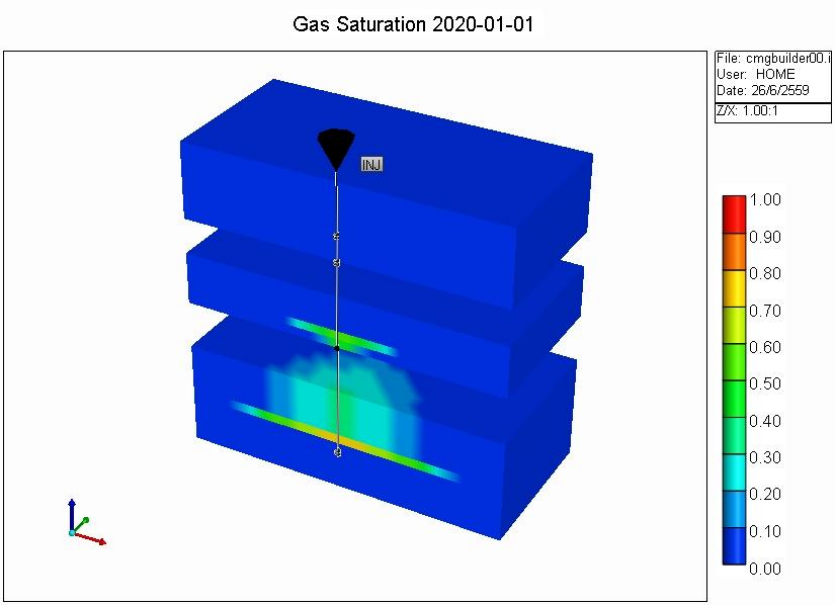

a. side view (5 years) and b. 3D view (5 years) in all layer at Well 3

a.

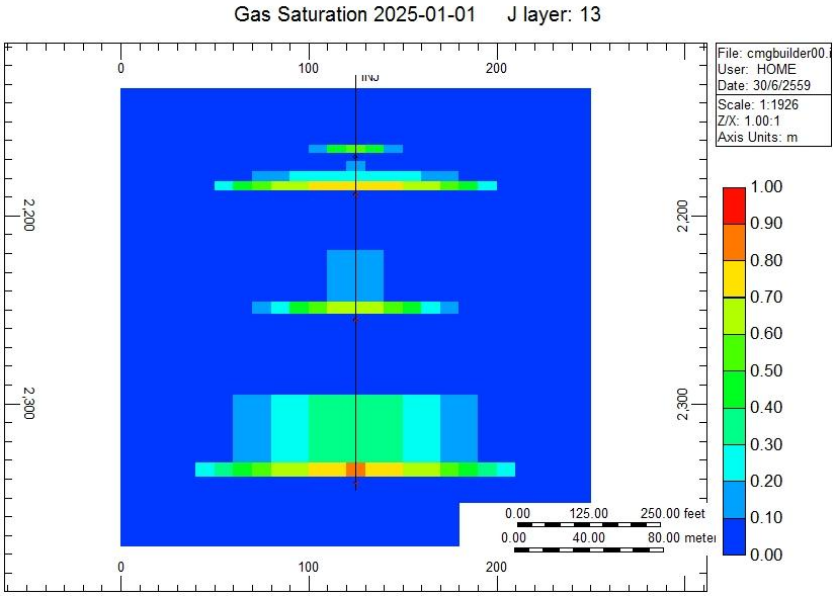

b.

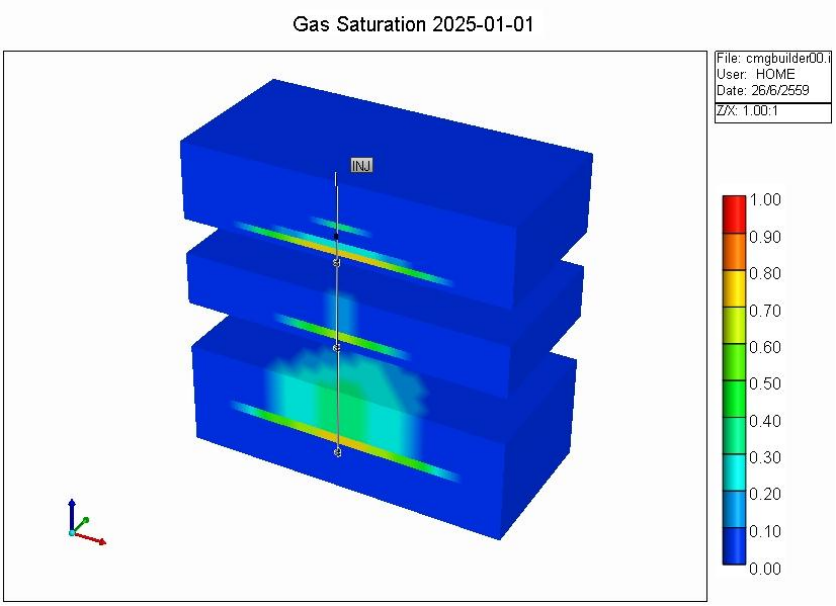

a. side view (10 years) and b. 3D view (10 years) in all layer at Well 3

a.

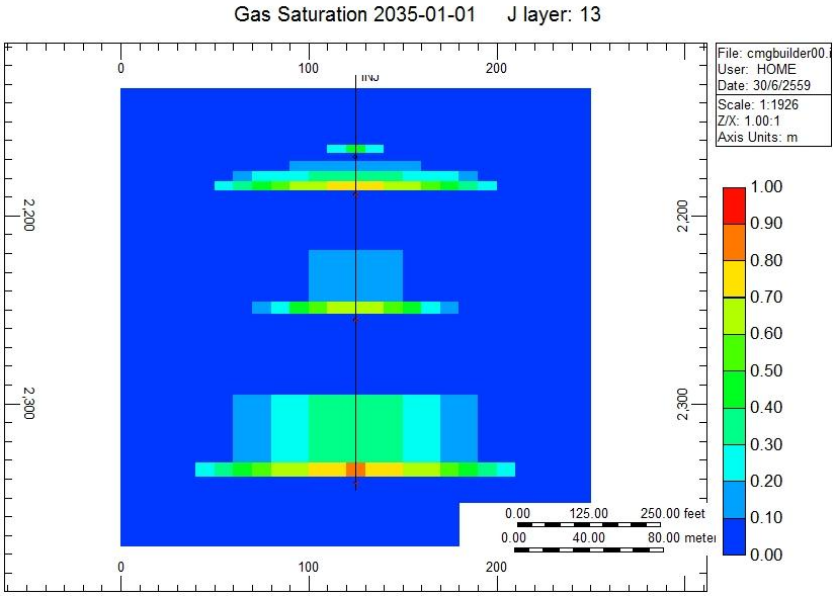

b.

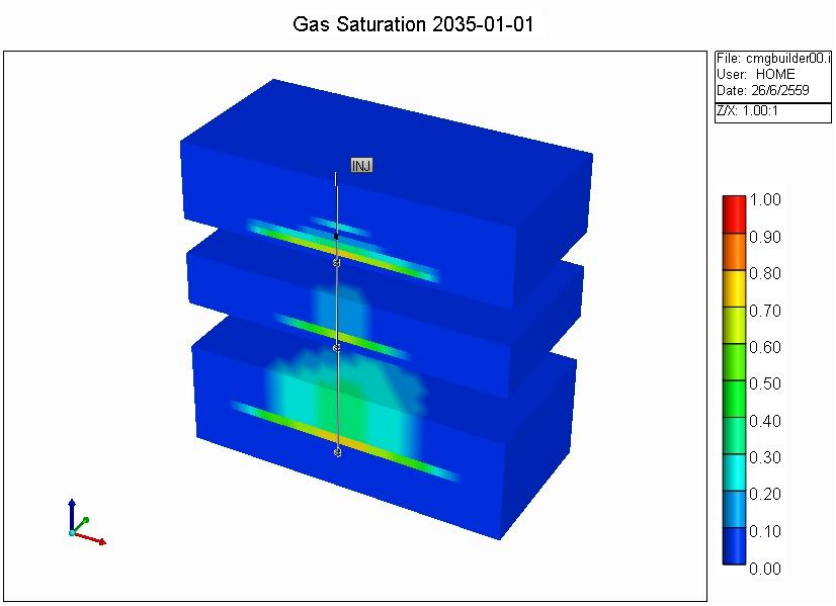

a. side view (20 years) and b. 3D view (20 years) in all layer at Well 3

a.

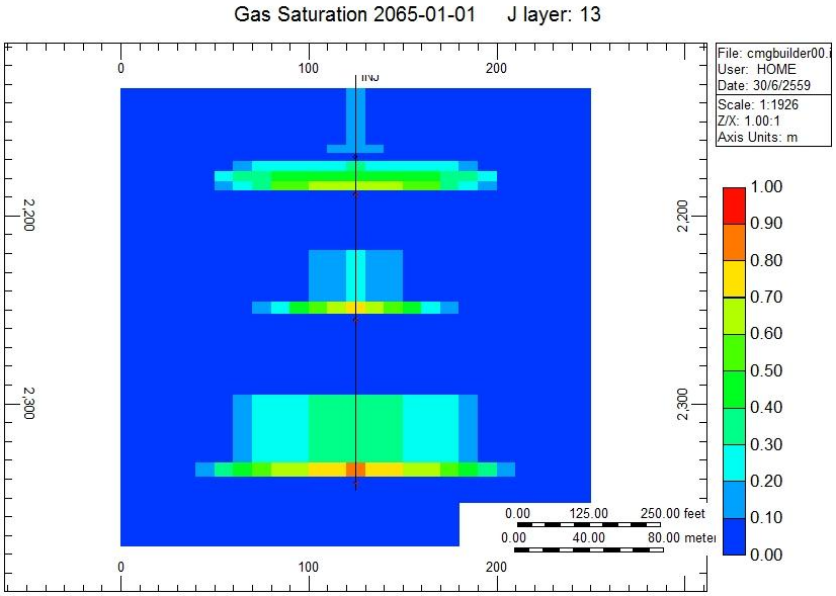

b.

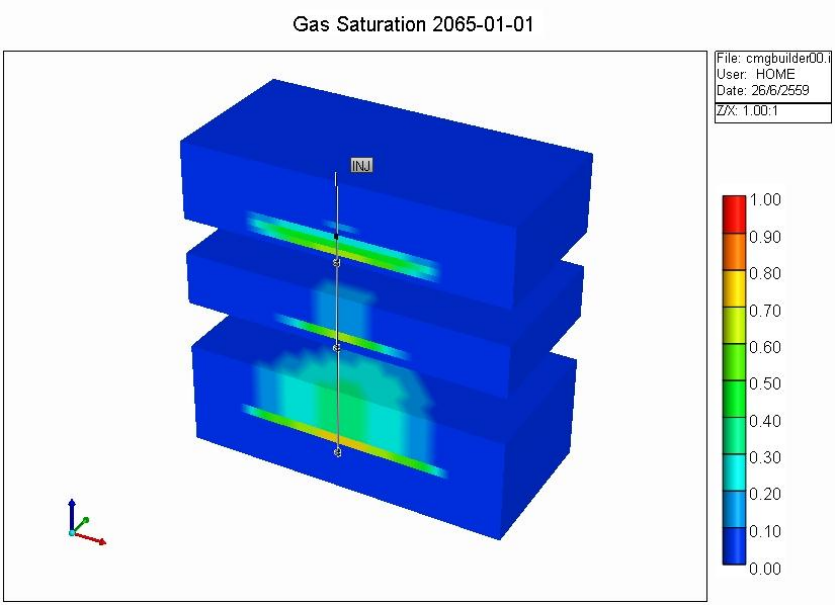

a. side view (50 years) and b. 3D view (50 years) in all layer at Well 3

All layer at 2,000 t/d injection rate.

a.

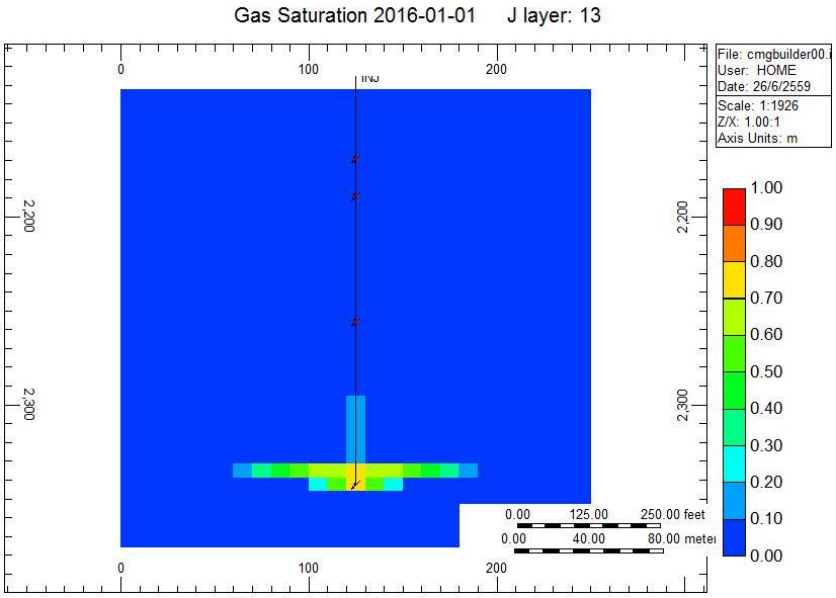

b.

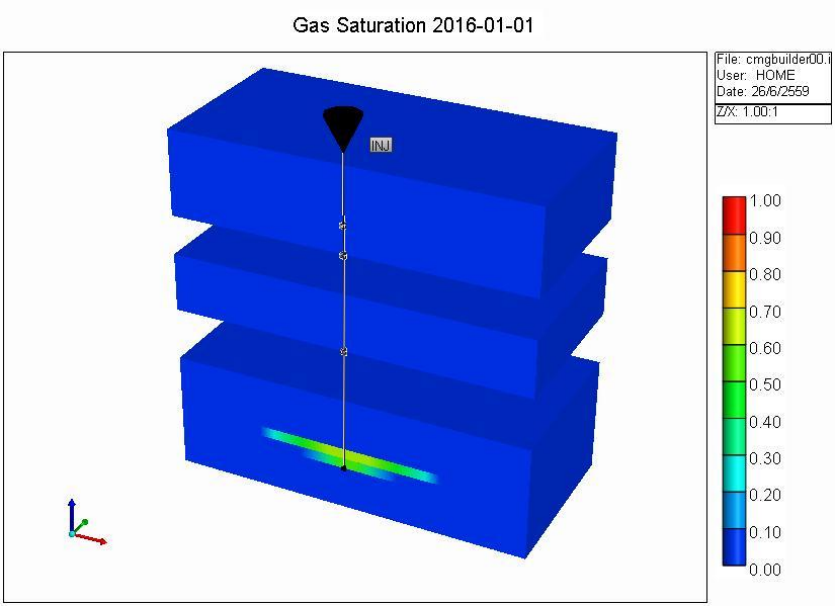

a. side view (1 year) and b. 3D view (1 year) in all layer at Well 3

a.

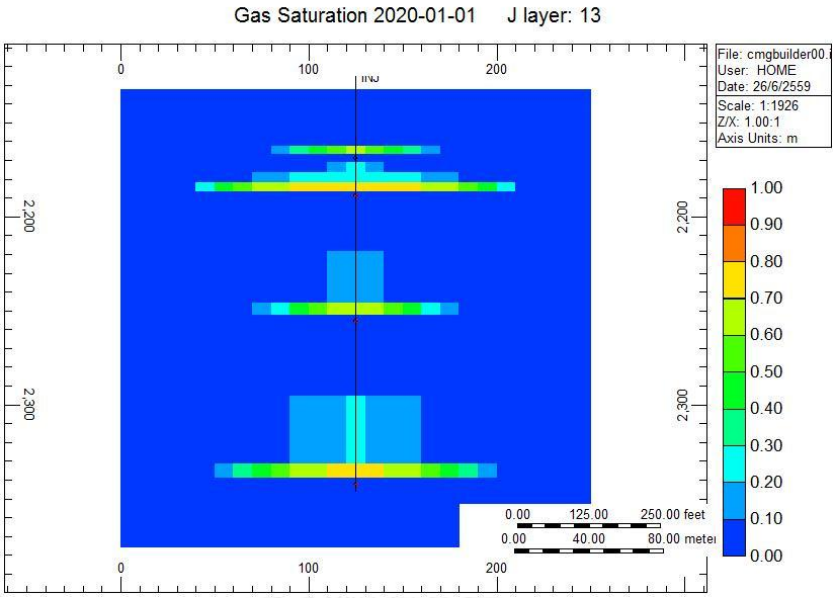

b.

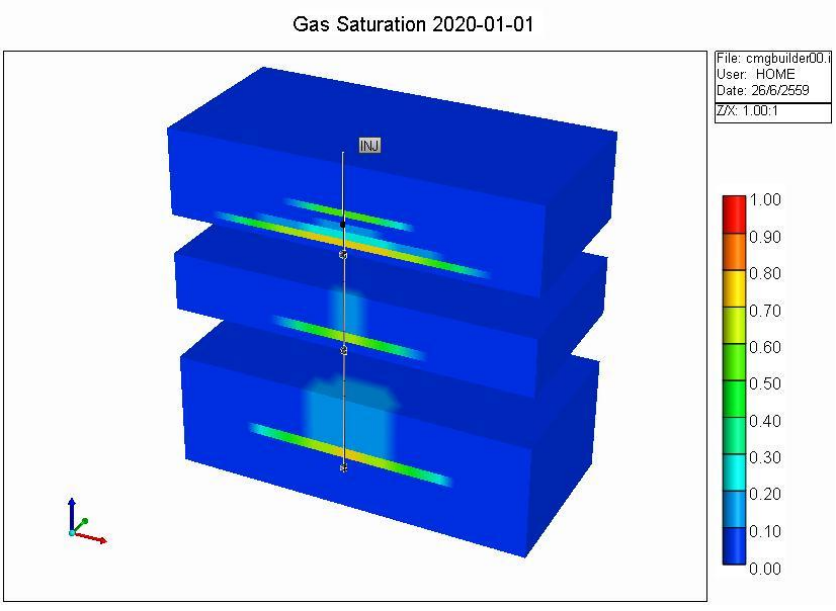

a. side view (5 years) and b. 3D view (5 years) in all layer at Well 3

a.

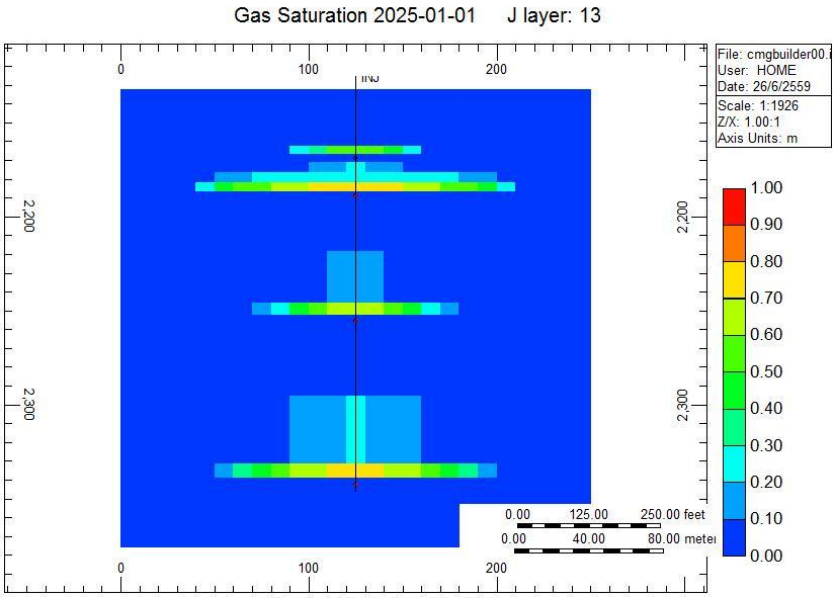

b.

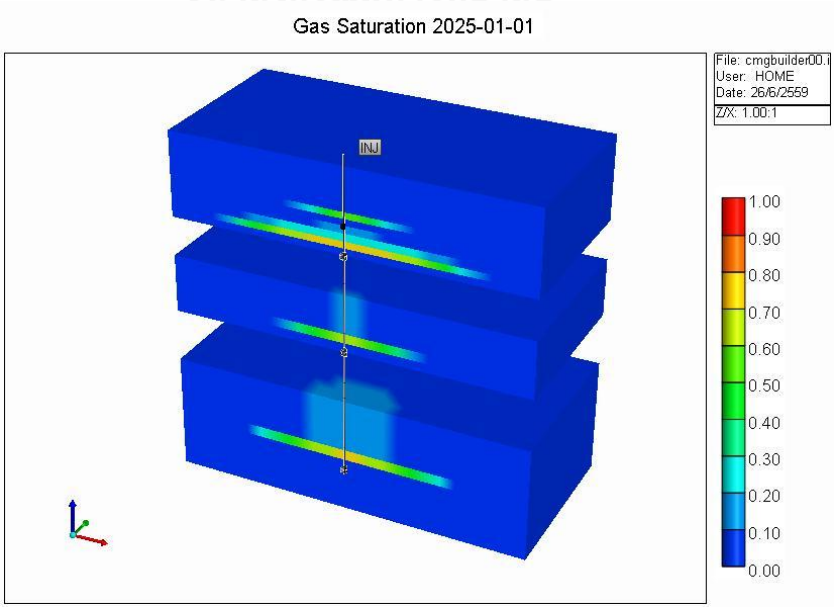

a. side view (10 years) and b. 3D view (10 years) in all layer at Well 3

a.

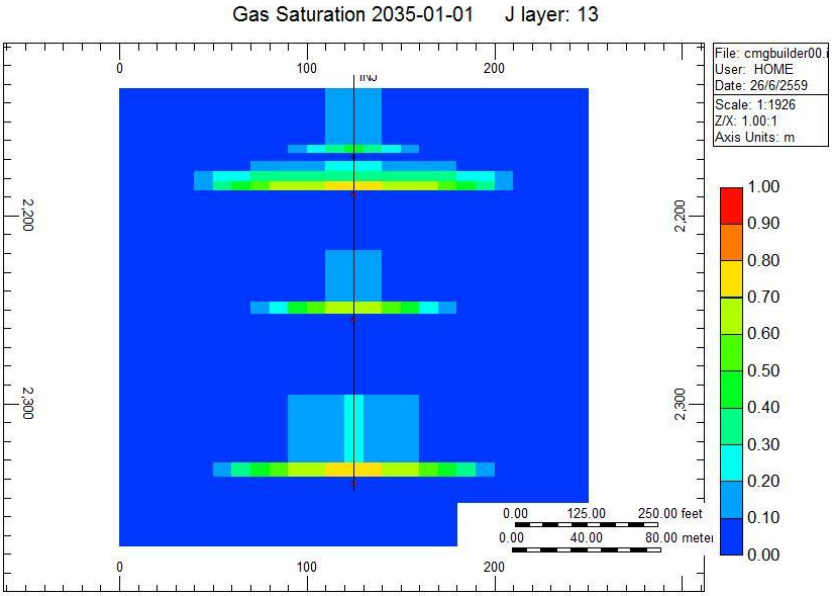

b.

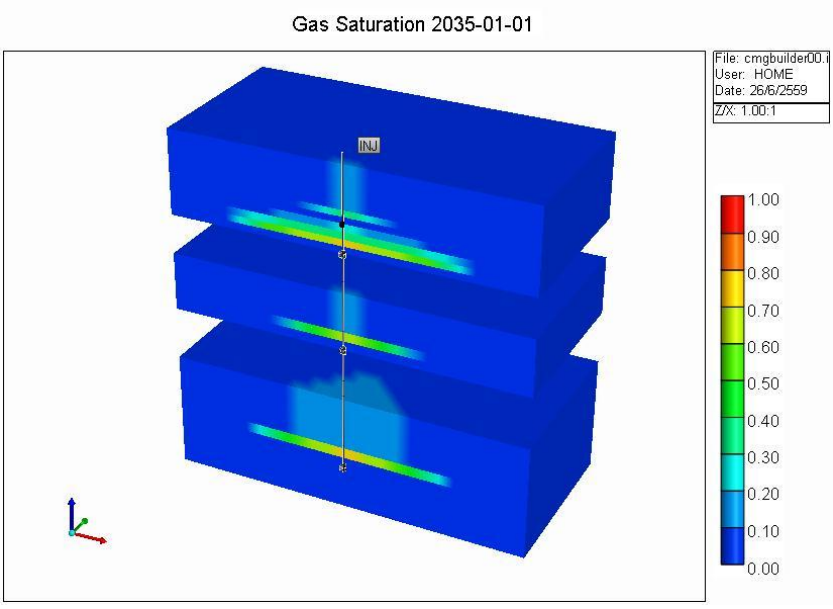

a. side view (20 years) and b. 3D view (20 years) in all layer at Well 3

a.

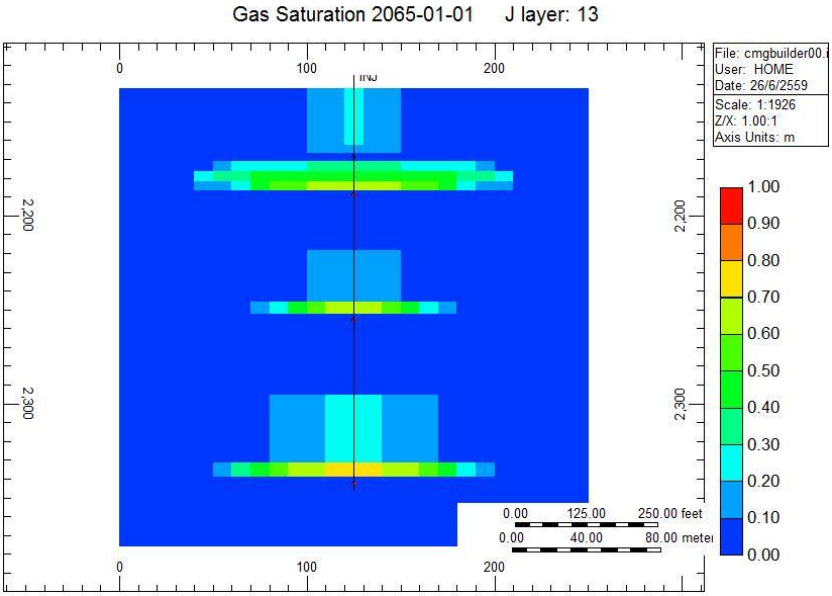

b.

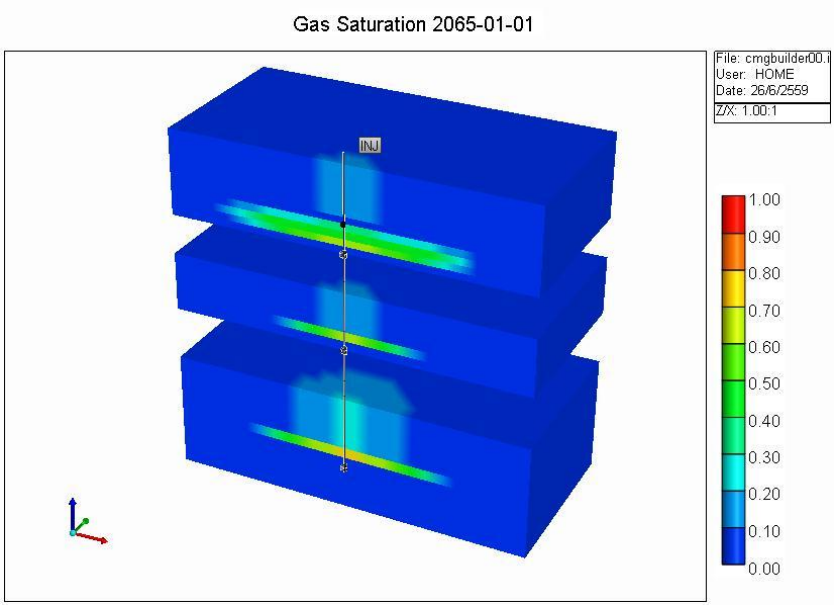

a. side view (50 years) and b. 3D view (50 years) in all layer at Well 3

All layer at 3,000 t/d injection rate.

a.

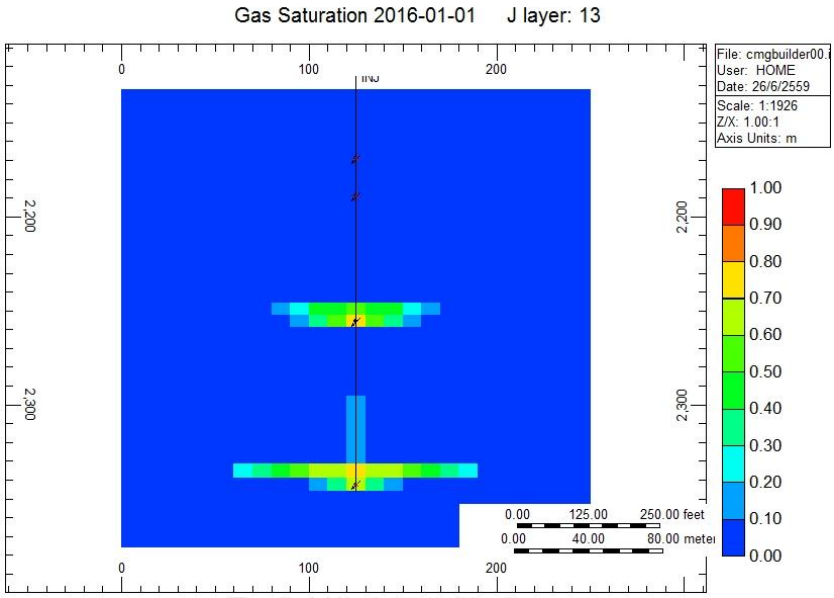

b.

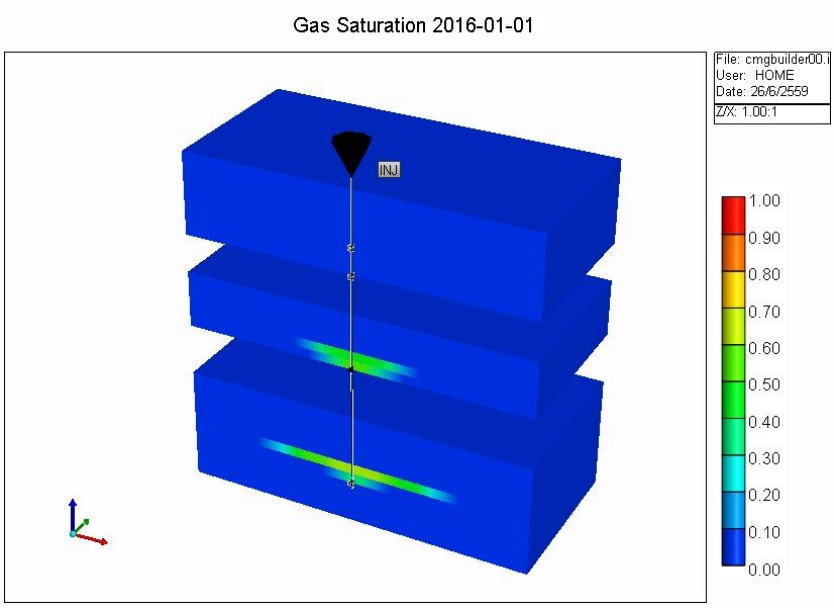

a. side view (1 year) and b. 3D view (1 year) in all layer at Well 3

a.

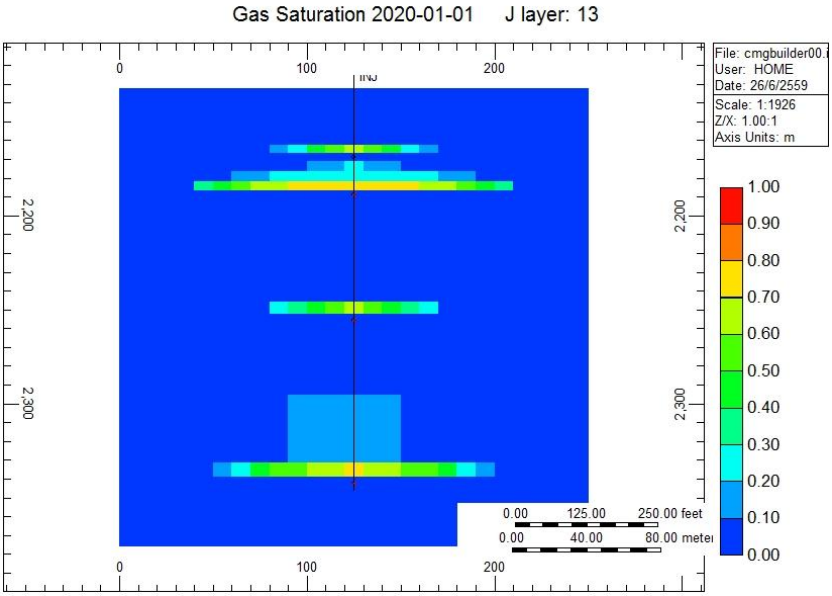

b.

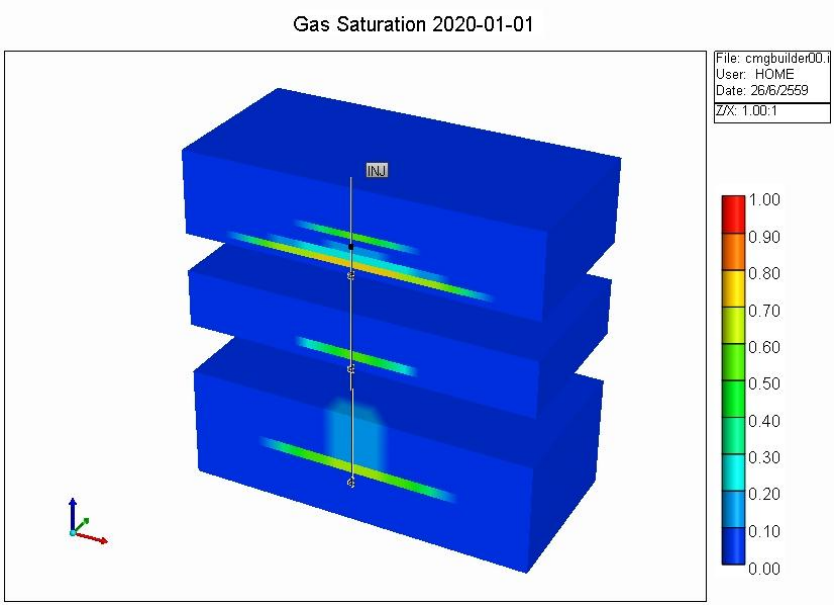

a. side view (5 years) and b. 3D view (5 years) in all layer at Well 3

a.

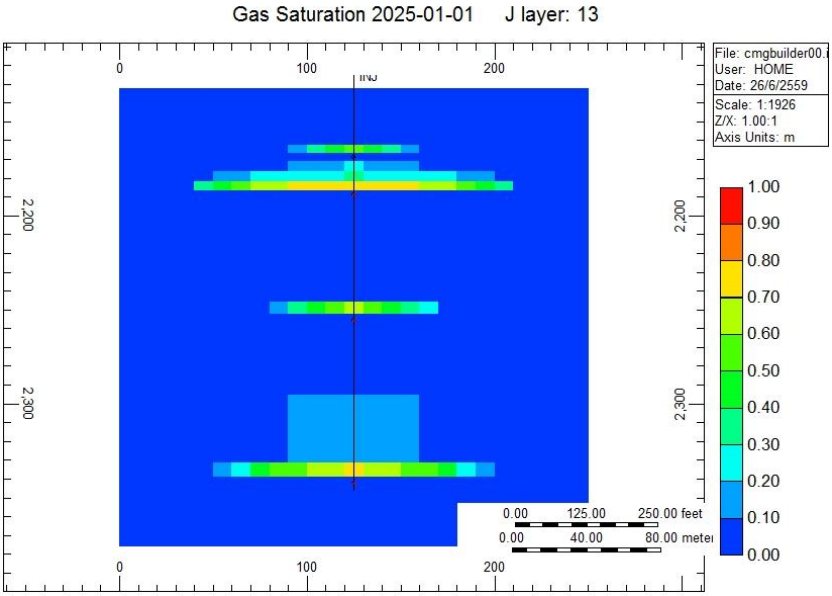

b.

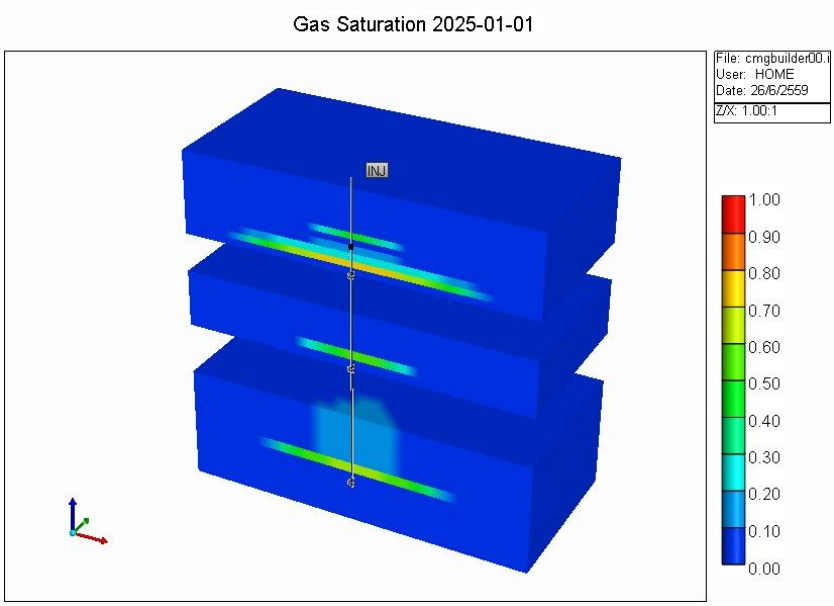

a. side view (10 years) and b. 3D view (10 years) in all layer at Well 3

a.

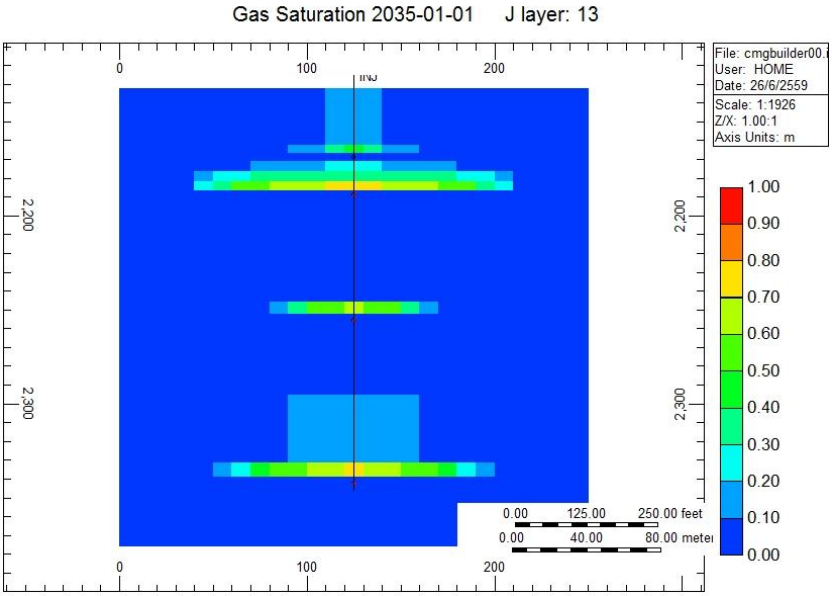

b.

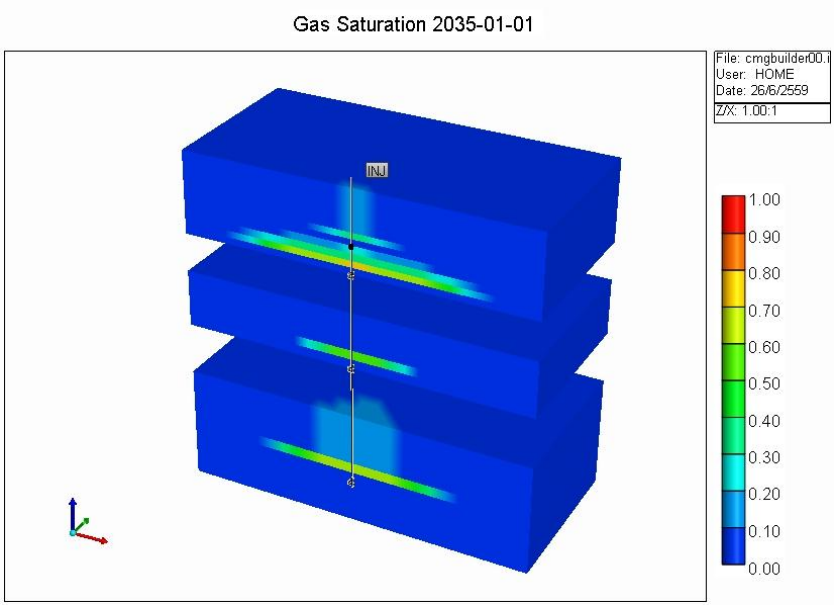

a. side view (20 years) and b. 3D view (20 years) in all layer at Well 3

a.

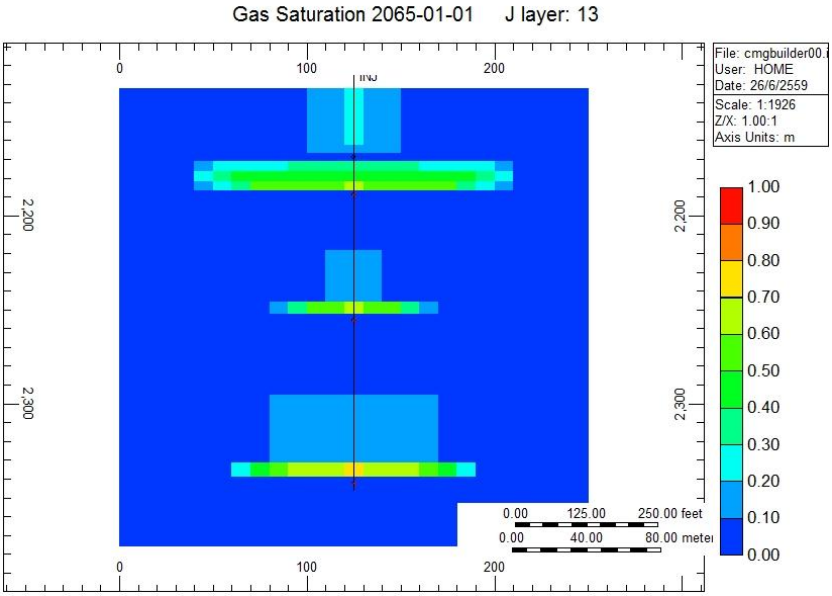

b.

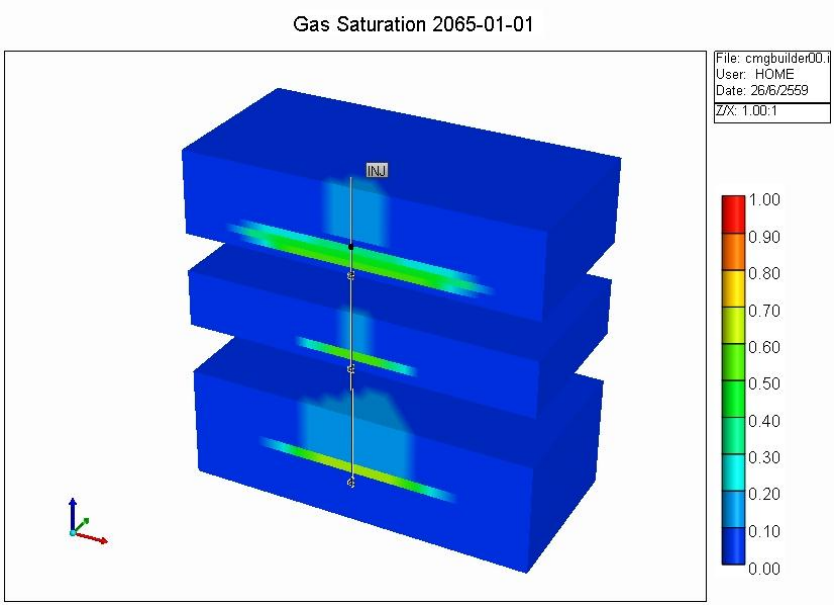

a. side view (50 years) and b. 3D view (50 years) in all layer at Well 3

All layer at 4,000 t/d injection rate.

a.

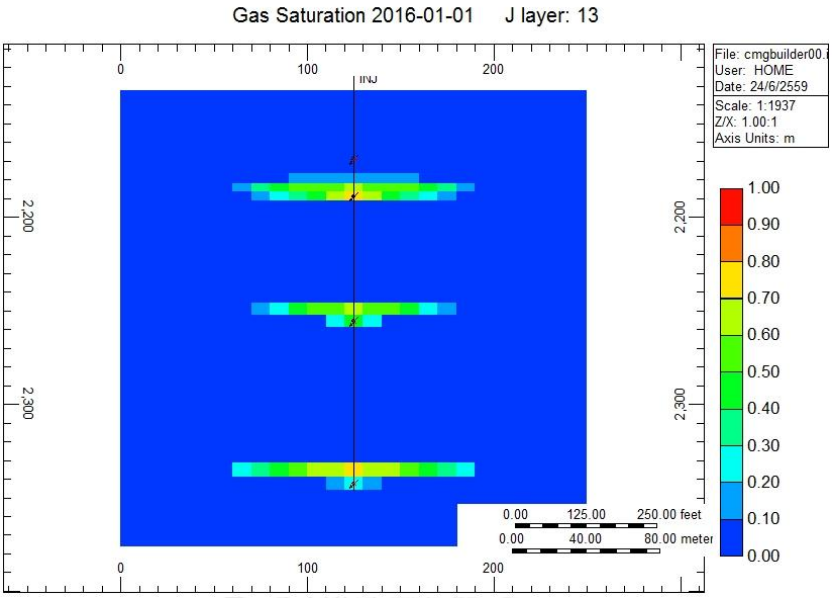

b.

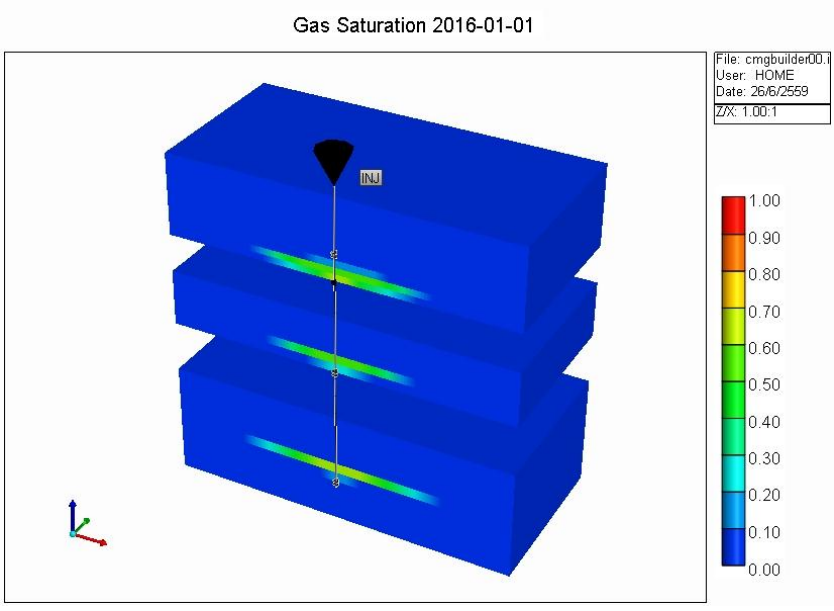

a. side view (1 year) and b. 3D view (1 year) in all layer at Well 3

a.

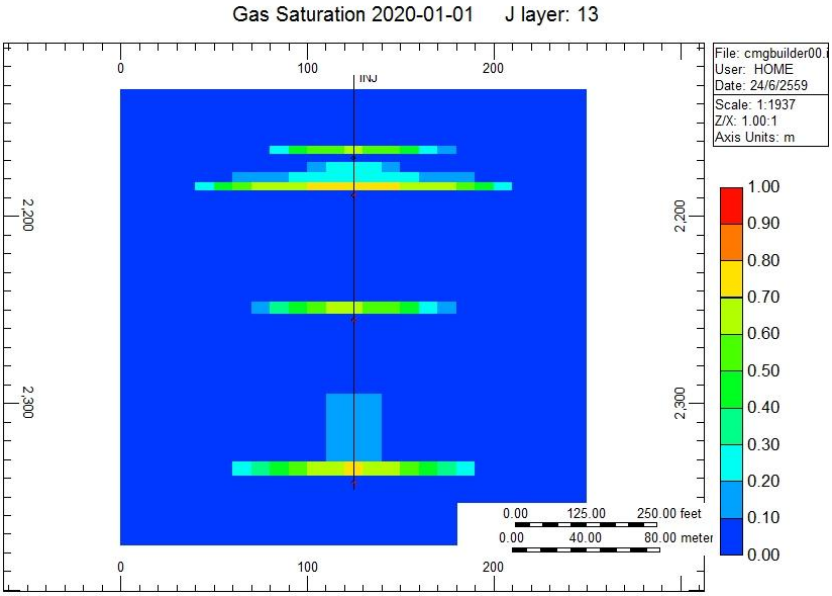

b.

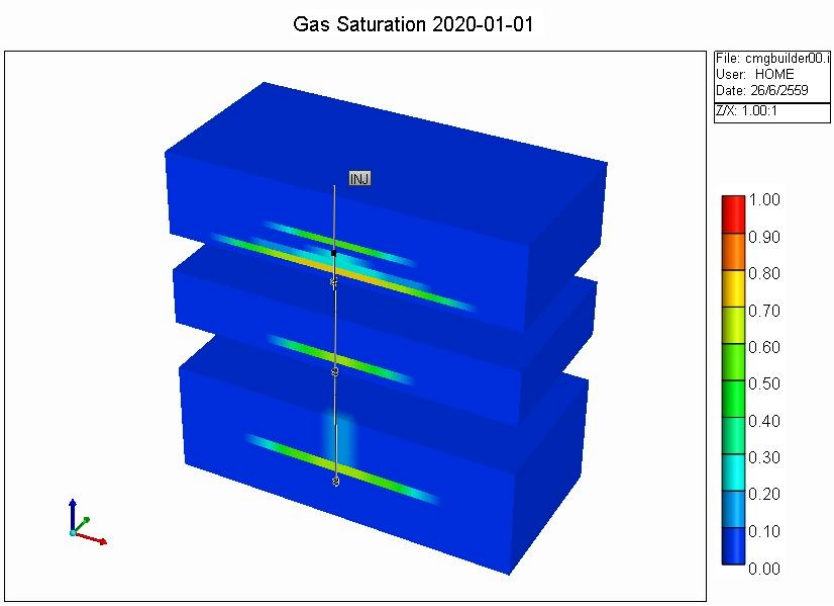

a. side view (5 years) and b. 3D view (5 years) in all layer at Well 3

a.

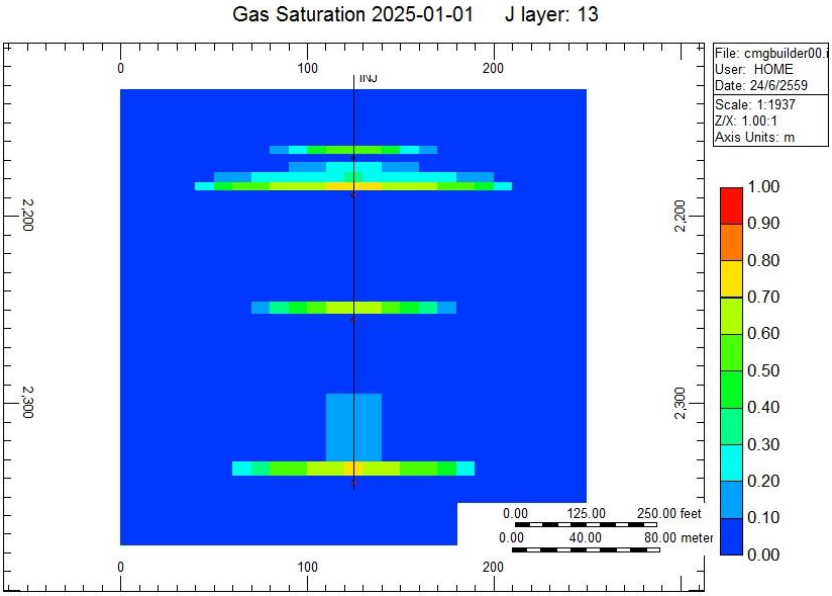

b.

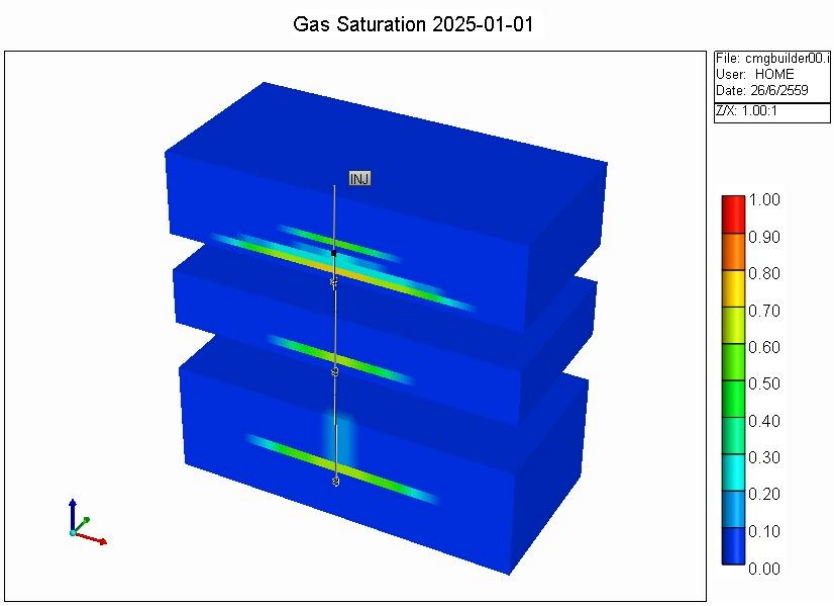

a. side view (10 years) and b. 3D view (10 years) in all layer at Well 3

a.

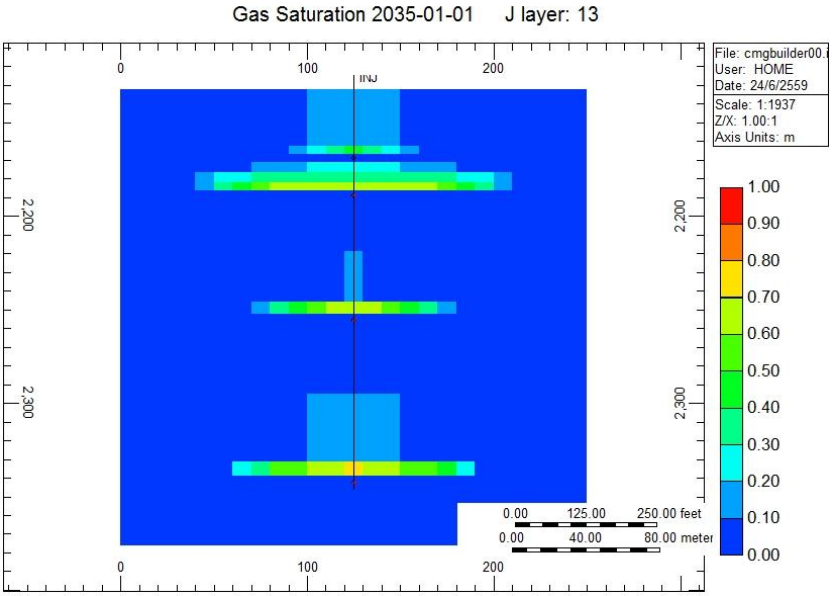

b.

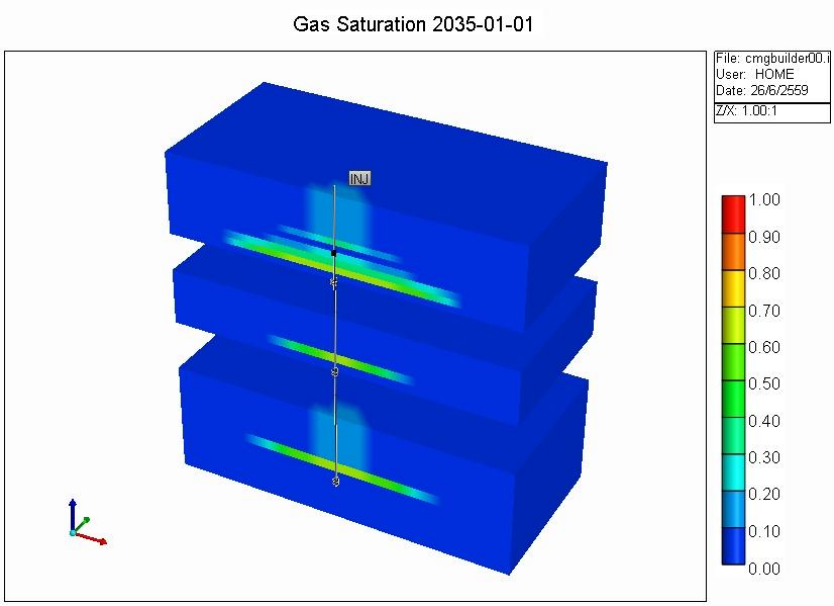

a. side view (20 years) and b. 3D view (20 years) in all layer at Well 3

a.

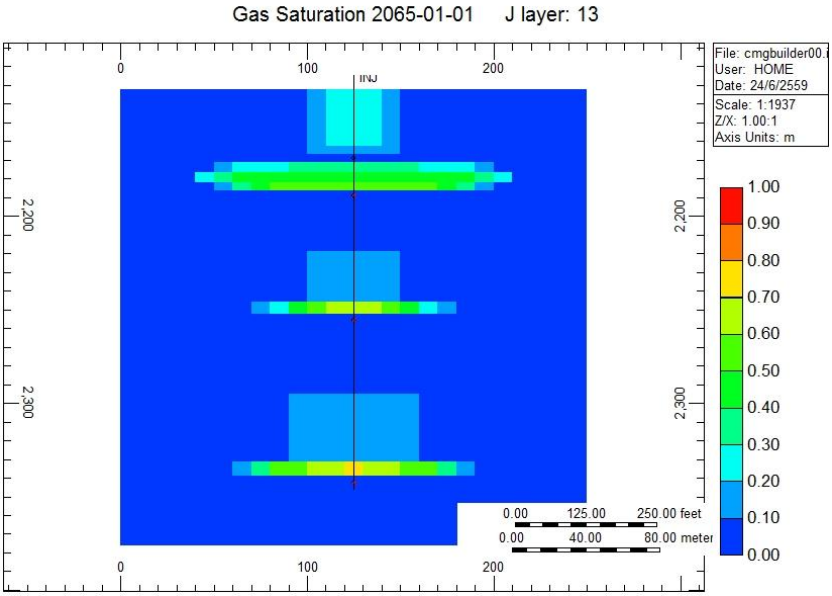

b.

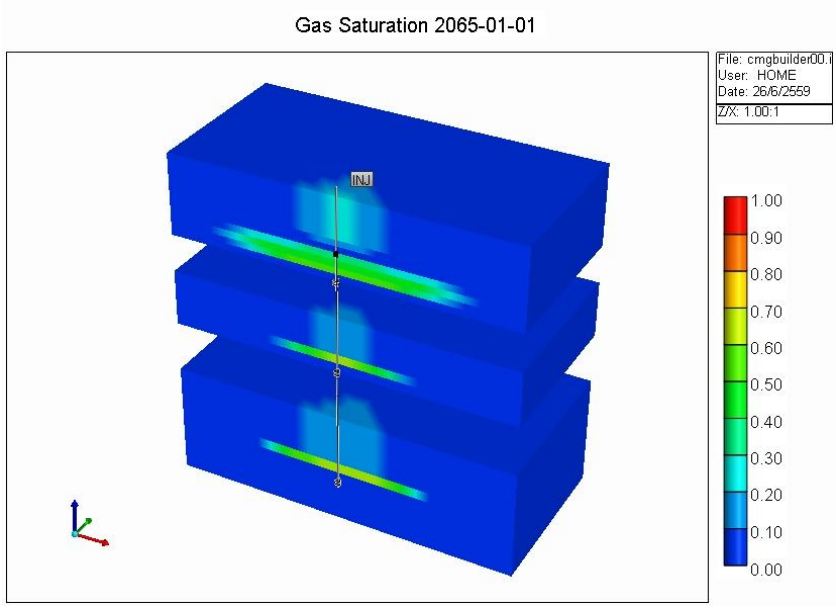

a. side view (50 years) and b. 3D view (50 years) in all layer at Well 3

VITA

Miss Monthicha Rawangphai was born on January 1, 1991 in Songkla province, The south of Thailand. She received her Bachelor degree in Sciences from Department of Earthsciences, Faculty of Sciences, Kasetsart University in 2013. After graduation, she has been a student in the Master' Degree program in georesource Engineering at Department of Mining and Petroleum Engineering, Faculty of Engineering, Chulalongkorn University.